frontiers | Research Topics

Nutrition and behavior as determinants of host-associated microbiomes

Edited by
Yvonne Vallès and M. Pilar Francino

Published in
Frontiers in Microbiology

ISSN 1664-8714
ISBN 978-2-8897-4685-9
DOI 10.3389/978-2-8897-4685-9

About Frontiers

Frontiers is more than just an open access publisher of scholarly articles: it is a pioneering approach to the world of academia, radically improving the way scholarly research is managed. The grand vision of Frontiers is a world where all people have an equal opportunity to seek, share and generate knowledge. Frontiers provides immediate and permanent online open access to all its publications, but this alone is not enough to realize our grand goals.

Frontiers journal series

The Frontiers journal series is a multi-tier and interdisciplinary set of open-access, online journals, promising a paradigm shift from the current review, selection and dissemination processes in academic publishing. All Frontiers journals are driven by researchers for researchers; therefore, they constitute a service to the scholarly community. At the same time, the *Frontiers journal series* operates on a revolutionary invention, the tiered publishing system, initially addressing specific communities of scholars, and gradually climbing up to broader public understanding, thus serving the interests of the lay society, too.

Dedication to quality

Each Frontiers article is a landmark of the highest quality, thanks to genuinely collaborative interactions between authors and review editors, who include some of the world's best academicians. Research must be certified by peers before entering a stream of knowledge that may eventually reach the public - and shape society; therefore, Frontiers only applies the most rigorous and unbiased reviews. Frontiers revolutionizes research publishing by freely delivering the most outstanding research, evaluated with no bias from both the academic and social point of view. By applying the most advanced information technologies, Frontiers is catapulting scholarly publishing into a new generation.

What are Frontiers Research Topics?

Frontiers Research Topics are very popular trademarks of the *Frontiers journals series*: they are collections of at least ten articles, all centered on a particular subject. With their unique mix of varied contributions from Original Research to Review Articles, Frontiers Research Topics unify the most influential researchers, the latest key findings and historical advances in a hot research area.

Find out more on how to host your own Frontiers Research Topic or contribute to one as an author by contacting the Frontiers editorial office: frontiersin.org/about/contact

Nutrition and behavior as determinants of host-associated microbiomes

Topic editors

Yvonne Vallès — The University of the West Indies, Cave Hill, Barbados

M. Pilar Francino — Fundación para el Fomento de la Investigación Sanitaria y Biomédica de la Comunitat Valenciana (FISABIO), Spain

Citation

Vallès, Y., Francino, M. P., eds. (2023). *Nutrition and behavior as determinants of host-associated microbiomes*. Lausanne: Frontiers Media SA.

doi: 10.3389/978-2-8897-4685-9

Table of contents

frontiers in Microbiology

EDITORIAL
published: 21 February 2022
doi: 10.3389/fmicb.2021.835394

Editorial: Nutrition and Behavior as Determinants of Host-Associated Microbiomes

Yvonne Vallès[1*†] *and M. Pilar Francino*[2,3†]

[1] *The University of the West Indies-Cave Hill Campus, Cave Hill, Barbados,* [2] *Fundación para el Fomento de la Investigación Sanitaria y Biomédica de la Comunitat Valenciana (FISABIO), Valencia, Spain,* [3] *CIBER en Epidemiología y Salud Pública, Madrid, Spain*

Keywords: animal, microbiome, modulation, nutrition, behavior

Editorial on the Research Topic

Nutrition and Behavior as Determinants of Host-Associated Microbiomes

Symbiotic relationships are dynamic in that adjustments are continuously made by the sets of organisms involved in the association. When considering microbiomes and their hosts, factors such as nutrition, behavior and a changing environment will affect both the host and its microbiome's composition, dynamics, and function. As our understanding of the role of microbiomes in the host's health grows, so does the thirst for knowledge on mechanisms of microbiome modulation. Here we present a collection of works that range from exploring natural microbiome variability under different geographical regions, to evaluating the effects of dietary and psychosocial factors on the human microbiome, to developing potential nutritional approaches to improve human and animal health and to increase efficiency and productivity in various animal systems.

As an example of natural microbiome variability, Liu et al. explore microbiome composition in three populations of yaks that inhabit three different regions of the environmentally heterogeneous Qinghai-Tibetan plateau. The Qinghai-Tibetan plateau is the largest and highest plateau in the world enclosing regions that vary vastly in altitude [from 500 m above sea level (a.s.l) at the foot of the Himalaya to 8,848 m a.s.l. at mount Everest], annual precipitation (from areas with 300 mm to others with 3,000 mm) and temperature, among other environmental factors (Favre et al., 2014). Yet, it is the home of 12 yak breeds, an extremely hardy indigenous ruminant found across the plateau (Liu et al.). Fascinatingly, Liu et al. demonstrate that the microbiome's diversity and composition will reflect the geographical region the yak population inhabits. Importantly, the soil of the Qinghai-Tibetan plateau is low in selenium (Se), so that Se deficiency is widespread in the yak and sheep that graze in this extreme environment. Cui et al. show that Se supplementation to the forage-based feed of Tibetan sheep improves fermentation and rumen microbial community structure, increasing livestock health and productivity.

In view of the indirect and unwanted connection of ruminants to climate change, Bharanidharan et al. explore the associations among cattle feeding systems (separate feeding vs. total mixed ration), breeds, rumen microbiota composition and CH_4 emissions. Interestingly, breeds independently of the feeding system have differential rumen microbial communities, with Hanwoo steers being higher CH_4 emitters than Holstein steers, but the use of a separate feeding system is more effective at reducing CH_4 emissions regardless of the cattle breed.

The gut microbiota also has an important effect on the nutritional physiology of pigs. Petry et al. and Long and Venema explore the possibility of modulating the swine gut microbiota by feeding the pigs with a corn-based feed supplemented with xylanase and a chemically pre-treated rapeseed meal, respectively. These studies come as a necessity, as the diet used in the swine industry presents a high proportion of dietary fiber, which the pig's intestine has no capacity to metabolize, decreasing

OPEN ACCESS

Edited and reviewed by:
Francesca Bottacini, Munster Technological University, Ireland

***Correspondence:**
Yvonne Vallès
kyvovas@gmail.com

These authors have contributed equally to this work

Specialty section:
This article was submitted to Microbial Symbioses, a section of the journal Frontiers in Microbiology

Received: *14 December 2021*
Accepted: *29 December 2021*
Published: *21 February 2022*

Citation:
Vallès Y and Francino MP (2022) Editorial: Nutrition and Behavior as Determinants of Host-Associated Microbiomes. Front. Microbiol. 12:835394. doi: 10.3389/fmicb.2021.835394

the productivity of the swine industry. In both cases, the supplementation of corn-based feed with xylanase and the chemical pre-treatment of rapeseed increase microbial community diversity and fiber degradability potential.

Focussing on a different food production industry, Huang et al. examine the effect of cassava starch-based feed on the microbiome composition and intestinal health of a carnivorous fish, the largemouth bass. Starch is an inexpensive feed ingredient, but carnivorous fishes are not well-adapted to its use. Interestingly, a significant decrease of beneficial bacteria abundance is observed in fish fed with a high-starch diet, with subsequent development of enteritis. To modulate the microbiome and prevent the development of enteritis, the authors propose the use of probiotics, reintroducing the lost beneficial bacteria and increasing productivity.

The influence of diet on the microbiome is not only of importance in animals raised for food but also in animal pets. The impact of modern lifestyles, characterized by higher energy intake packaged in smaller food bites with an increase in sedentarism, affects our pets, as a reflection of human behavior and nutrition. Therefore, current trends of increase in disorders such as diabetes and obesity are not unique to humans but extend to our pets as well. In their study, Li and Pan, examine the effect of a high protein low carbohydrate (HLPC) diet recommended for weight management vs. a control diet (CON: higher carbohydrate percentage with lower protein percentage) on the gut microbiome of lean and obese cats. Interestingly, the different diets do not influence the lean cat's microbiota, while significant differences are observed between the obese cats fed with HPLC and CON diets, where the HPLC-fed obese cat's microbiome has a greater abundance of short-chain fatty acid producers that could eventually be used in weight management therapies.

Overall, these various studies in animal systems illustrate the vast potential of microbiome modulation as a strategy to improve health in both pets and farm animals, as well as productivity in animal-based food industries.

Finally, we report several studies on the human's gut microbiome that (1) validate once again the fact that there is an inherent individual variability in microbiota functionality, as shown by Riva et al. regarding individual ability to metabolize rutin, a bioactive polyphenolic compound with antioxidant, antiaging, and anti-neurodegenerative properties; (2) demonstrate the possibility of positively modulating the microbiome by adding tannin wood extracts to food and in particular quebracho and tara, as Molino et al. show that their addition is significantly associated to an increased presence of *Akkermansia* and beneficial short-chain fatty acid producers; and (3) indicate that the disruption of an equilibrated microbiome is affected by more than just physical cues, with psychological and behavioral cues as well-influencing microbiome development. In their study, Rodriguez et al. show that the antenatal psychological status of the mother can disrupt the infant's gut microbiome through the transmission of a suboptimal maternal microbial community, a negative effect on breast milk immune properties, and an adverse impact on the duration of breastfeeding.

AUTHOR CONTRIBUTIONS

All authors listed have made a substantial, direct, and intellectual contribution to the work and approved it for publication.

ACKNOWLEDGMENTS

We would like to thank all the authors that have contributed to this Research Topic, the reviewers that have provided their time and expertise, and the Frontiers editorial staff for their support.

REFERENCES

Favre, A., Päckert, M., Pauls, S. U., Jähnig, S. C., Uhl, D., Michalak, I., et al. (2014). The role of the uplift of the Qinghai-Tibetan plateau for the evolution of tibetan biotas. *Biol. Rev.* 90, 236–253.

Conflict of Interest: The authors declare that the research was conducted in the absence of any commercial or financial relationships that could be construed as a potential conflict of interest.

Publisher's Note: All claims expressed in this article are solely those of the author and do not necessarily represent those of their affiliated organizations, or those of the publisher, the editors and the reviewers. Any product that may be evaluated in this article, or claim that may be made by its manufacturer, is not guaranteed or endorsed by the publisher.

frontiers in Microbiology

ORIGINAL RESEARCH
published: 16 October 2020
doi: 10.3389/fmicb.2020.591462

Differential Responses to Dietary Protein and Carbohydrate Ratio on Gut Microbiome in Obese vs. Lean Cats

Qinghong Li†* and *Yuanlong Pan*†

Nestlé Purina Research, St. Louis, MO, United States

More than 60% of domestic cats in the United States are either overweight or obese (OW). High-protein low-carbohydrate (HPLC) diets have been recommended for weight management for humans and pets. Gut microbes can influence the host's health and metabolism. Less is known about feline gut microbiomes compared to other species. Thirty-nine lean (LN) and OW domestic short-haired cats (median age, 7.2 years) with median body fat of 15.8 and 32.5%, respectively, were enrolled in a two-phase study. All cats were fed the control diet (CON) with 32.4% protein and 32.3% carbohydrate for 8 weeks followed by another 8 weeks of intervention where half of the cats continued the CON diet while the other half were switched to a HPLC diet with 51.4% protein and 11.6% carbohydrate. The goal was to understand how the HPLC diet influenced gut microbiota in obese vs. lean cats. The 16S rRNA gene profiling study revealed a significant impact on gut microbiome by dietary protein and carbohydrate ratio. The effect was more pronounced in OW cats than LN cats. While no microbial taxon was different between groups in LN cats, compositional changes occurred at different taxonomical ranks in OW cats. At the phylum level, *Fusobacteria* became more abundant in HPLC-fed cats than in CON-fed cats. At the genus level, five short-chain fatty acid (SCFA) producers had altered compositions in response to the diets: *Faecalibacterium* and *Fusobacterium* are more abundant in HPLC-fed cats while the abundances of *Megasphaera*, *Bifidobacterium*, and *Veillonella* increased in CON-fed cats. Predicted microbial gene networks showed changes in energy metabolism and one-carbon metabolism pathways. Our study demonstrated differential responses to HPLC diet between obese vs. lean cats and opportunities to explore these SCFA-producers for weight management in cats.

Keywords: cat, microbiome, protein, carbohydrate, obesity, diet, feline

OPEN ACCESS

Edited by:
Yvonne Vallès,
The University of the West Indies, Cave Hill, Barbados

Reviewed by:
Umesh D. Wankhade,
University of Arkansas for Medical Sciences, United States
Maryam Dadar,
Razi Vaccine and Serum Research Institute, Iran

***Correspondence:**
Qinghong Li
qinghong.li@rd.nestle.com

†***ORCID:***
Qinghong Li
orcid.org/0000-0002-2584-6024
Yuanlong Pan
orcid.org/0000-0002-9843-9948

Specialty section:
This article was submitted to Microbial Symbioses, a section of the journal Frontiers in Microbiology

Received: *04 August 2020*
Accepted: *17 September 2020*
Published: *16 October 2020*

Citation:
Li Q and Pan Y (2020) Differential Responses to Dietary Protein and Carbohydrate Ratio on Gut Microbiome in Obese vs. Lean Cats. Front. Microbiol. 11:591462. doi: 10.3389/fmicb.2020.591462

INTRODUCTION

Pet obesity has increased in the past two decades, and it currently is reported that more than 60% of pet cats are overweight or obese (OW)[1]. Comorbidities associated with excessive body weight include diabetes mellitus, cardiovascular diseases, musculoskeletal disorders, and many others. Thus, feline obesity poses not only health concerns for the cats, but also economical and emotional

[1]https://petobesityprevention.org/

issues for the owners. Obesity can be attributed to a combination of causes including increased energy intake, reduced energy expenditure and more efficient absorption in dietary nutrients, which has been associated with changes in microflora in the gastrointestinal (GI) tract of hosts (Ley et al., 2005; Turnbaugh et al., 2006). The GI tract is home of trillions of microorganisms that ferment and utilize unabsorbed dietary components (Sonnenburg et al., 2005). Some of the bacteria in the intestine and colon metabolize dietary carbohydrates to produce short-chain fatty acids (SCFAs) which are precursors for energy production (McNeil, 1984). In humans, an estimated 5–10% of absorbed energy comes from the colon (Bingham et al., 1982; McNeil et al., 1982). GI microbes in obese individuals are thought to be more efficient at extracting energy than those in lean individuals (Backhed et al., 2004; Turnbaugh et al., 2006). The ratio of *Firmicutes* to *Bacteroidetes* in the gut has been associated with obesity in dogs, mice, and humans (Ley et al., 2005, 2006; Ley, 2010; Li et al., 2017; Coelho et al., 2018). Potential mechanisms through which gut microbes contribute to host obesity include extraction of extra dietary energy, increased lipogenesis and accumulation of triglycerides in adipocytes (Benahmed et al., 2020).

The concept of using high-protein low-carbohydrate (HPLC) diets for weight loss has been known for many years (Riegler, 1976). Potential benefits of HPLC diets, including increased satiety, reduced hunger, loss of body fat, and retention of lean body mass, were reported in humans, rodents, and dogs (Bierer and Bui, 2004; Laflamme and Hannah, 2005; Kinzig et al., 2007; Kushner and Doerfler, 2008). HPLC diets have been shown to alter the gut microbiome in kittens (Hooda et al., 2013). In dogs, a HPLC diet altered the composition and function of the gut microbiota differentially based on body condition, with greater changes observed in OW dogs (Li et al., 2017; Coelho et al., 2018). However, studies of the gut microbiome of adults cats as affected by HPLC diets or by body composition are limited. In this study, we examined the effect of dietary protein and carbohydrate on gut microbiome in adult cats with and without excessive body fat.

The goal of this study was to understand how gut microbiome changes in response to a HPLC diet vs. a control diet (CON) diet in adult cats. Based on the previous studies in dogs and kittens, we hypothesized that there would be a significant shift in microbiota between HPLC and CON diets, and that effect would be greater in OW cats than cats with lean and healthy body condition (LN).

MATERIALS AND METHODS

Animals and Study Design

The study protocol was approved by the Institutional Animal Care and Use Committee of the Nestlé Purina PetCare Company. Twenty OW domestic short-haired neutered male or female cats and 19 sex-, breed-, and age-matched LN cats were selected for a two-phase 16-week study. Cats with a body condition score (BCS) between 4 and 5 in the 9-point scale system (Laflamme, 1997) were considered for the LN group, while cats with BCS 7–9 were considered for the OW group. Body fat was determined by quantitative magnetic resonance (QMR) analysis using EchoMRI-Infants QMR Analyzer (Echo Medical Systems) to confirm body composition prior to randomization (T0): cats with $\leq$20% body fat were considered LN while those with $\geq$25% body fat were considered OW. Cats in each weight group were randomly assigned to two diet treatment groups balanced for sex, age, and body fat: the CON and the HPLC diet as the test diet (**Table 1**). During the baseline feeding phase, all cats were fed the CON diet for 8 weeks during which each cat's maintenance energy requirement (MER) was individually determined based on intake needed to maintain their body weight. Initially, MER (kilocalories) was estimated as 60 × body weight (kg) with a weekly adjustment made if body weight increased or decreased by more than 5% of their initial body weight. In the intervention phase, cats were switched to their assigned diet and fed to maintain body weight for another 8 weeks. Fecal samples were collected, and body fat percentages were measured using QMR after the baseline (T1) and intervention (T2) period.

Cats were individually housed with access to a group room with natural and supplemental lighting on a 12-h cycle. All cats received regular exercise in the activity room with other cats, routine grooming, and regular socialization by caretakers.

Diets

The study diets were formulated to be isocaloric, and to meet or exceed the maintenance nutrient requirement based on the guidelines of the Association of American Feed Control Officials. Both diets contained animal protein as a primary protein source. The protein level in the HPLC diet was adjusted by replacing grains with plant protein. Details in nutritional compositions of the diets are described in **Table 2**.

The 16S rRNA Gene Sequencing of the V3–V4 Region

Fresh fecal samples were collected within 15 min of defecation at T1 and T2 and were immediately frozen and stored at −80°C until use. Fecal DNA extraction was performed using PowerFecal DNA isolation kit (Mo Bio Laboratories) and quantified by Quant-It Pico Green (Thermo Fisher Scientific) according to manufacturer's protocols. The 16S rRNA gene library was constructed according to Illumina's 16S metagenomic sequencing library preparation guide. Sequencing was performed in an Illumina MiSeq machine with 500 cycles according to the previously described procedures (Li et al., 2017).

Bioinformatics Analysis

Each paired-end reads were merged and assembled into a single read using the software PEAR with default settings (Zhang et al., 2014), resulting in an average of 99.4% assembly. Unassembled reads and those with less than 350

Abbreviations: CON, control diet; FDR, false discovery rate; HPLC, high-protein low-carbohydrate diet; KEGG, Kyoto Encyclopedia of Genes and Genomes; LEfSe, linear discriminant analysis effect size; LN, lean and normal weight; OTU, operational taxonomic unit; OW, overweight or obese; PCoA, principal coordinate analysis; PD, phylogenetic diversity; PICRUSt, phylogenetic investigation of communities by reconstruction of unobserved states; SCFAs, short-chain fatty acids.

TABLE 1 | Physical characteristics of the cats.

	Lean and normal (LN)			Overweight or obese (OW)		
	HPLC	**CON**	***P*-value**	**HPLC**	**CON**	***P*-value**
N	10	9		10	10	
Sex						
Female	5	4		4	4	
Male	5	5		6	6	
Age	6.75 ± 4.49	6.49 ± 3.53	0.89	7.15 ± 2.50	7.08 ± 2.23	0.95
Body weight (kg)	4.03 ± 0.78	4.19 ± 0.69	0.63	5.85 ± 1.01	5.97 ± 0.82	0.77
Body condition score	5.0 ± 0.0	5.0 ± 0.0	n/a	7.3 ± 0.7	7.4 ± 0.5	0.71
Body fat (%)[a]						
T0	14.7 ± 3.7	14.6 ± 4.5	0.94	32.3 ± 5.4	33.9 ± 3.3	0.44
T1	14.4 ± 4.0	14.9 ± 3.9	0.77	31.4 ± 5.0	32.7 ± 4.0	0.52
T2	15.7 ± 3.0	16.7 ± 4.1	0.58	32.5 ± 5.4	33.7 ± 4.0	0.58
P-value (ANOVA)[b]	0.73	0.53		0.89	0.75	

[a] *Body fat is measured by quantitative magnetic resonance (QMR) before and after baseline feeding (T0 and T1, respectively), and after intervention (T2).*
[b] *Difference in body fat within each body type by diet group.*
Student's t-test is performed unless indicated otherwise. HPLC, high-protein low-carbohydrate diet; CON, control diet; na, not applicable. Continuous variables are expressed as mean ± standard error.

or greater than 475 nucleotides were discarded. Chimeric reads were detected using UCHIME (Edgar et al., 2011) and discarded. Reads were de-replicated, sorted and clustered into operational taxonomic units (OTUs) based on minimal 97% identity using the UPARSE-OTU clustering algorithm and the greengenes database (v. 13.8) (Edgar, 2010, 2013). Taxonomy assignment was performed using the k-mer-based K-nearest neighbor search algorithm implemented in Mothur (version 1.39.5) (Schloss et al., 2009) by searching the reference sequence file from the greengenes database (Quast et al., 2013). Sequence alignment was performed using PyNAST (Caporaso et al., 2010a). Phylogenetic tree was built from the aligned sequences using FastTree (Price et al., 2009, 2010). Microbial compositional data in the OTU table was normalized using total sum scaling where relative abundance was calculated for each microbial taxa. Low abundance taxa with less than 0.01% in relative abundance in all samples were removed. Faith's phylogenetic diversity (PD), Shannon diversity, and observed species indexes were calculated using the QIIME script "alpha_rarefaction." Beta diversity on Bray–Curtis, weighted and unweighted UniFrac dissimilarity matrix was calculated using "beta_diversity_through_plots" (Lozupone et al., 2011). Rarefactions on the OTU table were performed to the maximal depth of 20,000 reads. QIIME (version 1.9.1) functions were called for making taxonomy assignment, OTU table and phylogenetic tree (Caporaso et al., 2010b).

TABLE 2 | Nutrition compositions in HPLC and CON diets.

Content (%)	**HPLC**	**CON**
Moisture	7.82	7.98
Protein	51.35	32.43
Carbohydrate	11.60	32.30
Fat	14.60	14.30
Total dietary fiber	12.70	11.20
Soluble dietary fiber	1.18	0.79
Insoluble dietary fiber	11.50	10.40
Ash	10.3	8.80
Calculated ME (kcal/g)	3.45	3.48

HPLC, high-protein low-carbohydrate diet; CON, control diet; ME, metabolizable energy.

Statistical Analysis

ANOVA analysis followed by Tukey's *post hoc* test was performed to compare alpha diversity between groups. Permutational multivariate analysis of variance (PERMANOVA) was performed to compare beta diversity (Oksanen et al., 2019). Student's *t*-test was performed to test the null hypothesis that the means of the first or second principal component (PC), PC1 or PC2, between groups were equal. The distance from T1 and T2 in each cat was calculated using the unweighted UniFrac dissimilarity matrix and compared across four body condition-diet groups using ANOVA followed by Tukey's *post hoc* test. To identify significant taxa between groups, only taxa with at least 50% of non-zero values in at least one group were considered and non-parametric Kruskal–Wallis test was performed followed by Dunn's multiple comparison with Benjamini–Hochberg adjustment. Multivariate analysis by linear models (MaAsLin) was performed to find associations between clinical variables and microbial features (Morgan et al., 2012). Linear discriminant analysis (LDA) effect size (LEfSe) (Segata et al., 2011) and Random Forest machine learning with 500 trees were performed to select microbial markers that contributed most to the separation between groups using the MicrobiomeAnalyst web portal (Dhariwal et al., 2017). To evaluate functional changes in gut microbial metagenomes due to diet intervention, phylogenetic investigation of communities by reconstruction of unobserved states (PICRUSt) (Langille et al., 2013) was performed on the compositional data to estimate

Kyoto Encyclopedia of Genes and Genomes (KEGG) orthologs and pathways, which were subject to LEfSe analysis. P values were adjusted to control false discovery rate (FDR) (Benjamini and Hochberg, 1995). Statistical computing was performed in R version 3.5.2. (R Core Team, 2015).

RESULTS

There were 10 males and 9 females in the LN group and 12 males and 8 females in the OW group (**Table 1**). The mean ages were 6.6 ± 0.9 (standard error) for LN cats and 7.1 ± 0.5 for OW cats ($P = 0.64$) while mean BCS for LN and OW cats were 5.0 ± 0.0 and 7.4 ± 0.13 ($P < 0.01$), respectively. At T0, the median body fat percentages were 14.0% (range, 6.9–17.3%) for LN males, 15.4% (range, 5.7–20.0%) for LN females, 32.0% (range, 26.4–37.0%) for OW males, and 34.8% (range, 28.8–45.8%) for OW females. At T2, one male and one female of the LN group had exceeded 20% body fat: means were 15.2% (10.5, 21.8%) for LN males, 17.1% (9.6, 20.8%) for LN females, 30.8% (26.2, 34.6%) for OW males, and 36.4% (29.9, 43.8%) for OW females. There was no significant change in body fat among T0, T1, and T2 ($P_{ANOVA} > 0.05$ in all cases, **Table 1**). All cats were healthy throughout the study except that one HPLC-fed LN cat (LN-HPLC) who developed a health issue unrelated to the diet after T1 and whose T2 sample was not collected.

A total of 4,809,360 paired-end sequences were generated from 77 fecal samples, with a median 61,903 sequences per sample (range, 31,538–82,908). After assembly and quality trimming, the median was 48,352 sequences (range, 24,445–67,643) per sample (**Supplementary Table 1**). The median length of the assembled sequences was 440 nucleotides. A operational taxonomic units (OTUs) table with 77 samples and 1,635 was constructed.

Dietary Effects on Gut Microbial Diversities

To assess richness and evenness in gut microbial communities in each cat, Faith's PD, Shannon diversity and Observed Species indexes were calculated (**Supplementary Table 2**). Although no difference was found between OW and LN cats ($P > 0.05$) at T1 after all cats were fed the same CON diet, a significant difference was found at T2 ($P < 0.05$ for both Faith's PD and Shannon indexes, **Figures 1A,B**). Tukey's *post hoc* test showed significant differences in Faith's PD between LN-HPLC cats and OW-CON cats (mean = 27.0 and 30.5, respectively, $P = 0.019$) and in Shannon diversity between LN-CON cats and OW-CON cats (mean = 4.46 and 5.45, respectively, $P = 0.022$). A similar trend was found in Observed Species index ($P_{ANOVA} = 0.057$).

To explore the effects of diet, sex, and body condition on gut microbial composition, beta diversity indexes

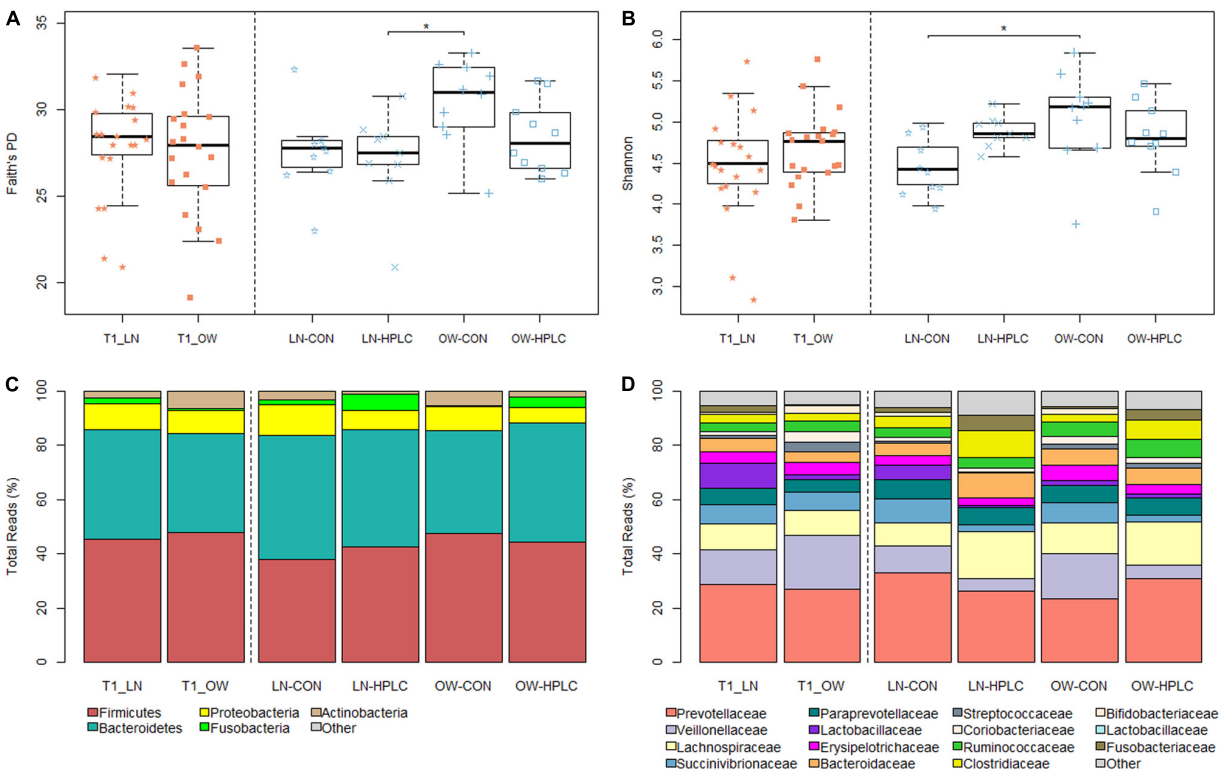

FIGURE 1 | Faith's PD **(A)** and Shannon diversity **(B)** indexes after baseline feeding (T1, orange) and intervention (T2, blue). Relative abundances of gut microbiota in the phylum level **(C)** and family level **(D)**. LN, lean cats; OW, overweight or obese cats; HPLC, high-protein, low-carbohydrate diet; CON, control diet. Adjusted *$P < 0.05$.

based on Bray–Curtis, weighted and unweighted UniFrac metrics were calculated (**Supplementary Table 2**) (Lozupone and Knight, 2015). At T1, while no difference was found in fecal microbiomes in the principal coordinate analysis (PCoA) analysis due to sex or prospective diet groups ($P > 0.10$ in both cases, **Figure 2A** and **Supplementary Figure 1A**), a significant difference was found between OW and LN cats ($P = 0.047$, unweighted UniFrac, **Supplementary Figure 1B**). No difference was found between the prospective diet groups in either LN or OW cats (**Supplementary Figures 1C,D**).

The dietary intervention had a significant impact on fecal microbial communities (**Figure 2B** and **Supplementary Table 2**). Significant changes were observed among the four body condition-diet groups, OW-HPLC, OW-CON, LN-HPLC, and LN-CON, using the unweighted UniFrac distance, ($P_{PERMANOVA}$ = 1.0e-06). Dietary effect was greater in OW cats than in LN cats ($P_{PERMANOVA}$ = 2.9e-05, $P_{PERMANOVA}$ = 0.008, respectively, **Figures 2C,D**). The distribution of samples along the first and second principal coordinates, PC1 and PC2, was also analyzed. A significant difference along PC1 was found due to diet or body condition (P = 2.8e-06, P = 0.046, respectively, **Figure 3A**). No difference was found on PC2 ($P > 0.05$ in both cases). Significant changes were observed on the distance from T1 to T2 based

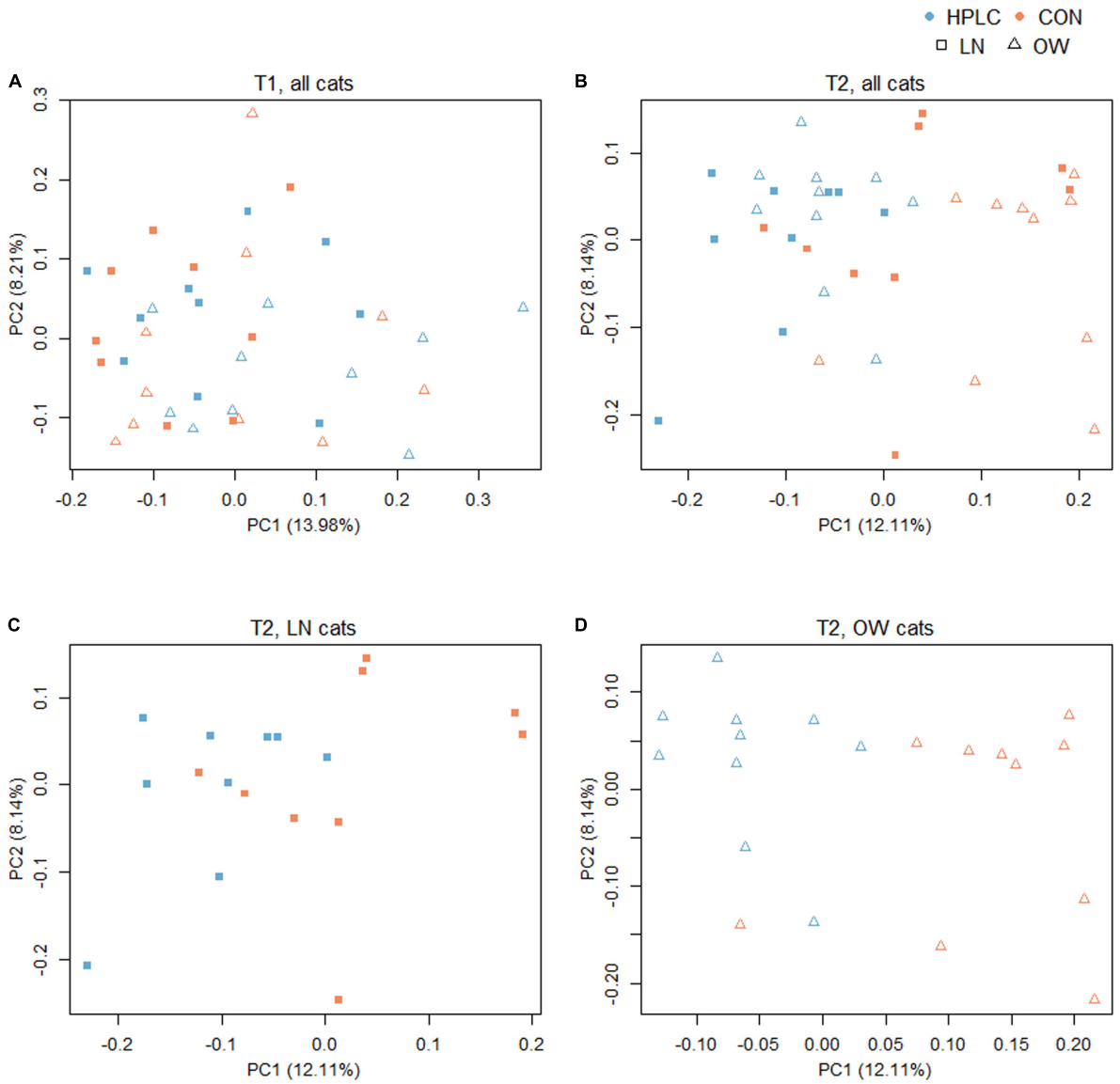

FIGURE 2 | Principal coordinates analysis based on unweighted UniFrac distance metric with **(A)** all cats at T1, **(B)** all cats at T2, **(C)** LN cats at T2, and **(D)** OW cats at T2. Squares represent LN cats; triangles represent OW cats. Blue and orange represent HPLC and CON diets respectively. The percentages of data variation explained by the first two principal coordinates are indicated on the *x* and *y* axes. LN, lean cats; OW, overweight or obese cats; HPLC, high-protein, low-carbohydrate diet; CON, control diet.

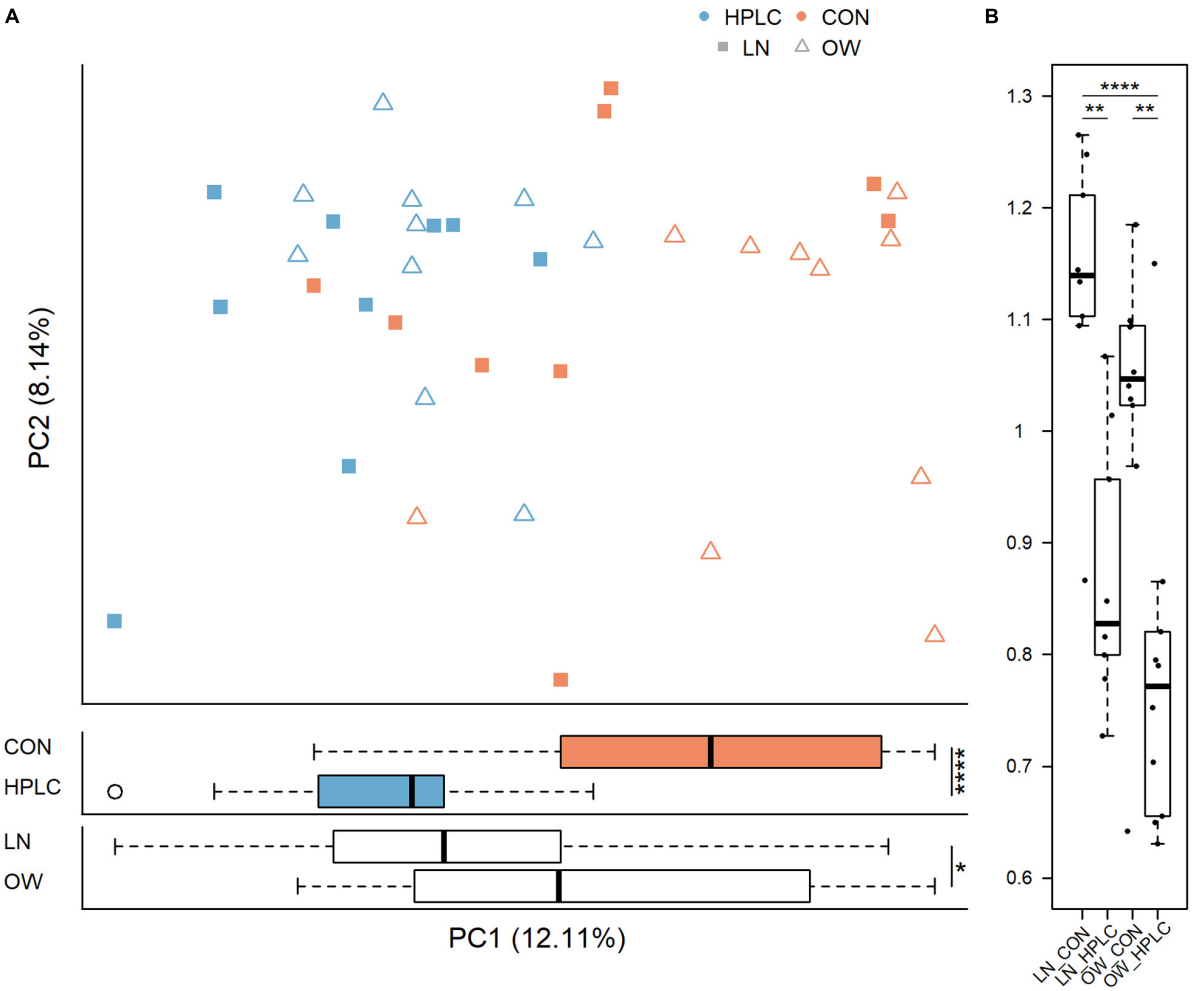

FIGURE 3 | Principal coordinate analysis based on **(A)** unweighted UniFrac distance metric (top panel) and sample distribution along PC1 by diet (middle panel) and by body condition (bottom panel). **(B)** Differences in unweighted UniFrac distance from T1 to T2 for each cat are calculated and plotted for the four groups. LN, lean cats; OW, overweight or obese cats; HPLC, high-protein, low-carbohydrate diet; CON, control diet. *P*-values from student's *t*-test **(A)** and Tukey's post hoc test **(B)**: $^{*}P < 0.05$, $^{**}P < 0.01$, $^{***}P < 0.001$, $^{****}P < 0.0001$.

on unweighted UniFrac dissimilarity matrix (P = 8.9e-06, **Figure 3B**).

Multivariate linear modeling was performed to assess any association between microbial abundance and clinical variables such as age, sex, body weight, BCS, and body fat. No significant association was found.

Gut Microbiota Between OW vs. LN Cats

No taxonomic change was found at T1 after adjusting for multiple testing errors (FDR > 0.05 in all cases, **Supplementary Table 3**). Two phyla showed opposite trends: *Fusobacteria* was more abundant in LN cats while *Actinobacteria* was enriched in OW cats. But the differences did not reach statistical significance (P = 0.057 and 0.054, respectively, **Figure 1C**). Similar trends were found in the families of *Fusobacteriaceae* and *Coriobacteriaceae* (phylum Actinobacteria) (P = 0.057 and 0.030, respectively, **Figure 1D**). At the genus level, *Firmicutes*, *Butyrivibrio*, *Bulleidia*, *Dialister*, and *Acidaminococcus* were more abundant in OW cats while *Fusobacterium* was less abundant when compared to LN cats (P = 0.009, 0.010, 0.020, 0.057, 0.058, respectively, FDR > 0.05 in all cases; **Supplementary Table 3**).

Dietary Intervention Changes Gut Microbiota in OW Cats

Effects of diet intervention on bacterial compositions were examined at the phylum, family, genus, and species levels in OW cats (**Table 3** and **Supplementary Table 4**). The abundance of *Fusobacteria* was increased by more than eight fold in HPLC cats compared to CON cats (FDR = 0.001, **Figure 1C**). At the family level, the abundances of *Fusobacteriaceae, Clostridiaceae, Lachnospiraceae, Ruminococcaceae, Mogibacteriaceae,* and *Peptococcaceae* were increased while those of *Veillonellaceae, Bifidobacteriaceae, Porphyromonadaceae,* and *Rikenellaceae* were decreased in HPLC vs. CON cats (FDR < 0.05 in all

TABLE 3 | Differential taxa between diet groups in obese or overweight (OW) cats.

Rank	Taxonomy	*P* (KW)	FDR	*P* (T1 vs. T2-CON)	*P* (T1 vs. T2-HPLC)	*P* (T2-CON vs. T2-HPLC)	FC (HPLC/CON)
Phylum	Fusobacteria	0	0.001	0.651	0	0	8.1
Family	Fusobacteriaceae	0	0.004	0.651	0	0	8.1
Family	Veillonellaceae	0	0.004	0.691	0	0.003	−3.4
Family	Bifidobacteriaceae	0.002	0.018	0.527	0.003	0.004	−711
Family	Clostridiaceae	0.007	0.036	0.851	0.007	0.02	2.3
Family	Lachnospiraceae	0.007	0.036	0.31	0.005	0.099	1.4
Family	Ruminococcaceae	0.008	0.036	0.174	0.006	0.196	1.4
Family	Mogibacteriaceae	0.011	0.037	0.048	0.02	0.619	1.8
Family	Peptococcaceae	0.01	0.037	0.171	0.009	0.228	1.6
Family	Porphyromonadaceae	0.012	0.038	0.013	0.877	0.029	−3.5
Family	Rikenellaceae	0.015	0.041	0.022	0.505	0.021	−8.1
Genus	*Faecalibacterium*	0	0.002	0.868	0	0.001	4.5
Genus	*Megasphaera*	0	0.002	0.851	0	0.001	−83.4
Genus	*Fusobacterium*	0	0.003	0.651	0	0	8
Genus	*Veillonella*	0	0.004	0.691	0	0.003	−3.4
Genus	*Bifidobacterium*	0.002	0.019	0.527	0.003	0.004	−711
Species	*prausnitzii*	0	0.002	0.868	0	0.001	4.5
Species	*gnavus*	0	0.004	0.974	0	0.001	5
Species	*cylindroides*	0.001	0.011	0.892	0.002	0.003	na
Species	*dolichum*	0.003	0.022	0.091	0.043	0.002	na
Species	*ruminis*	0.006	0.031	0.374	0.004	0.068	na
Species	*plebeius*	0.01	0.042	0.596	0.008	0.048	−2.6
Species	*hiranonis*	0.012	0.043	0.487	0.009	0.073	2.1

CON, control diet; HPLC, high-protein low-carbohydrate diet; T1, at the end of baseline feeding; T2, at the end of intervention; FDR, false discovery rate; FC, fold change; na, not applicable. Non-parametric Kruskall–Wallis (KW) test was performed among three groups of cats: T1, T2-HPLC, and T2-CON, followed by Dunn's multiple comparison with Benjamini–Hochberg adjustment. P-values were adjusted to control for false discovery rate (FDR). Only significant taxa (FDR < 0.05) were shown.

cases, **Figure 1D** and **Supplementary Figure 2**). In addition, the abundances of five genera shifted in OW cats: increases in *Faecalibacterium* and *Fusobacterium* but decreases in *Megasphaera*, *Veillonella*, and *Bifidobacerium* were found in HPLC-fed cats when compared to CON-fed cats (FDR < 0.05 in all cases, **Figure 4** and **Table 3**). *Clostridium* showed an increase in CON-fed vs. HPLC-fed cats. But the change did not reach statistical significance after adjusting for multiple testing ($P = 0.007$, $FDR = 0.057$).

Four species, *Faecalibacterium prausnitzii*, *Ruminococcus gnavus*, Clostridium *hiranonis*, and *E*ubacterium *dolichum*, had increased abundances while three others, *Eubacterium cylindroides*, *Lactobacillus ruminis*, and *Bacteroides plebeius*, decreased (FDR < 0.05 in all cases, **Table 3**) in HPLC cats vs. CON cats.

No change in any taxonomic rank was found between diets in LN cats (FDR > 0.05, **Supplementary Table 4**).

Biomarkers and Machine Learning

LEfSe analysis identified four genera using the selection criteria of FDR < 0.05 and $\log_{10}(LDA) > 3.0$ (**Supplementary Table 5**). *Fusobacterium* and *Faecalibacterium* were more abundant in OW-HPLC cats while abundances of *Megasphaera* and *Bifidobacterium* were decreased (**Figure 5A**). No genus had a significant change between diets in LN cats using the same selection criteria.

Random Forest machine learning selected top 10 genera including *Fusobacterium, Faecalibacterium, Megasphaera, Bifidobacterium*, *Roseburia*, *Sutterella*, *Clostridium*, *Catenibacterium*, *Blautia,* and *Parabacteroides* (**Figure 5B**). The four genera with the greatest predictive power belonged to three phyla: *Megasphaera* and *Faecalibacterium* (*Firmicutes*), *Fusobacterium* (*Fusobacteria*), and *Bifidobacterium* (*Actinobacteria*). The resulting random forest classifier achieved an out-of-bag (OOB) error rate of 5% (**Supplementary Figure 3**).

Predicted Metagenomic Functions

LEfSe analysis identified nine KEGG pathways in OW cats using the selection criteria of $P < 0.01$ and $\log_{10}(LDA) > 2.5$ (**Supplementary Table 6**). No pathway was identified in LN cats. These pathways, all of which were enriched in CON-fed OW cats, included pathways involved in energy metabolism (glycolysis and gluconeogenesis, pyruvate metabolism, propianoate metabolism, fatty acid metabolism, and TCA cycle), and folate biosynthesis and one-carbon metabolic (one-carbon pool by folate) pathways. In addition, peptidase, tryptophan metabolism, and lysine degradation pathways were also identified as different between diets in OW cats.

DISCUSSION

High-protein low-carbohydrate diets have been suggested as a tool for body weight management for decades with potential benefits including increased satiety, reduced hunger, and preservation of lean body mass during weight reduction in

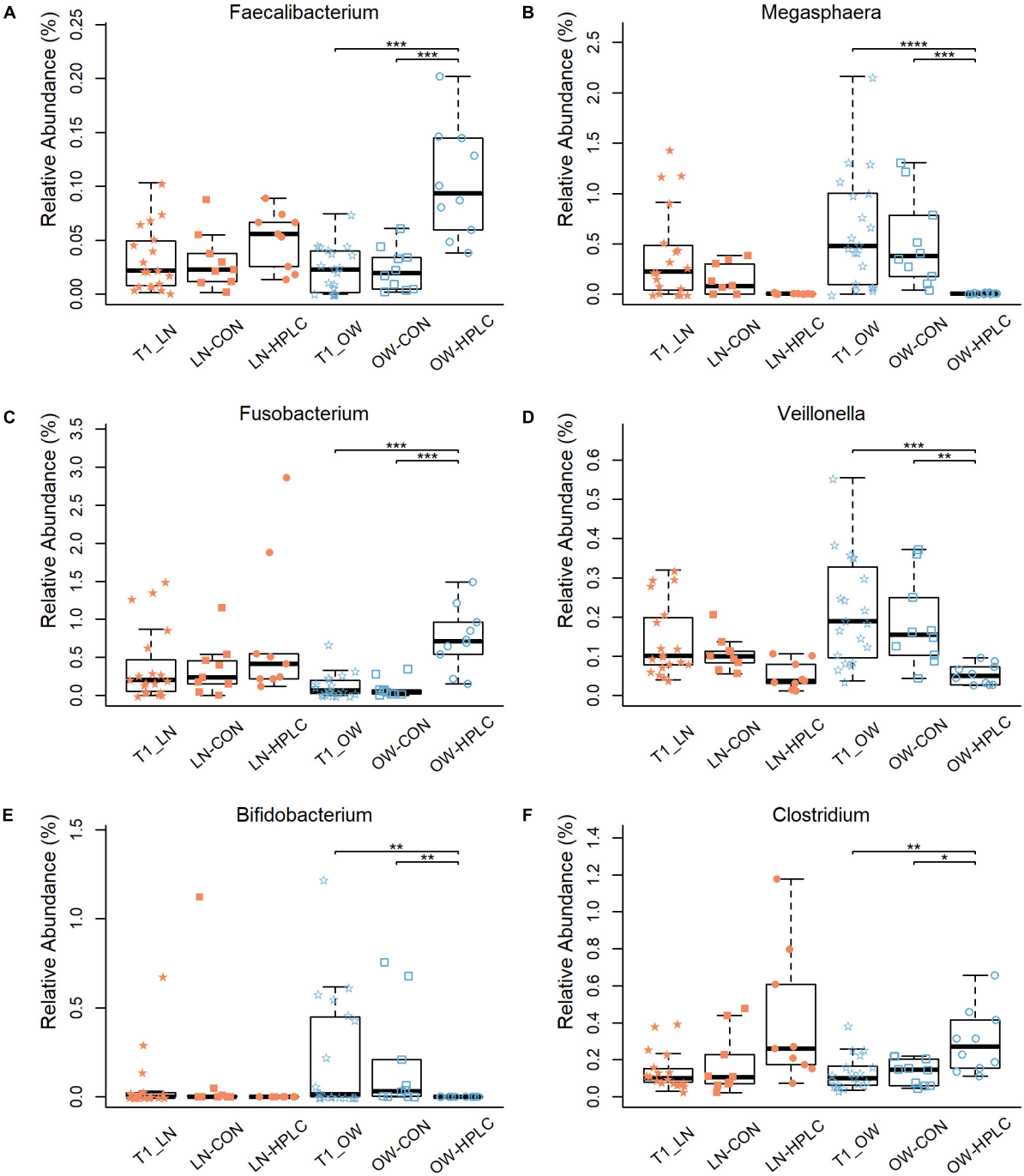

FIGURE 4 | Differences in relative abundance of six bacterial genera: **(A–F)** *Faecalibacterium, Megasphaera, Fusobacterium, Veillonella, Bifidobacterium,* and *Clostridium*. Samples are from the T2 time point unless indicated otherwise. LN, lean cats; OW, overweight or obese cats; HPLC, high-protein, low-carbohydrate diet; CON, control diet. *P*-values were corrected for multiple testing (FDR): *FDR < 0.05, **FDR < 0.01, ***FDR < 0.001, ****FDR < 0.0001.

humans and animals (Riegler, 1976; Nobels et al., 1989; Diez et al., 2002; Bierer and Bui, 2004; Laflamme and Hannah, 2005; Kushner and Doerfler, 2008). The GI microbiota plays an important role in utilizing unabsorbed food components and extracting energy from food. In this study, we examined differential responses to the HPLC diet in gut microbiomes in obese vs. lean cats. To minimize the confounding effect of body weight changes on gut microbiota, cats were fed to maintain body weight throughout the entire study.

No difference in alpha diversity was observed between LN and OW cats fed the same CON for an 8 weeks period at T1. Similar observations were reported in obese vs. lean dogs

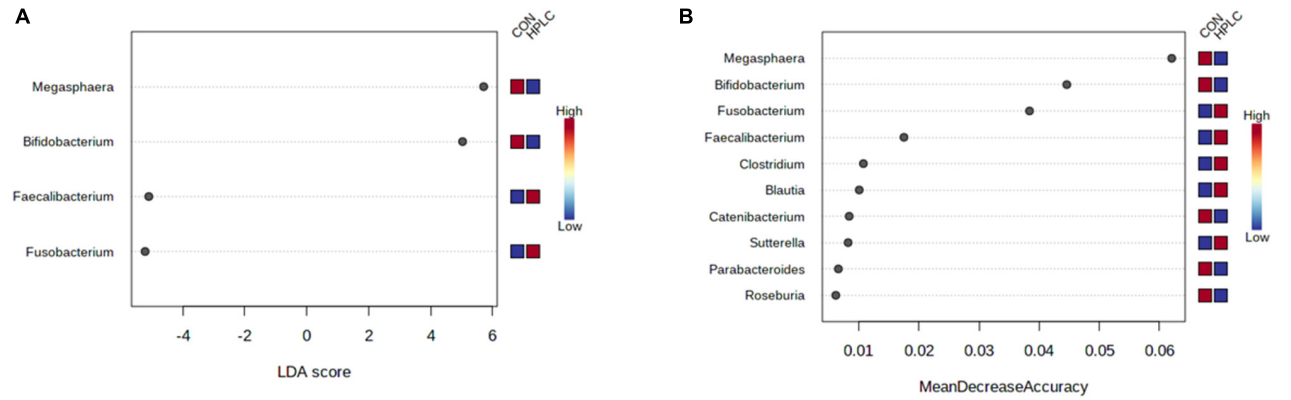

FIGURE 5 | (A) LEfSe analysis identifies four genera significantly different between OW-HPLC vs. OW-CON cats. Selection criteria: $\log_{10}(LDA) > 3.0$ and FDR < 0.05. **(B)** Top 10 genera with the most discriminant powers by Random Forest machine learning with 500 trees. LN, lean cats; OW, overweight or obese cats; HPLC, high-protein, low-carbohydrate diet; CON, control diet.

(Handl et al., 2013; Li et al., 2017). Shannon diversity showed differences between LN and OW cats fed on the CON diet for additional 8 weeks at T2. It is thus possible that the difference between body conditions was initially masked by a confounding dietary effect which diminished at T2. Fischer et al. (2017) reported differences in Faith's PD but not Shannon diversity between lean vs. obese cats. But no change was found before and after weight loss in obese cats. It is difficult to fully assess these results with the relatively small number of microbiome studies available in cats compared to those in humans and other mammals.

Consistent with other microbiome studies on feline feces, *Firmicutes, Bacteroidetes, Proteobacteria, Actinobacteria,* and *Fusobacteria* are the five most predominant phyla. Interestingly, *Bacteroidetes* represented less than 1% of the phyla in kitten feces but its abundance increased significantly in adult cats, presumably at the expense of *Firmicutes* and *Actinobacteria* (Hooda et al., 2013; Fischer et al., 2017). Gut microbiomes shift in response to dietary changes in humans and animals (Wu et al., 2011; David et al., 2014; Li et al., 2017; Coelho et al., 2018). While no clustering was found in the PCoA plot between the two prospectively assigned diet groups at T1, a diet effect on GI microbial compositions became apparent at T2, with greater effects in OW cats than LN cats. Our results appear to be in agreement with the kitten study where distinct clusters were formed due to changes in dietary protein and carbohydrate ratio (Hooda et al., 2013). Body condition had a significant effect based on unweighted UniFrac and Bray–Curtis distance (both $P < 0.05$) at T1, but this effect diminished at T2 ($P > 0.05$), possibly masked by diet effect. Many bacterial taxonomic changes were found in the genus level in OW cats compared with little change in LN cats. Similar findings were reported in a dog study (Li et al., 2017). More research is needed to understand the mechanism underlying the differential responses to protein/carbohydrate change between obese vs. lean pets.

In contrast to findings in humans and rodents (Ley et al., 2006; Turnbaugh et al., 2009; Ley, 2010), Fischer et al. (2017) reported significantly more *Firmicutes* but less *Bacteroidetes* in neutered lean cats vs. obese cats. However, no change in either phylum was observed between OW vs. LN cats in the current study. An increase in *Fusobacteria* abundance was found in LN cats when compared to OW cats (2.38 vs. 0.67%, respectively, $P = 0.057$) at T1, although the difference did not reach statistical significance. The abundance of *Fusobacteria* in OW cats was increased in response to HPLC diet (HPLC 3.89% vs. CON 0.48%, respectively, FDR = 0.01) at T2. Interestingly, the findings reported in the kitten study were more drastic, where *Fusobacteria* comprised more than 12% of the microbiome in kittens fed a HPLC diet compared to merely 0.1% in those fed a moderate-protein moderate-carbohydrate diet (Hooda et al., 2013).

Five SCFA-producing genera had altered abundances in OW cats after the dietary intervention: the abundances of *Megasphaera*, *Veillonella*, and *Bifidobacterium* were decreased while those of *Faecalibacterium* and *Fusobacterium* were increased in HPLC-fed vs. CON-fed OW cats. In humans, a large increase in *Megasphaera* abundance with decreases in *Bifidobacterium* and *Faecalibacterium* were reported in obese individuals vs. normal ones (Turnbaugh et al., 2006; Furet et al., 2010; Schwiertz et al., 2010; Brandt and Aroniadis, 2013; Verdam et al., 2013). The exact species of *Megasphaera* that were increased in obese people was undetermined, but was thought to be one of the SCFA producers that can ferment excess carbohydrates into SCFAs and improve energy absorption (Holt, 1994; Turnbaugh et al., 2006). Thus, a decrease in *Megasphaera* may suggest a beneficial effect of the HPLC diet for weight loss in OW cats. The *Bifidobacterium* spp. possess a large number of genes involved in carbohydrate metabolism in their genomes (Lee and O'Sullivan, 2010), thus it is not surprising that this genus became more abundant in CON group vs. HPLC group. *Faecalibacterium* with a sole known species *F. prausnitzii*, is one of the most abundant and important commensal bacteria in humans, accounting for more than 5% of total bacteria in human feces (Louis et al., 2010; Arumugam et al., 2011). It is a butyrate-producing bacterium in the phylum of *Firmicutes* with anti-inflammatory effects *in vivo* and *in vitro* (Sokol et al., 2008). It has been documented that the

abundance of *F. prausnitzii* was decreased in rats (Liu et al., 2014; Mu et al., 2016), pigs (Boudry et al., 2013), and dogs (Schmidt et al., 2018) fed high protein diets. To the contrary, the HPLC diet increased *F. prausnitzii* abundances in the feces of kittens (Hooda et al., 2013) and in this study, adult cats. The cat is considered an obligate carnivore that has evolved on diets rich in protein. Thus, it is conceivable that cats, which have a higher protein requirement than humans and many other mammals, may have a different response in their gut microbiota to high protein diets. Both *Veillonella* and *Fusobacterium* are SCFA producers albeit they responded differently to dietary protein and carbohydrate change in cats. The *Veillonella* spp. cannot utilize carbohydrates, but its genome encompasses genes for a major metabolic pathway which converts lactate into acetate and propionate, a SCFA with benefits in exercise endurance and athletic performance in humans and rodents (van den Bogert et al., 2013; Scheiman et al., 2019). *Fusobacterium* spp. genomes encode enzymes in the butyrate biosynthesis pathway and produce acetate and butyrate primarily through amino acid fermentation (Vital et al., 2014). Synthesis of SCFAs can activate molecular pathways that lead to lipogenesis and triglyceride accumulation in adipocytes (Benahmed et al., 2020). Thus, it is possible that decreases in *Megasphaera*, *Veillonella*, and *Bifidobacterium* may lead to reduced lipogenesis, triglyceride accumulation, and energy absorption, while increases in *Faecalibacterium* confer anti-inflammatory and immunomodulatory benefits in HPLC-fed cats compared to CON-fed OW cats.

Phylogenetic investigation of communities by reconstruction of unobserved states analysis provides an overview of microbial gene networks in the system's level. Nine pathways were enriched in OW-CON cats compared to OW-HPLC cats. Due to the high carbohydrate content in the CON, it is not surprising to see changes in pathways involved in energy metabolism. Gut bacteria use a specific group of enzymes called CAZymes (carbohydrate-active enzymes) to break down complex carbohydrates into simple sugars (Cantarel et al., 2012), which can be further metabolized for energy through glycolysis. Glycolysis produces pyruvate, which can be converted into carbohydrates via gluconeogenesis or fatty acids through a reaction with acetyl-CoA. In addition, pyruvate can produce energy via TCA cycle if oxygen is present or via fermentation without oxygen. Gut bacteria synthesize folic acid *de novo* providing important dietary source of folates for animals. Besides being important one-carbon donors or acceptors, folic acid mediate the important one-carbon metabolism which supports multiple physiological processes including biosynthesis, amino acid homeostasis, epigenetic regulation, and redox defense (Ducker and Rabinowitz, 2017). The significance of these pathways which are based on imputed metagenomes from 16S rRNA gene composition data in CON-fed OW cats should be validated by whole metagenome sequencing.

CONCLUSION

In summary, our study demonstrated a strong influence of dietary protein carbohydrate ratio on gut microbiota in adult cats. There was a significant difference in alpha diversity between OW and LN cats after 16 weeks on the CON diet. The dietary effect was evidenced in the PCoA analysis. Importantly, the effect was more prominent in OW cats than LN cats. The five predominant phyla in the feces of adult cats were *Firmicutes*, *Bacteroidetes*, *Fusobacteria*, *Actinobacteria*, and *Proteobacteria*. The OW cats had a higher *Firmicutes*/*Bacteroidetes* ratio than LN cats, although the difference did not reach statistical significance. In a metagenomic analysis between obese vs. lean twins, 75% obesity-enriched genes belonged *Actinobacteria* while the other 25% came from *Firmicutes* (Turnbaugh et al., 2009). Remarkably, the OW cats had three times as many *Actinobacteria* as their LN counterparts (P = 0.054). In humans, *Fusobacteria* was positively associated with obesity (Andoh et al., 2016; Gao et al., 2018; Crovesy et al., 2020). To the contrary, a decrease in *Fusobacteria* was observed in OW cats vs. LN cats (P = 0.057). More studies are needed to confirmed the findings. However, the HPLC diet increased *Fusobacteria* abundance in OW cats to a level comparable to that in LN cats. Changes in numerous SCFA-producers and carbohydrate-fermenters were observed. While no significant taxa change was found in LN cats, five genera were changed in OW cats: *Faecalibacterium* and *Fusobacterium* were more abundant while *Megasphaera*, *Veillonella*, and *Bifidobacerium* became less abundant in HPLC-fed cats compared to CON-fed cats. On the pathway level, changes in energy and one-carbon metabolisms were noticed. Future metagenomics sequencing and analysis may provide additional resolutions in the species or even strain levels and opportunity to better understand metagenomic changes in the systems level.

DATA AVAILABILITY STATEMENT

The sequence and meta data in the study can be obtained through the accession number PRJNA661962 from the Sequence Read Archive database.

ETHICS STATEMENT

The animal study was reviewed and approved by the Institutional Animal Care and Use Committee of the Nestlé Purina PetCare Company.

AUTHOR CONTRIBUTIONS

QL conceived the study, participated in the feeding study, performed data analysis and interpretation, and wrote the manuscript. YP designed the diets, performed diet analysis, participated in the feeding study, and reviewed the manuscript. Both authors contributed to the article and approved the submitted version.

FUNDING

The study was funded by the Nestlé Purina PetCare Company. The funder was not involved in the study design, collection, analysis, interpretation of data, the writing of this article or the decision to submit it for publication.

ACKNOWLEDGMENTS

We would like to thank Mark Miller, Brandon Singer, and Dr. Tammy Platt for organizing and running the animal study and for sample collections, Hallie Barnett for QMR measurements, Dr. Heidi Gordon for veterinary care and services, Patricia Turpin and Cindy Steeby for laboratory assistance, Barb Peters for technical assistance, Dr. Sandeep Bhatnagar for making the diets, Jeffrey Labuda for fecal DNA extraction and 16S rRNA gene sequencing, and Dr. Dorothy Laflamme for critical review of the manuscript.

SUPPLEMENTARY MATERIAL

The Supplementary Material for this article can be found online at: https://www.frontiersin.org/articles/10.3389/fmicb.2020.591462/full#supplementary-material

Supplementary Figure 1 | Principal coordinates analysis (PCoA) based on unweighted UniFrac distance metric on **(A)** sex, **(B)** body condition, and diet in **(C)** LN cats and **(D)** OW cats at T1. The percentages of data variation explained by the first two principal coordinates are indicated on the *x* and *y* axes.

Supplementary Figure 2 | Differences in relative abundances of ten bacterial families. T1 samples are denoted. *P* values were corrected for multiple testing (FDR). *FDR < 0.05, **FDR < 0.01, ***FDR < 0.001.

Supplementary Figure 3 | Performance of Random Forest machine learning classifier over number of trees.

Supplementary Table 1 | Sequence distribution by sample, assembly, and passage rates.

Supplementary Table 2 | Alpha- and beta-diversities between groups at T1 and T2. ANOVA and Tukey's *post hoc* test were applied to compare alpha diversities while PERMANNOVA is used to compare beta diversities.

Supplementary Table 3 | Changes in taxonomical abundances between OW and LN cats at T1. *P*-values from Mann–Whitney U test are obtained and adjusted for multiple testing error.

Supplementary Table 4 | Comparison of the diet groups at the phylum, family, genus, and species levels in OW and LN cats using Kruskal–Wallis test followed by Dunn's multiple comparison with Benjamini–Hochberg adjustment. *P*-values are adjusted for multiple testing error using false discovery rate (FDR).

Supplementary Table 5 | LEfSe analysis on bacterial genus between OW-HPLC vs. OW-CON cats. LEfSe selection criteria: FDR < 0.05 and $\log_{10}$ (*LDA*) > 3.0.

Supplementary Table 6 | PICRUSt-predicted KEGG metagenomic orthologous functions between OW-HPLC and OW-CON cats. KO pathways were selected using $P < 0.05$ and $\log_{10}$ (*LDA*) > 2.5.

REFERENCES

Andoh, A., Nishida, A., Takahashi, K., Inatomi, O., Imaeda, H., Bamba, S., et al. (2016). Comparison of the gut microbial community between obese and lean peoples using 16S gene sequencing in a Japanese population. *J. Clin. Biochem. Nutr.* 59, 65–70. doi: 10.3164/jcbn.15-152

Arumugam, M., Raes, J., Pelletier, E., Le Paslier, D., Yamada, T., Mende, D. R., et al. (2011). Enterotypes of the human gut microbiome. *Nature* 473, 174–180. doi: 10.1038/nature09944

Backhed, F., Ding, H., Wang, T., Hooper, L. V., Koh, G. Y., Nagy, A., et al. (2004). The gut microbiota as an environmental factor that regulates fat storage. *Proc. Natl. Acad. Sci. U.S.A.* 101, 15718–15723. doi: 10.1073/pnas.0407076101

Benahmed, A. G., Gasmi, A., Dosa, A., Chirumbolo, S., Mujawdiya, P. K., Aaseth, J., et al. (2020). Association between the gut and oral microbiome with obesity. *Anaerobe* 14:102248. doi: 10.1016/j.anaerobe.2020.102248

Benjamini, Y., and Hochberg, Y. (1995). Controlling the false discovery rate: a practical and powerful approach to multiple testing. *J. R. Stat. Soc. Ser. B* 57, 289–300. doi: 10.1111/j.2517-6161.1995.tb02031.x

Bierer, T. L., and Bui, L. M. (2004). High-protein low-carbohydrate diets enhance weight loss in dogs. *J. Nutr.* 134, 2087S–2089S. doi: 10.1093/jn/134.8.2087S

Bingham, S., Cummings, J. H., and Mcneil, N. I. (1982). Diet and health of people with an ileostomy. 1. Dietary assessment. *Br. J. Nutr.* 47, 399–406. doi: 10.1079/bjn19820051

Boudry, G., Jamin, A., Chatelais, L., Gras-Le Guen, C., Michel, C., and Le Huerou-Luron, I. (2013). Dietary protein excess during neonatal life alters colonic microbiota and mucosal response to inflammatory mediators later in life in female pigs. *J. Nutr.* 143, 1225–1232. doi: 10.3945/jn.113.175828

Brandt, L. J., and Aroniadis, O. C. (2013). An overview of fecal microbiota transplantation: techniques, indications, and outcomes. *Gastrointest. Endosc.* 78, 240–249. doi: 10.1016/j.gie.2013.03.1329

Cantarel, B. L., Lombard, V., and Henrissat, B. (2012). Complex carbohydrate utilization by the healthy human microbiome. *PLoS One* 7:e28742. doi: 10.1371/journal.pone.0028742

Caporaso, J. G., Bittinger, K., Bushman, F. D., Desantis, T. Z., Andersen, G. L., and Knight, R. (2010a). PyNAST: a flexible tool for aligning sequences to a template alignment. *Bioinformatics* 26, 266–267. doi: 10.1093/bioinformatics/btp636

Caporaso, J. G., Kuczynski, J., Stombaugh, J., Bittinger, K., Bushman, F. D., Costello, E. K., et al. (2010b). QIIME allows analysis of high-throughput community sequencing data. *Nat. Methods* 7, 335–336. doi: 10.1038/nmeth.f.303

Coelho, L. P., Kultima, J. R., Costea, P. I., Fournier, C., Pan, Y., Czarnecki-Maulden, G., et al. (2018). Similarity of the dog and human gut microbiomes in gene content and response to diet. *Microbiome* 6:72. doi: 10.1186/s40168-018-0450-3

Crovesy, L., Masterson, D., and Rosado, E. L. (2020). Profile of the gut microbiota of adults with obesity: a systematic review. *Eur. J. Clin. Nutr.* 74, 1251–1262. doi: 10.1038/s41430-020-0607-6

David, L. A., Maurice, C. F., Carmody, R. N., Gootenberg, D. B., Button, J. E., Wolfe, B. E., et al. (2014). Diet rapidly and reproducibly alters the human gut microbiome. *Nature* 505, 559–563. doi: 10.1038/nature12820

Dhariwal, A., Chong, J., Habib, S., King, I. L., Agellon, L. B., and Xia, J. (2017). MicrobiomeAnalyst: a web-based tool for comprehensive statistical, visual and meta-analysis of microbiome data. *Nucleic Acids Res.* 45, W180–W188. doi: 10.1093/nar/gkx295

Diez, M., Nguyen, P., Jeusette, I., Devois, C., Istasse, L., and Biourge, V. (2002). Weight loss in obese dogs: evaluation of a high-protein, low-carbohydrate diet. *J. Nutr.* 132, 1685S–1687S. doi: 10.1093/jn/132.6.1685S

Ducker, G. S., and Rabinowitz, J. D. (2017). One-carbon metabolism in health and disease. *Cell Metab.* 25, 27–42. doi: 10.1016/j.cmet.2016.08.009

Edgar, R. C. (2010). Search and clustering orders of magnitude faster than BLAST. *Bioinformatics* 26, 2460–2461. doi: 10.1093/bioinformatics/btq461

Edgar, R. C. (2013). UPARSE: highly accurate OTU sequences from microbial amplicon reads. *Nat. Methods* 10, 996–998. doi: 10.1038/nmeth.2604

Edgar, R. C., Haas, B. J., Clemente, J. C., Quince, C., and Knight, R. (2011). UCHIME improves sensitivity and speed of chimera detection. *Bioinformatics* 27, 2194–2200. doi: 10.1093/bioinformatics/btr381

Fischer, M. M., Kessler, A. M., Kieffer, D. A., Knotts, T. A., Kim, K., Wei, A., et al. (2017). Effects of obesity, energy restriction and neutering on the faecal microbiota of cats. *Br. J. Nutr.* 118, 513–524. doi: 10.1017/s0007114517002379

Furet, J. P., Kong, L. C., Tap, J., Poitou, C., Basdevant, A., Bouillot, J. L., et al. (2010). Differential adaptation of human gut microbiota to bariatric surgery-induced weight loss: links with metabolic and low-grade inflammation markers. *Diabetes* 59, 3049–3057. doi: 10.2337/db10-0253

Gao, X., Zhang, M., Xue, J., Huang, J., Zhuang, R., Zhou, X., et al. (2018). Body Mass Index Differences in the Gut Microbiota Are Gender Specific. *Front. Microbiol.* 9:1250. doi: 10.3389/fmicb.2018.01250

Handl, S., German, A. J., Holden, S. L., Dowd, S. E., Steiner, J. M., Heilmann, R. M., et al. (2013). Faecal microbiota in lean and obese dogs. *FEMS Microbiol. Ecol.* 84, 332–343. doi: 10.1111/1574-6941.12067

Holt, J. G. (1994). *Bergey's Manual of Determinative Bacteriology*. Baltimore: Lippincott Williams & Wilkins.

Hooda, S., Vester Boler, B. M., Kerr, K. R., Dowd, S. E., and Swanson, K. S. (2013). The gut microbiome of kittens is affected by dietary protein:carbohydrate ratio and associated with blood metabolite and hormone concentrations. *Br. J. Nutr.* 109, 1637–1646. doi: 10.1017/s0007114512003479

Kinzig, K. P., Hargrave, S. L., Hyun, J., and Moran, T. H. (2007). Energy balance and hypothalamic effects of a high-protein/low-carbohydrate diet. *Physiol. Behav.* 92, 454–460. doi: 10.1016/j.physbeh.2007.04.019

Kushner, R. F., and Doerfler, B. (2008). Low-carbohydrate, high-protein diets revisited. *Curr. Opin. Gastroenterol.* 24, 198–203. doi: 10.1097/mog.0b013e3282f43a87

Laflamme, D. P. (1997). Development and validation of a body condition score system for dogs: a clinical tool. *Canine Pract.* 22, 10–15.

Laflamme, D. P., and Hannah, S. S. (2005). Increased dietary protein promotes fat loss and reduces loss of lean body mass during weight loss in cats. *Int. J. Appl. Res. Vet. Med.* 3, 62–68.

Langille, M. G., Zaneveld, J., Caporaso, J. G., Mcdonald, D., Knights, D., Reyes, J. A., et al. (2013). Predictive functional profiling of microbial communities using 16S rRNA marker gene sequences. *Nat. Biotechnol.* 31, 814–821. doi: 10.1038/nbt.2676

Lee, J. H., and O'Sullivan, D. J. (2010). Genomic insights into bifidobacteria. *Microbiol. Mol. Biol. Rev.* 74, 378–416. doi: 10.1128/mmbr.00004-10

Ley, R. E. (2010). Obesity and the human microbiome. *Curr. Opin. Gastroenterol.* 26, 5–11. doi: 10.1097/mog.0b013e328333d751

Ley, R. E., Backhed, F., Turnbaugh, P., Lozupone, C. A., Knight, R. D., and Gordon, J. I. (2005). Obesity alters gut microbial ecology. *Proc. Natl. Acad. Sci. U.S.A.* 102, 11070–11075. doi: 10.1073/pnas.0504978102

Ley, R. E., Turnbaugh, P. J., Klein, S., and Gordon, J. I. (2006). Microbial ecology: human gut microbes associated with obesity. *Nature* 444, 1022–1023. doi: 10.1038/4441022a

Li, Q., Lauber, C. L., Czarnecki-Maulden, G., Pan, Y., and Hannah, S. S. (2017). Effects of the dietary protein and carbohydrate ratio on gut microbiomes in dogs of different body conditions. *MBio* 8, e1703–e1716. doi: 10.1128/mBio.01703-16

Liu, X., Blouin, J. M., Santacruz, A., Lan, A., Andriamihaja, M., Wilkanowicz, S., et al. (2014). High-protein diet modifies colonic microbiota and luminal environment but not colonocyte metabolism in the rat model: the increased luminal bulk connection. *Am. J. Physiol. Gastrointest. Liver Physiol.* 307, G459–G470. doi: 10.1152/ajpgi.00400.2013

Louis, P., Young, P., Holtrop, G., and Flint, H. J. (2010). Diversity of human colonic butyrate-producing bacteria revealed by analysis of the butyryl-CoA:acetate CoA-transferase gene. *Environ. Microbiol.* 12, 304–314. doi: 10.1111/j.1462-2920.2009.02066.x

Lozupone, C., Lladser, M. E., Knights, D., Stombaugh, J., and Knight, R. (2011). UniFrac: an effective distance metric for microbial community comparison. *ISME. J.* 5, 169–172. doi: 10.1038/ismej.2010.133

Lozupone, C. A., and Knight, R. (2015). The UniFrac significance test is sensitive to tree topology. *BMC. Bioinformatics* 16:211. doi: 10.1186/s12859-015-0640-y

McNeil, N. I. (1984). The contribution of the large intestine to energy supplies in man. *Am. J. Clin. Nutr.* 39, 338–342. doi: 10.1093/ajcn/39.2.338

McNeil, N. I., Bingham, S., Cole, T. J., Grant, A. M., and Cummings, J. H. (1982). Diet and health of people with an ileostomy. 2. Ileostomy function and nutritional state. *Br. J. Nutr.* 47, 407–415. doi: 10.1079/bjn19820052

Morgan, X. C., Tickle, T. L., Sokol, H., Gevers, D., Devaney, K. L., Ward, D. V., et al. (2012). Dysfunction of the intestinal microbiome in inflammatory bowel disease and treatment. *Genome Biol.* 13, R79.

Mu, C., Yang, Y., Luo, Z., Guan, L., and Zhu, W. (2016). The colonic microbiome and epithelial transcriptome are altered in rats fed a high-protein diet compared with a normal-protein diet. *J. Nutr.* 146, 474–483. doi: 10.3945/jn.115.223990

Nobels, F., Van Gaal, L., and De Leeuw, I. (1989). Weight reduction with a high protein, low carbohydrate, calorie-restricted diet: effects on blood pressure, glucose and insulin levels. *Neth. J. Med.* 35, 295–302.

Oksanen, J., Blanchet, F. G., Friendly, M., Kindt, R., Legendre, P., Mcglinn, D., et al. (2019). *vegan: Community Ecology Package. R Package Version 2.5-6*.

Price, M. N., Dehal, P. S., and Arkin, A. P. (2009). FastTree: computing large minimum evolution trees with profiles instead of a distance matrix. *Mol. Biol. Evol.* 26, 1641–1650. doi: 10.1093/molbev/msp077

Price, M. N., Dehal, P. S., and Arkin, A. P. (2010). FastTree 2–approximately maximum-likelihood trees for large alignments. *PLoS One* 5:e9490. doi: 10.1371/journal.pone.0009490

Quast, C., Pruesse, E., Yilmaz, P., Gerken, J., Schweer, T., Yarza, P., et al. (2013). The SILVA ribosomal RNA gene database project: improved data processing and web-based tools. *Nucleic Acids Res.* 41, D590–D596.

R Core Team (2015). *R: A Language and Environment for Statistical Computing*. Vienna: R Foundation for Statistical Computing.

Riegler, E. (1976). [Weight reduction by a high protein, low carbohydrate diet (author's transl)]. *Med. Klin.* 71, 1051–1056.

Scheiman, J., Luber, J. M., Chavkin, T. A., Macdonald, T., Tung, A., Pham, L. D., et al. (2019). Meta-omics analysis of elite athletes identifies a performance-enhancing microbe that functions via lactate metabolism. *Nat. Med.* 25, 1104–1109. doi: 10.1038/s41591-019-0485-4

Schloss, P. D., Westcott, S. L., Ryabin, T., Hall, J. R., Hartmann, M., Hollister, E. B., et al. (2009). Introducing mothur: open-source, platform-independent, community-supported software for describing and comparing microbial communities. *Appl. Environ. Microbiol.* 75, 7537–7541. doi: 10.1128/aem.01541-09

Schmidt, M., Unterer, S., Suchodolski, J. S., Honneffer, J. B., Guard, B. C., Lidbury, J. A., et al. (2018). The fecal microbiome and metabolome differs between dogs fed Bones and Raw Food (BARF) diets and dogs fed commercial diets. *PLoS One* 13:e0201279. doi: 10.1371/journal.pone.0201279

Schwiertz, A., Taras, D., Schafer, K., Beijer, S., Bos, N. A., Donus, C., et al. (2010). Microbiota and SCFA in lean and overweight healthy subjects. *Obesity* 18, 190–195. doi: 10.1038/oby.2009.167

Segata, N., Izard, J., Waldron, L., Gevers, D., Miropolsky, L., Garrett, W. S., et al. (2011). Metagenomic biomarker discovery and explanation. *Genome Biol.* 12, R60.

Sokol, H., Pigneur, B., Watterlot, L., Lakhdari, O., Bermudez-Humaran, L. G., Gratadoux, J. J., et al. (2008). Faecalibacterium prausnitzii is an anti-inflammatory commensal bacterium identified by gut microbiota analysis of Crohn disease patients. *Proc. Natl. Acad. Sci. U.S.A.* 105, 16731–16736. doi: 10.1073/pnas.0804812105

Sonnenburg, J. L., Xu, J., Leip, D. D., Chen, C. H., Westover, B. P., Weatherford, J., et al. (2005). Glycan foraging in vivo by an intestine-adapted bacterial symbiont. *Science* 307, 1955–1959. doi: 10.1126/science.1109051

Turnbaugh, P. J., Hamady, M., Yatsunenko, T., Cantarel, B. L., Duncan, A., Ley, R. E., et al. (2009). A core gut microbiome in obese and lean twins. *Nature* 457, 480–484. doi: 10.1038/nature07540

Turnbaugh, P. J., Ley, R. E., Mahowald, M. A., Magrini, V., Mardis, E. R., and Gordon, J. I. (2006). An obesity-associated gut microbiome with increased capacity for energy harvest. *Nature* 444, 1027–1031.

van den Bogert, B., Boekhorst, J., Smid, E. J., Zoetendal, E. G., and Kleerebezem, M. (2013). Draft Genome Sequence of Veillonella parvula HSIVP1, Isolated from the Human Small Intestine. *Genome Announc.* 1:e00977-13.

Verdam, F. J., Fuentes, S., De Jonge, C., Zoetendal, E. G., Erbil, R., Greve, J. W., et al. (2013). Human intestinal microbiota composition is associated with local and systemic inflammation in obesity. *Obesity* 21, E607–E615.

Vital, M., Howe, A. C., and Tiedje, J. M. (2014). Revealing the bacterial butyrate synthesis pathways by analyzing (meta)genomic data. *mBio* 5:e00889.

Wu, G. D., Chen, J., Hoffmann, C., Bittinger, K., Chen, Y. Y., Keilbaugh, S. A., et al. (2011). Linking long-term dietary patterns with gut microbial enterotypes. *Science* 334, 105–108. doi: 10.1126/science.1208344

Zhang, J., Kobert, K., Flouri, T., and Stamatakis, A. (2014). PEAR: a fast and accurate illumina paired-end reAd mergeR. *Bioinformatics* 30, 614–620. doi: 10.1093/bioinformatics/btt593

Conflict of Interest: QL and YP are current employees of the Nestlé Purina PetCare Company.

frontiers in Microbiology

ORIGINAL RESEARCH
published: 19 November 2020
doi: 10.3389/fmicb.2020.588264

Pretreatment of Rapeseed Meal Increases Its Recalcitrant Fiber Fermentation and Alters the Microbial Community in an *in vitro* Model of Swine Large Intestine

Cheng Long[1,2] *and Koen Venema*[1,2]*

[1] *Faculty of Science and Engineering, Centre for Healthy Eating and Food Innovation, Maastricht University Campus Venlo, Venlo, Netherlands,* [2] *School of Nutrition and Translational Research in Metabolism (NUTRIM), Maastricht University, Maastricht, Netherlands*

OPEN ACCESS

Edited by:
M Pilar Francino, Fundación para el Fomento de la Investigación Sanitaria y Biomédica de la Comunitat Valenciana (FISABIO), Spain

Reviewed by:
Sergio Perez-Burillo, University of Granada, Spain
Adamantini Kyriacou, Harokopio University, Greece

***Correspondence:**
Koen Venema
k.venema@maastrichtuniversity.nl

Specialty section:
This article was submitted to Microbial Symbioses, a section of the journal Frontiers in Microbiology

Received: *28 July 2020*
Accepted: *06 October 2020*
Published: *19 November 2020*

Citation:
Long C and Venema K (2020) Pretreatment of Rapeseed Meal Increases Its Recalcitrant Fiber Fermentation and Alters the Microbial Community in an in vitro Model of Swine Large Intestine. Front. Microbiol. 11:588264. doi: 10.3389/fmicb.2020.588264

The aim of current study was to investigate in an *in vitro* study how enzymatic and chemical pretreated rapeseed meal (RSM) influences the fiber fermentation and microbial community in the swine large intestine. RSM was processed enzymatically by a cellulase (CELL), two pectinases (PECT), or chemically by an alkaline (ALK) treatment. 16S rRNA gene sequencing data was performed to evaluate changes in the gut microbiota composition, whereas short-chain fatty acid (SCFA) production (ion-chromatography) and non-starch polysaccharides (NSP) composition (using monoclonal antibodies; mAbs) were used to assess fiber degradation. The results showed that ALK, CELL, PECT1, and PECT2 changed microbial community composition, increased the predicted abundance of microbial fiber-degrading enzymes and pathways, and increased acetic acid, propionic acid, butyric acid, and total SCFA production. The increased microbial genera positively correlated with SCFA production. Monoclonal antibody analyses showed that the cell wall polysaccharide structures of RSM shifted after ALK, CELL, PECT1, and PECT2 treatment. The degradation of NSP during the fermentation period was dynamic, and not continuous based on the epitope recognition by mAbs. This study provides the first detailed analysis of changes in the swine intestinal microbiota due to RSM modified by ALK, CELL, PECT1, and PECT2, which altered the microbial community structure, shifted the predicted functional metagenomic profile and subsequently increased total SCFA production. Our findings that ALK, CELL, PECT1, and PECT2 increased fiber degradability in RSM could help guide feed additive strategies to improve efficiency and productivity in swine industry. The current study gave insight into how enzymatic treatment of feed can alter microbial communities, which provides good opportunity to develop novel carbohydrase treatments, particularly in swine feed.

Keywords: cell wall polysaccharides, rapeseed meal, pig gut microbiota, pectinase, cellulase

INTRODUCTION

Rapeseed meal (RSM), a by-product of rapeseed oil production, is not only a suitable protein source for swine feed but also a potentially energy source. RSM contains 20 to 40% non-starch polysaccharides (NSP) (Slominski and Campbell, 1990; Simbaya et al., 1995). The primary cell walls of RSM consist of pectin and xyloglucan and its cellulose microfibrils are interlinked with xyloglucan via hydrogen bonds forming a stiff network (Carpita and Gibeaut, 1993). Pectins are linked to each other and cross-linked between pectin and hemicellulose, and between pectin and cellulose (Broxterman and Schols, 2018). Pectins, consisting of homogalacturonan, rhamnogalacturonan, xylogalacturonan, arabinogalactan and arabinan, are the major polysaccharides present in the dehulled rapeseed meal (Eriksson et al., 1997). In the secondary cell wall of RSM, the main carbohydrates are 4-O-methyglucuronoxylan, xyloglucan, and cellulose. A drawback of using RSM in animal feed is that the complex cell wall polysaccharides cannot be utilized by endogenous enzymes from monogastric animals (e.g., pigs), and also can only partly be fermented by the microbial community in the gastrointestinal tract (GIT) of the pig.

Therefore, the animal feed sector seeks opportunities to enhance degradability of NSP of feedstuffs, in order to improve its potential as a nutrient source for domestic animals. Previous research showed that physical processing technologies, such as hammer milling, pelleting, wet-milling, extrusion, and mild hydrothermal acid treatment, had limited effect on recalcitrant NSP structures (de Vries et al., 2012, 2013). As a result, more efficient solutions are needed to modify the cell wall architecture and allow the gut microbiota to utilize the complex carbohydrates. Former research has shown that NSP-degrading enzymes, such as cellulase and pectinases, could open the cell wall structure and improve NSP degradability (Giraldo et al., 2007, 2008). Previous studies showed that addition of pectolytic enzymes improved degradability of NSP of RSM *in vitro* (Pustjens et al., 2012) and in broilers (de Vries et al., 2014; Pustjens et al., 2014). However, none of the above studies investigated how the gut microbiota was affected by the modified RSM or by the feed enzymes. It is important to know this, as NSP can only be fermented by microbes. Bindelle et al. (2011) demonstrated that NSP-degrading enzymes increased abundances of cellulolytic *Ruminococcus*- and xylanolytic *Clostridium*-like bacteria and altered fermentation patterns of barley cultivars and wheat products. Torok and colleagues (Torok et al., 2008) investigated changes in gut microbial population in response to the supplementation of an NSP-degrading enzyme (containing β-glucanase, xylanase, and protease activities) in a barley-based diet in chickens, and the results showed that microbial composition revealed distinct clusters correlating with un-supplemented and enzyme supplemented birds. Previous research reported that the pre-treatment of feed stuffs with carbohydrases can cause the release of reducing sugars and other hydrolysis materials, promoting chemotactic response in specific bacteria, and stimulating their attachment to feed particles, and thereby growth of these microbes (Beauchemin et al., 2003; Giraldo et al., 2007; Ribeiro et al., 2015, 2018).

In the present study, RSM (predigested with digestive enzymes) was treated independently with two kinds of pectinases (PECT1 and PECT2), one cellulase (CELL), or alkaline (ALK), and afterwards the untreated and treated RSM preparations were fermented in the Swine Large Intestine *in vitro* Model (SLIM) (Long et al., 2020a). The aim of the current study was to investigate whether fermentation by the swine gut microbiota of treated RSM was improved compared to untreated RSM, and whether the microbiota composition and activity were changed.

MATERIALS AND METHODS

Substrate Preparation

Rapeseed meal (Brassica napus, Cargill N.V., Antwerp, Belgium; 2011) was obtained from a commercial feed mill (Agrifirm B.V., Utrecht, Netherlands). Preparation method I (predigestion of RSM after carbohydrase or alkaline treatment) (**Figure 1**): to 200 g of RSM 40 mL 10*gastric electrolyte concentrate solution (GES, 310 g sodium chloride, 110 g potassium chloride, 15 g calcium chloride di-hydrate, and 4840 g ultrapure water) and 360 mL ultrapure water were added. The pH was adjusted to 5.5 and then nothing (CON), 10 mL of alkaline (ALK, 6 M NaOH), or the following carbohydrases were added CELL (Accellerase 1000, Sigma-Aldrich, Missouri, United States), PECT1 (Pectinex Ultra SP, Novozymes A/S, Bagsvaerd, Denmark), or PECT2 (Multifect Pectinase, DuPont Industrial Biosciences, Genencor division, Rochester, NY). CELL has cellobiohydrolases, endoglucanases, beta-glucosidases, and hemi-cellulases activities. PECT1 has pectin esterase and polygalacturonase activities. PECT2 mainly has pectinase and some hemicellulase activities. Enzyme preparations were added to the RSM (25 mL/kg DM) and incubated at 37°C for 2 h, with occasional shaking (every 30 min), while ALK was incubated overnight at 4°C. Enzyme preparations were then heated at 100°C for 5 min to inactive enzymes. Afterwards, for all five samples, 120 mL GES was added and pH adjusted to 3 to continue with the gastric incubation according to the predigestion protocol as described elsewhere (Sáyago-Ayerdi et al., 2017). After predigestion, the slurry was centrifuged (8.000 *g*, at 4°C, for 20 min) and dialysis was performed for the supernatants. For dialysis, a dialyzer (Sureflux, Nipro Europe Group Companies, Mechelen, Belgium) was used with a peristaltic pump to remove small digestion products and water. After reduction of the total volume to ∼450–500 mL, supernatant was mixed with pellet, and freeze-dried. Method II

Abbreviations: RSM, rapeseed meal; CON, control, RSM without treatment; CELL, cellulase, Accellerase 1000, RSM treated with CELL; PECT, pectinase; PECT1, Pectinex Ultra SP, RSM treated with PECT1; PECT2, Multifect Pectinase, RSM treated with PECT2; ALK, alkaline, 6 M NaOH, RSM treated with ALK; _B, for carbohydrase- or ALK-treatment prior to digestion; _A, for carbohydrase- or ALK-treatment after digestion; SCFA, short chain fatty acids; NSP, non-starch polysaccharides; GIT, gastrointestinal tract; SLIM, Large Intestine in intro Model; GES, gastric electrolyte concentrate solution; TIM-2, TNO (gastro-) Intestinal Model of colon; SIEMP, standard ileal efflux medium of pigs; mAbs, Monoclonal antibodies; BSA, bovine serum albumin; TMB, tetramethylbenzidine; ASV, amplicon sequence variant; XG; xyloglucan; RG-I, Rhamnogalacturonan I; AG, arabinogalactan; RG-I/AG, arabinogalactan side chains of RG-I.

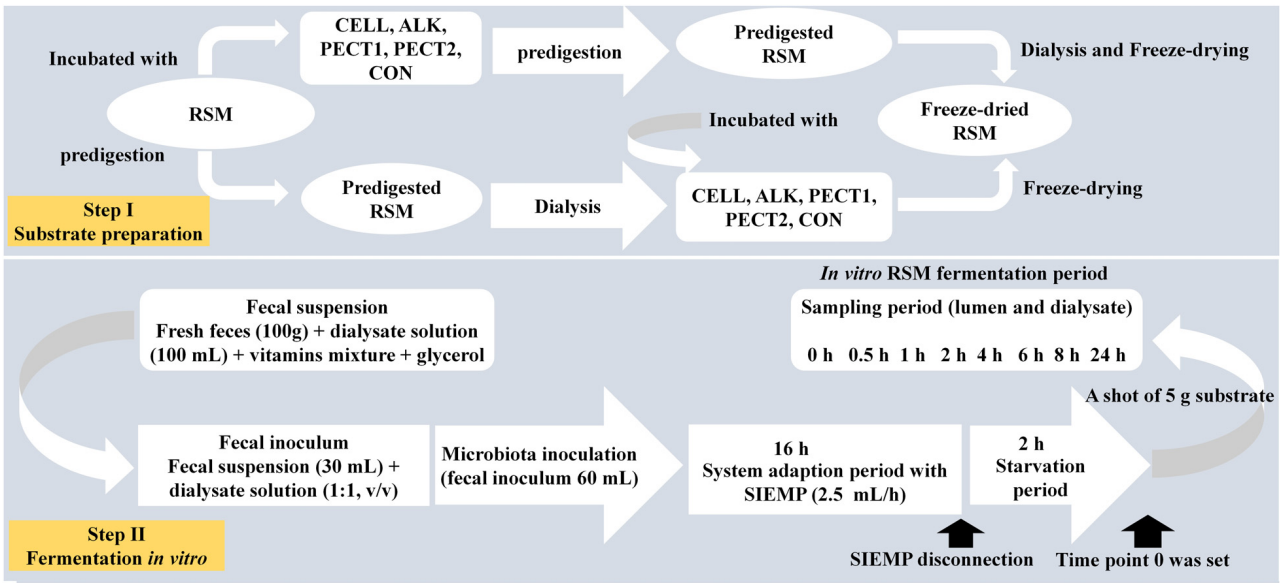

FIGURE 1 | Schematic experimental setup for fiber fermentation in the Swine Large Intestine *in vitro* model (SLIM).

(predigestion of RSM before carbohydrase or alkaline treatment) (**Figure 1**): four batches of 200 g RSM were predigested as described before (Sáyago-Ayerdi et al., 2017) and then dialyzed. Afterwards, 55 mL 10*GES was added, and pH adjusted to 5.5, after which 10 mL of ALK, or 10 mL of CELL, PECT1, or PECT2 treatment (25 mL/ kg DM) commenced, respectively. Enzyme preparations were incubated at 37°C for 2 h with occasional shaking (every 30 min), and ALK was incubated overnight at 4°C. Afterwards, enzyme preparations were heated at 100°C for 5 min to inactive enzymes, and pH was neutralized to 6.5–7 with HCl or NaOH, and the samples were freeze-dried. Samples are differentiated by the suffix _B (for before) or _A (for after) (e.g., PECT1_A) for carbohydrase- or ALK-treatment prior to and after digestion, respectively.

Fermentation in the Swine *in vitro* Large Intestinal Model (SLIM)

The setup of SLIM was as follows: a fully computer-controlled *in vitro* model based on TIM-2 (Minekus et al., 1999) was used to mimic the swine large intestine (Long et al., 2020a). The pH (5.9) was controlled by continuous addition of 2 M sodium hydroxide. Standard ileal efflux medium of pigs (SIEMP) was used to simulate the materials entering the colon. The SIEMP, adapted from Gibson et al. (1988) and described in Long et al. (2020a), contained the following components (g/L): 74.6 maize starch, 9.0 xylan, 19.0 pectin, 9.0 amylopectin, 9.0 arabinogalactan, 9.0 arabinoxylan, 9.0 xyloglucan, 31.5 Tween 80, 43.7 casein, 0.7 ox-bile, 43.7 bactopepton, 4.7 $K_2HPO_4.3H_2O$, 0.009 $FeSO_4.7H_2O$, 8.4 NaCl, 0.8 $CaCl_2.2H_2O$, 0.7 $MgSO_4.7H_2O$, 0.05 bile, 0.02 haemin and 0.3 cysteine∘HCl, plus 1.5 mL of a vitamin mixture containing (per liter): 1 mg menadione, 0.5 mg vitamin B12, 2 mg D-biotin, 10 mg pantothenate, 5 mg p-aminobenzoic, 4 mg thiamine and 5 mg nicotinamide acid. The pH was adjusted to 5.9. Dialysis liquid contained (per liter): 2.5 g $K_2HPO_4.3H_2O$, 0.005 g $FeSO_4.7H_2O$, 4.5 g NaCl, 0.45 g $CaCl_2.2H_2O$, 0.05 g bile, 0.5 g $MgSO_4.7H_2O$ and 0.4 g cysteine∘HCl, plus 1 mL of the vitamin mixture. All medium components were purchased at Tritium Microbiology (Eindhoven, Netherlands). The pig fecal inoculum was a standardized microbiota from growing pigs, freshly collected from the floor (48 pens with 6 pigs/pen, Hypor Libra x Hypor Maxter, Hendrix Genetics, Boxmeer, Netherlands), but only material from the top was selected (so not toughing the floor). Feces was pooled and mixed with dialysate as described before (Long et al., 2020a).

In order to create a complete anaerobic environment, SLIM with 90 mL dialysate in each of the 4 individual units was flushed with gaseous nitrogen for at least 3 h before incorporating the standardized microbiota. Thirty mL of the standardized microbiota was added to each SLIM-unit, making the total volume 120 mL. **Figure 1** shows the experimental set-up for fiber addition to SLIM. The microbiota was adapted to the model with SIEMP for 16 h. During the adaptation phase, SIEMP was added into each SLIM-unit at a rate of 2.5 mL/h through the feeding syringe. At the end of the adaptation period, a 2-h starvation period was performed, which was used to allow all the carbohydrates within SIEMP to be fermented. Afterwards, a shot of 5 grams of the different RSMs was given to the system at time point 0 h, and incubation was continued for 24 h after that (**Figure 1**).

Sample Collection

Samples from lumen (n = 2) and spent dialysate (n = 2) were collected at time point 0, 0.5, 1, 2, 4, 6, 8, and 24 h (t0, t0.5, t1, t2, t4, t6, t8, and t24). They were snap-frozen in liquid nitrogen and stored until analyses. Lumen samples were used to analyze

microbiota composition and polysaccharides structures, and both lumen and dialysis samples were analyzed for short chain fatty acid (SCFA) concentrations.

Sequencing of the V3-V4 Region of the 16S rRNA Gene

Microbial DNA extraction and sequencing of the V3-V4 region of the 16S rRNA gene were performed by BaseClear B.V. (Leiden, Netherlands). Briefly, genomic DNA extraction was performed using the Quick-DNA^{TM} Fecal/Soil Microbe Miniprep Kit (Zymo Research, California, United States) according to the manufacturer's instructions. Barcoded amplicons from the V3-V4 region of 16S rRNA genes were generated using a 2-step PCR. 10–25 ng genomic DNA was used as template for the first PCR with a total volume of 50 μL using the 341F (5′-CCTACGGGNGGCWGCAG-3′) and the 785R (5′-GACTACHVGGGTATCTAATCC-3′) primers (Klindworth et al., 2013) appended with Illumina adaptor sequences. PCR products were purified (QIAquick PCR Purification Kit, Venlo, Netherlands) and the size of the PCR products were checked on a Fragment analyzer (Advanced Analytical, Ankeny, United States) and quantified by fluorometric analysis. Purified PCR products were used for the 2nd PCR in combination with sample-specific barcoded primers (Nextera XT index kit, Illumina, CA, United States). Subsequently, PCR products were purified, checked on a Fragment analyzer and quantified, followed by multiplexing, clustering, and sequencing on an Illumina MiSeq with the paired-end (2×) 300 bp protocol and indexing. The sequencing run was analyzed with the Illumina CASAVA pipeline (v1.8.3) and demultiplexed based on sample-specific barcodes.

Bioinformatics Analysis

The demultiplexed raw sequences obtained from BaseClear were processed using the QIIME2 pipeline (Bolyen et al., 2019). In short, reads were imported and quality filtered and dereplicated with q2-dada2 (Callahan et al., 2016). Next, dada2 was performed with paired-end reads and truncations parameters were as follows:the first 17 and 14 base pairs were trimmed off in forward and reverse reads, respectively. And at position 280 base pairs the fragment was truncated in forward reads, and at position 230 base pairs for the reverse reads. The processed sequences were used for all the downstream analyses. Alpha-diversity (Shannon index) and β-diversity (weighted and unweighted UniFrac) were analyzed by the q2-phylogeny plugin[1].

Phylogenetic Investigation of Communities by Reconstruction of Unobserved States, PICRUSt2

The PICRUSt2 software (Douglas et al., 2019) was used to predict microbial functional abundances based on marker gene sequences. KEGG database was used to predict the results.

[1]https://github.com/qiime2/q2-diversity

Chemical Analyses

Short-Chain Fatty Acids Analyses

Samples from lumen and dialysate were analyzed by Brightlabs (Venlo, Netherlands) for determination of concentrations of SCFA. Ion exclusion chromatography (IEC) was applied on an 883 Ion Chromatograph (IC; Metrohm, Switzerland), using a Transgenomic IC Sep ICE-ION-300 column (30 cm length, 7.8 mm diameter, and 7 μm particles) and a MetroSep RP2 Guard. The mobile phase consists of 1.5 mM aqueous sulphuric acid. Samples were centrifuged (21,000 *g*, 10 min) and the clear supernatant was filtered through a 0.45 μm PFTE filter and diluted with mobile phase (for lumen 1:5, for dialysate 1:2). Ten microliters were loaded on the column by an autosampler 730 (Metrohm). Molecules were eluted according to their pKa.A column flow rate of 0.4 ml*min^{-1} was used. The temperature of the column was 65°C. The organic acids were detected using suppressed conductivity detection.

Glycome Profiling

Sample preparation

Lumen samples from each time point and treatment were freeze-dried, after which they were dissolved at 1 mg/mL in deionized water, and stored at −20°C as stock solutions.

Monoclonal antibodies (mAbs)

mAbs were obtained as hybridoma cell culture supernatants from CarboSource (Atlanta, GA, United States)[2] (**Supplementary File 1**).

ELISA

The ELISA protocol was slightly modified from Pattathil et al. (2010). In brief, samples prepared above were applied (50 μL of 100 μg/mL in deionized water per well) to Costar 3598 96-well plates (Corning Life Sciences, New Yok, United States) and were dried to the well surfaces by evaporation overnight at 37°C. Control wells contained deionized water. The plates were blocked with 200 μL of 1% (w/v) bovine serum albumin (BSA) in Tris-buffered saline (50 mM Tris–HCl, pH 7.6, containing 100 mM sodium chloride) for 1 h. Blocking agent was removed by aspiration, and 50 μL of undiluted hybridoma supernatant were added to each well and incubated for 1 h at room temperature. Supernatant was removed and wells were washed three times with 200 μL of 0.1% (w/v) BSA in Tris-buffered saline (wash buffer). Peroxidase-conjugated goat anti-mouse IgG, anti-mouse IgM, goat anti-rat IgG, or goat anti-rat IgM antibodies (Sigma-Aldrich), depending on the primary antibody used, were diluted 1:5,000 in wash buffer, and 50 μL were added to each well and incubated for 1 h. Wells were then washed five times with 200 μL of wash buffer. Next, 3,3′,5,5′-tetramethylbenzidine (TMB) solution (Sigma-Aldrich, St. Louis, United States) was freshly prepared according to the manufacturer's instructions, and 50 μL were added to each well. After 20 min, the reaction was stopped by adding 50 μl of 0.5 N sulfuric acid to each well. The OD of each well was read at a wavelength of 450 nm

[2]http://www.carbosource.net/

using a Multi-mode microplate reader (BioTek Synergy HTX, Abcoude, Netherlands).

Polysaccharide panel screening

Polysaccharide panel screening of mAbs was carried out by ELISA against all lumen samples immobilized to 96-well plates. Duplicate preparations of each polysaccharide were used for all experiments reported here. Binding data was visualized in R via ComplexHeatmap package (Gu et al., 2016).

Statistics

Analysis of covariance (ANCOVA) was applied to compare α-diversities (Shannon index), relative abundances of taxa at genus level and predicted abundance of microbial functional profile among different RSM treatments and time points by using package lme4 in R version 3.5.3[3]. Visualizations were performed in STAMP (Parks et al., 2014). The amplicon sequence variant (ASV) table (feature table of QIIME2) was normalized and filtered in R. The table was normalized via division by the sum of sequences in a given sample and multiplied by the minimum sum across all samples. Relative abundances were filtered as follows: values below a relative abundance threshold of 0.01% were not taken into account; taxa with a median relative abundance <1% in all groups were not considered for statistical analysis. White's non-parametric *t*-test was applied to compare between CON and treatments.

Permutational multivariate analysis of variance [PERMANOVA (Anderson, 2005)] was performed to test the significance of β-diversity distances in QIIME2 (weighted and unweighted UniFrac) between non-processed and processed RSM. The results were visualized in R (R version 3.5.3).

Pearson correlations between continuous meta-variables and taxonomic variables were calculated and visualized in R. Parameters were set as follows: Missing values for meta-variables were handled as NO imputation (replacing missing data with substituted); zeros were kept for the calculation of correlation; a minimum number of 0.1% was considered for calculation; a minimum of 4 paired observations were required for calculation of correlations. *P*-values were corrected using the Benjamini-Hochberg method. A *q*-value (corrected *P*-value) <0.05 was considered significant.

RESULTS

Characteristics of Non-processed and Processed RSM

A comprehensive set of 155 plant cell wall glycan-directed monoclonal antibodies was used to screen untreated RSM by a ELISA-based assay (Pattathil et al., 2010, 2012), and 34 antibodies reacted with RSM (data not shown). These were subsequently used in the current study to obtain information on the presence and relative abundance of specific epitopes that are characteristic of the different types of polymers in untreated RSM and RSM processed by ALK, CELL, PECT1, and PECT2.

Figure 2 shows that both increases and decreases in epitope recognition occurred in ALK, CELL, PECT1, and PECT2 compared to CON. Samples from after (_A) and before (_B) predigestion clustered together according to each treatment, which indicated _A and _B from the same treatment had similar epitope accessibility. ALK strongly increased binding of non-fucosylated XG mAbs, while CELL, PECT1, and PECT2 led to disappearance of those compared to CON, regardless of _A and _B treatment. All the treatments increased the binding of "Linseed Mucilage RG-I group" directed mAbs, but had little effect on Xylan-2 and RG-Ic group compared to CON. Binding of MAC204 (AG-1), which is binding to gum tragacanth and to lettuce and green tomato RG-I preparations (arabinogalactan), disappeared with ALK_A, ALK_B, and CELL_B, while increased binding of CCRC-M107 (AG-2), which binds to linear and branched arabinans and RG-I preparations from diverse plants but does not bind to larch arabinogalactan (Pattathil et al., 2010), was observed in ALK_A and ALK_B. CELL_A, CELL_B, PECT1_A, PECT1_B, and PECT2_B led to disappearance of the binding of mAbs of "pectic backbone group" and CCRC-M 133, which also binds to linear and branched arabinans and RG-I preparations from diverse plants but do not bind to larch arabinogalactan. ALK, PECT1, and PECT2 increased binding of mAbs directed against the arabinogalactan side chains of RG-I (RG-I/AG).

ALK, CELL, PECT1, and PECT2 Significantly Changed Microbiota Composition Compared to CON as Evaluated by Unweighted UniFrac

To determine the changes in composition of the gut microbiota fed with a shot of 5 g CON, ALK, CELL, PECT1, or PECT2, a comparison of microbiota based on sequencing the V3-V4 region of the 16S rRNA gene was performed. Shannon indices significantly decreased at t4, t6, t8 and t24, compared to that of t0 (**Supplementary File 2** and **Supplementary Figure S1A**). When data from all of the time points were pooled, there were no significant differences among CON, ALK, CELL, PECT1, and PECT2 in Shannon index (**Supplementary File 2** and **Supplementary Figure S1B**). Phylogeny based UniFrac methodology was then used to compare the β-diversity of the microbial communities between microbiota fed with non-processed and processed RSM. Unweighted UniFrac analysis (**Figure 3**) shows that samples from processed RSM (ALK, CELL, PECT1, and PECT2) significantly (P = 0.004) separated from non-processed RSM (CON), and samples from different processing method clustered together. Samples from CON, ALK, CELL, PECT1, and PECT2 all clustered together (P = 0.125) with respect to weighted UniFrac (**Supplementary File 2** and **Supplementary Figure S2**).

There were no significant differences between microbiota fed with RSM predigested before or after carbohydrase

[3]https://www.r-project.org/

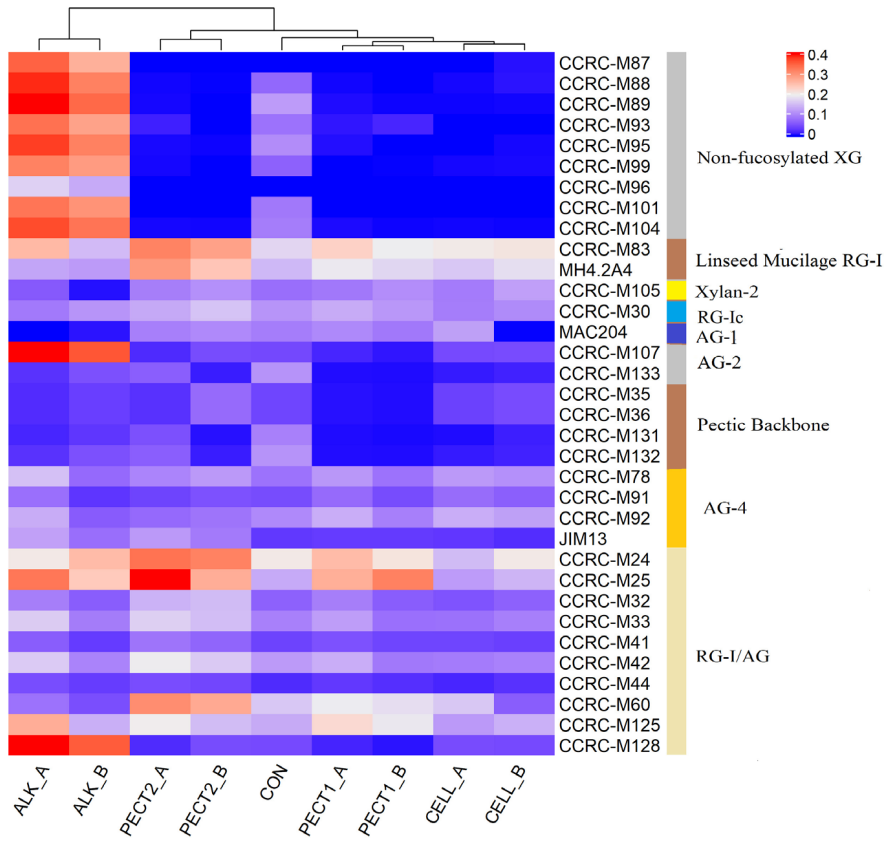

FIGURE 2 | Glycome profiling of non-processed and processed RSM. The binding response data of the mAbs are presented as heatmap using a blue-white-red scale indicating the intensity of the ELISA signal (blue, white, and red colors depict no, medium, and strong binding, respectively). The mAbs (indicated by their codes) are grouped based on the cell wall glycans they predominantly recognize as shown in the panel on right-hand side of the figure. _A, RSM was treated after predigestion, _B; RSM was treated before predigestion. XG, xyloglucan; RG-I, rhamnogalacturonan I; AG, arabinogalactan; RG-I/AG, arabinogalactan side chains of RG-I.

or ALK treatment with respect to both α-diversity (**Supplementary File 2** and **Supplementary Figure S3**), or β-diversity (data not shown), which indicated method I and method II of processing RSM had little effect on microbiota composition. Glycome profiling of RSM (**Figure 2**) also shows that samples from after and before processing clustered together according to each treatment, which indicated their polysaccharide compositions were similar to each other.

Relative abundances of taxa within the pig microbiotas fed with non-processed and processed RSM were compared to identify significantly different bacterial taxa. At genus level (**Figure 4**), seven genera were significant higher in relative abundance after ALK, CELL, PECT1, and PECT2 treatment compared to CON. These were *Ruminococcaceae NK4A214* group, *Ruminococcaceae UCG-002*, *Ruminococcaceae UCG-005*, *Roseburia*, *Anaerotruncus*, *Bifidobacterium*, *Christensenellaceae R-7* group, and *Selenomonas*. For genera *Christensenellaceae R-7* group and *Ruminococcaceae UCG-005*, their relative abundances were also higher in ALK and PECT1 compared to CELL. Instead, the relative abundances of *Prevotella* 7, an unclassified genus from *Prevotellaceae*, and *Prevotellaceae* UCG-001 were significantly decreased after feeding ALK, CELL, PECT1, and PECT2 compared to microbiota fed with CON. The relative abundance of *Succinivibrionaceae UCG-001* was significant higher in ALK and PECT1 compared to CON.

PICRUSt2 Analyses Revealed That Microbial Functional Abundances Related to Carbohydrate Metabolism and SCFA Production Were Significantly Increased With Processed RSM Compared to CON

PICRUSt2 was performed to the 16S rRNA gene data to predict metagenomic functional profiles. In this study we focused on carbohydrate metabolism related microbial functions (**Figure 5**). The relative abundances of fiber degradation pathways, beta-glucosidase [EC:3.2.1.21], beta-mannosidase [EC:3.2.1.25], and cellobiose phosphorylase [EC:2.4.1.20], were significant higher in ALK, CELL, PECT1, and PECT2 compared to CON, whereas conversely that of alpha-L-fucosidase [EC:3.2.1.51] was significant higher in

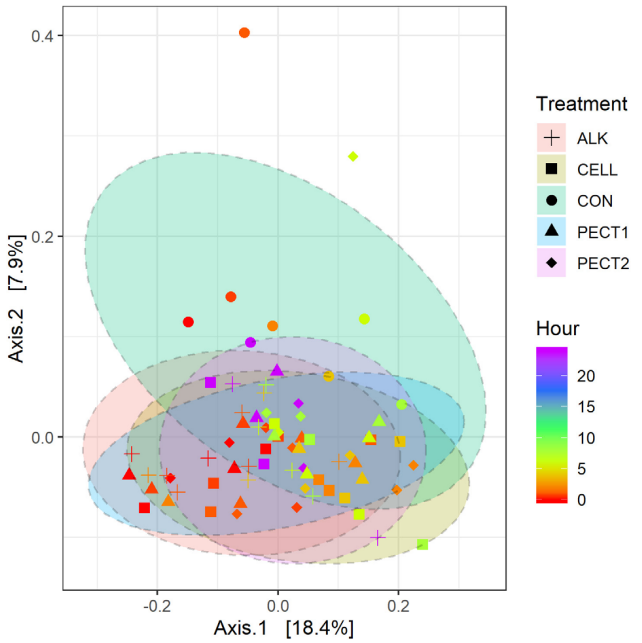

FIGURE 3 | Principal coordinate analysis (PCoA) plot generated based on an unweighted UniFrac matrix. Samples were grouped by shape and color representing the treatment and time point they belonged to, respectively: CON (sphere), ALK (plus), PECT1 (triangle), PECT2 (diamond), CELL (square); a red-green-purple scale was used to indicate the fermentation time (red and purple depict start and end of the fermentation period).

CON compared to ALK, CELL, PECT1, and PECT2. For cellobiose phosphorylase [EC:2.4.1.20], the relative abundance in ALK was also significant higher than those of CELL, PECT1, and PECT2.

Six microbial pathways related to fermentation were significant higher in relative abundance when microbiotas were fed with ALK, CELL, PECT1, and PECT2 compared to microbiota fed with CON. These pathways were pyruvate dehydrogenase E1 component, short-chain fatty acids transporter, mannose-1-phosphate guanylyltransferase, superpathway of glucose and xylose degradation, and L-lysine fermentation to acetate and butanoate. The relative abundance of lactose/L-arabinose transport system permease protein was significant higher in ALK, PECT1, and PECT2 compared to CON.

Table 1 shows that the cumulative acetic, propionic, and butyric acid and total SCFA production were higher in ALK, CELL, PECT1, and PECT2 compared to CON. For acetic acid, more than 2 times greater production was observed when the microbiota was fed with ALK, CELL, PECT1, and PECT2 compared to when the microbiota was fed with CON. The production of propionic, butyric acid and total SCFA in ALK, CELL, PECT1, and PECT2 were more than 1.6 times higher than that in CON, except for propionic (1.3 times), and butyric acid (1.4 times) production in ALK.

Glycome Profiling Shows That Binding of mAbs in Digests Were Dynamic During the *in vitro* Fermentation in SLIM

To investigate the dynamic changes of polysaccharides structure in CON, ALK, CELL, PECT1, and PECT2 during *in vitro* fermentation, a time series of sampling was performed and the set of 34 mAbs was used to screen the lumen digests. **Figure 6** shows that no or few binding signals were observed in Non-fucosylated XG, AG-2, and Pectic Backbone mAbs upon feeding CON, ALK, CELL, PECT1, and PECT2 at all time points.

No binding of CCRC-M83 that specifically bind to Linseed Mucilage RG-I was observed at t0 in all treatments (just prior to addition of the fiber shots), and binding signals appeared afterwards. For ALK, binding of CCRC-M83 decreased from t0.5 to t2, increased again at t4, and decreased to the lowest value at t24. For CELL, binding of CCRC-M83 decreased from t0.5 to t2, stabilized from t4 to t8, and decreased to the lowest value at t24. For CON, binding increased from t0.5 to t1, decreased from t2 to t6, increased at t8, and decreased to the lowest value at t24. For PECT1, binding increased from t0.5 to t4, and then decreased progressively until t24. For PECT2, binding increased slightly from t0.5 to t8, and then decreased to the lowest value at t24.

In terms of Xylan-2 recognizing mAb (i.e., CCRC-M105), weak bindings were detected at all time points after t0 with CELL and CON. Increased binding of CCRC-M105 was observed from t0.5 to t1 in ALK and the amount of binding decreased from t2 to t4, slightly increased again at t6, and then decreased until t24. For PECT1, increased binding of CCRC-M105 was observed from t0.5 to t6, which decreased afterward until t24. Binding for PECT2 was dynamic from t0.5 to t24, but the lowest binding was observed at t24.

As for the RG-Ic recognizing mAb (i.e., CCRC-M30), binding of CCRC-M30 was lower in ALK, PECT1, and PECT2 according to each time point compared to CELL and CON, but binding over time was dynamic. With respect to the AG-4 mAbs (recognizing arabinogalactans), weak and dynamic binding was observed at each time point in all treatments.

With respect to RG-I/AG mAbs, more active mAbs were observed compared to other groups of mAbs in all treatments. Within RG-I/AG mAbs, amount of binding of CCRC-M25 and CCRC-M60 were stronger than other RG-I/AG mAbs in all treatments, and their amount of binding were fluctuating during the whole fermentation period and still existed at t24 in all treatments.

Correlation Between Microbiota Abundance and SCFA Production and mAb Binding

Pearson correlation analyses were performed to investigate the relationship between the relative abundance of microbial genera and SCFA production at each time point (**Figure 7**). Seven genera (*Bifidobacterium*, *Collinsella*, *Denitrobacterium*, *Olsenella*, *Coriobacteriaceae*.1, *Bacteroidales S24-7* group.2, and *Acetitomaculum*) had significant negative correlation

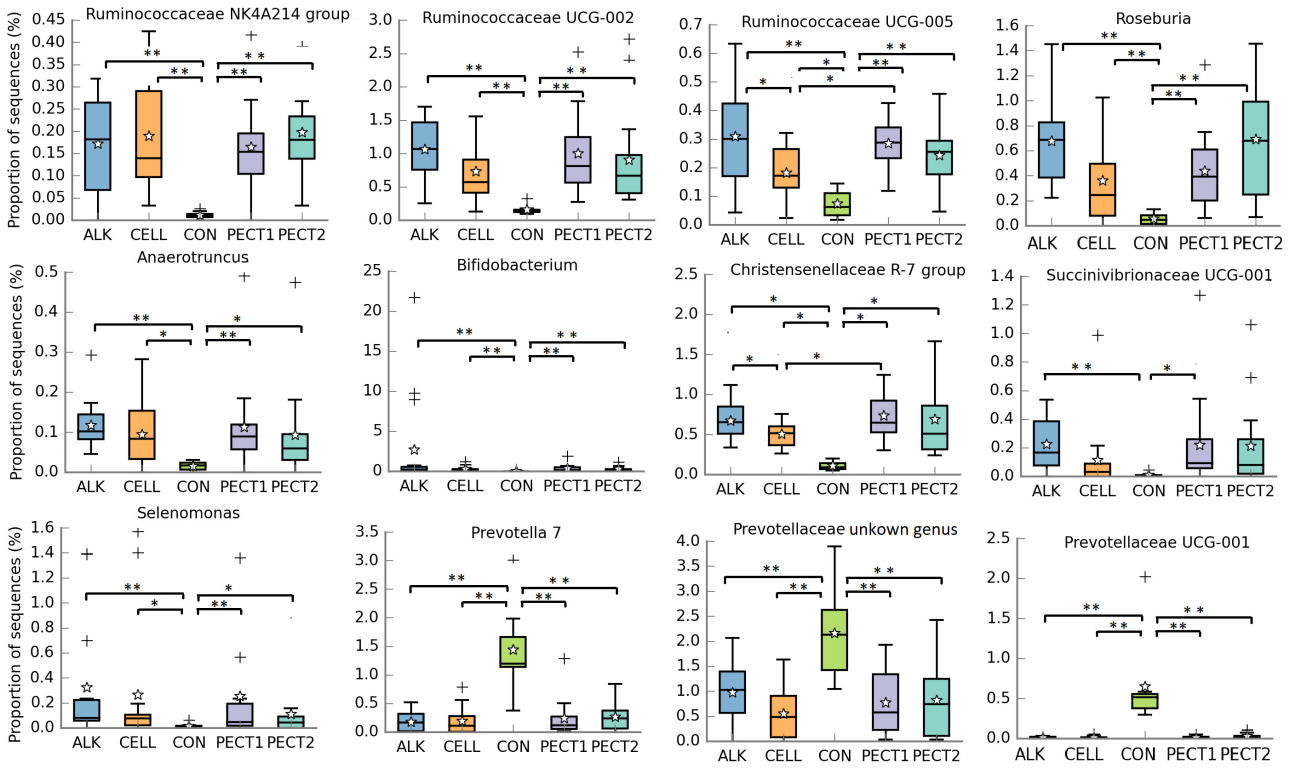

FIGURE 4 | Significantly different relative abundances of microbial genera upon treatment with ALK, CELL, CON, PECT1, and PECT2. The relative abundances of genera in pre-treated RSM compared to CON were analyzed by ANCOVA. *$P < 0.05$; **$P < 0.01$. The stars represent the group means while the middle bars of the boxplots represent the median and the plusses represent outliers.

with propionic acid, butyric acid, valeric acid and total SCFA production. Within these, *Bacteroidales S24-7* group.2, *Olsenella*, *Coriobacteriaceae*.1, and *Acetitomaculum* also significantly negatively correlated with acetic acid. Eight genera (*Bacteroidales S24-7* group.1, *Prevotella* 9, *Faecalibacterium*, *Ruminococcaceae UCG-005*, *Ruminococcus* 2, *Selenomonas*, *Succinivibrio*, and *Succinivibrionaceae UCG-001*) significantly positively correlated with acetic acid, propionic acid, butyric acid, valeric acid and total SCFA production. Within these, *Ruminococcus* 2 and *Succinivibrio* also had significant positive correlation with caproic acid. *Bacteroidales S24-7* group, *Sarcina*, and *Oribacterium* had significant positive correlation with propionic acid, butyric acid, valeric acid and total SCFA production. *Roseburia*, *Ruminococcaceae NK4A214* group and *Ruminococcaceae UCG-002* significantly positively correlated with acetic acid, propionic acid, butyric acid and total SCFA production. *Prevotella* 7 significantly positively correlated with propionic acid, valeric acid, caproic acid, and total SCFA production.

The correlation between binding of mAbs and relative abundance of microbial genera was also analyzed. Within the mAbs that recognizing non-fucosylated XG, CCRC-M93 had significant negative correlation with *Bacteroidales S24-7* group.1, *Christensenellaceae R-7* group, [*Eubacterium*] *nodatum* group, *Blautia*, *Lachnospira*, *Lachnospiraceae NK3A20* group, *Roseburia*, *Ruminococcaceae UCG-005*, *Ruminococcus* 2, *Subdoligranulum*, *Catenibacterium*, *Catenisphaera*, *Succiniclasticum*, and *Succinivibrionaceae UCG-001*. CCRC-M96 significantly negatively correlated with *Bacteroidales S24-7* group.2 and *Acetitomaculum*, while it significantly positively correlated with *Anaerotruncus*. CCRC-M99 had significant negative correlation with Dorea and *Ruminococcus* 2, whereas it had significant positive correlation with *Megasphaera*. CCRC-M104 had significant positive correlation with *Prevotellaceae UCG-001*, while it negatively correlated with *Ruminococcaceae UCG-002*.

MH4.2A4 that recognizes linseed mucilage RG-I had significant negative correlations with *Bacteroidales S24-7* group.1, *Ruminococcaceae NK4A214* group, and *Ruminococcaceae UCG-005*.

CCRC-M105 that binds to Xylan-2 had significant negative correlations with *Prevotellaceae*.1, *Family XIII UCG*-001, *Acidaminococcus*, and *Megasphaera*, whereas it positively correlated with *Ruminococcus* 2 and *Subdoligranulum*.

CCRC-M30, binding to RG-Ic, had significant positive correlations with *Denitrobacterium*, *Olsenella*, *Bacteroidales S24-7* group.2, and *Acetitomaculum*, while it significantly negatively correlated with *Roseburia*, *Faecalibacterium*, *Ruminococcaceae UCG-002*, *Ruminococcaceae UCG-005*, *Selenomonas*, and *Succinivibrionaceae UCG-001*.

MAC204, that recognizing AG-1, significantly negatively correlated with *Denitrobacterium*, *Olsenella*, *Bacteroidales S24-7* group.2, *Acetitomaculum*, and *Roseburia*, while it had significant positive correlations with *Lactobacillus*, *Sarcina*, *Roseburia*,

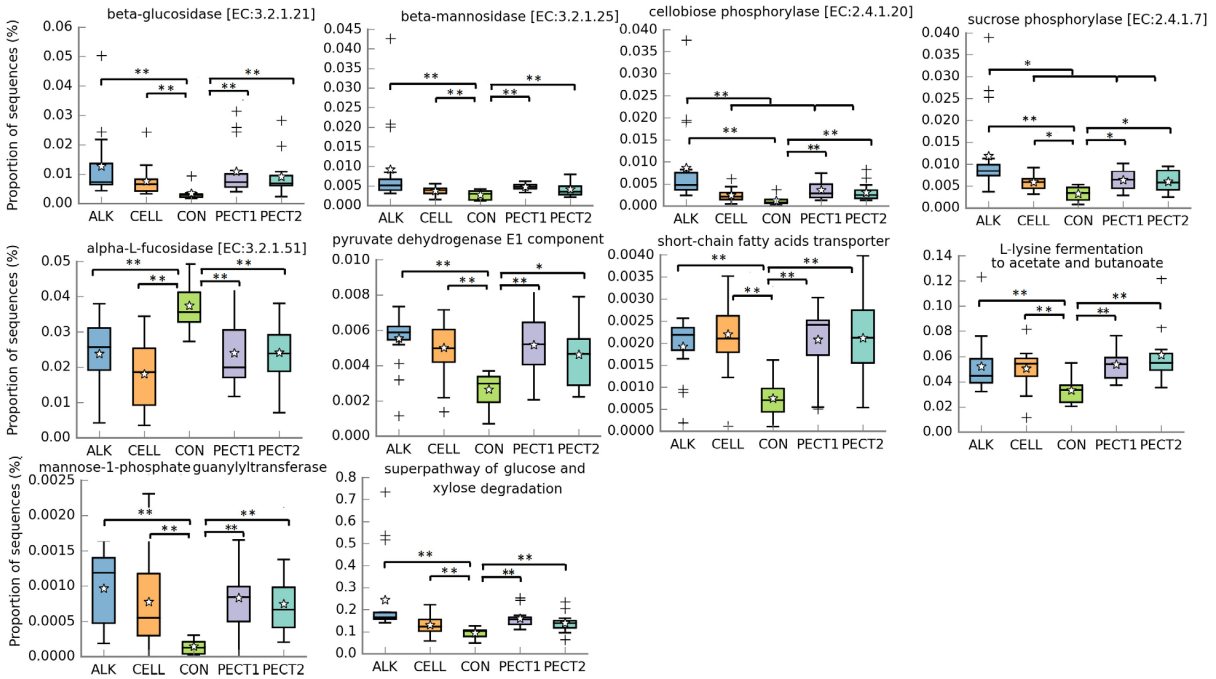

FIGURE 5 | Significantly different metagenomic functions in relative abundance among ALK, CELL, CON, PECT1, and PECT2. The predicted abundances of microbial functional profile in pre-treated RSM compared to CON were analyzed by ANCOVA. *$P < 0.05$; **$P < 0.01$. The stars represent the group means while the middle bars of the boxplots represent the median and the plusses represent outliers.

TABLE 1 | Fold change of cumulative Acetic, Propionic, and Butyric acid, and total short-chain fatty acid production during fermentation of ALK, PECT1, PECT2, and CELL compared to CON.

Treatment	Acetic acid	Propionic acid	Butyric acid	Total SCFA
ALK	2.0	1.3	1.6	1.4
CELL	2.3	1.7	1.8	1.7
PECT1	2.2	1.6	1.6	1.6
PECT2	2.5	1.9	1.8	1.8

Ruminococcaceae NK4A214 group, *Ruminococcaceae UCG-002*, *Ruminococcaceae UCG-005*, and *Selenomonas*.

CCRC-M133, binding to AG-2, significantly negatively correlated with *Denitrobacterium*, *Prevotella* 7, *Prevotellaceae UCG-001*, *Acetitomaculum*, and *Subdoligranulum*, while it positively correlated with *Ruminococcaceae UCG-002*.

CCRC-M131, that binds to pectic backbone, had significant negative correlation with *Denitrobacterium*, *Olsenella*, *Bacteroidales S24-7* group.2, *Prevotellaceae UCG-001*, *Acetitomaculum*, and *Subdoligranulum*, while it positively correlated with *Lactobacillus*, *Anaerotruncus*, and *Ruminococcaceae UCG-002*.

With respect to mAbs binding to AG-4, CCRC-M78 had significant negative correlation with *Bifidobacterium*, and *Christensenellaceae R-7* group, whereas it significantly positively correlated with *Prevotellaceae UCG-001*. CCRC-M91 had significant negative correlation with *Denitrobacterium*, *Olsenella*, and *Acetitomaculum*, and CCRC-M91 and CCRC-M92 significantly positively correlated with *Lactobacillus*. JIM13 had significant negative correlation with *Subdoligranulum*.

As for mAbs binding to RG-I/AG, they had significant negative correlation with *Bacteroidales S24-7* group (CCRC-M32), *Bacteroidales S24-7* group.2 (CCRC-M32 and M125), *Lactobacillus* (CCRC-M24), [*Eubacterium*] *nodatum* group (CCRC-M60), *Acetitomaculum* (CCRC-M42), *Blautia* (CCRC-M60), *Coprococcus* 3 (CCRC-M24), *Ruminococcaceae NK4A214* group (CCRC-M32, M41, M44, and M60), *Ruminococcaceae UCG-002* (CCRC-M44), *Ruminococcaceae* UCG-005 (CCRC-M32, M44, and M60) *Subdoligranulum* (CCRC-M 42), and *Succiniclasticum* (CCRC-M125). Significantly positive correlations were observed with *Olsenella* (CCRC-M44), *Bacteroidales S24-7* group (CCRC-M128), *Prevotella* 7 (CCRC-M24 and M128), *Prevotellaceae UCG-001* (CCRC-M 24 and M128), *Prevotellaceae* (CCRC-M128), *Lactobacillus* (CCRC-M42), *Lachnospira* (CCRC-M128), *Ruminococcus* 2 (CCRC-M128), *Subdoligranulum* (CCRC-M128), and *Succinivibrio* (CCRC-M128).

DISCUSSION

Cell Wall Polysaccharides Composition of Differently Pretreated RSM

Cell wall polysaccharides of RSM (*Brassica napus*) were comprehensively studied by chemical methods (Pustjens et al.,

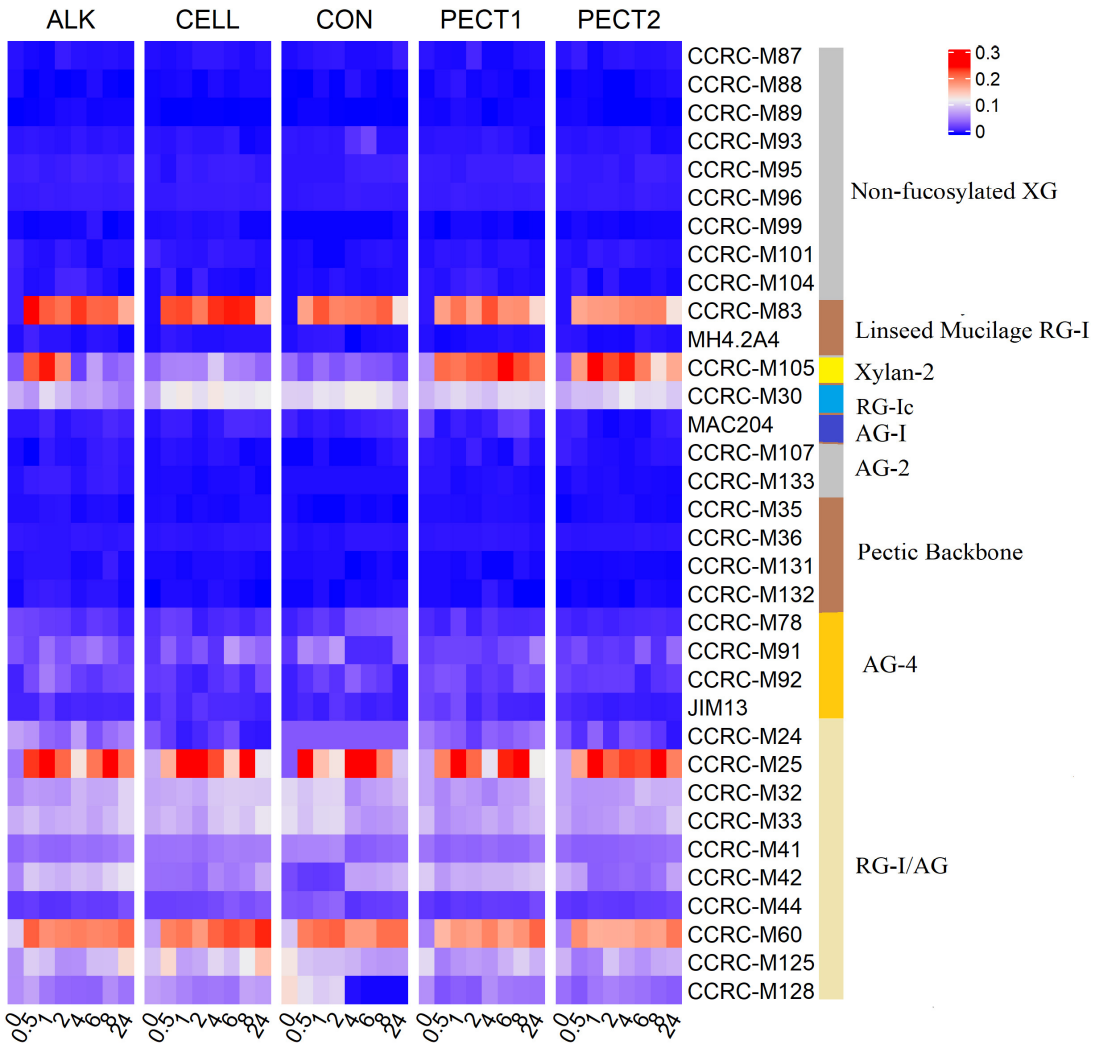

FIGURE 6 | Glycome profiling of lumen digests during *in vitro* fermentation of ALK, CELL, CON, PECT1, and PECT2 at time point 0, 0.5, 1, 2, 4, 6, 8, and 24 h. The binding response data are presented as heatmap using a blue-white-red scale indicating the strength of the ELISA signal (blue, white, and red colors depict no, medium, and strong binding, respectively). The mAbs are grouped based on the cell wall glycans they predominantly recognize as shown in the panel on the right-hand side of the figure. XG, xyloglucan; RG-I, rhamnogalacturonan I; AG, arabinogalactan; RG-I/AG, arabinogalactan side chains of RG-I.

2013), which showed that they generally consisted of arabinan, homogalacturonan, Rhamnogalacturonan I (RG-I), type II arabinogalactan (AG), and xyloglucan (XG) (Siddiqui and Wood, 1977). In a previous study (Long et al., 2020b), we determined the monosaccharide constituent composition, which was in line with Pustjens et al. (2013). Our current findings with the mAbs are also in line with this, since non-fucosylated XG-, RG- I-, pectic backbone-, and AG-recognizing mAbs bound to CON. By similar reasoning, xylan was also detected in CON, which was not reported before, although it is not entirely clear how much cross-reactivity the mAbs show.

ALK treatment intensively increased binding of mAbs that specifically bind to non-fucosylated XG (**Figure 2**). This is consistent with previous finding that alkali could extract XG from hemicellulose (Pustjens et al., 2013), which led to XG being detected by the mAbs in the current study. Previous research also demonstrated that XG is linked via hydrogen bonds to the surface of cellulose microfibrils, which is extractable with alkali, but not accessible by enzyme (Pauly et al., 1999). However, enzymatic treatments (PECT1, PECT2, and CELL) led to a disappearance of binding non-fucosylated XG-specific mAbs compared to CON, which was unexpected. It could be that XG might become entrapped by other cell wall structures after pectinase or cellulase treatment. It is unknown whether this kind of the hidden phenomenon would reduce the degradability of XG.

Enzymatic treatments increased binding of linseed mucilage RG-I-specific mAbs and some mAbs directed against the arabinogalactan side chains of RG-I (RG-I/AG), and reduced binding of some mAbs directed to pectic backbone, which indicated that PECT1 and PECT2 broke down pectic backbone and exposed RG-I and its

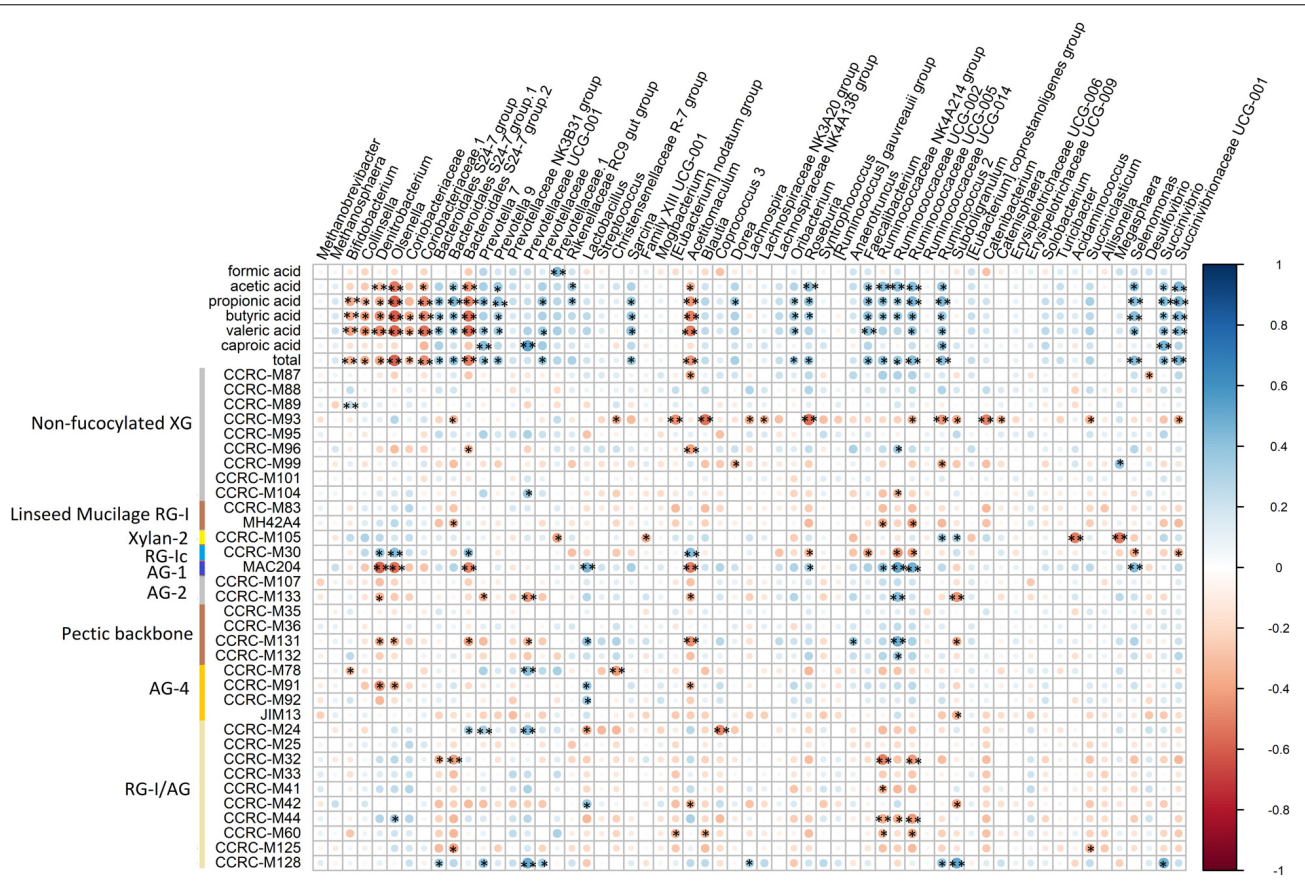

FIGURE 7 | Correlation between core bacterial genera, and SCFA and binding of mAbs. Statistical significance was determined for all pairwise comparisons using Pearson's method. $^{*}P < 0.05$; $^{**}P < 0.01$. Size of the circles indicates correlation strength, which bigger sizes meaning higher correlations. Blue circles represent positive correlations (correlation coefficients from 0 to 1), whereas red circles represent negative correlations (correlation coefficients from 0 to –1). total, total SCFA production. The mAbs are grouped based on the cell wall glycans they predominantly recognize as shown in the panel on the left-hand side of the figure. XG, xyloglucan; RG-I, rhamnogalacturonan I; AG, arabinogalactan; RG-I/AG, arabinogalactan side chains of RG-I.

arabinogalactan side chains. These results are supported by a previous study showing that PECT1 and PECT2 degraded pectic backbone and released RG-I and its arabinogalactan side chains (Pustjens et al., 2013). Moreover, RG-I attached to cellulose microfibrils can be released by cellulase (Oechslin et al., 2003), while at the same time it might block the accessibility of pectic backbone because of the shifting of the polysaccharides structure.

ALK treatment led to the disappearance of binding of mAbs that specifically bind to AG-1 while it increased binding of mAbs that specifically binding to AG-2, which indicated that ALK could cause arabinogalactan to be physically entrapped in other cell wall structures, while linear and branched arabinan become accessible (Pattathil et al., 2010).

They were lower in amount of binding of mAbs in AG-4 from ALK_B, PECT1_B, PECT2_B, and CELL_B, compared to ALK_A, PECT1_A, PECT2_A, and CELL_A, respectively. This indicated that small fragments were produced in AG-4 group after enzymatic and chemical treating RSM, which were dialyzed out in ALK_B, PECT1_B, PECT2_B, and CELL_B during the subsequent predigestion treatment. Overall, both enzymatic and chemical processed RSM can release some polysaccharides but physically entrap or shield some others at the same time.

Community Structure of Swine Microbiota Fed With Differently Pretreated RSM

PERMANOVA tests suggested significant differences ($P = 0.004$) in community structure between all pre-treatments and the CON group, though no significant differences were detected between the pre-treatments (**Figure 3**). Dietary fiber is known to have a considerable effect on gut microbiota composition (Flint, 2012; Yatsunenko et al., 2012; Cotillard et al., 2013). Glycome profiling of non-processed and processed RSM showed that polysaccharides structures were differentially shifted due to ALK, PECT1, PECT2, and CELL treatment in the current study, which were consistent with previous studies (Pustjens et al., 2012; de Vries et al., 2014). These observations might explain the specific genus changes in microbiota composition after microbiotas fed with ALK, PECT1, PECT2, and CELL compare to CON (**Figure 4**), despite the

differential effect of the different treatments as assessed by the glycome profiling.

In order to understand which microbes were significantly influenced by dietary supplementation of processed RSM, microbial genera were compared among the five treatments (**Figure 4**). The relative abundances of *Ruminococcaceae NK4A214* group, *Ruminococcaceae UCG-002*, *Ruminococcaceae UCG-005*, *Roseburia*, *Bifidobacterium*, and *Christensenellaceae R-7* group were significantly increased in ALK, PECT1, PECT2, and CELL (**Figure 4**). Research has shown that genera of family *Ruminococcaceae* contain major (hemi)cellulolytic and pectinolytic species (Pettipher and Latham, 1979; Nyonyo et al., 2014; Hartinger et al., 2019a). Thus, microbes from family *Ruminococcaceae* play an important role in degrading (hemi)cellulose and pectin in their activity against recalcitrant fiber (Shinkai and Kobayashi, 2007; Flint et al., 2008). Previous research demonstrated that the higher the relative abundance of *Ruminococcaceae NK4A214* group, the higher the fiber degradability (Hartinger et al., 2019b). This observation was consistent with the current study, which showed that the SCFA production (which is usually used as evaluation of fiber degradability *in vitro*) was also higher in ALK, CELL, PECT1, and PECT2 compared to CON. Furthermore, our study also showed that the relative abundance of *Ruminococcaceae NK4A214* group, as well as *Ruminococcaceae UCG-002* and *Ruminococcaceae UCG-005*, significantly correlated with acetic acid, propionic acid, butyric acid, and (not surprisingly) total SCFA production. *Roseburia* is a well-known butyrate-producing bacteria (Duncan et al., 2002), and a primary degrader of β-mannans (La Rosa et al., 2019). The significant increase in abundance of this genus was accordance with the increased butyric acid production in the current study (**Table 1**), and increased predicted abundance of beta-mannosidases (EC.3.2.1.25) in the processed RSM groups (**Figure 5**). *Bifidobacterium* is suggested to be a common cross-feeding bacteria for sugar utilization (Cockburn and Koropatkin, 2016). Previous research has been shown that *Bifidobacterium bifidum* relies on the presence of a primary degrader in order to grow with either resistant starch or xylan both *in vitro* (Turroni et al., 2015) and *in vivo* (Turroni et al., 2016). It has also been reported that numerous *Bifidobacterium* species grew to higher cell densities accompanied by upregulating their respective saccharolytic pathways when grown in co-culture compared to their growth in monoculture (Milani et al., 2015). This finding was in accordance with the current study, where the relative abundance of *Bifidobacterium* was much higher than that of other genera, especially in ALK (data not shown). Alternatively, synergy existed among genera that were targeting the same substrates, possibly by specializing in degrading different motifs within the molecule. However, this might also lead to a competitive environment when the fermentation continues after 24 h. For instance, when a specific motif for a particular microbe runs out, the microbe might start to utilize another motif."

The relative abundance of *Christensenellaceae R-7* group increased after enzymatic and chemical treatment, which was consistent with a previous study where rumen microbiota was fed with fibrinolytic enzyme-treated wheat straw (Ribeiro et al., 2020). *Christensenellaceae* plays an important role in degrading fiber (Mao et al., 2015) and producing acetic and butyric acid (Morotomi et al., 2012). All the observations above were supported by former reports that feed processed by carbohydrase enzymes could stimulate growth of specific microbes (Giraldo et al., 2007, 2008; Long et al., 2020c). It can be speculated that the pre-treatment of feed stuffs with carbohydrases causes the release of hydrolysis materials (presumably oligosaccharides), which promote the chemotactic response of specific bacteria, and stimulates their attachment to insoluble feed particles (this attachment is known as biofilm formation), thereby leading to growth of these microbes (Beauchemin et al., 2003; Giraldo et al., 2007; Ribeiro et al., 2015, 2018).

Fiber Degradation and SCFA Production

Enzymatic and chemical treatment on RSM increased the amount of acetic acid, propionic acid, butyric acid, and thereby total SCFA production (**Table 1**). This observation was consistent with the predicted functional profiles related to carbohydrate metabolism, where the relative abundance of fiber breakdown and fermentation enzymes and pathways increased (**Figure 5**). This finding was in accordance with previous studies that addition of pectolytic enzymes improved degradability of non-starch polysaccharides (NSP) of RSM *in vitro* (Pustjens et al., 2012) and in broilers (de Vries et al., 2014; Pustjens et al., 2014). Giraldo et al. also reported that supplementation of exogenous cellulase increased SCFA production (Giraldo et al., 2007). Previous research demonstrated that supplementation of carbohydrase on feed before feeding could increase microbial protein production, ruminal cellulolytic bacterial numbers, and ruminal fibrinolytic activity. Thus, the findings above indicate that the enzymatic and chemical treatment on RSM could sufficiently open cell wall architecture (refer to **Figure 2**), to enable effective accessibility of NSP to bacterial degradation enzymes, and subsequently stimulate expression of microbial saccharolytic pathways.

No bindings of mAbs recognizing non-fucosylated XG were observed in lumen samples after the microbiota was fed with ALK or CON (**Figure 6**), which was unexpected as binding signals were seen in the substrates themselves prior to addition to SLIM (**Figure 2**). The hypothesis could be entertained that XG was immediately utilized by bacteria before our first sampling time point (after 30 min), or that the XG structures were unable to be recognized by the mAbs after supplementing them to lumen, due to entrapment by other molecules. Binding signals still existed at t24 for all mAbs that showed signal at the t0.5 time point, which indicated that these structures cannot be degraded any further or more fermentation time was needed. Glycome profiling showed that binding of mAbs recognizing each polysaccharide structure/epitope were dynamic during the 24 h fermentation period (**Figure 6**). It is not unlikely that certain polysaccharide structure, such as (hemi)cellulose and pectin, were exposed to microbes stage by stage, due to ever increasing degradation of the cell wall structures over time. For instance, bacteria should break down side-chain AG before they

can utilize RG-I. However, this hypothesis should be validated in future study.

The increased in abundance of *Ruminococcaceae NK4A214* group, *Ruminococcaceae UCG-002*, and *Ruminococcaceae UCG-005* in enzymatic and chemical treated RSM groups showed negative correlations with XG, RG-I, and RG-I/AG (arabinogalactan side chains of RG-I), and positively correlated with AG-1, AG-2, and pectic backbone. These observations suggested that ALK, CELL, PECT1, and PECT2 stimulated these genera to utilize XG, RG-I, and arabinogalactan side chains of RG-I, and exposed AG-1, AG-2, and pectic backbone to other bacteria in the current study. The abundance of *Roseburia* and *Succinivibrionaceae UCG-001* in enzymatic and chemical treated RSM groups had negative correlations with XG and AG-1, which suggested that the treatments on RSM stimulated these genera to degrade XG and AG-1. A possible model of action can be explained by the adhesion theory of Cellulolytic Bacteria (Miron et al., 2001), which supposes that the (in our case) enzymatic and chemical treatments on RSM stimulate attachments of microbes to specific polysaccharides structures (Meale et al., 2014), which lead the bacteria to degrade them. However, the mechanism of exogenous enzymes enhanced degradation of plant cell walls is complex, with many interrelated factors, and requires further studies. Moreover, degradation of fibers requires a plethora of microbial enzymes as indicated for instance by the numerous PUL-loci needed by *Bacteroides thetaiotaomicron* to breakdown pectin.

CONCLUSION

The present study clearly demonstrated that both enzymatic and chemical pre-treatment on RSM shifted its cell wall polysaccharide structure, subsequently altering microbial community composition and functional profile compared to untreated RSM, and eventually increased fiber degradability as evaluated by SCFA production. Furthermore, glycome profiling showed that the abundance of cell wall polysaccharides were dynamically changed during fermentation, and did not continuously decrease during the fermentation period. Our findings that ALK, CELL, PECT1 and PECT2 increased fiber degradability in RSM could help guide feed additive strategies to improve efficiency and productivity in swine industry. The current study gave insight into how feed enzyme modulate microbial status, which provides good opportunity to develop novel carbohydrase, particularly in swine feed.

DATA AVAILABILITY STATEMENT

The datasets presented in this study can be found in online repositories. The names of the repository/repositories and accession number(s) can be found in the article/ **Supplementary Material**.

AUTHOR CONTRIBUTIONS

KV and CL designed and planned the experiment. CL performed the data analyses and drafted the manuscript. KV revised and contributed to the manuscript. Both authors read and approved the final manuscript.

FUNDING

This study was funded by the Centre for Healthy Eating and Food Innovation (HEFI) of Maastricht University – Campus Venlo and has been made possible with the support of the Dutch Province of Limburg with a grant to HEFI, HEFI-1venk15-25. CL received a Ph.D. scholarship from the China Scholarship Council under the Chinese Government Graduate Student Overseas Study Program (Grant No. 201603250050).

ACKNOWLEDGMENTS

For CCRC antibodies "Generation of the CCRC-series of monoclonal antibodies used in this work was supported by a grant from the NSF Plant Genome Program (DBI-0421683)." For JIM and MAC antibodies "Distribution of the JIM and MAC antibodies used in this work was supported in part by NSF grants DBI-0421683 and RCN 009281." We thank Sanne Verbruggen and Jessica Verhoeven for sharing their experience in running TIM-2, and Rob van Dinter for technical support. This manuscript has been released as a pre-print at Research Square (Long and Venema, 2020).

SUPPLEMENTARY MATERIAL

The Supplementary Material for this article can be found online at: https://www.frontiersin.org/articles/10.3389/fmicb.2020.588264/full#supplementary-material

REFERENCES

Anderson, M. J. (2005). *Permutational Multivariate Analysis of Variance*. Auckland: University of Auckland, 32–46.

Beauchemin, K. A., Colombatto, D., Morgavi, D. P., and Yang, W. Z. (2003). Use of exogenous fibrolytic enzymes to improve feed utilization by ruminants. *Anim. Sci. J.* 81, E37–E47.

Bindelle, J., Pieper, R., Montoya, C. A., Van Kessel, A. G., and Leterme, P. (2011). Nonstarch polysaccharide-degrading enzymes alter the microbial community and the fermentation patterns of barley cultivars and wheat products in an *in vitro* model of the porcine gastrointestinal tract. *FEMS Microbiol. Ecol.* 76, 553–563. doi: 10.1111/j.1574-6941.2011.01074.x

Bolyen, E., Rideout, J. R., Dillon, M. R., Bokulich, N. A., Abnet, C. C., AlGhalith, G. A., et al. (2019). Reproducible, interactive, scalable and extensible microbiome data science using QIIME 2. *Nat. Biotechnol.* 37, 852–857. doi: 10.1038/s41587-019-0209-9

Broxterman, S. E., and Schols, H. A. (2018). Interactions between pectin and cellulose in primary plant cell walls. *Carbohyd. Polym.* 192, 263–272. doi: 10.1016/j.carbpol.2018

Callahan, B. J., Mcmurdie, P. J., Rosen, M. J., Han, A. W., Johnson, A. J. A., and Holmes, S. P. (2016). DADA2: high-resolution sample inference from Illumina amplicon data. *Nat. Methods* 13:581. doi: 10.1038/nmeth

Carpita, N. C., and Gibeaut, D. M. (1993). Structural models of primary cell walls in flowering plants: consistency of molecular structure with the physical properties of the walls during growth. *Plant J.* 3, 1–30. doi: 10.1111/j.1365-313x.1993.tb00007.x

Cockburn, D. W., and Koropatkin, N. M. (2016). Polysaccharide degradation by the intestinal microbiota and its influence on human health and disease. *J. Mol. Biol.* 428, 3230–3252. doi: 10.1016/j.jmb.2016.06.021

Cotillard, A., Kennedy, S. P., Kong, L. C., Prifti, E., Pons, N., Chatelier, E. L., et al. (2013). Dietary intervention impact on gut microbial gene richness. *Nature* 500, 585–588. doi: 10.1038/nature12480

de Vries, S., Pustjens, A. M., Kabel, M. A., Salazar-Villanea, S., Hendriks, W. H., and Gerrits, W. J. J. (2013). Processing technologies and cell wall degrading enzymes to improve nutritional value of dried distillers grain with solubles for animal feed: an in vitro digestion study. *J. Agric. Food Chem.* 61, 8821–8828. doi: 10.1021/jf4019855

de Vries, S., Pustjens, A. M., Schols, H. A., Hendriks, W. H., and Gerrits, W. J. J. (2012). Improving digestive utilization of fiber-rich feedstuffs in pigs and poultry by processing and enzyme technologies: a review. *Anim. Feed Sci. Technol.* 178, 123–138. doi: 10.1016/j.anifeedsci.2012.10.004

de Vries, S., Pustjens, A., Kabel, M., Kwakkel, R., and Gerrits, W. (2014). Effects of processing technologies and pectolytic enzymes on degradability of nonstarch polysaccharides from rapeseed meal in broilers. *Poult. Sci.* 93, 589–598. doi: 10.3382/ps.2013-03476

Douglas, G. M., Maffei, V. J., Zaneveld, J., Yurgel, S. N., Brown, J. R., Taylor, C. M., et al. (2019). PICRUSt2: an improved and extensible approach for metagenome inference. *BioRxiv* doi: 10.1101/672295

Duncan, S. H., Hold, G. L., Barcenilla, A., Stewart, C. S., and Flint, H. J. (2002). Roseburia intestinalis sp. nov., a novel saccharolytic, butyrate-producing bacterium from human faeces. *Int. J. Syst. Evol. Microbiol.* 52, 1615–1620. doi: 10.1099/00207713-52-5-1615

Eriksson, I., Andersson, R., and Åman, P. (1997). Extraction of pectic substances from dehulled rapeseed. *Carbohydr. Res.* 301, 177–185. doi: 10.1016/S0008-6215(97)00096-7

Flint, H. J. (2012). The impact of nutrition on the human microbiome. *Nutr. Rev.* 70, S10–S13. doi: 10.1111/j.1753-4887.2012.00499.x

Flint, H. J., Bayer, E. A., Rincon, M. T., Lamed, R., and White, B. A. (2008). Polysaccharide utilization by gut bacteria: potential for new insights from genomic analysis. *Nat. Rev. Microbiol.* 6, 121–131. doi: 10.1038/nrmicro1817

Gibson, G. R., Cummings, J. H., and Macfarlane, G. T. (1988). Use of a three-stage continuous culture system to study the effect of mucin on dissimilatory sulfate reduction and methanogenesis by mixed populations of human gut bacteria. *Appl. Environ. Microbiol.* 54, 2750–2755. doi: 10.1128/aem.54.11.2750-2755.1988

Giraldo, L. A., Tejido, M. L., Ranilla, M. J., and Carro, M. D. (2007). Effects of exogenous cellulase supplementation on microbial growth and ruminal fermentation of a high-forage diet in Rusitec fermenters. *Anim. Sci. J.* 85, 1962–1970. doi: 10.2527/jas.2006-318

Giraldo, L. A., Tejido, M. L., Ranilla, M. J., and Carro, M. D. (2008). Influence of direct-fed fibrolytic enzymes on diet digestibility and ruminal activity in sheep fed a grass hay-based diet. *Anim. Sci. J.* 86, 1617–1623. doi: 10.2527/jas.2007-0343

Gu, Z. G., Eils, R., and Schlesner, M. (2016). Complex heatmaps reveal patterns and correlations in multidimensional genomic data. *Bioinformatics* 32, 2847–2849. doi: 10.1093/bioinformatics/btw313

Hartinger, T., Edwards, J. E., Expósito, R. G., Smidt, H., ter Braak, C. J. F., Gresner, N., et al. (2019a). Differently pre-treated alfalfa silages affect the *in vitro* ruminal microbiota composition. *Front. Microbiol.* 10:2761. doi: 10.3389/fmicb.2019.02761

Hartinger, T., Gresner, N., and Südekum, K.-H. (2019b). *In vitro* ruminal fermentation characteristics of alfalfa silages in response to different pre-ensiling treatments. *Anim. Feed Sci. Technol.* 258:114306. doi: 10.1016/j.anifeedsci.2019.114306

Klindworth, A., Pruesse, E., Schweer, T., Peplies, J., Quast, C., Horn, M., et al. (2013). Evaluation of general 16S ribosomal RNA gene PCR primers for classical and next-generation sequencing-based diversity studies. *Nucleic Acids Res.* 41:e1. doi: 10.1093/nar/gks808

La Rosa, S. L., Leth, M. L., Michalak, L., Hansen, M. E., Pudlo, N. A., Glowacki, R., et al. (2019). The human gut firmicute *Roseburia intestinalis* is a primary degrader of dietary β-mannans. *Nat. Commun.* 10:905.

Long, C., and Venema, K. (2020). Pretreatment of rapeseed meal increases its recalcitrant fibre fermentation and alters the microbial community in an in vitro model of swine large intestine. *Res. Square.* [Preprint]. doi: 10.21203/rs.3.rs-34955/v1

Long, C., De Vries, S., and Venema, K. (2020a). Polysaccharide source altered ecological network, functional profile, and short-chain fatty acid production in a porcine gut microbiota. *Benef. Microb.* 11, 591–610. doi: 10.3920/bm2020.Q210006

Long, C., de Vries, S., and Venema, K. (2020c). Differently pre-treated rapeseed meals affect *in vitro* swine gut Microbiota composition. *Front. Microbiol.* 11. doi: 10.3389/fmicb.2020.570985

Long, C., Rösch, C., de Vries, S., Schols, H. A., and Venema, K. (2020b). Cellulase and alkaline treatment improves intestinal microbial degradation of recalcitrant fibres of rapeseed meal in pigs. *J. Agr. Food Chem.* doi: 10.1021/acs.jafc.0c03618

Luis, A. S., Briggs, J., Zhang, X., Farnell, B., Ndeh, D., Labourel, A., et al. (2018). Dietary pectic glycans are degraded by coordinated enzyme pathways in human colonic Bacteroides. *Nat. Microbiol.* 3, 210–219. doi: 10.1038/s41564-017-0079-1

Mao, S., Zhang, M., Liu, J., and Zhu, W. (2015). Characterising the bacterial microbiota across the gastrointestinal tracts of dairy cattle: membership and potential function. *Sci. Rep.* 5:16116. doi: 10.1038/srep16116

Meale, S. J., Beauchemin, K. A., Hristov, A. N., Chaves, A. V., and McAllister, T. A. (2014). Board-invited review: opportunities and challenges in using exogenous enzymes to improve ruminant production. *Anim. Sci. J.* 92, 427–442. doi: 10.2527/jas.2013-6869

Milani, C., Lugli, G. A., Duranti, S., Turroni, F., Mancabelli, L., Ferrario, C., et al. (2015). Bifidobacteria exhibit social behavior through carbohydrate resource sharing in the gut. *Sci. Rep.* 5:15782. doi: 10.1038/srep15782

Minekus, M., Smeets-Peeters, M., Bernalier, A., Marol-Bonnin, S., Havenaar, R., Marteau, P., et al. (1999). A computer-controlled system to simulate conditions of the large intestine with peristaltic mixing, water absorption and absorption of fermentation products. *Appl. Microbiol. Biotechnol.* 53, 108–114. doi: 10.1007/s002530051622

Miron, J., Ben-Ghedalia, D., and Morrison, M. (2001). Invited review: adhesion mechanisms of rumen cellulolytic bacteria. *J. Dairy Sci.* 84, 1294–1309. doi: 10.3168/jds.S0022-0302(01)70159-2

Morotomi, M., Nagai, F., and Watanabe, Y. (2012). Description of *Christensenella* minuta gen. nov., sp. nov., isolated from human faeces, which forms a distinct branch in the order *Clostridiales*, and proposal of *Christensenellaceae* fam. nov. *Int. J. Syst. Evol. Microbiol.* 62, 144–149. doi: 10.1099/ijs.0.026989-0

Nyonyo, T., Shinkai, T., and Mitsumori, M. (2014). Improved culturability of cellulolytic rumen bacteria and phylogenetic diversity of culturable cellulolytic and xylanolytic bacteria newly isolated from the bovine rumen. *FEMS Microbiol. Ecol.* 88, 528–537. doi: 10.1111/1574-6941.12318

Oechslin, R., Lutz, M. V., and Amadò, R. (2003). Pectic substances isolated from apple cellulosic residue: structural characterisation of a new type of rhamnogalacturonan I. *Carbohydr. Polym.* 51, 301–310. doi: 10.1016/S0144-8617(02)00214-X

Parks, D. H., Tyson, G. W., Hugenholtz, P., and Beiko, R. G. (2014). STAMP: statistical analysis of taxonomic and functional profiles. *Bioinformatics* 30, 3123–3124. doi: 10.1093/bioinformatics/btu494

Pattathil, S., Avci, U., Baldwin, D., Swennes, A. G., McGill, J. A., Popper, Z., et al. (2010). A comprehensive toolkit of plant cell wall glycan-directed monoclonal antibodies. *Plant Physiol.* 153, 514–525. doi: 10.1104/pp.109.151985

Pattathil, S., Avci, U., Miller, J. S., and Hahn, M. G. (2012). Immunological approaches to plant cell wall and biomass characterization: glycome profiling. *Methods Mol. Biol.* 908, 61–72.

Pauly, M., Albersheim, P., Darvill, A., and York, W. S. (1999). Molecular domains of the cellulose/xyloglucan network in the cell walls of higher plants. *Plant J.* 20, 629–639. doi: 10.1046/j.1365-313X.1999.00630.x

Pettipher, G. L., and Latham, M. J. (1979). Production of enzymes degrading plant cell walls and fermentation of cellobiose by *Ruminococcus flavefaciens* in batch and continuous culture. *Microbiology* 110, 29–38. doi: 10.1099/00221287-110-1-29

Pustjens, A. M., de Vries, S., Gerrits, W. J., Kabel, M. A., Schols, H. A., and Gruppen, H. (2012). Residual carbohydrates from in vitro digested processed rapeseed (*Brassica napus*) meal. *J. Agric. Food Chem.* 60, 8257–8263. doi: 10.1021/jf301160m

Pustjens, A. M., de Vries, S., Schols, H. A., Gruppen, H., Gerrits, W. J., and Kabel, M. A. (2014). Understanding carbohydrate structures fermented or resistant to fermentation in broilers fed rapeseed (*Brassica napus*) meal to evaluate the effect of acid treatment and enzyme addition. *Poult. Sci.* 93, 926–934. doi: 10.3382/ps.2013-03519

Pustjens, A. M., Schols, H. A., Kabel, M. A., and Gruppen, H. (2013). Characterisation of cell wall polysaccharides from rapeseed (*Brassica napus*) meal. *Carbohydr. Polym.* 98, 1650–1656. doi: 10.1016/j.carbpol.2013.07.059

Ribeiro, G. O., Badhan, A., Huang, J., Beauchemin, K. A., Yang, W., et al. (2018). New recombinant fibrolytic enzymes for improved in vitro ruminal fiber degradability of barley straw. *Anim. Sci.* 96, 3928–3942. doi: 10.1093/jas/sky251

Ribeiro, G. O., Gonçalves, L. C., Pereira, L. G. R., Chaves, A. V., Wang, Y., Beauchemin, K. A., et al. (2015). Effect of fibrolytic enzymes added to a *Andropogon gayanus* grass silage-concentrate diet on rumen fermentation in batch cultures and the artificial rumen (Rusitec). *Animal* 9, 1153–1162. doi: 10.1017/S1751731115000221

Ribeiro, G. O., Gruninger, R. J., Jones, D. R., Beauchemin, K. A., Yang, W. Z., Wang, et al. (2020). Effect of ammonia fiber expansion-treated wheat straw and a recombinant fibrolytic enzyme on rumen microbiota and fermentation parameters, total tract digestibility, and performance of lambs. *Anim. Sci.* 98:skaa116. doi: 10.1093/jas/skaa116

Sáyago-Ayerdi, S. G., Zamora-Gasga, V. M., and Venema, K. (2017). Prebiotic effect of predigested mango peel on gut microbiota assessed in a dynamic in vitro model of the human colon (TIM-2). *Food Res. Int.* 118, 89–95. doi: 10.1016/j.foodres.2017.12.024

Shinkai, T., and Kobayashi, Y. (2007). Localization of ruminal cellulolytic bacteria on plant fibrous materials as determined by fluorescence in situ hybridization and real-time PCR. *Appl. Environ. Microbiol.* 73, 1646–1652. doi: 10.1128/AEM.01896-06

Siddiqui, I. R., and Wood, P. J. (1977). Carbohydrates of rapeseed: a review. *J. Sci. Food Agric.* 28, 530–538. doi: 10.1002/jsfa.2740280610

Simbaya, J., Slominski, B. A., Rakow, G., Campbell, L. D., Downey, R. K., and Bell, J. M. (1995). Quality characteristics of yellow-seeded Brassica seed meals: Protein, carbohydrate, and dietary fiber components. *J. Agric. Food Chem.* 43, 2062–2066. doi: 10.1021/jf00056a020

Slominski, B. A., and Campbell, L. D. (1990). Non-starch polysaccharides of canola meal: quantification, digestibility in poultry and potential benefit of dietary enzyme supplementation. *J. Sci. Food Agric.* 53, 175–184. doi: 10.1002/jsfa.2740530205

Torok, V. A., Ophel-Keller, K., Loo, M., and Hughes, R. J. (2008). Application of methods for identifying broiler chicken gut bacterial species linked with increased energy metabolism. *Appl. Environ. Microbiol.* 74, 783–791. doi: 10.1128/AEM.01384-07

Turroni, F., Milani, C., Duranti, S., Mancabelli, L., Mangifesta, M., Viappiani, A., et al. (2016). Deciphering bifidobacterial-mediated metabolic interactions and their impact on gut microbiota by a multi-omics approach. *ISME J.* 10, 1656–1668. doi: 10.1038/ismej.2015.236

Turroni, F., Özcan, E., Milani, C., Mancabelli, L., Viappiani, A., van Sinderen, D., et al. (2015). Glycan cross-feeding activities between bifidobacteria under *in vitro* conditions. *Front. Microbiol.* 6:1030. doi: 10.3389/fmicb.2015.01030

Wang, Y., McAllister, T. A., Rode, L. M., Beauchemin, K. A., Morgavi, D. P., Nsereko, V. L., et al. (2001). Effects of an exogenous enzyme preparation on microbial protein synthesis, enzyme activity and attachment to feed in the Rumen Simulation Technique (Rusitec). *Br. J Nutr.* 85, 325–332. doi: 10.1079/BJN2000277

Yatsunenko, T., Rey, F. E., Manary, M. J., Trehan, I., Dominguez-Bello, M. G., Contreras, M., et al. (2012). Human gut microbiome viewed across age and geography. *Nature* 486, 222–227. doi: 10.1038/nature11053

Conflict of Interest: The authors declare that the research was conducted in the absence of any commercial or financial relationships that could be construed as a potential conflict of interest.

frontiers in Microbiology

ORIGINAL RESEARCH
published: 21 December 2020
doi: 10.3389/fmicb.2020.585428

Conversion of Rutin, a Prevalent Dietary Flavonol, by the Human Gut Microbiota

*Alessandra Riva[1], Ditta Kolimár[2], Andreas Spittler[3], Lukas Wisgrill[4], Craig W. Herbold[1], László Abrankó[2] and David Berry[1,5]**

[1] Centre for Microbiology and Environmental Systems Science, Department of Microbiology and Ecosystem Science, Division of Microbial Ecology, University of Vienna, Vienna, Austria, [2] Faculty of Food Science, Department of Applied Chemistry, Szent István University, Budapest, Hungary, [3] Core Facility Flow Cytometry, Department of Surgery, Research Lab, Medical University of Vienna, Vienna, Austria, [4] Division of Neonatology, Pediatric Intensive Care and Neuropediatrics, Department of Pediatrics and Adolescent Medicine, Medical University of Vienna, Vienna, Austria, [5] Joint Microbiome Facility of the Medical University of Vienna and the University of Vienna, Vienna, Austria

The gut microbiota plays a pivotal role in the conversion of dietary flavonoids, which can affect their bioavailability and bioactivity and thereby their health-promoting properties. The ability of flavonoids to metabolically-activate the microbiota has, however, not been systematically evaluated. In the present study, we used a fluorescence-based single-cell activity measure [biorthogonal non-canonical ammino acid-tagging (BONCAT)] combined with fluorescence activated cell sorting (FACS) to determine which microorganisms are metabolically-active after amendment of the flavonoid rutin. We performed anaerobic incubations of human fecal microbiota amended with rutin and in the presence of the cellular activity marker L-azidohomoalanine (AHA) to detect metabolically-active cells. We found that 7.3% of cells in the gut microbiota were active after a 6 h incubation and 26.9% after 24 h. We then sorted BONCAT-positive cells and observed an enrichment of *Lachnospiraceae* (*Lachnoclostridium* and *Eisenbergiella*), *Enterobacteriaceae, Tannerellaceae*, and *Erysipelotrichaceae* species in the rutin-responsive fraction of the microbiota. There was marked inter-individual variability in the appearance of rutin conversion products after incubation with rutin. Consistent with this, there was substantial variability in the abundance of rutin-responsive microbiota among different individuals. Specifically, we observed that *Enterobacteriaceae* were associated with conversion of rutin into quercetin-3-glucoside (Q-glc) and *Lachnospiraceae* were associated with quercetin (Q) production. This suggests that individual microbiotas differ in their ability to metabolize rutin and utilize different conversion pathways.

Keywords: dietary bioactives, rutin, gut microbiota, fluorescence activated cell sorting, rutin metabolism, inter-individual variability

OPEN ACCESS

Edited by:
M. Pilar Francino, Fundación para el Fomento de la Investigación Sanitaria y Biomédica de la Comunitat Valenciana (FISABIO), Spain

Reviewed by:
Federico Rey, University of Wisconsin-Madison, United States
Stefano Raimondi, University of Modena and Reggio Emilia, Italy

***Correspondence:**
David Berry
david.berry@univie.ac.at;
berry@microbial-ecology.net

Specialty section:
This article was submitted to Microbial Symbioses, a section of the journal Frontiers in Microbiology

Received: *20 July 2020*
Accepted: *02 December 2020*
Published: *21 December 2020*

Citation:
Riva A, Kolimár D, Spittler A, Wisgrill L, Herbold CW, Abrankó L and Berry D (2020) Conversion of Rutin, a Prevalent Dietary Flavonol, by the Human Gut Microbiota. Front. Microbiol. 11:585428. doi: 10.3389/fmicb.2020.585428

INTRODUCTION

Flavonoids are a group of bioactive polyphenolic compounds present in a wide variety of plant-based foodstuffs. Rutin (Q-3-*O*-rutinoside) is a flavonol glycoside composed of Q and rutinose, a disaccharide of rhamnose and glucose, and represents the most consumed flavonol (3.75% in Europe and in the United Kingdom) (Zamora-Ros et al., 2016). Dietary sources of rutin include tea,

Abbreviations: FACS, fluorescence activated cell sorting; Q, quercetin; Q-glc, quercetin-3-glucoside.

green asparagus, onions, buckwheat, wine, eucalyptus, apples, as well as berries (de Araujo et al., 2013; Kumar and Pandey, 2013; Amaretti et al., 2015). Rutin has been shown to have anti-oxidant properties (Ghorbani, 2017) and to exert anti-aging effects on human dermal fibroblasts and human skin (Choi et al., 2016). It also has anti-neurodegenerative properties (Enogieru et al., 2018) and exhibits protective effects against hyperglycemia, dyslipidemia, liver damage, and cardiovascular disorders (Ghorbani, 2017). Additionally, the rutin degradation products Q-glc and Q have been found to have anti-inflammatory, anti-oxidant, and anti-mutagenic properties (Gibellini et al., 2011; Kumar and Pandey, 2013; Hobbs et al., 2018). Q-glc also possesses anti-hypertensive, hypolipidemic effects (Gibellini et al., 2011; Kumar and Pandey, 2013; Hobbs et al., 2018) and Q has been reported to ameliorate atherosclerosis and dyslipidemia (Salvamani et al., 2014).

The bioavailability of these dietary flavonoids depends on intestinal absorption, which is determined by their chemical composition and, in particular, by the nature of glycosylation (Matsumoto et al., 2004). The glyco-conjugates of Q are poorly absorbed in the upper intestinal tract and accumulate in the large intestine. In the colon, members of the gut microbiota can hydrolyze rutin or other glyco-conjugates, removing the sugar moiety and permitting the absorption of the aglycone (Cardona et al., 2013; Amaretti et al., 2015). Therefore, the colonic microbiota is responsible for the extensive breakdown of the original flavonoid structures into low-molecular-weight phenolic metabolites (Cardona et al., 2013). Currently, it is estimated that 500–1000 different microbial species inhabit the gastrointestinal tract, reaching the highest concentration in the colon (up to 10^{12} cells per gram of feces) (Thursby and Juge, 2017). Bacteria that metabolize rutin possess α-rhamnosidases that transform rutin into Q-glc and/or β-glucosidases that either convert Q-glc into Q (Braune and Blaut, 2016) or convert rutin directly into Q (Olthof et al., 2003). A limited number of bacteria have so-far been shown to have rutin-metabolizing capabilities in pure culture. α-rhamnosidases involved in deglycosylation of flavonoids have been characterized in *Lactobacillus acidophilus*, *Lactobacillus plantarum* (Beekwilder et al., 2009), and *Bifidobacterium dentium* (Bang et al., 2015). The capability to degrade rutin into Q was reported for *Bacteroides uniformis*, *Bacteroides ovatus* (Bokkenheuser et al., 1987), and *Enterococcus avium* (Shin et al., 2016). *Parabacteroides distasonis* was shown produce both Q-glc and Q via α-rhamnosidase and β-glucosidase activity (Bokkenheuser et al., 1987), and *Eubacterium ramulus* and *Enterococcus casseliflavus* are able to convert Q-glc in Q (Schneider et al., 1999).

Previous studies of rutin conversion by gut bacteria have involved screening strain collections, which gives limited insight into identifying which bacteria are actually involved in metabolizing rutin in the complex gut microbial community. In the present study, we identified cells in the gut microbiota that became metabolically-active upon rutin amendment using the cellular activity marker L-azidohomoalanine (AHA). By sorting active cells and profiling active and total communities using 16S rRNA gene amplicon sequencing, we were able to identify specific taxa enriched in rutin-treated samples. We observed marked inter-individual variability in both the extent of rutin degradation product formation as well as the abundance of the rutin-responsive microbial community. Our findings present new insights into rutin metabolism by different microbiotas in healthy individuals, which will be useful for future studies on flavonol metabolism in health as well as in disease conditions.

MATERIALS AND METHODS

Sample Collection

Fresh fecal samples were collected from 10 healthy subjects (seven females and three males, age mean ± SD:30.5 ± 5.8; BMI:mean ± SD: 22.19 ± 2.9). All participants followed an omnivore diet. Participants with antibiotic, probiotic, or prebiotic usage in the previous 6 months were excluded. The study was approved by, and conducted in accordance, with the University of Vienna ethics committee (Reference number 00161) and written informed consent was signed by all enrolled participants.

Anaerobic Incubations

Fresh stool samples were immediately introduced into an anaerobic tent (85% N_2, 10% CO_2, 5% H_2). All reagents were introduced into the anaerobic tent 2 days before the experiment to ensure that they were anaerobic by the start of the experiment. 10 mL phosphate-buffered saline (PBS) was added to 1 g of fecal sample. The suspension was homogenized by vigorous shaking and vortexing. Samples were left for 15 min to allow large particles to settle and subsequentally serially-diluted 1:10 twice. The serial 1:10 dilutions were necessary to avoid background noise and autofluorescence in the Cy5 [biorthogonal non-canonical ammino acid-tagging (BONCAT)] signal. Samples were incubated in autoclaved Hungate tubes in the presence of 1 mM of the non-canonical amino acid *L*-AHA (baseclick GmbH, Germany) and 500 μM rutin dissolved in dimethyl sulfoxide (DMSO; Sigma–Aldrich). A negative control containing DMSO and a positive control with 2 mg/mL of glucose were used for each experiment. An abiotic control for each time point was included to assess the chemical stability of rutin under the incubation conditions. Samples were incubated under anaerobic condition with a final volume of 5 mL for 0, 6, or 24 h. Subsequently, samples were centrifuged at 14,000 r/min for 10 min and the supernatant was collected and diluted with equal volume of pure acetonitrile (ACN) in order to stabilize the supernatant samples and then stored at −20°C for liquid chromatography-high resolution mass spectrometry (LC-HRMS) analysis. Part of the sample was frozen for nucleic acid extraction and part was washed twice in PBS and then fixed in 1:1 ethanol:PBS for FACS sorting.

Liquid Chromatography-High Resolution Mass Spectrometry (LC-HRMS)

Acetonitrile (LC-MS grade) and formic acid were purchased from VWR. High purity water (18.2 MΩ cm^{-1}) was used for dilution of samples and the preparation of mobile phases (Milli-Q Synergy/Elix water purification system, Merck).

Authentic reference standards of rutin, Q-3-*O*-glucoside and Q were purchased from Sigma–Aldrich (>94%, HPLC) and Extrasynthese (>99%, HPLC), respectively. Supernatants from the incubations were immediately centrifuged and aliquots for HPLC analysis were removed and equal volume of ACN was added. Samples were kept frozen until analysis. The ACN-stabilized samples were thawed and homogenized by vortexing. 100 μL was diluted 1:4 in water to decrease ACN content to 10%. The diluted sample was filtered through a 0.22 μm pore polytetrafluoroethylene syringe filter (Cronus, LabHut Ltd.), and 5 μL were injected into the LC system. Chromatographic separation was achieved on a Phenomenex Kinetex EVO C18 100 × 2.1 mm, 2.6 μm column utilizing an Agilent 1200 HPLC system. The column was operated at 30°C. The binary mobile phase consisted of H_2O with 0.1% formic acid (eluent A) and ACN (eluent B). The flow rate was set to 0.4 mL min^{-1}. Gradient separation was started at 5% B and linearly increased to reach 90% in 9 min. The eluent was kept constant at 90% B until 11.5 min and then the column was re-equilibrated at the initial conditions for 11.5 min. The effluent of the LC system was connected to an Agilent 6530 high-resolution, accurate mass quadrupole/time-of-flight mass spectrometer equipped with a dual sprayer electrospray ion source (ESI-Q/TOFMS). The mass spectrometry was run in full scan (MS-only) mode scanning from *m/z* 50–1700 in negative ionization mode. A continuous reference mass correction was applied using purine and HP-921 [Hexakis(1H,1H,3H-perfluoropropoxy)phosphazene] as reference substances. The ion source temperature was maintained at 325°C and capillary and fragmentor voltages were set to −4000 and 140 V, respectively. The Mass Hunter Workstation software package (B02.01) was used for data acquisition and data evaluation. Quantification of rutin, Q glucoside, and Q was performed with external calibration using reference standards.

BONCAT Labeling of Microbial Cells

Cu(I)-catalyzed click labeling of chemically-fixed microbial cells was performed on slides as described previously (Hatzenpichler et al., 2014). Briefly, fixed samples were immobilized on glass slides, dried in a 46°C hybridization oven, and dehydrated and permeabilized by placing slides for 3 min sequentially in 50, 80, and 96% ethanol. Then, 1.25 μL of 20 mM CuSO4, 2.50 μL of 50 mM tris[(1-hydroxypropyl-1H-1,2,3-triazol-4-yl)methyl]amine (THPTA) (baseclick GmbH, Germany), and 0.30 μL of alkyne dye (in DMSO) (Jena Bioscience, Germany) were mixed and allowed to react for 3 min at room temperature (RT) in the dark. In the meantime, 12.5 μL of freshly-prepared 100 mM sodium ascorbate (Sigma–Aldrich) and 12.5 μL of 100 mM aminoguanidine hydrochloride (Sigma–Aldrich) were added to 221 μL 1 × PBS (pH 7.4). Then, the dye premix was added to this solution, the tube inverted once and samples were covered by 30 μL of solution. Slides were transferred into a humid chamber and incubated in the dark at RT for 30 min. Afterward, slides were washed three times for 3 min each in 1 × PBS and then treated with an increasing ethanol series (3 min each in 50, 80, and 96% ethanol) and air-dried (Hatzenpichler et al., 2014). 1:1000 DNA stain, 4′, 6 diamidino-2-phenylindole (DAPI) solution (in PBS), was applied for 5 min and then slides were washed in cold MILLI-Q water (Millipore GmbH, Vienna, Austria). Samples were embedded with CitiFluor (Agar Scientific Ltd., Stansted, United Kingdom) if used immediately or stored at −20°C. Representative BONCAT pictures of a fecal sample incubated with rutin at 6 and 24 h and a negative control containing DMSO are shown in **Supplementary Figure 1**. Representative BONCAT picture of a fecal sample incubated with the glucose positive control is shown in **Supplementary Figure 2**. For FACS sorting, in-solution click labeling was performed immediately before FACS sorting. For click labeling, 300–500 μL fixed samples were centrifuged at 10,000 r/min for 10 min and re-suspended in 96% ethanol. The pellet was left for 3 min at RT and then centrifuged 10,000 r/min for 5 min. A master mix containing the dye solution was prepared as described above. Samples were suspended in 60–100 μL of solution and incubated in the dark at RT for 30 min. Afterward, samples were washed three times by centrifugation with 1x PBS (Hatzenpichler et al., 2014). Immediately before sorting, samples were filtered with a 35 μm nylon mesh using BD tubes 12 × 75 mm (BD, Germany).

Image Acquisition and Analysis

20–30 images were collected for each sample with an epifluoresce microscope (Zeiss-Axio-imager, Germany). Image analysis was performed using the software *digital image analysis in microbial ecology* (Daime) and the biovolume fraction, the fraction of BONCAT-labeled biomass (Cy5-labeled) relative to the total biomass (DAPI-labeled), was calculated (Daims et al., 2006).

Fluorescence Activated Cell Sorting (FACS)

For flow cytometry sorting, bacteria were labeled in Cy5 dye as previously described, and analyzed on an ultra high-speed cell sorter MoFlo Astrios EQ (Beckman Coulter, Brea, CA, United States) using the Summit v6.2 software (Beckman Coulter). To standardize the daily measurement and to assess the size of the bacteria, calibration beads (silica beads 100, 500, and 1000 nm, Kisker Biotech, Steinfurt, Germany) having a refractive index close to biological material were recorded. The sorting of Cy5-labeled bacteria was performed as follows: In a first scatter plot, the 561 nm SSC Height-Log parameter was set vs. the 488 nm FSC1 Height-Log parameter. To reduce electronic noise, the triggering signal was set on the 561 nm SSC parameter. A second dot plot 488 nm FSC1-Height-Log vs. 488 nm SSC-Height-Log showed in a first measurement the different sizes of the silica beads and in the following measurements the scattering of the bacteria. Bacteria were then pre-gated and displayed on a third scatter plot with 488 nm SSC area log axes vs. 640 nm 671/30-Area-Log axes. Cy5-positive bacteria were then sorted out into tubes with a maximum event rate of 50,000 events per second. Reanalysis of the samples showed a purity of >99%. An overview of the gating strategy and FACS selectivity analysis is shown in **Supplementary Figures 3**, **4**. In order to assess the technical reproducibility of the method, absolute cell count was performed with the cell sorter FACS Melody (BD, Germany) and BONCAT-positive cells were counted in triplicate for each sample (**Supplementary Figures 5A,B**). Absolute

counting beads (CountBright™, Invitrogen, ThermoFisher Scientific, Austria) were used for cell counts according to the manufacturer's instructions.

DNA Extraction and 16S rRNA Gene Amplicon Sequencing

DNA extraction was performed for both total microbial community and the FACS-sorted fraction using the QiAmp mini DNA extraction kit (Qiagen) following the protocols for bacteria according to the manufacturer's instructions. PCR amplification was performed with a two-step barcoding approach according to Herbold et al. (2015) using 16S rRNA gene primers targeting most bacteria (V3–V4 region of the 16S rRNA gene) (S-D-Bact-0341-b-S-17 [5′-CCTACGGGNGGCWGCAG-3′] and S-D-Bact-0785-a-A-21 [5′-GACTACHVGGGTATCTAATCC-3′]. The barcoded amplicons were purified with ZR-96 DNA Clean-up Kit (Zymo Research, United States) and quantified using the Quant-iT™ PicoGreen® dsDNA Assay (Invitrogen, United States) (Herbold et al., 2015). An equimolar library was constructed by pooling samples, and the resulting library was sent for sequencing on the Illumina MiSeq platform at Microsynth AG (Balgach, Switzerland).

Sequence Processing and Data Analysis

16S rRNA gene sequence data were sorted into libraries according to Herbold et al. (2015) and processed into amplicon sequence variants (ASVs) using the Divisive Amplicon Denoising Algorithm (DADA2) (Callahan et al., 2016) and classified using the RDP classifier (Wang et al., 2007) as implemented in Mothur (Schloss et al., 2009). Sequencing libraries were subsampled to a smaller number of reads than the smallest library (subsampled to 1000 reads) to avoid biases related to uneven library depth. 1000 reads were sufficient to maintain a high coverage per library (mean Good's coverage: 99%). 16S rRNA gene sequence data have been deposited in the NCBI Short Read Archive under PRJNA622517. Statistical analysis was performed using R statistical software[1]. Statistical analysis to compare samples groups was performed using ANOVA, and with the R package DEseq2 (Love et al., 2014). The statistical significance of factors affecting microbiota composition was evaluated using non-parametric permutational multivariate analysis of variance (perMANOVA), significant clustering of groups was evaluated with analysis of similarities (ANOSIM), ordination was performed using redundancy analysis (RDA) and non-metric multidimensional scaling (NMDS) in the vegan package in R (Oksanen et al., 2010). Relative standard deviation (RSD) was calculated as standard deviation (SD)/mean to determine inter-individual variability across participants. Microbial community variation within participant was further determined using the UpSetR package in R, which employs a matrix-based layout to show intersections of sets and their sizes (Conway et al., 2017). Alpha and beta diversity metrics were also calculated with the vegan package. Variables are expressed as mean ± SD. A probability value (p-value) less than 0.05 was considered statistically significant and p-values were adjusted with the false discovery rate (FDR) method in the case of multiple comparison. Statistical analysis to compare producer groups was performed using ANOVA and Tukey test for multiple comparisons.

Screening Bacterial Genomes for Alpha-Rhamnosidase Genes

Uniprot[2] was queried using "alpha-L-rhamnosidase" as a query and filtered for "reviewed" entries. Entries were manually examined for confirmation of activity and to compile pfam motifs (El-Gebali et al., 2019). A single pfam motif, Bac_rhamnosid6H (PF17389), was common to all genes with confirmed alpha-rhamnosidase activity. Uniprot was subsequently queried using PF17389 and filtered for "reviewed" entries to determine specificity. All reviewed entries for PF17389 possessed confirmed alpha-rhamnosidase activity. All publicly-available genomes available at NCBI as 24 September 2020 (N = 268,330) were screened using PF17389 with hmmsearch (hmmer3[3]) and genes matching the pfam ($E < 10^{-6}$ and alignment over at least 300 amino acids) were extracted from the genomes. All extracted genes were back-screened against the Pfam-A database with hmmscan (hmmer3) and only those genes that matched PF17389 as a best-hit were retained as putative alpha-rhamnosidase. Genus-level assignments were inferred by string-matching genus labels (e.g., *Escherichia*) to the organism name associated to each searched genome.

RESULTS

Biotransformation of Rutin by the Gut Microbiota

In order to characterize the biotransformation of rutin by the gut microbiota and to identify metabolically-active bacteria after rutin amendment, we performed anaerobic incubations of freshly-collected stool contents amended with 500 μM rutin (**Figure 1**). This concentration is in line with previous studies and is consistent with a reasonable dietary intake (Amaretti et al., 2015; Zamora-Ros et al., 2016). Over the course of the incubations, there was a slight but not statistically-significant reduction in rutin (one-way ANOVA, p = 0.41, n = 10, molar recovery: 97%; **Figure 2A**), probably caused by the high dilution applied in the anaerobic incubation. However, Q-glc and Q appeared after incubation with biomass (p = 0.019 and 0.036 for Q-glc and Q, respectively, n = 10; **Figures 2B,C**), indicating that rutin was actively transformed by the gut microbiota. Low levels of Q-glc were present in all time zero samples (**Figure 2B**), which may be because rutin preparations were either not completely purified or chemically degraded to Q-glc during storage. Interestingly, there was substantial variation in the amount of Q-glc and Q formed during incubation with the gut microbiota, suggesting considerable inter-individual variability in the capacity to metabolize rutin by different gut microbial communities (**Figures 2D,E**). Moreover, we have screened

[1]https://www.r-project.org/

[2]https://www.uniprot.org

[3]http://hmmer.org/

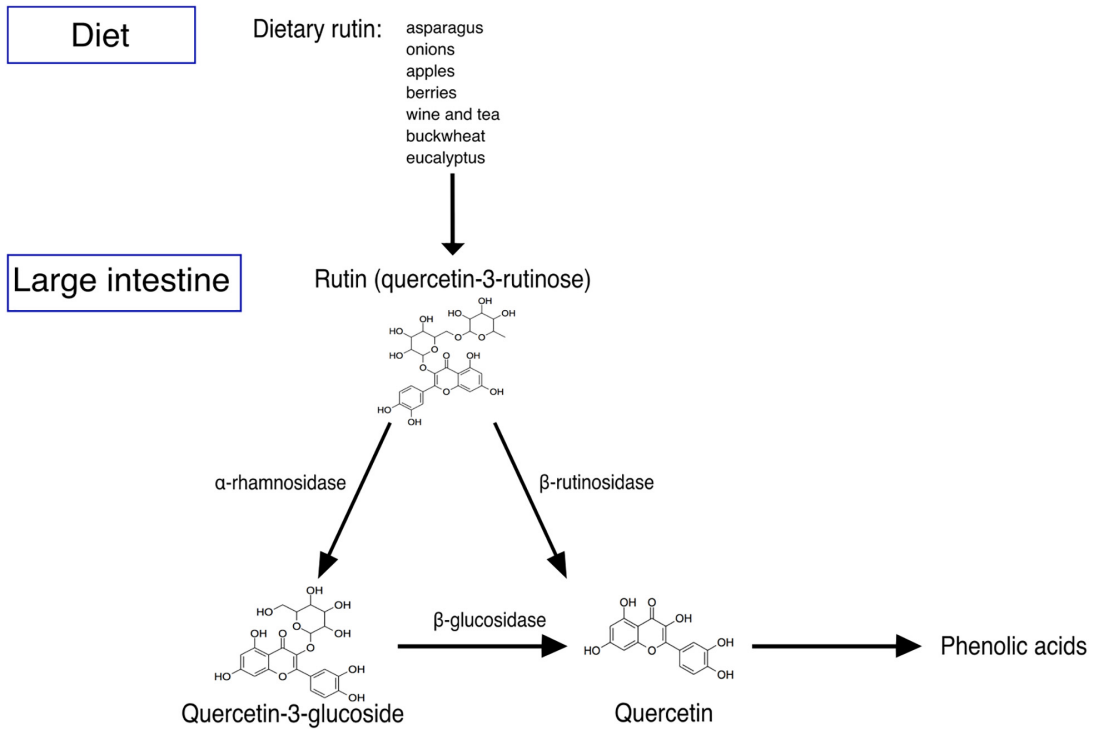

FIGURE 1 | Schematic representation of rutin degradation. Rutin is present in a wide variety of foods. Rutin is not well absorbed in the small intestine of humans, and thus is transported into the colon and metabolized by the gut microbiota into quercetin-3-glucoside and then quercetin or directly into quercetin. Quercetin may be subsequently degraded mainly into different phenolic acids.

the samples for some known Q metabolites (dihydroxyphenyl propionic acid hydroxyphenylacetic acid, dihydroxyphenylacetic acid, dihydroxybenzoic acid, hydroxybenzoic acid) and only a few samples showed hits and only with minor signals. Therefore, these hits and suspected metabolites were not included in the data evaluation.

The Core Metabolically-Active Microbiota in Rutin Amendments

As the capacity of dietary polyphenols to modulate the activity and/or composition of the gut microbiota is still poorly understood, we aimed to identify the metabolically-active microbial taxa upon rutin amendment. Rutin amendment activated a subset of the microbiota, and active cells were detected in almost all samples after 6 h of incubation with rutin, with an increasing number after 24 h (6 h: 7.3 ± 7.3%, 24 h: 26.9 ± 11.7% [mean ± SD]; *t*-test: $p = 0.0003$, $n = 20$) (**Figures 3A,B**). The diversity and the composition of the total microbial community did not change significantly during the short-term incubations (**Figures 4A,B**; perMANOVA, $p = 0.99$), indicating that the applied incubation conditions did not appreciably modify the composition of the microbiota (i.e., there was no strong "bottle effect"). However, the rutin-active fraction of the community, as determined by BONCAT activity labeling and FACS sorting, was significantly different from the total community. The diversity of the active fraction was lower than the total community (ANOVA, $p < 0.0001$ for the alpha diversity metrics; **Figure 4A**), and the NMDS ordination showed a clear separation of samples between the total community and the active fraction (perMANOVA, $p < 0.0001$; ANOSIM, $p = 0.001$) (**Figure 4B**). The most abundant taxa detected in the active fraction were *Bacteroidaceae*, *Enterobacteriaceae*, *Lachnospiraceae*, *Tannerellaceae*, and *Ruminococcaceae* (**Figure 5**). We found that members of the *Enterobacteriaceae* (*Escherichia/Shigella*), *Tannerellaceae* (*Parabacteroides*), *Erysipelotrichaceae* (*Erysipelatoclostridium*), and *Lachnospiraceae* (*Lachnoclostridium* and *Eisenbergiella*) were significantly increased in the active fraction compared to their respective total community samples (negative binomial distribution, Wald test, $p < 0.05$, $n = 20$). We then determined the prevalence of putative alpha-rhamnosidases (Bac_rhamnosid6H [PF17389]) in publicly-available genomes belonging to genera that comprised the core rutin-active community.

We further determined the proportion of database genomes that encoded a-Rhamnosidase for rutin-active genera (**Supplementary Figure 6A**) and non-active genera (**Supplementary Figure 6B**) and, in agreement with our experimental results, we found that putative alpha-rhamnosidases are common in genomes belonging genera that responded to the rutin amendment. We then used a non-parametric test to show that genomes randomly drawn from rutin-active genera would be expected to contain an a-Rhamnosidase more often than genomes randomly drawn from rutin-non-active genera (Mann–Whitney one-tailed test,

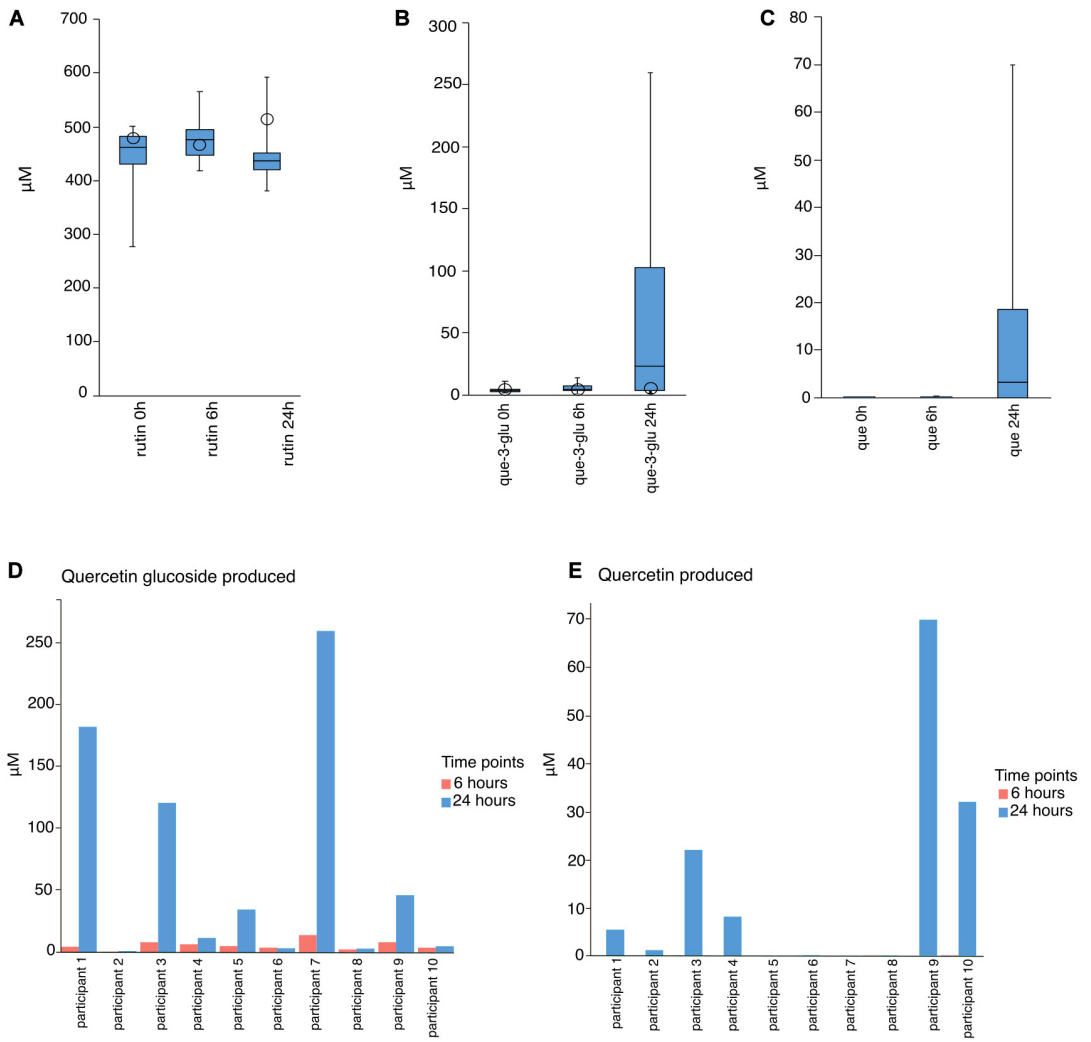

FIGURE 2 | Molar concentrations of rutin, quercetin-3-glucoside (Q-glc), and quercetin (Q) after 0, 6, and 24 h incubation. **(A–C)** Box and whisker plots of the combined results of incubation of rutin with the gut microbiota of 10 participants, as obtained from LC-HRMS analysis. Open circles indicate results of abiotic controls. **(D)** Q-glc and **(E)** Q concentrations in each incubation after 6 and 24 h.

$p = 0.041$, **Supplementary Figure 6C**), suggesting that the active genera are more likely to have database representatives that contain a-Rhamnosidase.

Microbial Community Composition Is Associated With Rutin Transformation Patterns

We observed that there was a large variability in the ASVs that were enriched in the active fraction of the community across the incubations from different donors. Only 13/97 and 23/91 ASVs were shared among all incubations at 6 and 24 h, respectively (**Supplementary Figures 7A,B**). We confirmed that the technical variability associated with the BONCAT procedure was much smaller than the observed biological variability (ANOVA; technical variation: $r^2 = 0.00085$, $p = 0.878$; biological variation: $r^2 = 0.999$, $p < 0.0001$; **Supplementary Figures 5A,B**).

We compared the inter-individual variability in the fraction of cells metabolically-activated by rutin with glucose, a compound that can be fermented by a large fraction of the gut microbiota, and found that inter-individual variability was higher in rutin amendments than glucose amendments (RSD 24 h rutin: 0.43, RSD 24 h glucose: 0.22; **Figure 3A** and **Supplementary Figure 2**). Consistent with this, we found that the microbial community varied significantly within participant in both the total community and active fraction (perMANOVA: $p < 0.0001$, **Supplementary Figures 7C,D**), which was in line with the observation that different cell morphologies were observed in the active fraction from different donors (**Figure 3B**). Though stool incubations from all participants led to the production of rutin degradation products, the pattern of rutin product formation was markedly different among different participants. We therefore divided the samples into the following groups: "High Q-glc producers," "High Q producers," and "Low producers." Based

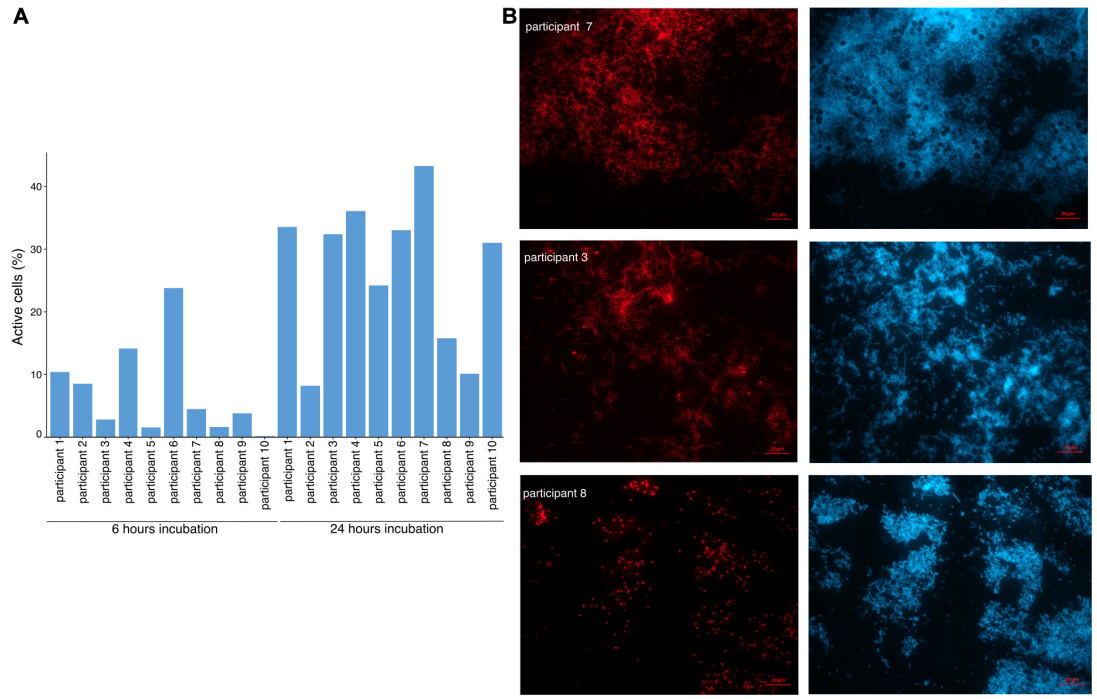

FIGURE 3 | The rutin-activated microbiota. **(A)** Relative abundance of metabolically-active cells in incubations. Relative standard deviation (RSD) was 1.0 for time 6 h and 0.43 for time 24 h. **(B)** Representative microscopic images of samples from three participants showing variability in cell morphology between donors. Active cells are represented in red (BONCAT-Cy5) and all cells are stained in blue (DAPI).

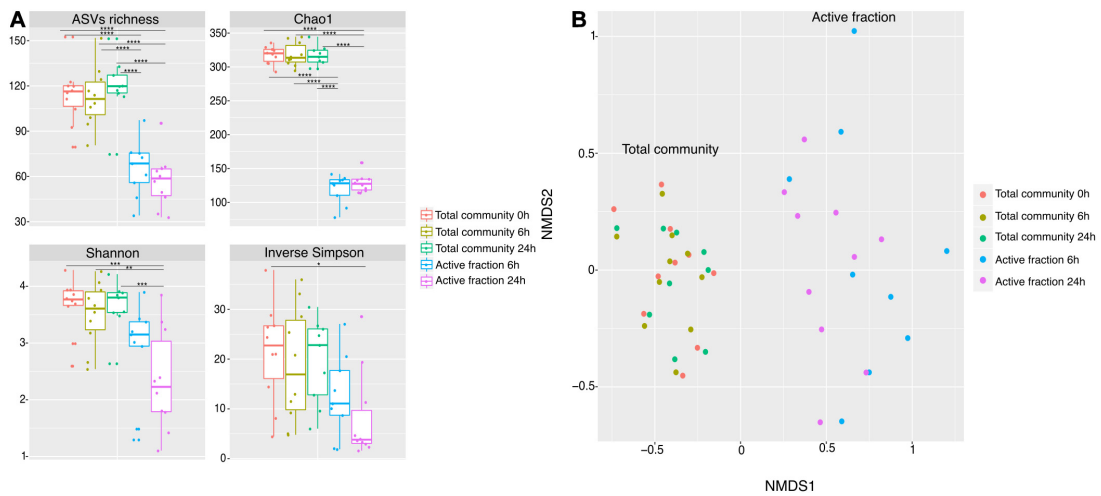

FIGURE 4 | Microbiota richness and diversity in metabolically-active community in rutin incubations. **(A)** Observed ASVs, Chao1 estimated richness, Shannon diversity, and inverse Simpson diversity estimators show significant difference between time points, active fraction and total community [ASVs richness, Chao1 and Shannon (ANOVA: $p < 0.0001$, $n = 50$), Inv. Simpson (ANOVA: $p = 0.020$, $n = 50$)]. Multiple comparisons are represented in the figure as asterisks. **(B)** NMDS ordination shows samples separation between the total community and the active fraction.

on these categories, we observed a significant clustering of both total community and active fraction samples in the RDA ordination (perMANOVA, total community: $p = 0.001$, active fraction: $p = 0.001$) (**Figures 6A,B**). In the active fraction, we observed an enrichment of *Enterobacteriaceae* (*Escherichia-Shigella*) in High Q-glc producers, and this taxon represented the majority of sequences recovered in the active fraction by 24 h (ANOVA: 0.0002, $n = 50$). In contrast, High Q producers had an enrichment of *Lachnospiraceae* (*Lachnoclostridium* and *Eisenbergiella*), which was the dominant taxon in the active fraction by 24 h (ANOVA: 0.0257, $n = 50$). Low producers had a trend, though not statistically significant,

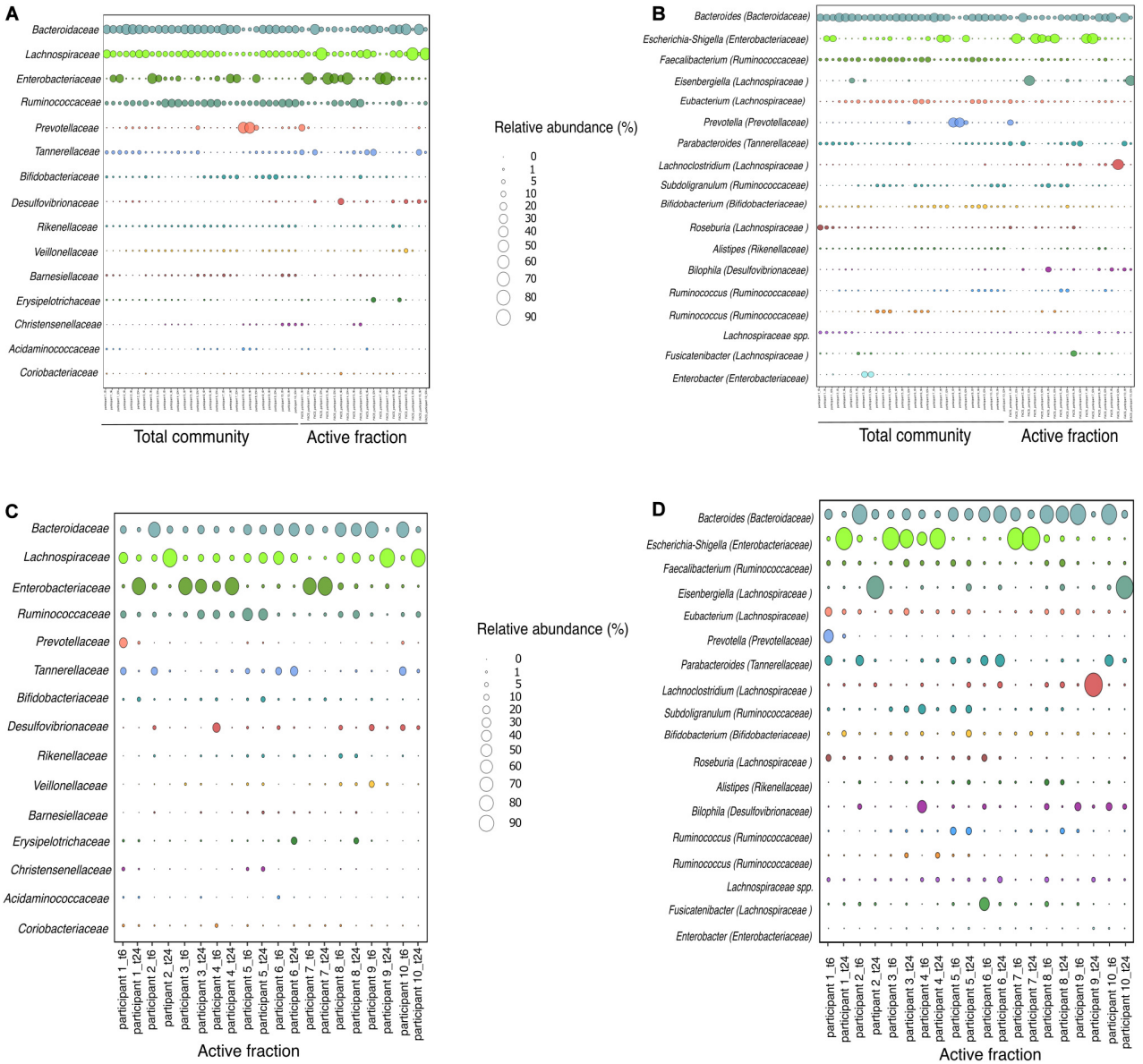

FIGURE 5 | Relative abundance of bacterial taxa based on 16S rRNA gene amplicon sequencing at family and genus level for each participant. **(A,B)** Relative abundance of the total community and the active fraction at time 6 and 24 h. **(C,D)** Relative abundance of the active fraction at time 6 or 24 h. Family and genera with relative abundance > 0.5 and > 1%, respectively, is shown.

toward enrichment in *Tannerellaceae* (*Parabacteroides*) and *Erysipelotricaceae* (*Erysipelatoclostridium*) in the active fraction (**Figure 6C** and **Supplementary Figures 6**, **8**).

DISCUSSION

The gut microbiota plays a key role in the conversion of dietary flavonoids. Though conversion of flavonoids by the microbiota has gained increasing interest (Braune and Blaut, 2016), key microbial players in flavonoid metabolism remain poorly characterized (Cardona et al., 2013). In this study, we investigated metabolism of the flavonoid rutin by the human gut microbiota. Rutin conversion products were detected in all tested donor stool incubations, but there was a dramatic variation in the amount of Q-glc and Q produced by different microbiotas. This suggests inter-individual variability in preference or capability for rutin metabolism. This is in line with a previous report of high person-to-person variation in the concentration of phenolic acids between 2 and 24 h incubation of stool with rutin (Jaganath et al., 2009).

Alpha diversity was lower in the active fraction compared to the total community, implying that a subset of the community is metabolically-activated by rutin. Indeed, we were able to identify

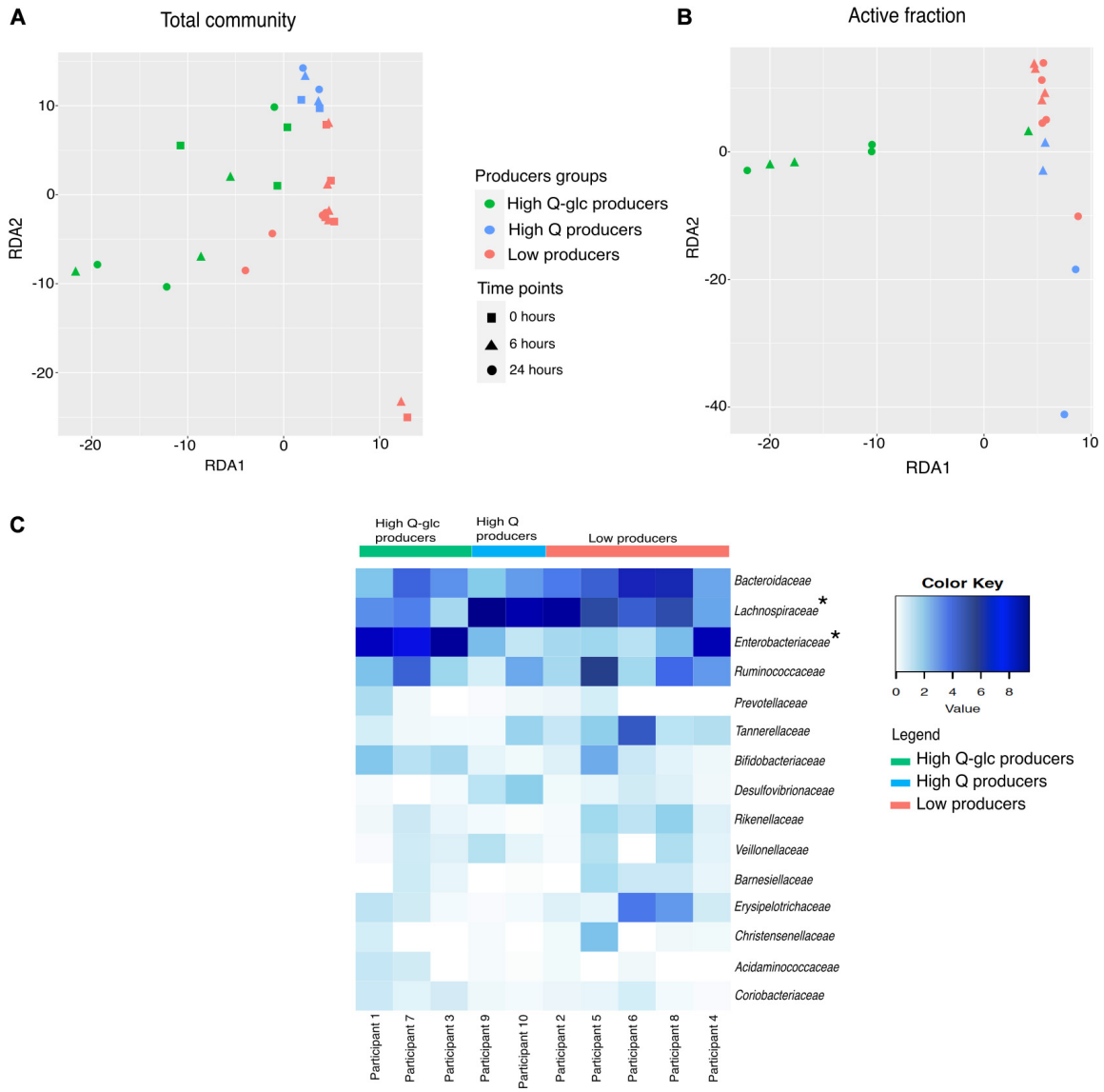

FIGURE 6 | Samples clusters based on rutin degradation pattern. Redundancy analysis shows sample clustering by degradation pattern in both the **(A)** total community [constrained variance explained:18.6%, RDA1 (14%), RDA2 (4.8%)] and **(B)** active fraction [constrained variance explained: 40.5%, RDA1 (36.3%), RDA2 (4.1%)]. **(C)** Family-level heatmap showing the square root transformed relative abundance of the active fraction divided by producer groups at 24 h. Significant changes in relative abundance (Low producers vs. High producers) are indicated with asterisks. *Enterobacteriaceae* increased in relative abundance in the High Q-glc producers. (High Q-glc producers vs. Low producers, $p = 0.0055$, High Q-glc producers vs. High-Q producers, $p = 0.0061$). *Lachnospiraceae* increased in relative abundance in the high-Q producers (High-Q producers vs. Low producers, $p = 0.0043$, High-Q producers vs. High Q-glc producers, $p < 0.00001$).

a percentage of 7.3 and 26.9% at time 6 and 24 h, respectively, of active cells with respect to the control without any amendment. Translational activity was likely still possible by these cells in the absence of additional amino acids in these short incubations via recycling of internal amino acids (Hatzenpichler et al., 2016).

In our study, the significant bacterial taxa selected are: *Lachnospiraceae* (*Lachnoclostridium*, *Eisenbergiella*), *Enterobacteriaceae* (*Escherichia*), *Tannerellaceae* (*Parabacteroides*), and *Erysipelotricaceae* (*Erysipelatoclostridium*). These bacteria may represent a "core rutin-selected microbiota" in healthy individuals. Members of the *Enterobacteriaceae* (*Escherichia coli*, *Escherichia fergusonii*, and *Enterobacter cloacae*) have been previously implicated in the O-deglycosylation and dehydroxylation of different flavonoids (Miyake et al., 1997; Hur et al., 2000; Zhao et al., 2014; Braune and Blaut, 2016). In a batch culture fermentation experiment, Tzounis et al. (2008) found that catechin, a flavan-3-ol monomers, promoted the growth of *E. coli* and Duda-Chodak (2012) found that rutin does not inhibit *E. coli* growth. In accordance with our findings, *P. distasonis* has been shown to produce both Q-glc and Q (Bokkenheuser et al., 1987) and the *Lachnospiraceae* member *Blautia* and *Eubacterium* were able to convert rutin in Q (Kim et al., 2014) and Q-glc

in Q, respectively. Based on rutin degradation capability and the identification of the core-rutin selective microbiota, we divided the donor microbiotas into high Q-glc, high Q, and low producers. We observed that members of *Enterobacteriaceae* (*Escherichia*) were associated Q-glc production, putatively due to expression of alpha-rhamnosidases that can act on rutin. We also found that *Lachnospiraceae* (*Lachnoclostridium* and *Eisenbergiella*) were associated with Q production, which may be due to expression of beta-rutinosidase enzymes or a combination of alpha-rhamnosidase and beta-glucosidase enzymes. In agreement with our experimental results, we found that putative alpha-rhamnosidases are common in genomes belonging genera that responded to the rutin amendment.

We did not screen for beta-rutinosidase and beta-glucosidase due to a lack of diagnostic bioinformatic tools for confident general inference of these activities. Beta-rutinosidase has not been identified in bacteria. The closest matches in Bacteria (by BLAST) of confirmed fungal beta-rutinosidases have only weak homology (< 30% identity) and are annotated as cellulases or cellulase-like enzymes. In addition, the carbohydrate-active enzyme (CAZY) database lists nine glycoside hydrolase families with individual members that have been shown to possess beta-glucoside activity (EC 3.2.1.21). However, each of the nine families also contain members that do not have known beta-glucosidase activity. Consequently, it is unclear which of the beta-glucosidases that are listed in CAZY will cleave glucose off of Q-glc specifically.

According to our findings, we hypothesize that inter-individual variability in rutin metabolism is driven by differences in the composition of the gut microbiota. Variation in rutin and other flavonoid metabolisms in humans may also be caused by host and environmental factors as diet and genetic polymorphism and differences in enzymatic activity (Almeida et al., 2018). In conclusion, individual microbiotas exert distinct capability in rutin utilization, showing a higher response in certain individuals, whereas others seem less capable in rutin utilization. Future research that takes into account functional gene analysis, diet, and host physiology will advance our understanding of the role of the gut microbiota in rutin degradation and provide opportunities to improve human health.

DATA AVAILABILITY STATEMENT

The datasets presented in this study can be found in online repositories. The names of the repository/repositories and accession number(s) can be found below: https://www.ncbi.nlm.nih.gov/, PRJNA622517.

ETHICS STATEMENT

The studies involving human participants were reviewed and approved by the University of Vienna ethics committee (Reference number 00161). The patients/participants provided their written informed consent to participate in this study.

AUTHOR CONTRIBUTIONS

DB, LA, and AR conceived and designed the experiments. AR performed the experiments and data analyses. AR and DK performed anaerobic incubation experiments. AS, LW, and AR performed FACS sorting. CH performed bioinformatics analyses. AR and DB wrote the manuscript. All authors gave approval to the final version of the manuscript.

FUNDING

This work was financially supported by Short Term Scientific Mission (FA 1403-POSITIVe) and the European Research Council (Starting Grant: FunKeyGut 741623). LA is grateful for the János Bolyai Research Scholarship of the Hungarian Academy of Sciences.

SUPPLEMENTARY MATERIAL

The Supplementary Material for this article can be found online at: https://www.frontiersin.org/articles/10.3389/fmicb.2020.585428/full#supplementary-material

REFERENCES

Almeida, A. F., Borge, G. I. A., Piskula, M., Tudose, A., Tudoreanu, L., Valentová, K., et al. (2018). Bioavailability of quercetin in humans with a focus on interindividual variation. *Compr. Rev. Food Sci. Food. Saf.* 17, 714–731. doi: 10.1111/1541-4337.12342

Amaretti, A., Raimondi, S., Leonardi, A., Quartieri, A., and Rossi, M. (2015). Hydrolysis of the rutinose-conjugates flavonoids rutin and hesperidin by the gut microbiota and bifidobacteria. *Nutrients* 7, 2788–2800. doi: 10.3390/nu7042788

Bang, S. H., Hyun, Y. J., Shim, J., Hong, S. W., and Kim, D. H. (2015). Metabolism of rutin and poncirin by human intestinal microbiota and cloning of their metabolizing alpha-L-rhamnosidase from *Bifidobacterium dentium*. *J. Microbiol. Biotechnol.* 25, 18–25. doi: 10.4014/jmb.1404.04060

Beekwilder, J., Marcozzi, D., Vecchi, S., de Vos, R., Janssen, P., Francke, C., et al. (2009). Characterization of rhamnosidases from *Lactobacillus plantarum* and *Lactobacillus acidophilus*. *Appl. Environ. Microbiol.* 75, 3447–3454. doi: 10.1128/AEM.02675-08

Bokkenheuser, V. D., Shackleton, C. H., and Winter, J. (1987). Hydrolysis of dietary flavonoid glycosides by strains of intestinal *Bacteroides* from humans. *Biochem. J.* 248, 953–956. doi: 10.1042/bj2480953

Braune, A., and Blaut, M. (2016). Bacterial species involved in the conversion of dietary flavonoids in the human gut. *Gut Microb.* 7, 216–234. doi: 10.1080/19490976.2016.1158395

Callahan, B. J., McMurdie, P. J., Rosen, M. J., Han, A. W., Johnson, A. J., and Holmes, S. P. (2016). DADA2: High-resolution sample inference from Illumina amplicon data. *Nat. Methods* 13, 581–583. doi: 10.1038/nmeth.3869

Cardona, F., Andres-Lacueva, C., Tulipani, S., Tinahones, F. J., and Queipo-Ortuno, M. I. (2013). Benefits of polyphenols on gut microbiota and implications in human health. *J. Nutr. Biochem.* 24, 1415–1422. doi: 10.1016/j.jnutbio.2013.05.001

Choi, S. J., Lee, S. N., Kim, K., Joo da, H., Shin, S., Lee, J., et al. (2016). Biological effects of rutin on skin aging. *Int. J. Mol. Med.* 38, 357–363. doi: 10.3892/ijmm.2016.2604

Conway, J. R., Lex, A., and Gehlenborg, N. (2017). UpSetR: an R package for the visualization of intersecting sets and their properties. *Bioinformatics* 33, 2938–2940. doi: 10.1093/bioinformatics/btx364

Daims, H., Lucker, S., and Wagner, M. (2006). daime, a novel image analysis program for microbial ecology and biofilm research. *Environ. Microbiol.* 8, 200–213. doi: 10.1111/j.1462-2920.2005.00880.x

de Araujo, M. E., Moreira Franco, Y. E., Alberto, T. G., Sobreiro, M. A., Conrado, M. A., Priolli, D. G., et al. (2013). Enzymatic de-glycosylation of rutin improves its antioxidant and antiproliferative activities. *Food Chem.* 141, 266–273. doi: 10.1016/j.foodchem.2013.02.127

Duda-Chodak, A. (2012). The inhibitory effect of polyphenols on human gut microbiota. *J. Physiol. Pharmacol.* 63, 497–503.

El-Gebali, S., Mistry, J., Bateman, A., Eddy, S. R., Luciani, A., Potter, S. C., et al. (2019). The Pfam protein families database in 2019. *Nucleic Acids Res.* 47, D427–D432. doi: 10.1093/nar/gky995

Enogieru, A. B., Haylett, W., Hiss, D. C., Bardien, S., and Ekpo, O. E. (2018). Rutin as a potent antioxidant: implications for neurodegenerative disorders. *Oxid. Med. Cell. Longev.* 2018:6241017. doi: 10.1155/2018/6241017

Ghorbani, A. (2017). Mechanisms of antidiabetic effects of flavonoid rutin. *Biomed. Pharmacother.* 96, 305–312. doi: 10.1016/j.biopha.2017.10.001

Gibellini, L., Pinti, M., Nasi, M., Montagna, J. P., De Biasi, S., Roat, E., et al. (2011). Quercetin and cancer chemoprevention. *Evid. Based Complement. Alternat. Med.* 2011:591356. doi: 10.1093/ecam/neq053

Hatzenpichler, R., Connon, S. A., Goudeau, D., Malmstrom, R. R., Woyke, T., and Orphan, V. J. (2016). Visualizing in situ translational activity for identifying and sorting slow-growing archaeal-bacterial consortia. *Proc. Natl. Acad. Sci. U.S.A.* 113, 4069–4078. doi: 10.1073/pnas.1603757113

Hatzenpichler, R., Scheller, S., Tavormina, P. L., Babin, B. M., Tirrell, D. A., and Orphan, V. J. (2014). In situ visualization of newly synthesized proteins in environmental microbes using amino acid tagging and click chemistry. *Environ. Microbiol.* 16, 2568–2590. doi: 10.1111/1462-2920.12436

Herbold, C. W., Pelikan, C., Kuzyk, O., Hausmann, B., Angel, R., Berry, D., et al. (2015). A flexible and economical barcoding approach for highly multiplexed amplicon sequencing of diverse target genes. *Front. Microbiol.* 6:731. doi: 10.3389/fmicb.2015.00731

Hobbs, C. A., Koyanagi, M., Swartz, C., Davis, J., Kasamoto, S., Maronpot, R., et al. (2018). Comprehensive evaluation of the flavonol anti-oxidants, alpha-glycosyl isoquercitrin and isoquercitrin, for genotoxic potential. *Food Chem. Toxicol.* 113, 218–227. doi: 10.1016/j.fct.2017.12.059

Hur, H. G., Lay, J. O. Jr., Beger, R. D., Freeman, J. P., and Rafii, F. (2000). Isolation of human intestinal bacteria metabolizing the natural isoflavone glycosides daidzin and genistin. *Arch. Microbiol.* 174, 422–428. doi: 10.1007/s002030000222

Jaganath, I. B., Mullen, W., Lean, M. E., Edwards, C. A., and Crozier, A. (2009). In vitro catabolism of rutin by human fecal bacteria and the antioxidant capacity of its catabolites. *Free Radic. Biol. Med.* 47, 1180–1189. doi: 10.1016/j.freeradbiomed.2009.07.031

Kim, M., Kim, N., and Han, J. (2014). Metabolism of *Kaempferia parviflora* polymethoxyflavones by human intestinal bacterium *Bautia* sp. MRG-PMF1. *J. Agric. Food. Chem.* 62, 12377–12383. doi: 10.1021/jf504074n

Kumar, S., and Pandey, A. K. (2013). Chemistry and biological activities of flavonoids: an overview. *Sci. World J.* 2013:162750. doi: 10.1155/2013/162750

Love, M. I., Huber, W., and Anders, S. (2014). Moderated estimation of fold change and dispersion for RNA-seq data with DESeq2. *Genome Biol.* 15:550. doi: 10.1186/s13059-014-0550-8

Matsumoto, M., Matsukawa, N., Mineo, H., Chiji, H., and Hara, H. (2004). A soluble flavonoid-glycoside, alphaG-rutin, is absorbed as glycosides in the isolated gastric and intestinal mucosa. *Biosci. Biotechnol. Biochem.* 68, 1929–1934. doi: 10.1271/bbb.68.1929

Miyake, Y., Yamamoto, K., and Osawa, T. (1997). Metabolism of antioxidant in lemon fruit (*Citrus limon* BURM. f.) by human intestinal bacteria. *J. Agric. Food Chem.* 45, 3738–3742. doi: 10.1021/jf970403r

Oksanen, J., Blanchet, F. G., Kindt, R., Legendre, P., McGlinn, D., and Minchin, P. R. (2010). *Vegan: Community Ecology Package, R Package Version 1.17.4*. Available online at: http://cran.r-project.org/ (accessed April 20, 2020).

Olthof, M. R., Hollman, P. C., Buijsman, M. N., van Amelsvoort, J. M., and Katan, M. B. (2003). Chlorogenic acid, quercetin-3-rutinoside and black tea phenols are extensively metabolized in humans. *J. Nutr.* 133, 1806–1814. doi: 10.1093/jn/133.6.1806

Salvamani, S., Gunasekaran, B., Shaharuddin, N. A., Ahmad, S. A., and Shukor, M. Y. (2014). Antiartherosclerotic effects of plant flavonoids. *Biomed. Res. Int.* 2014:480258. doi: 10.1155/2014/480258

Schloss, P. D., Westcott, S. L., Ryabin, T., Hall, J. R., Hartmann, M., Hollister, E. B., et al. (2009). Introducing mothur: open-source, platform-independent, community-supported software for describing and comparing microbial communities. *Appl. Environ. Microbiol.* 75, 7537–7541. doi: 10.1128/AEM.01541-09

Schneider, H., Schwiertz, A., Collins, M. D., and Blaut, M. (1999). Anaerobic transformation of quercetin-3-glucoside by bacteria from the human intestinal tract. *Arch. Microbiol.* 171, 81–91. doi: 10.1007/s002030050682

Shin, N. R., Moon, J. S., Shin, S. Y., Li, L., Lee, Y. B., Kim, T. J., et al. (2016). Isolation and characterization of human intestinal *Enterococcus avium* EFEL009 converting rutin to quercetin. *Lett. Appl. Microbiol.* 62, 68–74. doi: 10.1111/lam.12512

Thursby, E., and Juge, N. (2017). Introduction to the human gut microbiota. *Biochem. J.* 474, 1823–1836. doi: 10.1042/BCJ20160510

Tzounis, X., Vulevic, J., Kuhnle, G. G., George, T., Leonczak, J., Gibson, G. R., et al. (2008). Flavanol monomer-induced changes to the human faecal microflora. *Br. J. Nutr.* 99, 782–792. doi: 10.1017/S0007114507853384

Wang, Q., Garrity, G. M., Tiedje, J. M., and Cole, J. R. (2007). Naive Bayesian classifier for rapid assignment of rRNA sequences into the new bacterial taxonomy. *Appl. Environ. Microbiol.* 73, 5261–5267.

Zamora-Ros, R., Knaze, V., Rothwell, J. A., Hemon, B., Moskal, A., Overvad, K., et al. (2016). Dietary polyphenol intake in Europe: the European prospective investigation into cancer and nutrition (EPIC) study. *Eur. J. Nutr.* 55, 1359–1375. doi: 10.1007/s00394-015-0950-x

Zhao, M., Du, L., Tao, J., Qian, D., Shang, E. X., Jiang, S., et al. (2014). Determination of metabolites of diosmetin-7-O-glucoside by a newly isolated *Escherichia coli* from human gut using UPLC-Q-TOF/MS. *J. Agric. Food. Chem.* 62, 11441–11448. doi: 10.1021/jf502676j

Conflict of Interest: The authors declare that the research was conducted in the absence of any commercial or financial relationships that could be construed as a potential conflict of interest.

frontiers in Microbiology

ORIGINAL RESEARCH
published: 16 March 2021
doi: 10.3389/fmicb.2021.625782

Enrichment of Food With Tannin Extracts Promotes Healthy Changes in the Human Gut Microbiota

Silvia Molino[1†], Alberto Lerma-Aguilera[2†], Nuria Jiménez-Hernández[2,3], María José Gosalbes[2,3], José Ángel Rufián-Henares[1,4]* and M. Pilar Francino[2,3]**

[1]*Departamento de Nutrición y Bromatología, Instituto de Nutrición y Tecnología de los Alimentos, Centro de Investigación Biomédica, Universidad de Granada, Granada, Spain,* [2]*Area de Genòmica i Salut, Fundació per al Foment de la Investigació Sanitària i Biomèdica de la Comunitat Valenciana (FISABIO-Salut Pública), València, Spain,* [3]*CIBER en Epidemiología y Salud Pública, Madrid, Spain,* [4]*Instituto de Investigación Biosanitaria ibs.Granada, Granada, Spain*

OPEN ACCESS

Edited by:
Francesca Bottacini, Munster Technological University, Ireland

Reviewed by:
Simone Rampelli, University of Bologna, Italy
Ren-You Gan, Chinese Academy of Agricultural Sciences, China

***Correspondence:**
M. Pilar Francino
mpfrancino@gmail.com
María José Gosalbes
maria.jose.gosalbes@uv.es
José Ángel Rufián-Henares
jarufian@ugr.es

†These authors have contributed equally to this work

Specialty section:
This article was submitted to Microbial Symbioses, a section of the journal Frontiers in Microbiology

Received: *03 November 2020*
Accepted: *24 February 2021*
Published: *16 March 2021*

Citation:
Molino S, Lerma-Aguilera A, Jiménez-Hernández N, Gosalbes MJ, Rufián-Henares JÁ and Francino MP (2021) Enrichment of Food With Tannin Extracts Promotes Healthy Changes in the Human Gut Microbiota. Front. Microbiol. 12:625782. doi: 10.3389/fmicb.2021.625782

Food and food bioactive components are major drivers of modulation of the human gut microbiota. Tannin extracts consist of a mix of bioactive compounds, which are already exploited in the food industry for their chemical and sensorial properties. The aim of our study was to explore the viability of associations between tannin wood extracts of different origin and food as gut microbiota modulators. 16S rRNA amplicon next-generation sequencing (NGS) was used to test the effects on the gut microbiota of tannin extracts from quebracho, chestnut, and tara associated with commercial food products with different composition in macronutrients. The different tannin-enriched and non-enriched foods were submitted to *in vitro* digestion and fermentation by the gut microbiota of healthy subjects. The profile of the short chain fatty acids (SCFAs) produced by the microbiota was also investigated. The presence of tannin extracts in food promoted an increase of the relative abundance of the genus *Akkermansia*, recognized as a marker of a healthy gut, and of various members of the Lachnospiraceae and Ruminococcaceae families, involved in SCFA production. The enrichment of foods with tannin extracts had a booster effect on the production of SCFAs, without altering the profile given by the foods alone. These preliminary results suggest a positive modulation of the gut microbiota with potential benefits for human health through the enrichment of foods with tannin extracts.

Keywords: tannins, quebracho, chestnut, tara, *in vitro* digestion-fermentation, gut microbiota, short chain fatty acids

INTRODUCTION

In the last decades, the human microbiota has been the focus of great attention. Considering the genome of the entire microbial ecosystem, we can count a 100-fold higher number of genes compared to the human genome (Gilbert et al., 2018). The microbiome is involved in the modulation of human health, playing a role in several pathologies (i.e., metabolic diseases, inflammation, and neurological disorders; Ding et al., 2019). The human gut microbiota composition and function can be influenced by several factors. Among others, food and dietary components play a critical role in influencing the microbial ecosystem in the gastrointestinal

tract (Laitinen and Gueimonde, 2019; Cao et al., 2020). Diet is an essential factor in determining human health status and changes in macronutrients or in diet composition can rapidly modulate the composition and the metabolic functions of the intestinal microbiota (David et al., 2014). Thus, different types of foods have been investigated to understand the different response that they induce in the gut microbiota (Aguirre et al., 2016; Wu et al., 2019).

Tannin wood extracts comprehend a large group of botanical compounds with different properties, molecular weight, and structure, which can be obtained in huge amount by natural extraction from the wood and bark of different plants. Condensed tannins and hydrolysable tannins (including gallotannins and ellagitannins) are the two main categories (Serrano et al., 2009). These bioactive compounds are polyphenolic secondary metabolites, which plants use as a defense system against different aggressions, exerting a strong antimicrobial activity against pathogenic bacteria. In view of this, tannins have been investigated for their potential as alternatives to antibiotics, in particular for livestock animals (Díaz Carrasco et al., 2018; Farha et al., 2020). On the other hand, these compounds have also been widely studied *in vitro* and *in vivo* for bioactive effects similar to those of dietary fiber (Sieniawska, 2015).

The interaction of tannins with food has been well-described in relation with several sensorial aspects, such as astringency and bitter taste (Brossaud et al., 2001; Silva et al., 2017; Li et al., 2018; Pérez-Burillo et al., 2018). The structure of tannins gives them a distinctive tendency to bind to proteins and carbohydrates (Molino et al., 2019). For instance, both tannin molecular weight and degree of galloylation enhance their affinity for proteins, probably because tannin size determines the number of interaction sites. Nevertheless, larger tannin structures can cause steric hindrance and impede access to binding sites.

As mentioned, another interesting property of tannins is related to their fiber-like behavior since they are not broken down during gastrointestinal digestion and, hence, they are not absorbed at the small intestine. Therefore, they reach the large intestine where they can be used as substrate by gut microbes, which could result in potential prebiotic properties (Molino et al., 2018).

In light of this, we wanted to investigate if the association between different tannin extracts and a particular source of food could have modulatory effects on gut microbiota composition. We studied also the production of short chain fatty acids (SCFAs), which are good indicators of the effect of a foodstuff on the intestinal microbiota.

MATERIALS AND METHODS

Reagents

The reagents used for the *in vitro* digestion and fermentation were: potassium di-hydrogen phosphate, potassium chloride, magnesium chloride hexahydrate, sodium chloride, calcium chloride dihydrate, sodium mono-hydrogen carbonate, ammonium carbonate, and hydrochloric acid, all purchased from Sigma-Aldrich (Germany). The enzymes (salivary alpha-amylase and porcine pepsin) and bile acids (porcine bile extract) were obtained from Sigma-Aldrich, and porcine pancreatin was from Alfa Aesar (United Kingdom). The fermentation reagents (sodium di-hydrogen phosphate, sodium sulphide, tryptone, cysteine, and resazurin) were obtained from Sigma-Aldrich (Germany).

Short chain fatty acids standards (acetic acid, propionic acid, and butyric acid) were purchased from Sigma-Aldrich (Germany).

Plant Material

Three natural tannin extracts were chosen, which are representatives for the three main categories of tannins: quebracho wood extract (QUE; rich in a profisetinidin condensed tannin), chestnut wood extract (CHE; principally characterized by the presence of hydrolysable ellagitannins), and tara pods extract (TE; mainly represented by hydrolysable gallotannins). The tannin content in the extracts, determined by the International Organization of Vine and Wine (OIV) method (Aurand, 2017), was 80% for QUE, 72% for CHE, and 92% for TE. All the extracts were purchased from Silvateam Spa (San Michele di Mondoví, Italia), as powder. The extraction methods were all food grade, characterized by a natural hot water extraction.

Sample Preparation

Eight different food items, representing three types of products with different compositions in macronutrients were tested as potential tannin carriers: cereal-based foods [breakfast cereals (C), breakfast cereals with sugar (CS), and bread (B)], meat [meat (M) and meat with 30% fat (MF)], and dairy products [milk (L), low fat yogurt (Y), and full fat Greek yogurt (YG)]. All commercial products were bought in local supermarkets (Granada, Spain). The food samples were ground using an Ultraturrax (model T25, IKA, Spain) at 13,000 rpm. Then, the products were supplemented or not with 0.6% w/w of different tannin extracts (QUE, CHE, and TE). This amount of tannin extract added to food was decided based on our previous studies (data not shown). Since tannins can exert antimicrobial activity, it was critical to find a concentration effective for our purposes but not high enough as to affect negatively the gut microbes. On the other hand, we should use an amount of extracts that does not alter the flavor or the structure of the food matrix.

The samples were aliquoted and stored at −80°C until the *in vitro* digestion and fermentation processes. **Figure 1** summarizes the study design.

In vitro Digestion-Fermentation

Samples were *in vitro* digested and fermented following the method described by Pérez-Burillo et al. (2018). Briefly, three steps mimic those of gastrointestinal human digestion. The oral phase was carried out by adding 5 ml of simulated salivary fluid with α-amylase (75 U/ml) and 25 μl of $CaCl_2$ (0.3 M) to 5 g of food item alone or enriched with a tannin wood extract. The samples were then incubated for 2 min at 37°C. For the gastric phase, 10 ml of simulated gastric fluid with pepsin (2000 U/ml) and 5 μl of $CaCl_2$ (0.3 M) were added and the pH was lowered to 3.0 by adding 1 N HCl. The mix

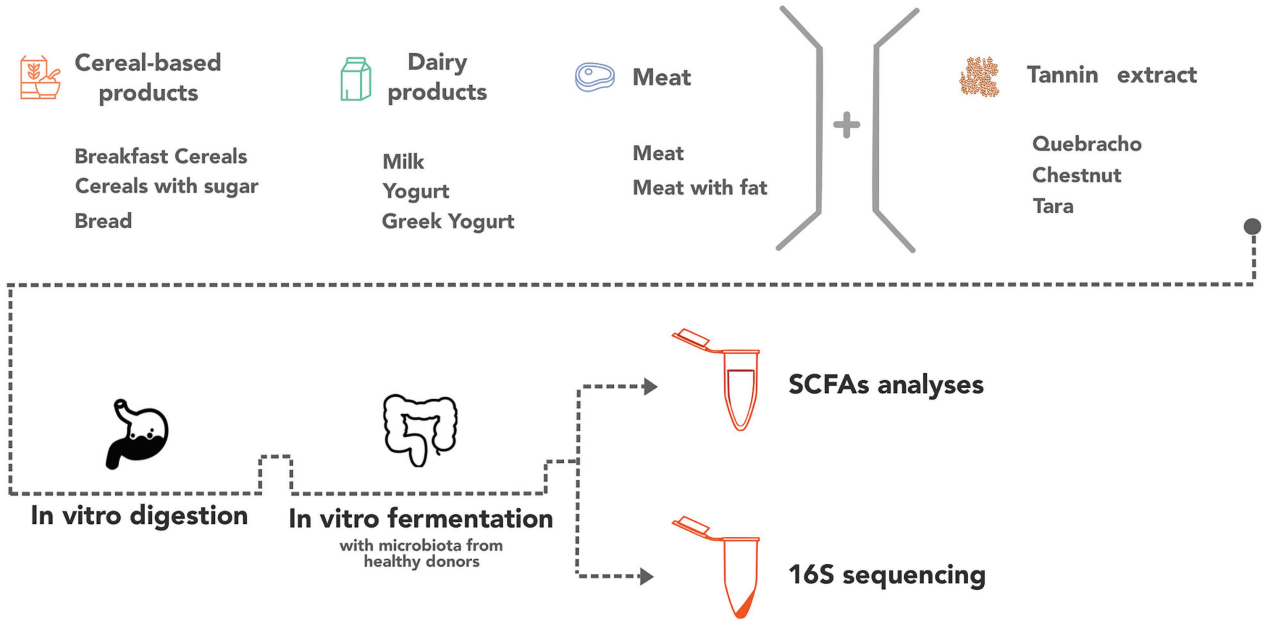

FIGURE 1 | Representation of the study design.

was then incubated at 37°C for 2 h. Finally, 20 ml of simulated intestinal fluid with pancreatin (13.37 mg/ml), bile salts (10 mM), and 40 µl of $CaCl_2$ (0.3 M) were added to the tube and the pH was raised to 7.0 with 1 N NaOH. The intestinal phase was followed by an incubation of the samples at 37°C for 2 h. A subsequent immersion of the tubes in iced water stopped the enzymatic reactions. The supernatants (potentially absorbed solution) were separated from the solid residue trough a centrifugation at 5000 rpm for 10 min at 4°C. To simulate the fraction that is not readily absorbed after digestion, 10% of the supernatant was added to the solid residue.

The fermentation was performed by adding 500 mg of the digested wet-solid residues deriving from digestion to 7.5 ml of fermentation final solution (peptone water + resazurine) and 2 ml of inoculum (32% feces w/v in phosphate buffer 100 mM, pH 7.0). We used an oligotrophic fermentation medium so that the food/tannin combination to be tested would be the only source of energy and nutrients for the microbiota. The inoculum was obtained by mixing the feces of six selected healthy volunteers, adult individuals (men or women) with a body mass index within the range 18.5–25 (University of Granada Ethics Committee approval no 1080/CEIH/2020). The selected people were not consuming any antibiotic or drug, and were following similar dietary patterns rich in vegetables, fruits, olive oil, and fish, typical of the Mediterranean diet.

In the tubes, an anaerobic atmosphere was produced by bubbling nitrogen through the mix, followed by an incubation at 37°C for 20 h, under oscillation. Immediately afterward, the samples were immersed in ice, to stop microbial activity, and centrifuged at 5,000 rpm for 10 min. The supernatant was collected as a soluble fraction potentially absorbed after fermentation and stored at −80°C, until the SCFA analyses. The solid residue, representing the non-absorbed fraction after fermentation, was also stored in order to perform 16S rRNA amplicon sequencing analyses (**Figure 1**).

DNA Extraction

Genomic DNA was extracted from the solid residues deriving from the fermentation process using the MagNA Pure LC JE379 platform (Roche) and DNA Isolation Kit III (Bacteria, Fungi; REF 03264785001), following the manufacturer's instructions, with a previous lysis with lysozyme at a final concentration of 0.1 mg/ml. DNA integrity was determined by agarose gel electrophoresis (0.8% w/v agarose in Tris-acetate-EDTA buffer) and DNA samples were quantified using a Qubit 3·0 Fluorometer (Invitrogen). All DNA samples were stored at −80°C until further processing.

High-Throughput Amplicon Sequencing

Total DNA (12 ng) was used as template for the amplification of the V3-V4 hypervariable region of the 16S rRNA gene. PCR primers were used as described by Klindworth et al. (2013), using the forward primer (5'-TCGT CGGC AGCG TCAG ATGT GTAT AAGA GACA GCCT ACGG GNGG CWGCA-G3') and reverse primer (5'-GTCT CGTG GGCT CGGA GATG TGTA TAAG AGAC AGGA CTAC HVGG GTAT CTAA TCC3'). We followed for the library construction the Illumina protocol for the small subunit ribosomal RNA gene (16S rRNA) Metagenomic Sequencing Library Preparation (Cod 15044223 RevA). Primers were fitted with adapter sequences added to the gene-specific sequences to make them compatible with the Illumina Nextera XT Index kit. Then, the amplicons were sequenced in an Illumina MiSeq sequencer according to the manufacturer's instructions in a 2 × 300 cycles paired-end

run (MiSeq Reagent kit v3). The data for the present study were deposited in the European Nucleotide Archive (ENA) at EMBL-EBI under accession number PRJEB41013.[1]

Bioinformatic Analyses

The sequence processing, assembly, amplicon sequence variants (ASVs) generation and annotation were performed in the DADA2 (v1.8.0) package from R (v3.6.0; Callahan et al., 2016). The filter and trimming parameters used were the following: maxN = 0, maxEE = c(2,5), truncQ = 0, trimLeft = c(17,21), truncLen = c(270,220), and rm.phix = TRUE. The merging process of the forward and reverse reads required a minimum overlap of 15 nucleotides and a maximum mismatch of 1. The reads were aligned using Bowtie2 against the human genome (GRCh38.p11) and matches were subsequently discarded (Langmead and Salzberg, 2012). The ASVs were generated by clustering sequences with 100% similarity. Taxonomic annotation was assigned by comparison to the SILVA 132 reference database using DADA2 v. 1.12 (Quast et al., 2013). Annotation was assigned at species level for 100% similarity matches or at the deepest possible taxonomic level in other cases.

SCFA Analysis

Short chain fatty acids production was assessed by analyzing acetic, propionic, and butyric acids, according to the procedure described by Molino et al. (2018). After the fermentation process, 1 ml of supernatant from the fermentation was centrifuged to remove solid particles, filtered through a 0.22 μm nylon filter, and finally transferred to a vial for UV-HPLC analysis. The sample did not require any pre-treatment before injection. The results were expressed as mmol of SCFAs per ml of fermented soluble fraction.

Statistical Analysis

Amplicon sequence variants with less than 10 counts in total were discarded. The ASV count table was normalized by total-sum scaling (TSS). Alpha and beta diversity measures were computed using various packages in the R platform. The Shannon diversity index, Chao1, and ACE richness estimators and Bray-Curtis dissimilarity index were obtained with the Vegan library (v2.5-2; Oksanen et al., 2012). Phylogeny-based measures such as Faith's phylogenetic diversity (PD) and the weighted UniFrac distance were computed using the picante (v1.8.2; Kembel et al., 2010) and GuniFrac packages (v1.1; Chen et al., 2012), respectively, after sequence alignment with msa (v1.4.3; Bodenhofer et al., 2015) and UPGMA tree-buiding with phangorn (v2.5.5; Schliep, 2011). In addition, principal component analysis (PCA), principal coordinate analysis (PCoA), and heatmaps were generated with in-house R scripts. Wilcoxon signed-rank tests with false discovery rate (FDR) adjustment for multiple comparisons were employed to evaluate differences in richness, diversity, and relative abundance of taxa among samples. The linear discriminant analysis (LDA) effect size (LEfSe) algorithm was applied to identify taxonomical biomarkers from different tannins (Segata et al., 2011). It combines Kruskal-Wallis and pairwise Wilcoxon rank-sum tests for statistical significance assessment and feature selection. Default parameters were used for significance ($p < 0.05$) and linear discriminant analysis threshold (<2.0).

Results of SCFA production are expressed as mean values of triplicates ($n = 3$) ± SD. One-way ANOVA with Bonferroni post-test correction was performed with the SPSS software (version 23, SPSS, Chicago, IL, United States) to determine significant differences among mean values on all the measured parameters.

RESULTS

To assess the bioactivity of tannin wood extracts of different origin and chemical composition, we chose three extracts representative of different classes of tannins: condensed tannins (QUE), ellagitannins (CHE), and gallotannins (TE). We evaluated the effect on the gut microbiota by adding the extracts to eight different sources of food grouped in three food types: cereal-based foods [breakfast cereals (C), breakfast cereals with sugar (CS), and bread (B)], meat [meat (M) and meat with 30% fat (MF)], and dairy products [milk (L), low fat yogurt (Y), and full fat Greek yogurt (YG)]. All the samples were subjected to an *in vitro* digestion-fermentation process designed to mimic natural digestion in the human oral, gastric, and intestinal chambers. The bioactivity was measured as the capacity to modify the gut microbiota in terms of taxonomic composition and SCFA production.

Comparisons of Microbiota Among Different Samples

The addition of tannin to the different food matrices determined a general trend of increase of the sample richness and diversity, as evaluated by different estimators and indexes: the Chao1 and ACE richness estimators, Faith's phylogenetic diversity (PD) and the Shannon diversity index that takes into account both richness and evenness (**Supplementary Table S1**). As an exception, microbiota richness and diversity rather decreased in cereal-based foods supplemented with CHE. **Figure 2** shows the increase in diversity detected when all food matrices are considered together for QUE (PD: adjusted $p = 0.035$; Shannon: adjusted $p = 0.023$) and TE (PD: adjusted $p = 0.035$; Shannon: adjusted $p = 0.023$), and the larger variability observed with the addition of CHE.

At the phylum level, the gut microbiota after *in vitro* fermentation of most samples was similar and dominated by Firmicutes and Bacteroidetes, followed by Proteobacteria, Verrucomicrobia and Actinobacteria, with some exceptions (**Figure 3**; **Supplementary Table S1**). Indeed, for meat (M and MF) enriched with tannin extracts, the relative abundance of Proteobacteria was higher ($p = 0.00084$, adjusted $p = 0.0051$), while that of Bacteroidetes was lower ($p = 0.027$, adjusted $p = 0.053$) compared to meat samples not enriched with tannins.

Principal coordinate analyses based on the Bray-Curtis dissimilarity index and the weighted UniFrac distance were performed to establish whether samples separate into clusters. As seen in **Figure 4**, PCo1 and PCo2 accounted for 61.47 and

[1]https://www.ebi.ac.uk/ena/browser/view/PRJEB41013

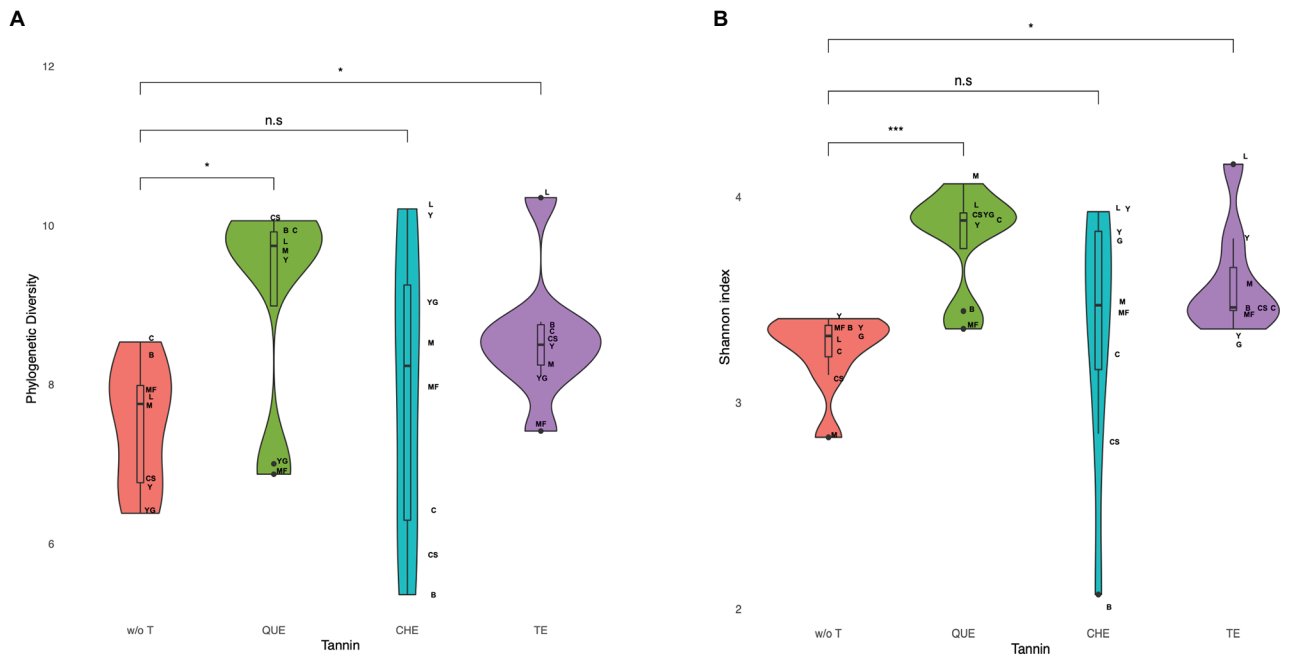

FIGURE 2 | Microbiota diversity measured as **(A)** phylogenetic diversity and **(B)** Shannon index in fermentations of food matrices with and without tannin extracts. Diversity increases for quebracho wood extract (QUE) and tara pods extract (TE) when all food matrices are considered together (p = 0.016, adjusted p = 0.023, and p = 0.008, adjusted p = 0.023, respectively). w/o T, without tannins; QUE, quebracho tannins extract; CHE, chestnut tannins extract; TE, tara tannins extract.

22.8%, respectively, of the total variation based on weighted UniFrac distances. All samples containing QUE and CHE clustered away from non-enriched foods, as did the milk and meat samples enriched with TE. The PCoA based on the Bray-Curtis index provided very similar results (**Supplementary Figure S1**). Thus, the results indicate that in most cases, the microbiota communities resulting from foods enriched with these tannin extracts are different from those of the food matrices alone.

More in depth, the obtained pattern of sample clustering does not reflect exclusively the tannin or the associated food matrix, but is rather influenced by both. Among the evaluated tannin extracts, QUE clustered most homogeneously, with all samples present in a single cluster independently of the matrix to which QUE was associated. In contrast, for CHE and TE, microbial composition depended on the food matrix. In the case of CHE, although all samples separated well from non-enriched foods, dairy and meat samples clustered with the QUE samples, whereas cereal-based foods did not. In the case of TE, the yogurt and cereal-based samples did not separate from non-enriched foods, whereas the milk and meat samples were located in the cluster containing all the QUE samples and the dairy and meat CHE samples. This suggests that TE only has an effect on the gut microbiota when added to meat or milk.

To identify the bacteria most generally affected by the addition of each of the tannins, we applied Wilcoxon signed-rank tests to compare bacterial relative abundances in all samples enriched with a given tannin vs. all samples containing no tannins. These comparisons identified a large number of genera for which abundance after tannin addition differed from that of non-enriched foods at nominal significance level, but only differences in QUE were still significant after adjusting for multiple comparisons (**Supplementary Figure S2**). Remarkably, with every tannin tested *Bacteroides* decreased (QUE: p = 0.008, adjusted p = 0.048; CHE: p = 0.008, adjusted p = 0.11; TE: p = 0.023, adjusted p = 0.14; **Figure 5A**) while *Akkermansia* increased (QUE: p = 0.008, adjusted p = 0.048; CHE: p = 0.008, adjusted p = 0.11; TE: p = 0.008, adjusted p = 0.079; **Figure 5B**). Wilcoxon signed-rank tests at family level (**Figure 5C**) confirmed that Bacteroidaceae decreased (QUE: p = 0.008, adjusted p = 0.031; CHE: p = 0.008, adjusted p = 0.049; TE p = 0.023, adjusted p = 0.103) and Akkermansiaceae increased (CHE: p = 0.008, adjusted p = 0.048; QUE: p = 0.008, adjusted p = 0.031; TE p = 0.008, adjusted p = 0.068) with each of the tannins, although, in this case, only the differences with QUE and CHE were significant after adjustment for multiple comparisons. In addition, several abundance changes were significant only with QUE, including decreases of the Bacteroidales families Prevotellaceae (adjusted p = 0.031), Barnesiellaceae (adjusted p = 0.031), and Tannerellaceae (adjusted p = 0.031), as well as increases of the Rickenellaceae (Bacteroidales; adjusted p = 0.047) and of several Clostridiales families [Ruminococcaceae (adjusted p = 0.031), Lachnospiraceae (adjusted p = 0.031), Christensenellaceae (adjusted p = 0.047), and Family XIII (adjusted p = 0.031)]. On the other hand, Peptostreptococcaceae (Clostridiales; adjusted p = 0.049) and the actinobacterial families Coriobacteriaceae (adjusted p = 0.048) and Bifidobacteriaceae (adjusted p = 0.048) augmented significantly only with CHE.

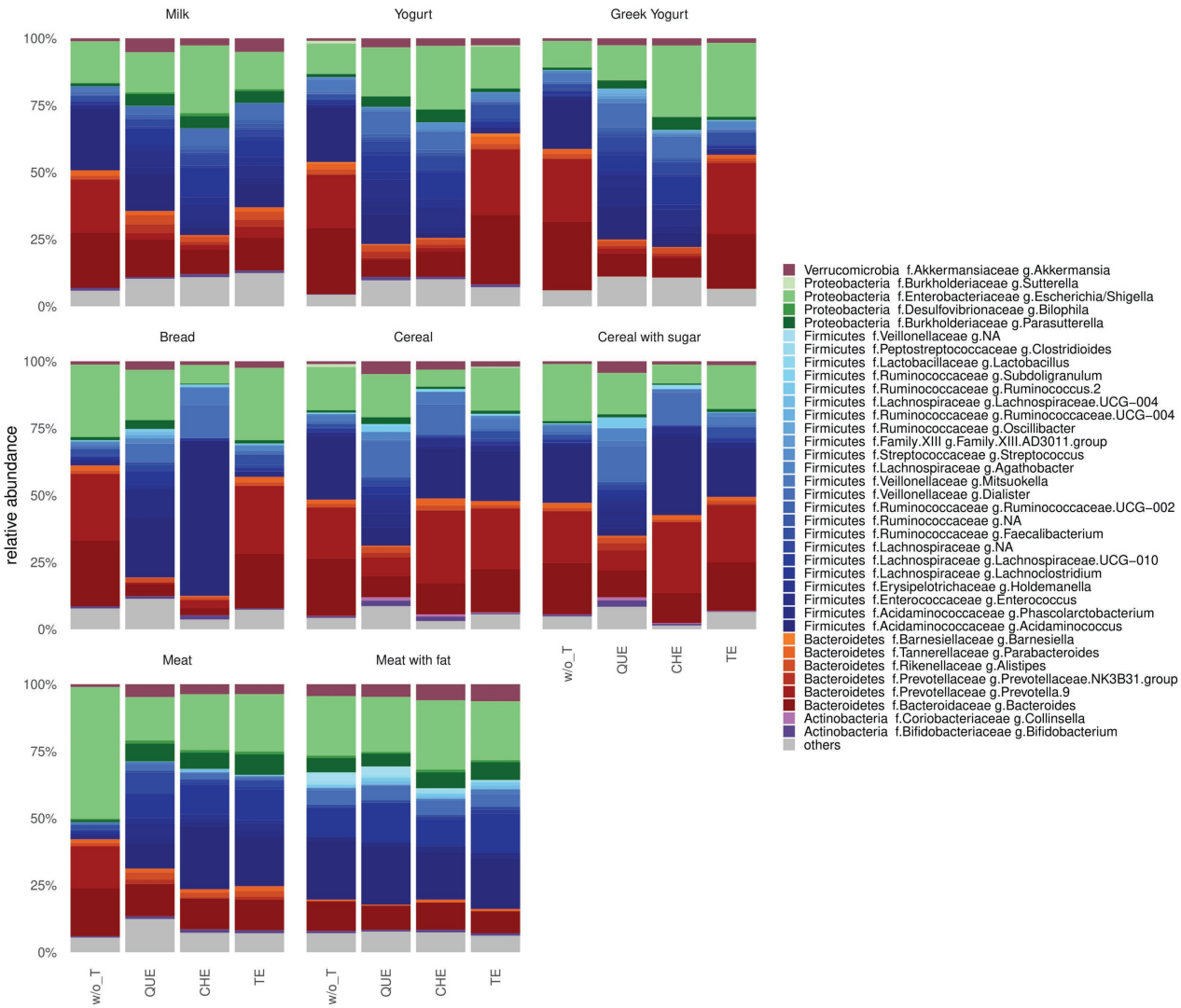

FIGURE 3 | Barplot of gut microbial community structure at genus level. w/o T, without tannins; QUE, quebracho tannins extract; CHE, chestnut tannins extract; TE, tara tannins extract. Relative abundance obtained by total-sum scaling (TSS) from genus-level abundance table. "Others" include genera with relative abundance lower than 1% for all conditions.

We also applied LEfSe analyses to identify the specific biomarkers that best characterize the microbiota changes generated by the addition of tannins within each of the three food groups [cereal-based foods (C, CS, and B), meat (M and MF), and dairy products (L, Y, and YG)]. The only group where significant differences were not detected between tannin-enriched and non-enriched matrices was that of meats. **Figure 6** depicts the over- and underrepresented genera (LDA score >3 and $p < 0.05$) in dairy sources and cereal-based foods enriched with the different tannin extracts, QUE, CHE, and TE. In most cases, genera increased rather than decreased with the addition of tannins, except in the case of CHE added to cereal-based foods, where several members of the Proteobacteria, Bacteroidetes, and Firmicutes were found to decrease, including various genera of the Ruminococcaceae and Lachnospiraceae families. *Sutterella* was the only genus that decreased in both food matrices with all of the tannins tested. No genus was overrepresented in both food matrices with all of the tannins, but *Akkermansia*, *Intestinimonas*, *Phascolarctobacterium*, and various unassigned Lachnospiraceae and Clostridiales Family XIII genera did increase in all cases except when cereal-based foods were enriched with CHE. It is interesting to note that several of the genera that decreased when CHE was added to carbohydrates actually increased when CHE was added to dairy (*Escherichia*, *Bilophila*, or *Lachnoclostridium*).

Finally, the differences generated by the addition of each tannin extract to each individual food matrix are represented as fold changes in **Supplementary Figure S3**, although further repetitions of each fermentation would be needed to assess their significance.

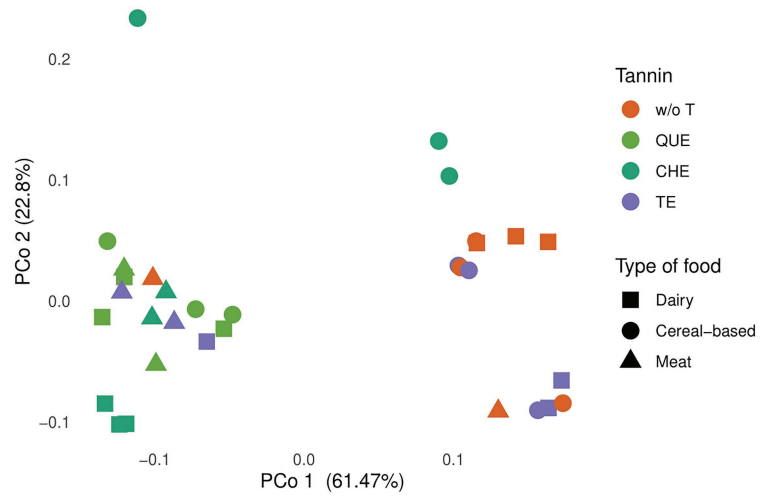

FIGURE 4 | Principal coordinate analysis (PCoA) plot of total variation based on weighted UniFrac distances among microbial communities in all profiled samples, evaluated at genus level. The food sources were grouped in three food types: cereal-based foods (breakfast cereals, breakfast cereals with sugar, and bread), meat (meat and meat with 30% fat), and dairy products (milk, low fat yogurt, and full-fat Greek yogurt). w/o T, without tannins, QUE, quebracho tannins extract; CHE, chestnut tannins extract; TE, tara tannins extract.

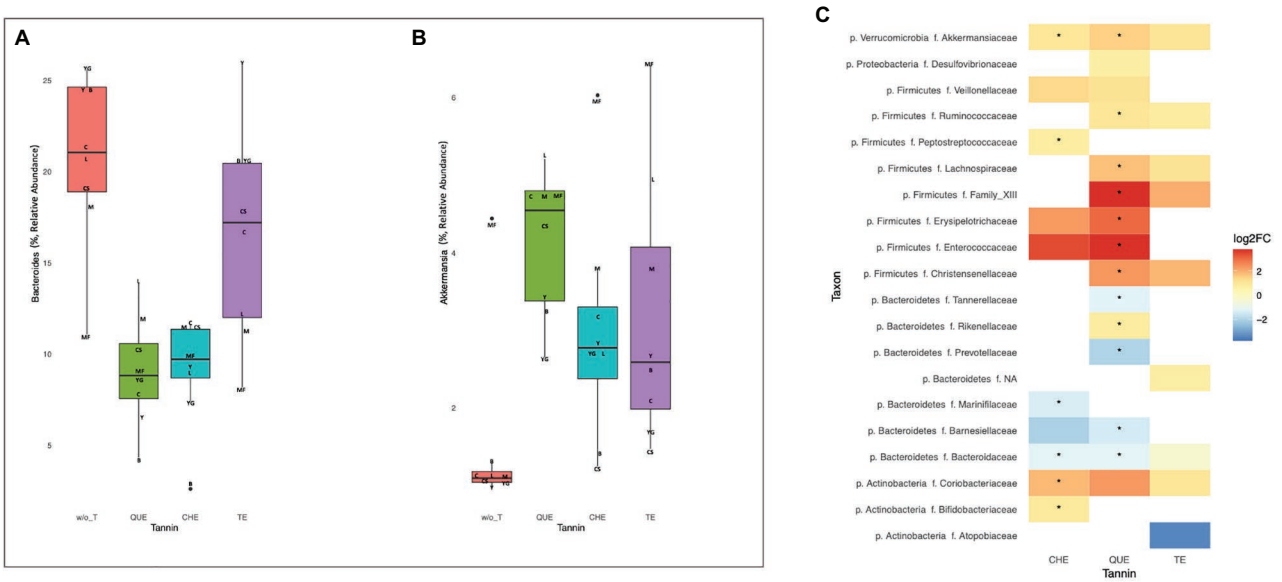

FIGURE 5 | Changes in microbiota composition with tannin addition in all foods. **(A)** Decrease of *Bacteroides* (QUE: $p = 0.0078$, adjusted $p = 0.048$; CHE: $p = 0.0078$, adjusted $p = 0.11$; TE: $p = 0.023$, adjusted $p = 0.14$) and **(B)** increase of *Akkermansia* (QUE: $p = 0.0078$, adjusted $p = 0.048$; CHE: $p = 0.0078$, adjusted $p = 0.11$; TE: $p = 0.0078$, adjusted $p = 0.079$) with every tannin tested. Initials indicate the different food matrices (C, breakfast cereals; CS, breakfast cereals with sugar; B, bread; M, meat; MF, meat with 30% fat; L, milk; Y, low fat yogurt; and YG, full-fat Greek yogurt). **(C)** Fold-changes in the relative abundance of bacterial families with each tannin. All changes significant at nominal level by Wilcoxon signed-rank tests are shown ($p < 0.05$). *Indicates statistically significant differences ($p < 0.05$) after correction for multiple testing.

Production of SCFAs

Short chain fatty acids are metabolites produced by gut microbial fermentation of carbohydrates, dietary fibers, proteins, and resistant starch. We focused on the release of the three principal subtypes: acetate, propionate, and butyrate. The PCA in **Figure 7A** depicts the similarity of the samples based on the relative abundance of each SCFA, showing that SCFA production is similar in fermentations of the same food group independently of the presence of the tannin extracts.

As expected, cereal-based foods released the highest amount of SCFAs (**Figure 7B**), producing, in decreasing order, acetic acid, propionic acid, and butyric acid. In foods with a higher

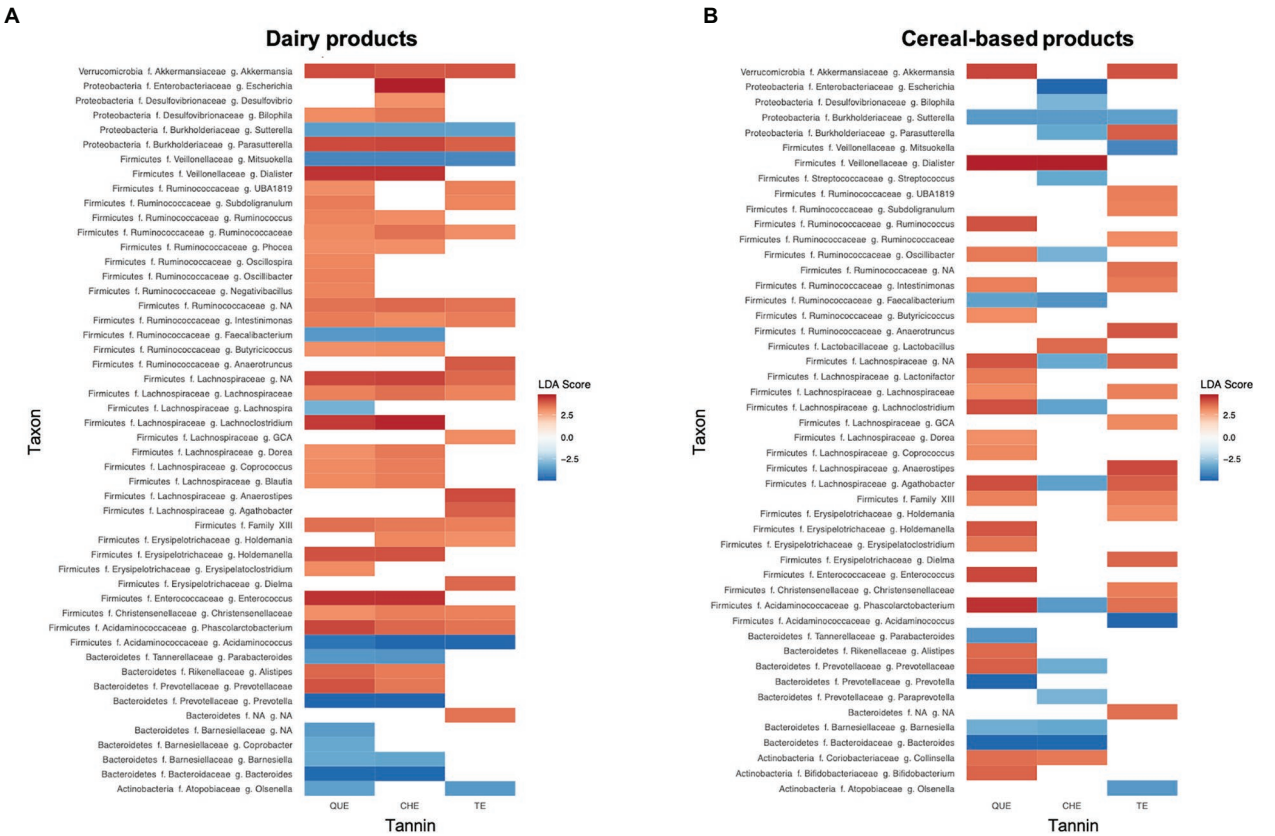

FIGURE 6 | Genera responsible for the main differences in gut microbiota composition due to the addition of tannin extracts to **(A)** dairy products and **(B)** cereal-based products, detected by Linear Discriminant Analysis (LDA) Effect Size (LEfSe). Differences are represented as LDA score (>3) by color gradient. All represented biomarkers are significant at $p < 0.05$. NA taxon refers to unclassified ASVs at f. (family) or g. (genus) level.

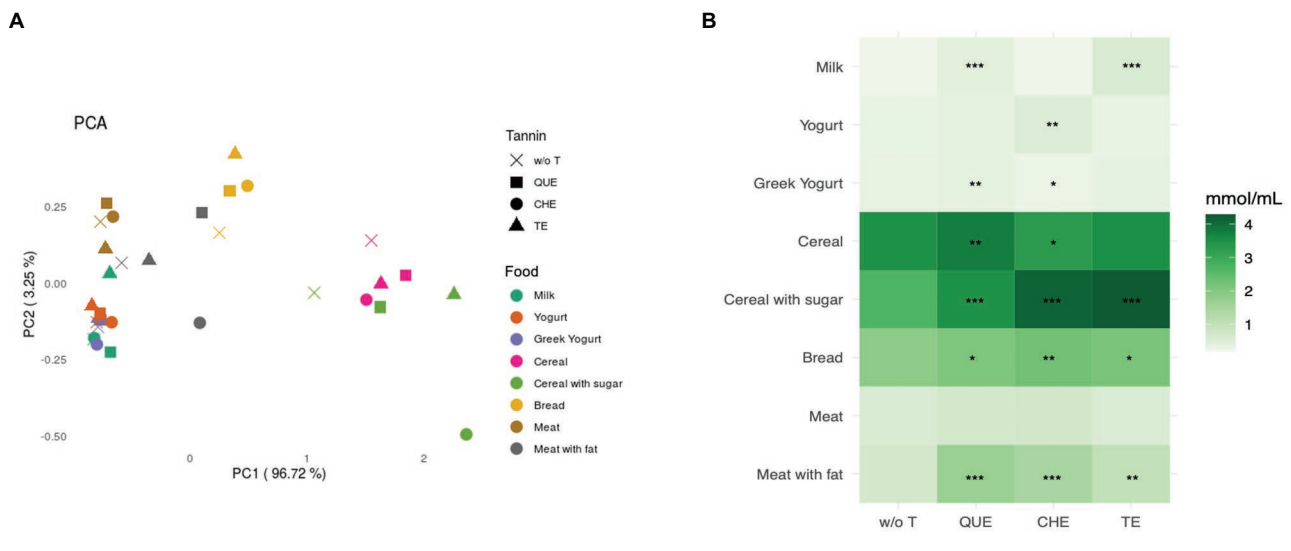

FIGURE 7 | Short chain fatty acids (SCFAs) released after *in vitro* fermentation of the food matrices with and without tannins. **(A)** Principal component analysis (PCA) based on Euclidean distance. **(B)** Sum of the concentration of SCFAs (in mmol/ml) per each sample, represented by color gradient as shown next to the heatmap. w/o T, without tannins; QUE, quebracho tannins extract; CHE, chestnut tannins extract; TE, tara tannins extract. *Indicates statistically significant differences by ANOVA and Bonferroni *post-hoc* test: $*p < 0.05$, $**p < 0.01$, $***p < 0.001$.

protein content, the ratio between acetic and propionic acid decreased, or even reversed, as in the case of M (**Table 1**). In most cases, the addition of tannins did not alter the relative production of the different SCFAs, but resulted in a booster effect (**Table 1**). Looking at the production of total SCFAs (**Figure 7B**), QUE, CHE, and TE nearly always resulted in a significant increase, particularly when they were combined with CS (QUE: adjusted $p < 0.001$, CHE: adjusted $p < 0.001$, and TE: adjusted $p < 0.001$) and MF (QUE: adjusted $p < 0.001$, CHE: adjusted $p < 0.001$, and TE: adjusted $p = 0.002$). On the contrary, when added to M, none of the three tannin extracts produced a statistically significant increase of total SCFAs. However, the addition of QUE, CHE, or TE to M induced a significant increase in the production of acetic acid compared to M without tannins, suggesting that they were exerting a booster effect on specific acetate-producing bacteria (**Table 1**).

Regarding differences among the three tannins, we detected several cases where only one or two of the extracts were effective at boosting overall SCFA production when added to specific foods (**Figure 7B**). Notably, within dairy foods, QUE was able to boost SCFA production in M and YG, whereas CHE and TE were only able to do so in Y and M, respectively. The measurements of specific SCFAs (**Table 1**) indicate that CHE and TE were able to boost the production of all three SCFAs in Y and M, respectively, whereas the other tannin extracts were not. QUE, on the other hand, had a significant booster effect on acetic and butyric acids in M, and on propionic acid in YG. This differential effect on specific SCFAs was, however, not sufficient to alter the overall profile of SCFA production in these foods, as observed in **Figure 7A**.

DISCUSSION

Effects on Microbiota Composition

The gut microbiota has a determinant role in maintaining human health. Specific foods and products containing prebiotics interact directly or indirectly with the microbiota, driving its composition and function (Laitinen and Gueimonde, 2019). In this context, tannins can modulate gut microbial composition and function, selectively inhibiting pathogens and promoting the growth of beneficial bacteria (Ozdal et al., 2016). Tannins are known also for their capacity to interact with proteins and carbohydrates, among other compounds. So, we were interested in investigating if the association of tannin extracts from different sources with different types of food matrices

TABLE 1 | Short chain fatty acids produced after the fermentation of the food source enriched or not with tannin extracts.

		Acetic acid	Propionic acid	Butyric acid
Milk	w/o T	0.117 ± 0.006	0.055 ± 0.000	0.047 ± 0.001
	QUE	0.269 ± 0.020*	0.063 ± 0.021	0.077 ± 0.000*
	CHE	0.120 ± 0.001	0.060 ± 0.001*	0.042 ± 0.004
	TE	0.174 ± 0.004*	0.302 ± 0.002*	0.107 ± 0.024*
Yogurt	w/o T	0.124 ± 0.009	0.115 ± 0.000	0.081 ± 0.008
	QUE	0.138 ± 0.003	0.149 ± 0.000*	0.091 ± 0.001
	CHE	0.244 ± 0.013*	0.158 ± 0.006*	0.098 ± 0.001*
	TE	0.067 ± 0.019*	0.151 ± 0.001*	0.092 ± 0.003
Greek yogurt	w/o T	0.139 ± 0.008	0.104 ± 0.001	0.088 ± 0.002
	QUE	0.152 ± 0.020	0.133 ± 0.010*	0.092 ± 0.000
	CHE	0.151 ± 0.002	0.047 ± 0.002*	0.087 ± 0.000
	TE	0.133 ± 0.006	0.133 ± 0.010*	0.090 ± 0.001
Cereals	w/o T	2.232 ± 0.033	1.181 ± 0.010	0.059 ± 0.000
	QUE	2.545 ± 0.027*	1.173 ± 0.009	0.068 ± 0.003
	CHE	2.259 ± 0.010	0.985 ± 0.038*	0.042 ± 0.005*
	TE	2.359 ± 0.009*	1.076 ± 0.011*	0.064 ± 0.001
Cereals with sugar	w/o T	1.832 ± 0.002	0.853 ± 0.006	0.016 ± 0.001
	QUE	2.379 ± 0.023*	1.002 ± 0.029*	0.075 ± 0.003*
	CHE	3.214 ± 0.018*	0.865 ± 0.008	0.047 ± 0.001*
	TE	2.957 ± 0.028*	1.259 ± 0.004*	0.054 ± 0.003*
Bread	w/o T	1.006 ± 0.005	0.754 ± 0.012	0.093 ± 0.010
	QUE	1.043 ± 0.022	0.912 ± 0.022*	0.122 ± 0.002*
	CHE	1.177 ± 0.025*	0.980 ± 0.013*	0.112 ± 0.003
	TE	1.041 ± 0.046	1.043 ± 0.001*	0.060 ± 0.002*
Meat	w/o T	0.039 ± 0.001	0.434 ± 0.026	0.104 ± 0.005
	QUE	0.068 ± 0.000*	0.510 ± 0.014*	0.115 ± 0.002
	CHE	0.134 ± 0.003*	0.488 ± 0.033	0.088 ± 0.000
	TE	0.110 ± 0.003*	0.367 ± 0.038*	0.093 ± 0.005
Meat with 30% fat	w/o T	0.255 ± 0.004	0.372 ± 0.019	0.069 ± 0.000
	QUE	0.842 ± 0.015*	0.765 ± 0.029*	0.074 ± 0.001
	CHE	0.951 ± 0.025*	0.419 ± 0.017*	0.075 ± 0.002
	TE	0.473 ± 0.002*	0.460 ± 0.021*	0.089 ± 0.001*

*The results are expressed as mmol/ml and data are represented as means ± SD (n = 3). w/o T, without tannins; QUE, quebracho tannins extract; CHE, chestnut tannins extract; TE, tara tannins extract. *Indicates statistically significant differences (p < 0.05) by ANOVA and Bonferroni post-hoc test between foods enriched with tannins and not.*

could determine a different response when interacting with the microbiota of healthy people. In particular, we decided to study tannins extracted from wood and bark of different plants, which are now finding new relevant applications in the food sector (Molino et al., 2019).

For most food matrices and tannins tested, tannin enrichment resulted in a change in the composition of the microbiota, compared with the fermentations employing the foods alone (**Figure 4**). Besides the increase in overall richness and diversity, the increase of the genus *Akkermansia* was one of the most general results in our study (**Figure 5B**). These are mucin-degrading bacteria, living in the mucus layer, recognized as markers of a healthy gut. In fact, several studies have highlighted their anti-inflammatory properties, and the ability to increase insulin sensitivity, and boost gut barrier function (Masumoto et al., 2016; Cires et al., 2017; Rinninella et al., 2019). These properties are also related to their production of propionate and butyrate (Venegas et al., 2019). Furthermore, some authors have proposed *Akkermansia* as a key player in the breakdown of phenolic compounds in the intestine (Li et al., 2015), suggesting a likely reason for the observed increase of this genus with the addition of tannins.

The addition of tannins (in particular QUE and CHE) also determined a decrease of *Bacteroides* and other genera and families of the order Bacteroidales (**Figure 5A**). *Bacteroides* is known to be implicated in proteolytic fermentation in the gut, so that the binding of proteins by tannins may be responsible for the decrease of these bacteria by rendering protein molecules unavailable for digestion (Smith and MacFarlane, 1998). Inhibitory effects of tannins on proteolytic bacteria and proteolytic enzyme activity have been proposed, likely due to coating of the protein surface leading to interference with the interaction of enzyme and substrate (McManus et al., 1981; Patra et al., 2012).

The interactions between tannins and food macromolecules may be different depending on the food matrices. Binding mechanisms between tannins and proteins or carbohydrates occur in a specific and selective way, mediated by hydrogen bonds and hydrophobic interactions (McManus et al., 1985; de Freitas and Nuno, 2012). Some factors related to these macromolecules may influence such interactions: size, charge, side chains, and conformation (Molino et al., 2019). Therefore, we expected that some effects of tannins would be dependent on the food matrix to which they were added.

In fact, we detected increases of the families Lachnospiraceae and Ruminococcaceae in most of the tannin-food combinations analyzed, except for the case of cereal-based foods supplemented with CHE (**Figure 6**). Several authors have reported an increase of the abundance of bacteria belonging to the Lachnospiraceae and Ruminococcaceae families when tannins were added to animal feed (Choy et al., 2014; Díaz Carrasco et al., 2018). Lachnospiraceae and Ruminococcaceae belong to the order Clostridiales, which encompasses mostly beneficial bacteria, including members that have been associated with the modulation of physiologic, metabolic, and immune processes in the gut and with prevention of inflammatory bowel disease. Furthermore, numerous genera of these families have been attributed the capacity to produce SCFAs (Lopetuso et al., 2013; Louis and Flint, 2017). Díaz Carrasco et al. (2018) observed the same trend of increment of the aforementioned Clostridiales families in chicken supplemented with a mix of QUE and CHE. In particular, they detected an increment of the genus *Faecalibacterium*, among others. In our analyses, *Faecalibacterium* rather decreased with addition of QUE and CHE to cereal-based and dairy products (**Figure 6**). However, addition of TE did determine a large increase of *Faecalibacterium* in C, CS, Y, and YG (**Supplementary Figure S2**), although *Faecalibacterium* increases did not reach significance when all cereal-based or dairy foods were considered together. This finding suggests that it will be interesting to analyze these individual food matrices supplemented with TE in further experiments to assess the significance of the *Faecalibacterium* increases independently in each of them.

Besides not showing an increase in Lachnospiraceae and Ruminococcaceae (**Figure 6**), cereal-based foods supplemented with CHE clustered far from the other samples (**Figure 4**) and, unlike other tannin-food combinations, showed a decrease in microbiota richness and diversity (**Supplementary Table S1**). These results could be related to a specific interaction between the hydrolysable ellagitannins contained in the chestnut wood extract and the fiber present in the evaluated food matrices. The inhibitory effects of ellagitannins on the activity of carbohydrate digestive enzymes, reported in the systematic review of Prpa et al. (2020), could also contribute to explain these differences.

Effects on SCFA Production

Tannins can act locally at intestinal level (especially non-absorbable tannins of high molecular weight), reaching the colonic gut microbiota. Herein, these compounds could be used by microorganisms, resulting in metabolites with different bioavailability, activity, or functional effect compared to the parent molecule (Serrano et al., 2009).

Tannins have been proposed as prebiotic substrates for gut microbes as these molecules favor SCFA production, have growth-promoting effects for beneficial bacteria, and/or could activate their metabolic functions. In our previous studies, we demonstrated a great production of SCFAs following *in vitro* digestion and fermentation of QUE and CHE (Molino et al., 2018). Now, our aim was to investigate whether the association of these extracts to various food sources could result in a booster effect or in an altered production of different SCFAs from that observed with the food sources alone.

It is well-known that carbohydrates exert a considerable prebiotic effect because polysaccharides act as a nutrient for the gut microbiota (Aguirre et al., 2016). Their metabolization by the microbiota results in the production, in decreasing order of proportion, of acetate, propionate, and butyrate. Generally, proteins are not a good source of prebiotics and they alter the profile of SCFA production. Increased fermentation of amino acids results in an elevated production of propionate, together with branched SCFAs, and some potentially harmful molecules such as amines or hydrogen disulfide (Diether and Willing, 2019). Here, we show that the combination of tannin extracts (QUE, CHE, and TE)

with the food matrices resulted in most cases in an increment of total SCFA production (**Figure 7B**). The increased SCFA production in presence of tannins may be potentially related to the synthesis of these compounds using the tannins or their metabolized products as substrates, or to the increased relative abundance and/or activity of gut microbiota species that ferment carbohydrates. Indeed, the increment in the relative abundances of both potential tannin metabolizers such as *Akkermansia* and carbohydrate fermenters/SCFA producers such as the Ruminococcaceae and Lachnospiraceae families suggests that both processes may be contributing to the boost in SCFA production.

The only case where none of the tannins led to any significant booster effect on total SCFA production was when combined with M. The strong protein-binding capacity is one of the distinguishing properties of tannins. This may have affected the potential interaction of the newly formed tannin-protein complexes with the microbiota, probably making the proteins less digestible and the tannins less available to exert their prebiotic action. The presence of a higher percentage of fat in MF may have reduced the formation of complexes between meat proteins and tannins, thus allowing greater interaction between tannins and the microbiota, resulting in a greater production of SCFAs.

Finally, our analyses revealed some differences in the modulation of SCFA production among the three tannin extracts (**Figure 7B**; **Table 1**). QUE (a condensed tannin), CHE (an ellagitannin), and TE (a gallotannin) have different chemical structures and it is well-known that the interaction between macromolecules and the different classes of tannins could differ (McManus et al., 1985; Baxter et al., 1997; Carn et al., 2012). However, although in some foods different tannins favored the synthesis of different SCFAs, this differential effect did not change the relative proportions of the SCFAs sufficiently to alter the expected profile favored by each food matrix. As illustrated in **Figure 7A**, the separation of the different samples according to SCFA production profile depended on the food sources (dairy products, meat, and cereal-based foods). So, the factor driving the clustering of SCFA profiles was the different nutritional composition of the food sources, not the tannin enrichment. It is possible that longer fermentation times might be needed to obtain significant differences in the effect of different tannins on the overall profile of SCFA production.

Our study may suffer some limitations related to the *in vitro* digestion and fermentation system. Indeed, some bacteria could need longer times for growth, so that the length of the fermentation experiment would not be sufficient to observe an increment of their relative abundance and/or their metabolic activity reflected in the production of SCFAs. An *in vivo* study could be more reliable because factors such as the interaction between the tannins and the gastrointestinal system could come into play. Furthermore, a long-term interventional study could allow investigating gradual changes in the composition of the intestinal microbiota and its functions. On the other hand, an *in vivo* study could introduce many confounding variables resulting in a disadvantage for the study of the interaction of tannins with specific food matrices.

In conclusion, the enrichment of foods with different composition (dairy products, cereal-based foods, and meat) with tannin extracts (QUE, CHE, and TE) evidenced the potential to influence host physiology through the modulation of the composition and the functionality of symbiotic bacteria in the gut. Our findings are in line with the considerations of Cires et al. (2017), which associated the consumption of condensed tannins with a shift to a healthier environment in the colonic ecosystem that could play a key role in the digestion and absorption of nutrients, but also in protecting the gastrointestinal system against pathogens. These preliminary results will pave the ground for the development of new functional foods within the framework of the European Commission research project Stance4Health. Indeed, these extracts, which are produced in a sustainable way, could represent new and cost-effective natural supplements to be exploited for their prebiotic effect, acting by boosting the production of SCFAs, which are crucial in the maintenance of gut and immune homeostasis. Depending on the matrix to which they were added, the new products could determine a different modulation of the composition and activity of the gut microbiota. In particular, QUE extracts generate the most homogeneous response across foods, whereas the effects of CHE and TE are more highly dependent on the food matrix. These new findings on the advantageous effects of tannins, and on the versatility provided by their combination with different foods, make of these compounds a promising new tool for the promotion of a healthy gut environment, with potential long-term benefits for metabolism and immunity.

DATA AVAILABILITY STATEMENT

The sequence data are available in the European Nucleotide Archive (ENA) under accession number PRJEB14013 (https://www.ebi.ac.uk/ena/browser/view/PRJEB41013).

AUTHOR CONTRIBUTIONS

SM, JAR-H, and MPF designed the research. SM, AL-A, and NJ-H conducted the experiments. SM and AL-A analyzed data and performed statistical analyses. AL-A conducted the bioinformatic analyses. SM and MPF wrote the manuscript. MJG, AL-A, and JAR-H provided significant advice and critically edited the manuscript. JAR-H obtained funding and coordinated the Stance4Health project. All authors contributed to the article and approved the submitted version.

FUNDING

This work was supported by the research project Stance4Health (contract no. 816303) from the European Commission (Research Executive Agency).

ACKNOWLEDGMENTS

This paper will form part of the doctoral thesis of SM, conducted within the context of the "Nutrition and Food Sciences Programme" at the University of Granada.

SUPPLEMENTARY MATERIAL

The Supplementary Material for this article can be found online at: https://www.frontiersin.org/articles/10.3389/fmicb.2021.625782/full#supplementary-material

REFERENCES

Aguirre, M., Eck, A., Koenen, M. E., Savelkoul, P. H. M., Budding, A. E., and Venema, K. (2016). Diet drives quick changes in the metabolic activity and composition of human gut microbiota in a validated in vitro gut model. *Res. Microbiol.* 167, 114–125. doi: 10.1016/j.resmic.2015.09.006

Aurand, J. (2017). Resolution OIV-OENO 574-2017 monograph on tannins – update of the method for determination of polyphenols.

Baxter, N. J., Lilley, T. H., Haslam, E., and Williamson, M. P. (1997). Multiple interactions between polyphenols and a salivary proline-rich protein repeat result in complexation and precipitation †. *Biochemistry* 36, 5566–5577.

Bodenhofer, U., Bonatesta, E., Horejš-Kainrath, C., and Hochreiter, S. (2015). Msa: an R package for multiple sequence alignment. *Bioinformatics* 31, 3997–3999. doi: 10.1093/bioinformatics/btv494

Brossaud, F., Cheynier, V., and Noble, A. C. (2001). Bitterness and astringency of grape and wine polyphenols. *Aust. J. Grape Wine Res.* 7, 33–39. doi: 10.1111/j.1755-0238.2001.tb00191.x

Callahan, B. J., McMurdie, P. J., Rosen, M. J., Han, A. W., Johnson, A. J. A., and Holmes, S. P. (2016). DADA2: high-resolution sample inference from Illumina amplicon data. *Nat. Methods* 13, 581–583. doi: 10.1038/nmeth.3869

Cao, Y., Liu, H., Qin, N., Ren, X., Zhu, B., and Xia, X. (2020). Impact of food additives on the composition and function of gut microbiota: a review. *Trends Food Sci. Technol.* 99, 295–310. doi: 10.1016/j.tifs.2020.03.006

Carn, F., Guyot, S., Baron, A., Pe, J., Buhler, E., and Zanchi, E. (2012). Structural properties of colloidal complexes between condensed tannins and polysaccharide hyaluronan. *Biomacromolecules* 13, 751–759. doi: 10.1021/bm201674n

Chen, J., Bittinger, K., Charlson, E. S., Hoffmann, C., Lewis, J., Wu, G. D., et al. (2012). Associating microbiome composition with environmental covariates using generalized UniFrac distances. *Bioinformatics* 28, 2106–2113. doi: 10.1093/bioinformatics/bts342

Choy, Y. Y., Quifer-Rada, P., Holstege, D. M., Frese, S. A., Calvert, C. C., Mills, D. A., et al. (2014). Phenolic metabolites and substantial microbiome changes in pig feces by ingesting grape seed proanthocyanidins. *Food Funct.* 5, 2298–2308. doi: 10.1039/C4FO00325J

Cires, M. J., Wong, X., Carrasco-Pozo, C., and Gotteland, M. (2017). The gastrointestinal tract as a key target organ for the health-promoting effects of dietary proanthocyanidins. *Front. Nutr.* 3:57. doi: 10.3389/fnut.2016.00057

David, L. A., Maurice, C. F., Carmody, R. N., Gootenberg, D. B., Button, J. E., Wolfe, B. E., et al. (2014). Diet rapidly and reproducibly alters the human gut microbiome. *Nature* 505, 559–563. doi: 10.1038/nature12820

de Freitas, V., and Nuno, M. (2012). Protein/polyphenol interactions: past and present contributions. Mechanisms of astringency perception. *Curr. Org. Chem.* 16, 724–746. doi: 10.2174/138527212799958002

Díaz Carrasco, J. M., Redondo, E. A., Pin Viso, N. D., Redondo, L. M., Farber, M. D., and Fernández Miyakawa, M. E. (2018). Tannins and bacitracin differentially modulate gut microbiota of broiler chickens. *Biomed. Res. Int.* 2018, 1–11. doi: 10.1155/2018/1879168

Diether, N. E., and Willing, B. P. (2019). Microbial fermentation of dietary protein: an important factor in diet–microbe–host interaction. *Microorganisms* 7:19. doi: 10.3390/microorganisms7010019

Ding, R. X., Goh, W. R., Wu, R. N., Yue, X. Q., Luo, X., Khine, W. W., et al. (2019). Revisit gut microbiota and its impact on human health and disease. *J. Food Drug Anal.* 27, 623–631. doi: 10.1016/j.jfda.2018.12.012

Farha, A. K., Yang, Q. Q., Kim, G., Li, H. B., Zhu, F., Liu, H. Y., et al. (2020). Tannins as an alternative to antibiotics. *Food Biosci.* 38:100751. doi: 10.1016/j.fbio.2020.100751

Gilbert, J., Blaser, M. J., Caporaso, J. G., Jansson, J., Lynch, S. V., and Knight, R. (2018). Current understanding of the human microbiome. *Nat. Med.* 24, 392–400. doi: 10.1038/nm.4517

Kembel, S. W., Cowan, P. D., Helmus, M. R., Cornwell, W. K., Morlon, H., Ackerly, D. D., et al. (2010). Picante: R tools for integrating phylogenies and ecology. *Bioinformatics* 26, 1463–1464. doi: 10.1093/bioinformatics/btq166

Klindworth, A., Pruesse, E., Schweer, T., Peplies, J., Quast, C., Horn, M., et al. (2013). Evaluation of general 16S ribosomal RNA gene PCR primers for classical and next-generation sequencing-based diversity studies. *Nucleic Acids Res.* 41, 1–11. doi: 10.1093/nar/gks808

Laitinen, K., and Gueimonde, M. (2019). Microbiota, food, and health. *Int. J. Mol. Sci.* 20, 4–6. doi: 10.3390/ijms20246329

Langmead, B., and Salzberg, S. L. (2012). Fast gapped-read alignment with Bowtie 2. *Nat. Methods* 9, 357–359. doi: 10.1038/nmeth.1923

Li, Z., Henning, S. M., Lee, R. P., Lu, Q. Y., Summanen, P. H., Thames, G., et al. (2015). Pomegranate extract induces ellagitannin metabolite formation and changes stool microbiota in healthy volunteers. *Food Funct.* 6, 2487–2495. doi: 10.1039/C5FO00669D

Li, S., Wilkinson, K. L., and Bindon, K. A. (2018). Compositional variability in commercial tannin and mannoprotein products. *Am. J. Enol. Vitic.* 69, 176–181. doi: 10.5344/ajev.2017.17057

Lopetuso, L. R., Scaldaferri, F., Petito, V., and Gasbarrini, A. (2013). Commensal clostridia: leading players in the maintenance of gut homeostasis. *Gut Pathog.* 5:1. doi: 10.1186/1757-4749-5-23

Louis, P., and Flint, H. J. (2017). Formation of propionate and butyrate by the human colonic microbiota. *Environ. Microbiol.* 19, 29–41. doi: 10.1111/1462-2920.13589

Masumoto, S., Terao, A., Yamamoto, Y., Mukai, T., Miura, T., and Shoji, T. (2016). Non-absorbable apple procyanidins prevent obesity associated with gut microbial and metabolomic changes. *Sci. Rep.* 6:31208. doi: 10.1038/srep31208

McManus, J. P., Davis, K. G., Beart, J. E., Gaffney, S. H., Lilley, T. H., and Haslam, E. (1985). Polyphenol interactions. Part 1. Introduction; some observations on the reversible complexation of polyphenols with proteins and polysaccharides. *J. Chem. Soc. Perkin Trans. 2* 9, 1429–1438. doi: 10.1039/p29850001429

McManus, J. P., Davis, K. G., Lilley, T. H., and Haslam, E. (1981). The association of proteins with polyphenols. *J. Chem. Soc. Chem. Commun.* 7, 309–311. doi: 10.1039/C3981000309b

Molino, S., Casanova, N. A., Rufián Henares, J. Á., and Fernandez Miyakawa, M. E. (2019). Natural tannin wood extracts as a potential food ingredient in the food industry. *J. Agric. Food Chem.* 68, 2836–2848. doi: 10.1021/acs.jafc.9b00590

Molino, S., Fernández-Miyakawa, M., Giovando, S., and Rufián-Henares, J. Á. (2018). Study of antioxidant capacity and metabolization of quebracho and chestnut tannins through in vitro gastrointestinal digestion-fermentation. *J. Funct. Foods* 49, 188–195. doi: 10.1016/j.jff.2018.07.056

Oksanen, A. J., Blanchet, F. G., Kindt, R., Legen, P., Minchin, P. R., O'Hara, R. B., et al. (2012). Vegan: Community Ecology Package. R package version 2.0-2.

Ozdal, T., Sela, D. A., Xiao, J., Boyacioglu, D., Chen, F., and Capanoglu, E. (2016). The reciprocal interactions between polyphenols and gut microbiota and effects on bioaccessibility. *Nutrients* 8, 1–36. doi: 10.3390/nu8020078

Patra, A. K., Min, B. -R., and Saxena, J. (2012). "Dietary tannins on microbial ecology of the gastrointestinal tract in ruminants" in *Dietary phytochemicals and microbes*. ed. A. K. Patra (Dordrecht: Springer Netherlands), 237–262.

Pérez-Burillo, S., Rufián-Henares, J. A., and Pastoriza, S. (2018). Towards an improved global antioxidant response method (GAR+): physiological-resembling in vitro digestion-fermentation method. *Food Chem.* 239, 1253–1262. doi: 10.1016/j.foodchem.2017.07.024

Prpa, E. J., Bajka, B. H., Ellis, P. R., Butterworth, P. J., Corpe, C. P., Hall, W. L., et al. (2020). A systematic review of in vitro studies evaluating the inhibitory effects of polyphenol-rich fruit extracts on carbohydrate digestive enzymes activity: a focus on culinary fruits consumed in Europe. *Crit. Rev. Food Sci. Nutr.* 1–21. doi: 10.1080/10408398.2020.1808585 [Epub ahead of print]

Quast, C., Pruesse, E., Yilmaz, P., Gerken, J., Schweer, T., Yarza, P., et al. (2013). The SILVA ribosomal RNA gene database project: improved data processing and web-based tools. *Nucleic Acids Res.* 41, 590–596. doi: 10.1093/nar/gks1219

Rinninella, E., Raoul, P., Cintoni, M., Franceschi, F., Miggiano, G. A. D., Gasbarrini, A., et al. (2019). What is the healthy gut microbiota composition? A changing ecosystem across age, environment, diet, and diseases. *Microorganisms* 7:14. doi: 10.3390/microorganisms7010014

Schliep, K. P. (2011). Phangorn: phylogenetic analysis in R. *Bioinformatics* 27, 592–593. doi: 10.1093/bioinformatics/btq706

Segata, N., Izard, J., Waldron, L., Gevers, D., Miropolsky, L., Garrett, W. S., et al. (2011). Metagenomic biomarker discovery and explanation. *Genome Biol.* 12:R60. doi: 10.1186/gb-2011-12-6-r60

Serrano, J., Puupponen-Pimiä, R., Dauer, A., Aura, A. M., and Saura-Calixto, F. (2009). Tannins: current knowledge of food sources, intake, bioavailability and biological effects. *Mol. Nutr. Food Res.* 53, 310–329. doi: 10.1002/mnfr.200900039

Sieniawska, E. (2015). Activities of tannins-from in vitro studies to clinical trials. *Nat. Prod. Commun.* 10, 1877–1884. doi: 10.1177/1934578X1501001118

Silva, M. S., García-Estévez, I., Brandão, E., Mateus, N., de Freitas, V., and Soares, S. (2017). Molecular interaction between salivary proteins and food tannins. *J. Agric. Food Chem.* 65, 6415–6424. doi: 10.1021/acs.jafc.7b01722

Smith, E. A., and MacFarlane, G. T. (1998). Enumeration of amino acid fermenting bacteria in the human large intestine: effects of pH and starch on peptide metabolism and dissimilation of amino acids. *FEMS Microbiol. Ecol.* 25, 355–368. doi: 10.1111/j.1574-6941.1998.tb00487.x

Venegas, D. P., De La Fuente, M. K., Landskron, G., González, M. J., Quera, R., Dijkstra, G., et al. (2019). Short chain fatty acids (SCFAs) mediated gut epithelial and immune regulation and its relevance for inflammatory bowel diseases. *Front. Immunol.* 10:277. doi: 10.3389/fimmu.2019.00277

Wu, Y., Wan, J., Choe, U., Pham, Q., Schoene, N. W., He, Q., et al. (2019). Interactions between food and gut microbiota: impact on human health. *Annu. Rev. Food Sci. Technol.* 10, 389–408. doi: 10.1146/annurev-food-032818-121303

Conflict of Interest: The authors declare that the research was conducted in the absence of any commercial or financial relationships that could be construed as a potential conflict of interest.

frontiers in Microbiology

ORIGINAL RESEARCH
published: 24 March 2021
doi: 10.3389/fmicb.2021.619970

Xylanase Supplementation Modulates the Microbiota of the Large Intestine of Pigs Fed Corn-Based Fiber by Means of a Stimbiotic Mechanism of Action

*Amy L. Petry[1], John F. Patience[1,2], Nichole F. Huntley[1], Lucas R. Koester[3], Michael R. Bedford[4] and Stephan Schmitz-Esser[1]**

[1]Department of Animal Science, Iowa State University, Ames, IA, United States, [2]Iowa Pork Industry Center, Iowa State University, Ames, IA, United States, [3]Department of Veterinary Microbiology and Preventive Medicine, Iowa State University, Ames, IA, United States, [4]AB Vista Feed Ingredients, Marlborough, United Kingdom

This research tested the hypothesis that xylanase modulates microbial communities within the large intestine of growing pigs fed corn-based fiber through a stimbiotic mechanism(s) of action (MOA). Sixty gilts were blocked by initial body weight, individually housed, and randomly assigned to one of four dietary treatments (n = 15): a low-fiber (LF) control, a high-fiber (HF) control containing 30% corn bran, HF+100 mg/kg xylanase (HF+XY), and HF+50 mg/kg arabinoxylan-oligosaccharide (HF+AX). Pigs were fed dietary treatments for 46 days. On day 46, pigs were euthanized, and mucosa and lumen contents were collected from the cecum and the colon. The V4 region of 16S rRNA genes was sequenced and clustered into 5,889, 4,657, 2,822, and 4,516 operational taxonomic units (OTUs), in the cecal contents and mucosa and colonic contents and mucosa, respectively. In cecal contents, HF+XY increased measures of α-diversity compared to LF ($p < 0.001$). Relative to LF, HF increased the prevalence of 44, 36, 26, and 8, and decreased 19, 9, 21, and 10, of the 200 most abundant OTUs from the cecal contents and mucosa and colonic contents and mucosa, respectively ($Q < 0.05$). Compared to LF, HF increased the abundance of OTUs from the *Treponema_2*, *Ruminococcus_1* genera, from the *Lachnospiraceae*, *Ruminococcaceae*, and *Prevotellaceae* families. In contrast, relative to LF, HF decreased *Turicibacter* and *Lactobacillus* in the cecal contents, and *Megasphaera* and *Streptococcus* in the mucosa. Relative to HF, HF+XY increased 32, 16, 29, and 19 and decreased 27, 11, 15, and 10 of the 200 most abundant OTUs from the cecal contents and mucosa and colonic contents and mucosa, respectively ($Q < 0.05$). The addition of xylanase to HF further increased the abundance of OTUs from the *Lachnospiraceae* and *Ruminococcaceae* families across the large intestine. Compared to HF, HF+XY increased the abundance of *Lactobacillus*, *Bifidobacterium*, and *Faecalibacterium* among all locations ($Q < 0.05$). However, HF+AX did not increase the prevalence of these genera in the large intestine. Supplementing xylanase to HF increased hidden-state predictions of microbial enzymes associated with arabinoxylan degradation, xylose metabolism, and short-chain fatty acid production. These data suggest xylanase elicits a stimbiotic MOA in the large intestine of pigs fed corn-based fiber.

Keywords: gut microbiota, insoluble fiber, stimbiotic, swine, xylanase, mucosa, colon, cecum

OPEN ACCESS

Edited by:
Dimitris G. Hatzinikolaou, National and Kapodistrian University of Athens, Greece

Reviewed by:
Zheng Ruan, Nanchang University, China
Ren-You Gan, Chinese Academy of Agricultural Sciences, China

***Correspondence:**
Stephan Schmitz-Esser
sse@iastate.edu

Specialty section:
This article was submitted to Microbial Symbioses, a section of the journal Frontiers in Microbiology

Received: *21 October 2020*
Accepted: *04 March 2021*
Published: *24 March 2021*

Citation:
Petry AL, Patience JF, Huntley NF, Koester LR, Bedford MR and Schmitz-Esser S (2021) Xylanase Supplementation Modulates the Microbiota of the Large Intestine of Pigs Fed Corn-Based Fiber by Means of a Stimbiotic Mechanism of Action. Front. Microbiol. 12:619970. doi: 10.3389/fmicb.2021.619970

INTRODUCTION

It is well established that pigs do not synthesize the endogenous enzymes required to digest dietary fiber (DF). Thus, pigs must rely on their gastrointestinal microbiota to ferment DF into metabolizable substrates (Varel and Yen, 1997). Modern swine diets are trending to contain increased concentrations of DF. This is often a consequence of mitigating rising feed costs by utilizing economically-priced industrial co-products. Many of these co-products fed to pigs are corn-based, and often shift the carbohydrate composition of the diet to favor DF, rather than starch (Acosta et al., 2020). It is well known that increasing DF can reduce nutrient and energy digestibility, impair hindgut fermentation, and decrease pig performance (Gutierrez et al., 2013; Weber et al., 2015). The DF innate to corn, and its co-products, is almost entirely insoluble and largely composed of arabinoxylans (Jaworski et al., 2015). Corn-based arabinoxylans are poorly fermented by resident microbiota due to their structural complexity and poor solubility (Bach Knudsen, 2014). One potential strategy to improve the fermentability of DF, and possibly mitigate its negative effects, is to include exogenous carbohydrases into the diet.

Xylanase is a logical carbohydrase to include in corn-based diets as it hydrolyzes the β-(1-4) glycosidic bonds of arabinoxylans (Dodd and Cann, 2009). Furthermore, it may improve DF fermentation by depolymerizing arabinoxylans into lower molecular weight fragments that are more soluble and fermentable (Pedersen et al., 2015). Indeed, xylanase often improves the nutrient and fiber digestibility of corn-based diets in the large intestine of the pig (Petry et al., 2019). Microbial fermentation largely occurs in the cecum and colon due to the dense microbial populations in these gastrointestinal regions (Jensen and Jørgensen, 1994). Additionally, there are increasing reports that supplementation of xylanase to swine benefits markers of improved gastrointestinal health, and commonly reduces finishing pig mortality in commercial production (Petry and Patience, 2020). These improvements in health are often postulated to result from modulation of microbial populations in the gut. However, there is a paucity of research investigating the composition of hindgut microbiota in pigs fed corn-based fiber supplemented with xylanase with a long adaptation period. Moreover, the *in vivo* mechanism(s) of action (MOA) of xylanase in the presence of corn-based DF has yet to be fully elucidated.

The *in-situ* release products of xylanase are likely arabinoxylan oligosaccharides (AXOS), and high molecular weight arabinoxylan polysaccharides. It has been reported that these AXOS can be rapidly fermented by the resident microbiota and modulate the gastrointestinal microbiota in the large intestine of poultry *via* a stimbiotic MOA (Bautil et al., 2020; González-Ortiz et al., 2020). However, there is a dearth of research in swine (Petry and Patience, 2020). A stimbiotic was defined by González-Ortiz et al. (2019), as "*an additive that stimulates a fiber-degrading microbiome resulting in an increase in fiber fermentability even though the additive itself contributes little to short chain fatty acid production*." The proposed mechanism of a stimbiotic is that it accelerates the capacity of the large intestine to more efficiently digest fiber by modulating microbial taxa that produce their own carbohydrases (Bautil et al., 2020; González-Ortiz et al., 2020). Therefore, the experimental objective was to characterize the modulation of hindgut microbiota due to increased corn-based fiber, xylanase, and directly-supplemented AXOS in pigs fed corn-based diets for 46 days. We hypothesized that the addition of xylanase or AXOS would modulate intestinal microbial communities to more effectively support fiber degradation through a stimbiotic MOA.

MATERIALS AND METHODS

Animals, Diets, and Experimental Design

The investigation into the gastrointestinal microbiota reported herein is in continuation of related research reported by Petry et al. (2020a,b). Readers are referred to Petry et al. (2020a) for greater detail on animal methods and diet compositions. Methods reported herein are adapted from Petry et al. (2020a), and are provided to briefly orient readers to the study design. All analytical methods exclusive to these data reported herein are provided.

Sixty growing gilts with an initial body weight of 25.4 ± 0.9 kg were used in three replicates (20 gilts per replicate) of a 46-day trial. Gilts were blocked by initial body weight and randomly assigned within a block to one of four dietary treatments: a low-fiber (LF) control with 7.5% neutral detergent fiber (NDF), a high-fiber (HF) control with 30% corn bran without solubles (NDF = 21.9%), HF+100 mg xylanase/kg (HF+XY; Econase XT 25P; AB Vista, Marlborough, United Kingdom) providing 16,000 birch xylan units per kg, and HF+50 mg arabinoxylan-oligosaccharide/kg (HF+AX; 3–7 degrees of polymerization). Pigs were individually housed and fed *ad libitum* for 36 days to provide adequate time for the pig and their microbiota, to adapt to dietary treatments. On day 36, pigs were moved to metabolism crates for a 10-day metabolism study reported by Petry et al. (2020a). During the metabolism study, pigs were limit fed 80% of the average daily feed intake determined based on the intake of the first replicate averaged across all treatments. The daily feed allotment was split into two feedings. Pigs were given *ad libitum* access to water throughout the duration of the total study.

Sample Collection

On day 46, pigs were fed half of their total daily feed allotment, and after consumption, were euthanized by captive bolt stunning and exsanguination. Pigs were necropsied for collection of lumen contents and mucosa from the cecum and colon. Approximately, 30 ml of cecal contents was collected, subsampled, snap-frozen in liquid nitrogen, and stored at −80°C pending DNA extraction. The apex of the cecum was isolated and rinsed with sterile phosphate buffered solution to remove remnants, and mucosal scrapings were carefully collected from the tissue, snap-frozen in liquid nitrogen, and stored at −80°C pending DNA extraction. Similarly, contents from the ascending portion of the spiral colon were collected, subsampled, and snap-frozen in liquid nitrogen, and stored at −80°C.

An approximately 4-cm long section proximal to the ascending spiral colon was isolated and flushed with sterile phosphate buffered solution. The colonic tissue was scraped for mucosa, and the scrapings were snap-frozen in liquid nitrogen and stored at −80°C pending DNA extraction.

DNA Extraction and 16S rRNA Gene Illumina MiSeq Sequencing

Total genomic DNA was extracted from cecal and colonic mucosa and contents using a DNeasy PowerLyzer PowerSoil Kit (Qiagen, Germantown, MD) according to the manufacturer's instructions. Extracted genomic DNA concentration and purity were evaluated using a ND-1000 spectrophotometer (NanoDrop Technologies, Rockland, DE), and subsequently stored at −80°C for later sequencing. All samples had 260:280 nm ratios above 1.84. Extracted DNA was adjusted to a total well concentration of 125 ng of DNA, and sequencing was conducted by the DNA facility at Iowa State University (Ames, IA).

PCR-amplified 16S rRNA gene sequencing was conducted using a previously established protocol designed to amplify bacteria and Arcaea (Caporaso et al., 2018). Concisely, one replicate per sample of extracted genomic DNA was amplified using Platinum™ Taq DNA Polymerase (Thermo Fisher Scientific, Waltham, MA). Mutual 16S rRNA bacterial primers 515F (5'-GTGYCAGCMGCCGCGGTAA-3'; 21) and 806R (5'-GG ACTACNVGGGTWTCTAAT-3'; 22) for the variable region V4 were utilized as previously described (Kozich et al., 2013). All samples underwent PCR with an initial denaturation step at 94°C for 3 min, followed by 35 PCR cycles (45 s of denaturing at 94°C, 20 s of annealing at 50°C, and 90 s of extension at 72°C), and concluded with a 10 min extension at 72°C. The subsequent PCR products were purified with a QIA quick 96 PCR Purification Kit (Qiagen Sciences Inc., Germantown, MD) according to the manufacturer's directions. The bar-coded amplicons were included at equivalent molar ratios and used for Illumina MiSeq paired-end sequencing with 250 bp read length and cluster generation with 10% PhiX control DNA on an Illumina MiSeq platform (Illumina Inc., San Diego, CA).

Sequence Analyses and Prediction of Functional Potential

Once sequencing was complete, corresponding overlapping paired-end reads was stitched to obtain an ultimate amplicon size of 255 bp. The sequencing data for each sample were screened for quality, and paired-end reads were combined using mothur (v.1.40.4). Sequences that contained ambiguous bases, were shorter than 250 bp, longer than 255 bp, contained homopolymers >8 bases in size, and potential chimeric sequences were removed. Remaining sequences were then clustered into operational taxonomic units (OTUs) with a 99% sequence similarity based on a distance matrix generated in mothur. Consensus taxonomy for OTUs was assigned using version 132 of the SILVA SSU database (Pruesse et al., 2007). Shannon, Simpson, and Chao1 α-diversity indices were calculated as previously described (Kim et al., 2017).

The hidden-state predictions of gene families and their abundance within a given location were constructed using the 2.3.0b version of Phylogenetic Investigation of Communities by Reconstruction of Unobserved States 2 (PICRUSt2), according to default parameters (Douglas et al., 2020). Briefly, representative 16S rRNA gene amplicon sequences for each OTU were aligned and placed into a phylogenetic tree with relation to reference genomes from the Integrated Microbial Genomes database using the provisions of HMMER, EPA-ng, and GAPPA (Barbera et al., 2019; Bengtsson-Palme et al., 2020; Czech et al., 2020).

Hidden-state gene predictions were determined by castor references based on nearest-sequenced taxon index, with a threshold of 2 (Louca and Doebeli, 2018). The hidden-state predictions of 2,381 enzymes were characterized from the Enzyme Commission (EC) database (Caspi et al., 2018). A total of 25 enzymes associated with arabinoxylan degradation, pentose metabolism, or short chain fatty acid (SCFA) production were selected (**Table 1**), normalized by predicted 16S rRNA gene copy number per OTU, and subsequentially analyzed using preplanned contrasts.

Statistical Analysis

Data were analyzed according to the following statistical model:

$$Y_{ijkl} = \mu + \tau_i + \upsilon_j + \rho_k + e_{ijkl}$$

Where Y_{ijkl} is the observed value for *l*th experimental unit within the *i*th level of dietary treatment of the *j*th block for

TABLE 1 | Enzymes associated with arabinoxylan degradation, pentose metabolism, or short chain fatty acid (SCFA) production that were selected for gene prediction-based analysis using Phylogenetic Investigation of Communities by Reconstruction of Unobserved States 2 (PICRUSt2).

Enzyme Commission (EC) number	Accepted name
1.1.1.9	D-xylulose reductase
1.1.1.27	L-lactate dehydrogenase
1.1.1.28	D-lactate dehydrogenase
2.3.1.8	Phosphate acetyltransferase
2.7.2.1	Acetate kinase
2.7.2.7	Butyrate kinase
2.7.2.15	Propionate kinase
2.7.1.17	Xylulose kinase
2.8.3.1	Propionate CoA-transferase
2.8.3.8	Acetate CoA-transferase
2.8.3.9	Butyrate-acetoacetate CoA-transferase
2.8.3.18	Succinyl-CoA:acetate CoA-transferase
3.1.1.73	Ferulic acid esterase
3.2.1.8	Endo-1,4-β-xylanase
3.2.1.22	Alpha-galactosidase
3.2.1.37	Xylan 1,4-β-xylosidase
3.2.1.55	Non-reducing end α-L-arabinofuranosidase
3.2.1.136	Glucuronoarabinoxylan endo-1,4-β-xylanase
3.2.1.139	Alpha-glucosiduronase
3.2.1.156	Oligosaccharide reducing-end xylanase
4.1.2.9	Phosphoketolase
5.3.1.5	Xylose isomerase
6.2.1.1	Acetate-CoA ligase
6.2.1.5	Succinyl-CoA synthetase (ADP-forming)
6.2.1.13	Acetate-CoA ligase (ADP-forming)

the *l*th pig in the *k*th replicate; μ is the general mean; τ_i is the fixed effect of the *i*th diet (i = 1–4); υ_j is the random effect of the *j*th block (j = 1–5); ρ_k is the random effect of the *k*th replicate (k = 1–3); and e_{ijkl} is the associated variance as described by the model for Y_{ijkl} (l = 1 through 60).

The top 200 individual OTUs, relative abundance of the 20 most abundant genera, and hidden-state predictions of the 25 microbial enzyme genes were analyzed using a negative binomial distribution in GLIMMIX procedure of SAS (Version 9.4, SAS Inst., Cary, NC), and they were offset by the total library count for a given sample. The MULTTEST procedure of SAS was used to correct p values for false discovery rates (Q values). For variables with a treatment $Q < 0.05$, the LOG_2 fold change and respective standard errors, were calculated comparing LF vs. HF, HF vs. HF+XY, and HF vs. HF+AX. Diversity indices were analyzed using PROC MIXED procedure of SAS. Least square means were separated using Fisher's Least Significant Difference test, and treatment differences were considered significant if $p < 0.05$.

RESULTS

Intestinal Microbiota Population Characteristics

A total of 9,280,410 sequences were obtained from all samples after size filtering, quality control, and chimera removal.

Cecum

From cecal content samples, a total of 2,707,536 high-quality reads were clustered into 5,889 OTUs and 213 genera, with a median of 41,672 sequences among samples. The five most abundant phyla (**Supplementary Figure S1A**; 97.5% of all OTUs) present included *Firmicutes* (64.44%), *Bacteroidetes* (27.33%), *Proteobacteria* (2.26%), *Actinobacteria* (2.04%), and *Spirochaetes* (1.40%). When characterized into families (**Supplementary Figure S1B**), the 20 most abundant families accounted for 96.22% of OTUs, and notably, *Prevotellaceae* (20.90%), *Ruminococcaceae* (19.40%), *Lachnospiraceae* (13.39%), *Clostridiaceae_1* (8.57%), and *Lactobacillaceae* (6.77%) were the five most abundant. Similarly, the 20 most abundant genera accounted for 70.57% of all classified OTUs (**Supplementary Figure S1C**), and notably *Clostridium_sensu_stricto_1* (8.7%), *Lachnospiraceae_unclassified* (7.84%), *Lactobacillus* (7.65%), *Ruminococcaceae_UCG-005* (5.25%), and *Allopreveotella* (5.07%) rounded out the top five.

A total of 2,551,171 high-quality reads from cecal mucosa samples were clustered into 4,657 OTUs and 234 genera, with a median of 41,672 sequences among samples. The five most abundant phyla among the cecal mucosa-associated microbiota accounted for 95.92% of all OTUs (**Supplementary Figure S1D**), and encompassed *Firmicutes* (53.08%), *Bacteroidetes* (31.59%), *Epsilonbacteraeota* (4.88%), *Proteobacteria* (4.11%), and *Spirochaetes* (2.27%). When further classified into families, the 20 most abundant accounted for 94.77% of all OTUs (**Supplementary Figure S1E**), and *Prevotellaceae* (23.44%), *Ruminococcaceae* (14.85%), *Lachnospiraceae* (10.46%), *Streptococcaceae* (6.08%), and *Lactobacillaceae* (5.55%) were the five most abundant. The 20 most abundant genera (**Supplementary Figure S1F**), comprised 70.22% of all OTUs, and *Allopreveotella* (7.26%), *Streptococcus* (6.08%), *Lactobacillus* (5.54%), *Ruminococcaceae_UCG-005* (5.25%), and *Lachnospiraceae_unclassified* (4.55%) were the five most abundant.

Colon

A total of 1,848,354 high-quality reads were obtained from colonic contents and clustered into 2,822 OTUs and 215 genera, with a median of 33,870 sequences among samples. The five most abundant phyla (**Supplementary Figure S2A**; 96.9% of all OTUs) included *Firmicutes* (66.03%), *Bacteroidetes* (24.42%), *Spirochaetes* (3.51%), *Proteobacteria* (1.50%), and *Euryarchaeota* (1.46%). The 20 most abundant families accounted for 95.6% of OTUs (**Supplementary Figure S2B**), and notably, *Ruminococcaceae* (18.36%), *Prevotellaceae* (18.04%), *Lachnospiraceae* (16.42%), *Clostridiaceae_1* (11.19%), and *Streptococcaceae* (6.29%) were the five most abundant. Likewise, the 20 most abundant genera comprised 67.4% of all OTUs (**Supplementary Figure S2C**), and *Clostridium_sensu_stricto_1* (11.05%), *Lachnospiraceae_unclassified* (8.72%), *Streptococcus* (6.29%), *Ruminococcaceae_UCG-005* (5.64%), and *Prevotellaceae_NK3B31_group* (4.53%) composed the five most abundant.

From colonic mucosa samples, a total of 2,173,348 high-quality reads were clustered into 4,516 OTUs and 253 genera, with a median of 37,554 sequences among samples. The five most abundant phyla (**Supplementary Figure S2D**; 94.2% of all OTUs) present included *Firmicutes* (55.74%), *Bacteroidetes* (27.54%), *Proteobacteria* (4.04%), *Spirochaetes* (3.85%), and *Epsilonbacteraeota* (3.04%). When characterized into families (**Supplementary Figure S2E**), the 20 most abundant accounted for 91.12% of OTUs, and *Ruminococcaceae* (19.59%), *Prevotellaceae* (16.57%), *Lachnospiraceae* (11.74%), *Streptococcaceae* (7.05%), and *Rikenellaceae* (4.74%) were the five most abundant. With regard to microbial genera, the 20 most abundant accounted for 63.50% of all classified OTUs in the colonic mucosa (**Supplementary Figure S2F**), and *Streptococcus* (7.05%), *Lachnospiraceae_unclassified* (6.46%), *Ruminococcaceae_UCG-005* (6.22%), *Clostridium_sensu_stricto_1* (4.62%), and *Prevotellaceae_NK3B31_group* (4.12%) were the five most abundant.

Alpha-Diversity

Chao1, Shannon, and Simpson indices of diversity, evenness and richness are depicted in **Figure 1**. For the cecal contents, HF+XY had the greatest Chao1, Shannon, and Simpson indices, with HF and HF+AX performing intermediately among treatments, and LF having the lowest ($p < 0.001$). Compared to LF, HF, HF+XY, and HF+AX had greater Chao1 and Shannon indices in the cecal mucosa ($p < 0.05$), but did not differ for the Simpson index ($p = 0.117$). Similarly, for colonic contents HF, HF+XY, and HF+AX had a greater Chao1 index than LF ($p = 0.041$). For the Shannon and Simpson indices, HF and HF+AX were greater than LF and HF+XY ($p < 0.05$). Shannon and Simpson indices did not differ among treatments in the colonic mucosa, but HF+XY had the greatest Chao1 index ($p = 0.042$).

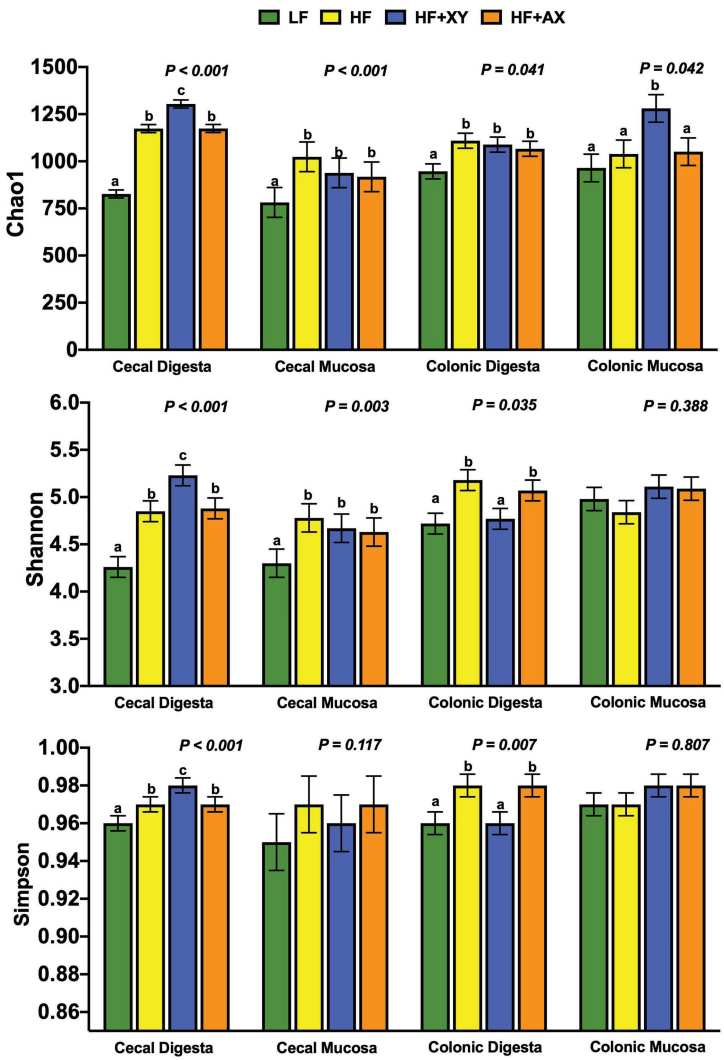

FIGURE 1 | Indices of α-diversity of microbial operational taxonomic units (OTUs) among treatments present in the contents and mucosa from the cecum and colon.

Dietary Treatment Modulation of Cecal and Colonic Microbiota

Figure 2 depicts the relative abundance of the five most abundant phyla and 20 most abundant genera among treatments within each location. The five most abundant phyla accounted for 96.5, 97.5, 97.3, and 97.7% of all characterized OTUs in cecal contents for LF, HF, HF+XY, and HF+AX, respectively. Whereas, the 20 most abundant genera among treatments accounted for 67.9, 69.7, 74.1, and 70.6% of all OTUs present in cecal contents for LF, HF, HF+XY, and HF+AX, respectively. In the cecal mucosa, the five most abundant phyla comprised 94.4, 96.4, 95.4, and 96.6% of all OTUs characterized in LF, HF, HF+XY, and HF+AX, respectively. Likewise, the 20 most abundant genera among microbiota characterized from cecal mucosa accounted for 67.8, 70.2, 71.8, and 71.6% of the OTUs characterized in LF, HF, HF+XY, and HF+AX, respectively.

In the colonic contents, the five most abundant phyla comprised 96.8, 96.8, 97.8, and 97.3% of all OTUs present in LF, HF, HF+XY, and HF+AX, respectively. Whereas, in the colonic mucosa, the five most abundant phyla accounted for 94, 92.6, 94, and 94.9% of the OTUs is present in LF, HF, HF+XY, and HF+AX, respectively. The 20 most abundant genera in the colonic contents composed 64.4, 68.5, 66.8, and 68.9% of the OTUs found in LF, HF, HF+XY, and HF+AX, respectively. Within the colonic mucosa, the 20 most abundant genera comprised 59.3, 63.2, 63.9, and 65.2% of OTUs found in in LF, HF, HF+XY, and HF+AX, respectively.

Treatment Modulation of Microbial Genera in the Cecum

Relative to LF, HF increased *Treponema_2* and *Ruminococcaceae_UCG-005*, and reduced *Turicibacter* and *Lactobacillus* in cecal

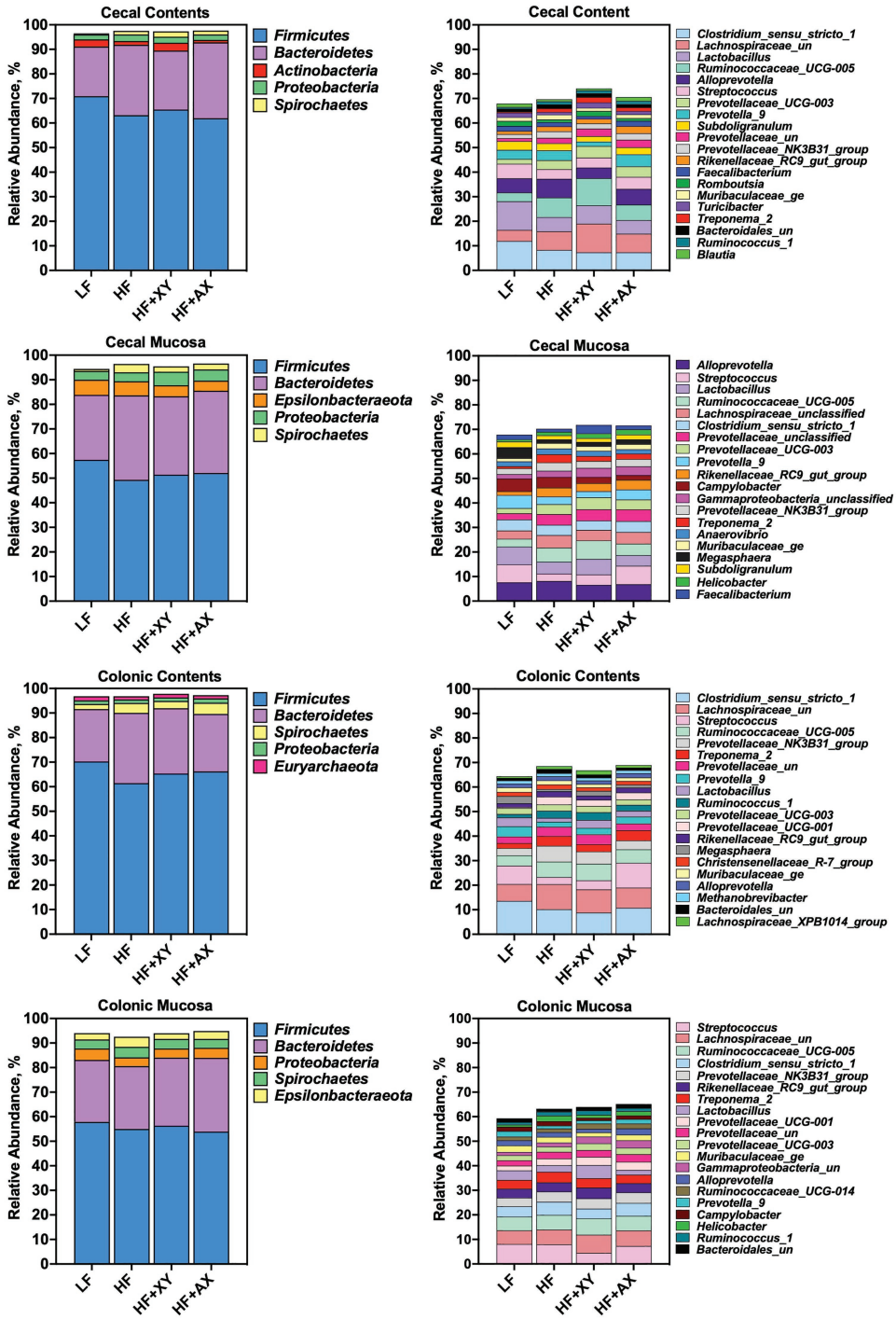

FIGURE 2 | The relative abundance of the five most abundant phyla and 20 most abundant genera among treatments found in the contents and mucosa from the cecum and colon.

contents (**Figure 3**; $Q < 0.05$). In the cecal mucosa, relative to LF, HF had a greater proportion of *Treponema_2* and *Rikenellaceae_RC9_gut_group*, and *Megasphaera* and *Streptococcus* were less abundant (**Figure 3**; $Q < 0.05$). The addition of xylanase to HF increased the presence of *Turicibacter*, *Romboutsia*, *Lachnospiraceae_unclassified*, and *Ruminococcaceae_UCG-005*, but decreased the prevalence of *Prevotella_9* and *Alloprevotella*, in the cecal contents ($Q < 0.05$). Relative to HF, HF+XY

increased *Faecalibacterium* in the cecal mucosa, and decreased the prevalence of *Campylobacter* ($Q < 0.05$). The 20 most abundant genera did not differ between HF and HF+AX in the cecal contents ($Q > 0.10$), but HF+AX did increase the abundance of *Streptococcus* and decreased the prevalence of *Campylobacter* ($Q < 0.05$).

Treatment Modulation of Microbial Genera in the Colon

In the colonic contents, relative to LF, HF increased the prevalence of *Prevotellaceae_UCG-001*, *Prevotellaceae_NK3B31_group*, *Ruminococcus_1*, and *Treponema_2*, but decreased the abundance of *Prevotella_9*, *Lactobacillus*, *Streptococcus*, and *Megasphaera* (**Figure 3**; $Q < 0.05$). Similarly, compared to LF, HF decreased the abundance of *Prevotella_9* and *Lactobacillus* in the colonic mucosa, but increased *Helicobacter* and *Ruminococcus_1* (**Figure 3**; $Q < 0.05$). Contrarily in the colonic contents, when compared to HF, HF+XY increased the abundance of *Megasphaera* and *Lactobacillus* but decreased the prevalence of *Rikenellaceae_RC9_gut_group* and *Treponema_2* ($Q < 0.05$). Moreover, the addition of xylanase to HF increased the abundance of *Lactobacillus*, *Gammaproteobacteria_unclassified*, and *Ruminococcaceae_UCG-014* in the colonic mucosa, but decreased the abundance of *Campylobacter*, *Streptococcus*, and *Helicobacter* ($Q < 0.05$). The addition of AXOS to HF increased *Streptococcus* and decreased *Prevotellaceae_NK3B31_group* in the colonic contents ($Q < 0.05$). Within the colonic mucosa, compared with the HF, HF+AX increased the abundance of *Prevotella_9* and *Gammaproteobacteria_unclassified*, but reduced the abundance of *Lactobacillus* ($Q < 0.05$).

Treatment Modulation of the 200 Most Abundant OTUs in the Cecal Contents

Compared to LF, HF significantly increased the prevalence of 44, and reduced 19, of the 200 most prevalent OTUs characterized from cecal contents (**Figure 4A**). Notably, among the 100 most abundant OTUs in the cecal contents, HF increased the prevalence of five OTUs from the genus *Ruminococcaceae_UCG-005* (OTUs #10, 23, 36, 58, and 63), two unclassified OTUs associated with the family *Lachnospiraceae* (OTUs #92 and 100), two OTUs from the genus *Rikenellaceae_RC9_gut_group* (OTUs #52 and 70), and five OTUs from the family *Prevotellaceae* (OTUs: *OTU_4_Alloprevotella*, *OTU_6_Prevotella_9*, *OTU_50_Prevotellaceae_UCG-001*, *OTU_81_Prevotellaceae_NK3B31_group*, and *OTU_90_Prevotella_1*). Interestingly, among the 100 most abundant OTUs in the cecal contents, HF significantly decreased

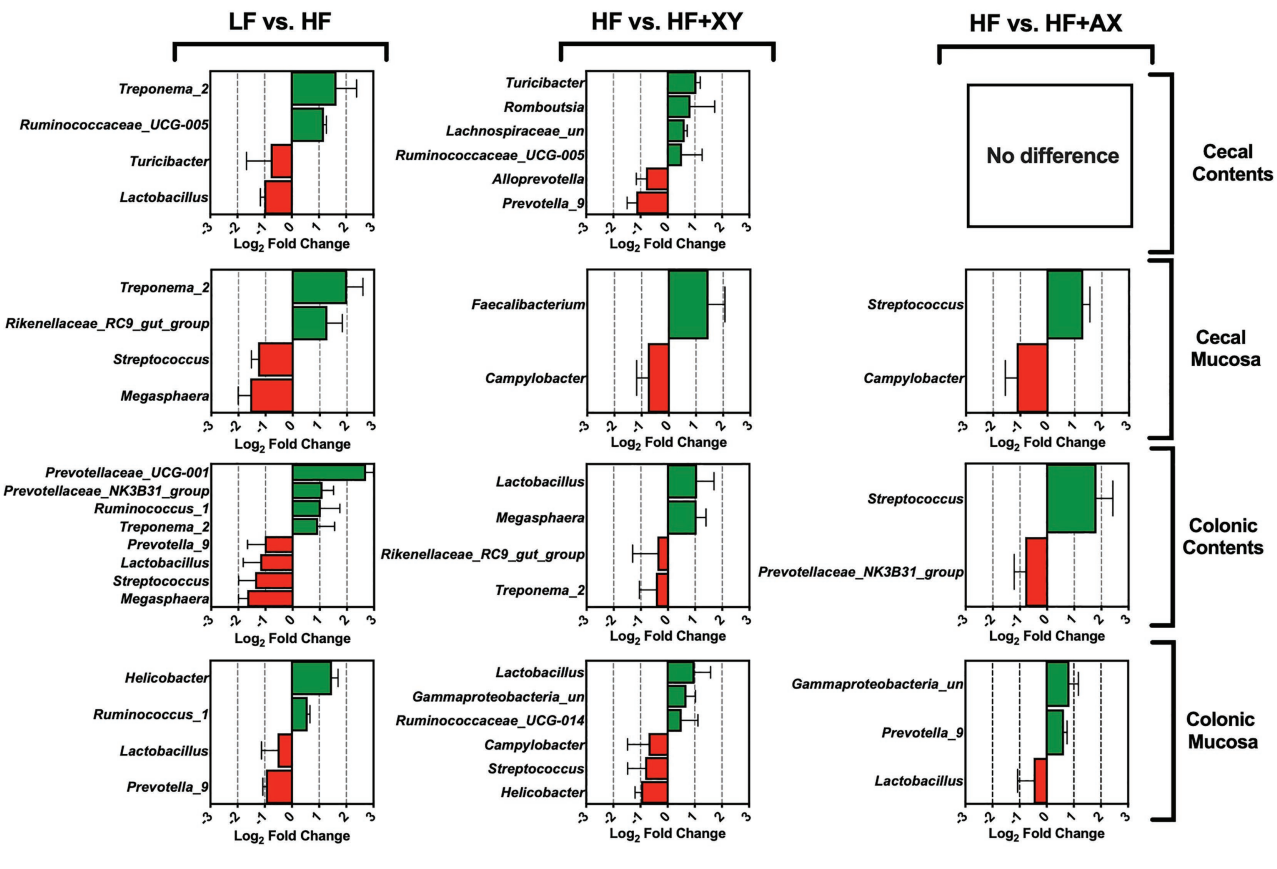

FIGURE 3 | The Log_2 fold change difference between LF vs. HF, HF vs. HF+XY, and HF vs. HF+AX for the 20 most abundant microbial genera in the contents and mucosa from the cecum and colon with a value of $Q < 0.05$.

the prevalence of *OTU_17_Clostridium_sensu_stricto_1*, *OTU_19_Lactobacillus*, *OTU_33_Blautia*, *OTU_53_Holdemanella*, *OTU_64_Subdoligranulum*, *OTU_67_Pseudoscardovia*, and *OTU_72_Bifidobacterium*. For OTUs 101 through 200 in the cecal contents, when compared to LF, HF increased the prevalence of four unclassified OTUs from the family *Lachnospiraceae* (OTUs #143, 146, 179, and 188), two OTUs from the genus *Rikenellaceae_RC9_gut_group* (OTUs #139 and 157), two OTUs from the genus *Treponema_2* (OTUs #141 and 177), five OTUs from the family *Ruminococcaceae* (OTUs #123, 142, 155, 163, and 167), and two from the genus *Oscillospira* (OTUs #127 and 194). However, relative to LF, HF decreased the abundance of *OTU_118_Terrisporobacter*, *OTU_131_Phascolarctobacterium*, *OTU_182_Ruminococcaceae_UCG-005*, *OTU_169_Lactobacillus*, *OTU_125_Catenibacterium*, *OTU_189_Lactobacillus*, and *OTU_128_Blautia*, in the cecal contents. The addition of xylanase to HF significantly increased 32, and decreased 27, of the 200 most prevalent OTUs characterized from cecal contents (**Figure 4B**). Notably, HF+XY increased the prevalence of seven unclassified OTUs from the family *Lachnospiraceae* (OTUs #92, 100, 143, 161, 175, 179, and 188), seven OTUs from the genus *Ruminococcaceae_UCG-005* (OTUs #23, 55, 58, 75, 87, 163, and 182), three OTUs from the genus *Lactobacillus* (OTUs #19, 169, and 189), two from the *Bifidobacterium* genus (OTUs # 27and 72), and increased the abundance of *OTU_160_Faecalibacterium*. Moreover, relative to HF, HF+XY decreased the prevalence of nine OTUs from the family *Prevotellaceae* (OTUs #4, 6, 81, 101, 102, 126, 134, 186, and 200) and decreased the abundance of *OTU_47_Agathobacter* and *OTU_129_Escherichia-Shigella* in the cecal contents. Compared to HF, HF+AX increased the abundance of 12, and decreased seven, of the 200 most prevalent OTUs characterized from cecal contents (**Figure 4C**).

Treatment Modulation of the 200 Most Abundant OTUs in the Cecal Mucosa

Compared to LF, HF significantly increased 36, and decreased nine, of the 200 most abundant OTUs characterized in the cecal mucosa (**Figure 5A**). In the cecal mucosa, relative to LF, HF increased the abundance of seven OTUs from the family *Ruminococcaceae* (OTUs #17, 54, 84, 100, 146, 154, and 159), five OTUs from the *Rikenellaceae_RC9_gut_group* genus (OTUs #19,45,131,145, and 161), five OTUs from the *Prevotellaceae* family (OTUs #16, 46, 89,104, 129), four OTUs from the *Muribaculaceae* family (OTUs #78,86,149, and 153), four OTUs associated with the *Treponema_2* genus (OTUs #29, 133, 173,and 189), and three unclassified OTUs from the *Lachnospiraceae* family (OTUs #66, 181, and 198). Interestingly, relative to LF, HF decreased the abundance of *OTU_1_Streptococcus*, *OTU_7_Megasphaera*, and *OTU_9_Prevotella_9*, in the cecal mucosa. Relative to HF, HF+XY significantly increased 16, and decreased 11, of the 200 most abundant OTUs characterized in the cecal mucosa (**Figure 5B**). Compared to HF, in the cecal mucosa, HF+XY increased the prevalence of three OTUs from the *Ruminococcaceae_UCG-005* genus (OTUs #54, 85, and 96), and three OTUs from the *Prevotellaceae* family (OTUs #16, 46, and 129). Interestingly, HF+XY also increased the prevalence of *OTU_31_Lactobacillus*, *OTU_67_Bifidobacterium*, *OTU_71_Succinivibrio*, *OTU_124_Catenibacterium*, and *OTU_172_Faecalibacterium* in the cecal mucosa. The addition of AXOS to HF significantly increased five, and decreased seven of the 200 most abundant OTUs (**Figure 5C**). Notably, HF+AX had a greater abundance of *OTU_1_Streptococcus* and *OTU_174_Helicobacter*, and decreased prevalence of *OTU_193_Selenomonas* and *OTU_160_Acetitomaculum*.

Treatment Modulation of the 200 Most Abundant OTUs in the Colonic Contents

Compared to LF, HF significantly increased 26, and decreased 21, of the 200 most abundant OTUs characterized in the colonic contents (**Figure 6A**). Relative to LF, HF increased the abundance of eight OTUs from the family *Ruminococcaceae* (OTUs #21, 92, 100, 113, 157, 170, 179, and 189), seven OTUs from the *Prevotellaceae* family (OTUs #5, 11, 18, 56, 70, 73, and 143), five unclassified OTUs from the *Lachnospiraceae* family (OTUs #41, 84, 86, 112, and 164), and increased the abundance of *OTU_130_Acetitomaculum* and *OTU_196_Akkermansia*. Interestingly, relative to LF, HF decreased the abundance of *OTU_2_Streptococcus*, *OTU_6_Megasphaera*, *OTU_76_Selenomonas*, *OTU_128_Dorea*, *OTU_141_Faecalibacterium*, *OTU_165_Phascolarctobacterium*, and *OTU_172_Methanosphaera* in the colonic contents. The addition of xylanase to HF significantly increased 29, and decreased 15, of the 200 most abundant OTUs characterized in the colonic contents (**Figure 6B**). Compared to HF, HF+XY increased the abundance of eight OTUs from the family *Ruminococcaceae* (OTUs #8, 21, 72, 83, 92, 100, 105, and 120), and five OTUs from the *Lachnospiraceae* family (OTUs #24, 30, 41, 59, 84, and 133) in the colonic contents. Moreover, compared to HF, HF+XY increased the abundance of *OTU_6_Megasphaera*, *OTU_79_Bifidobacterium*, *OTU_128_Dorea*, *OTU_141_Faecalibacterium*, *OTU_165_Phascolarctobacterium*, *OTU_172_Methanosphaera*, and *OTU_173_Catenibacterium* in the colonic contents. Compared to HF, HF+AX increased the abundance of nine, and decreased 12, of the 200 most prevalent OTUs characterized from colonic contents (**Figure 6C**). Notably, the addition of AXOS to HF increased the abundance of *OTU_2_Streptococcus*, *OTU_56_Alloprevotella_5*, *OTU_85_Coprococcus_1*, *OTU_125_Prevotella_7*, *OTU_128_Dorea*, *OTU_138_Treponema_2*, *OTU_172_Methanosphaera*, *OTU_173_Catenibacterium*, and *OTU_187_Spirochaetaceae_unclassified* in the colonic contents. However, HF+AX had decreased prevalence of *OTU_79_Bifidobacterium*, *OTU_140_Ruminococcaceae_NK4A214_group*, *OTU_143_Prevotellaceae_unclassified*, *OTU_144_Agathobacter*, *OTU_156_Acidaminococcus*, and *OTU_196_Akkermansia*, compared to HF in colonic contents.

Treatment Modulation of the 200 Most Abundant OTUs in the Colonic Mucosa

Relative to LF, HF significantly increased eight of the 200 most abundant OTUs characterized from colonic mucosa (**Figure 7A**): *OTU_176_Treponema_2*, *OTU_149_Treponema_2*,

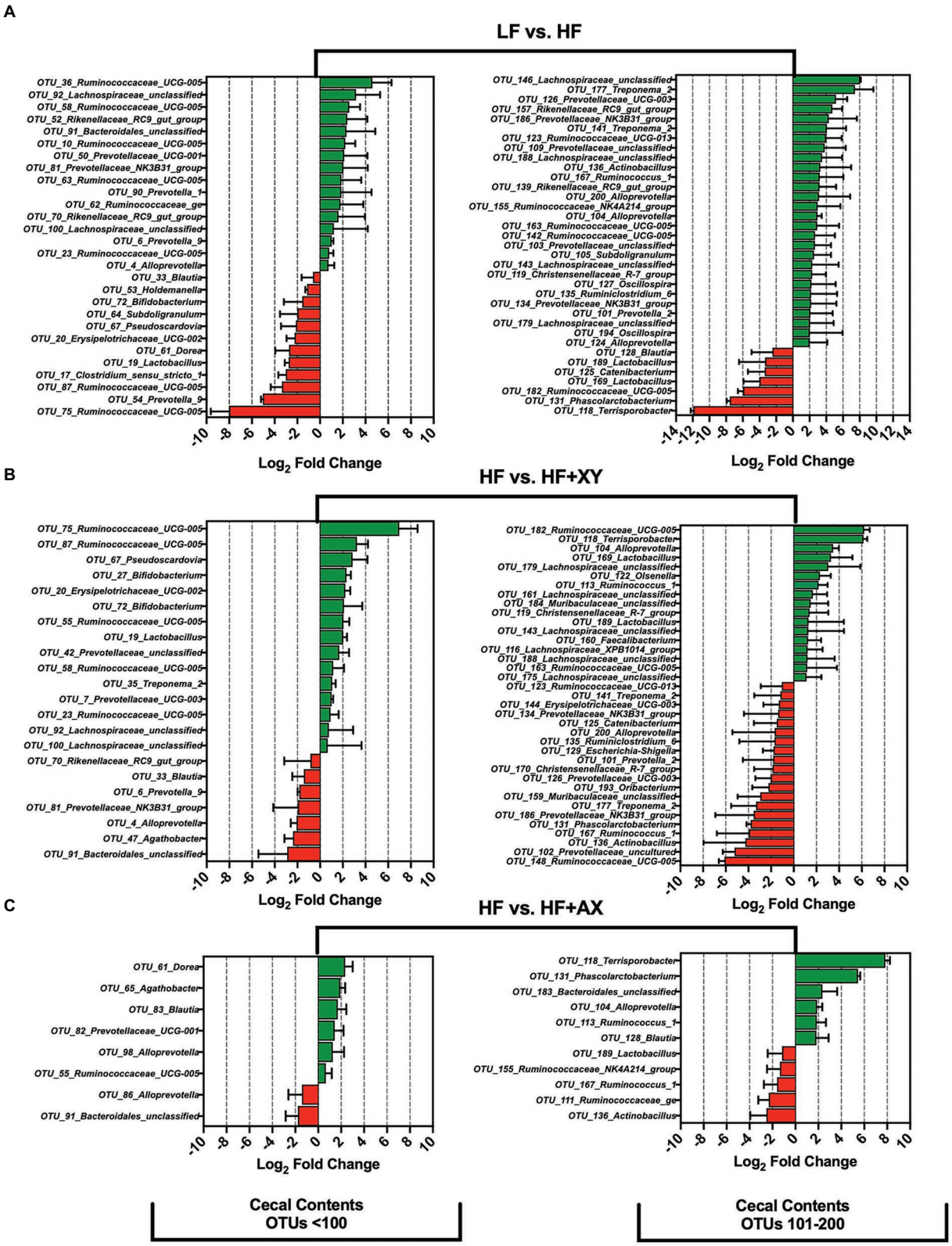

FIGURE 4 | The Log_2 fold change difference between **(A)** LF vs. HF, **(B)** HF vs. HF+XY, and **(C)** HF vs. HF+AX or OTUs with a contrast value of $Q < 0.05$ from the 200 most abundant OTUs among treatments present in the cecal contents.

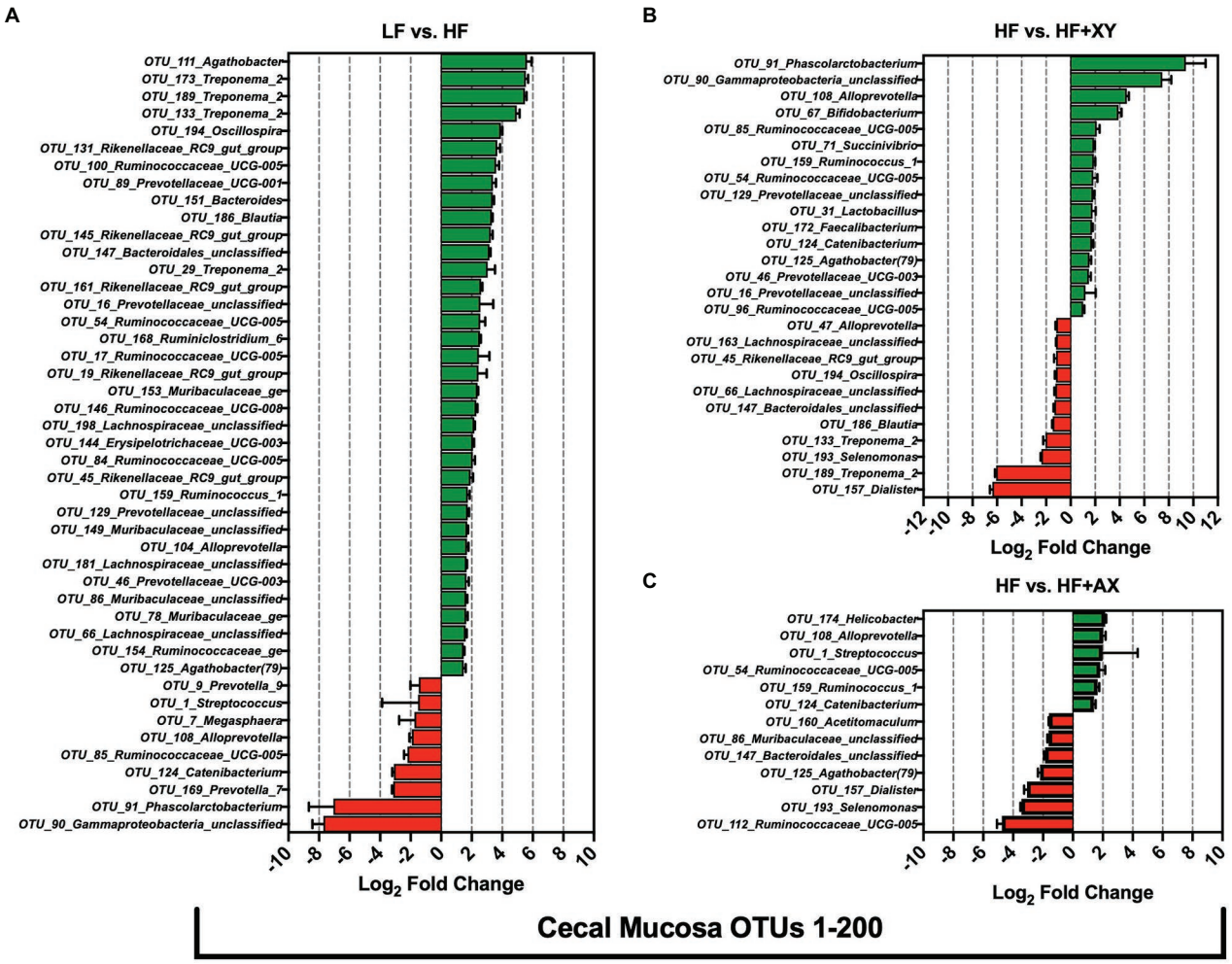

FIGURE 5 | The Log_2 fold change difference between **(A)** LF vs. HF, **(B)** HF vs. HF+XY, and **(C)** HF vs. HF+AX or OTUs with a contrast value of $Q < 0.05$ from the 200 most abundant OTUs among treatments present in the cecal mucosa.

OTU_98_Helicobacter, *OTU_147_Muribaculaceae_unclassified*, *OTU_11_Prevotellaceae_NK3B31_group*, *OTU_182_Lachnospiraceae_unclassified*, *OTU_87_Prevotellaceae_unclassified*, and *OTU_10_Streptococcus*. Moreover, compared to LF, HF had decreased abundance of 10 of the 200 most abundant OTUs characterized from colonic mucosa: *OTU_127_Lachnospiraceae_unclassified*, *OTU_189_Desulfovibrio*, *OTU_134_Treponema_2*, *OTU_158_Lachnospiraceae_unclassified*, *OTU_8_Megasphaera*, *OTU_187_Rikenellaceae_RC9_gut_group*, *OTU_81_Ruminococcaceae_UCG-010*, *OTU_117_Lactobacillus*, *OTU_31_dgA-11_gut_group*, and *OTU_3_Lactobacillus*. Relative to HF, HF+XY significantly increased 19, and decreased 10, of the 200 most abundant OTUs characterized from colonic mucosa (**Figure 7B**). Compared to HF, in the colonic mucosa, HF+XY increased the prevalence of five OTUs from the *Ruminococcaceae* family (OTUs #14, 30, 42, 122, 134, and 139), three OTUs from the *Lachnospiraceae* family (OTUs #80, 127, and 158), three OTUs from the *Lactobacillus* genus (OTUs #3, 117, and 124), two OTUs from the *Prevotellaceae* family (OTUs #85 and 104), and two OTUs from the *Rikenellaceae_RC9_gut_group* (OTUs #105 and 187). Moreover, HF+XY had a greater abundance of *OTU_47_Bifidobacterium*, *OTU_31_dgA-11_gut_group*, and *OTU_4_Gammaproteobacteria_unclassified* in the colonic mucosa. Contrarily, the addition of xylanase to HF reduced the abundance of *OTU_189_Desulfovibrio*, *OTU_176_Treponema_2*, *OTU_149_Treponema_2*, *OTU_56_Ruminococcaceae_UCG-005*, *OTU_79_Alloprevotella*, *OTU_97_Subdoligranulum*, *OTU_10_Streptococcus*, *OTU_98_Helicobacter*, *OTU_147_Muribaculaceae_unclassified*, and *OTU_182_Lachnospiraceae_unclassified* in the colonic mucosa. Relative to HF, HF+AX increased the abundance of eight OTUs in the colonic mucosa (**Figure 7C**): *OTU_42_Ruminococcaceae_UCG-014*, *OTU_158_Lachnospiraceae_unclassified*, *OTU_134_Treponema_2*, *OTU_127_Lachnospiraceae_unclassified*, *OTU_105_Rikenellaceae_RC9_gut_group*, *OTU_139_Ruminococcus_1*, *OTU_31_dgA-11_gut_group*, and *OTU_4_Gammaproteobacteria_unclassified*. Moreover, compared to HF, HF+AX had reduced

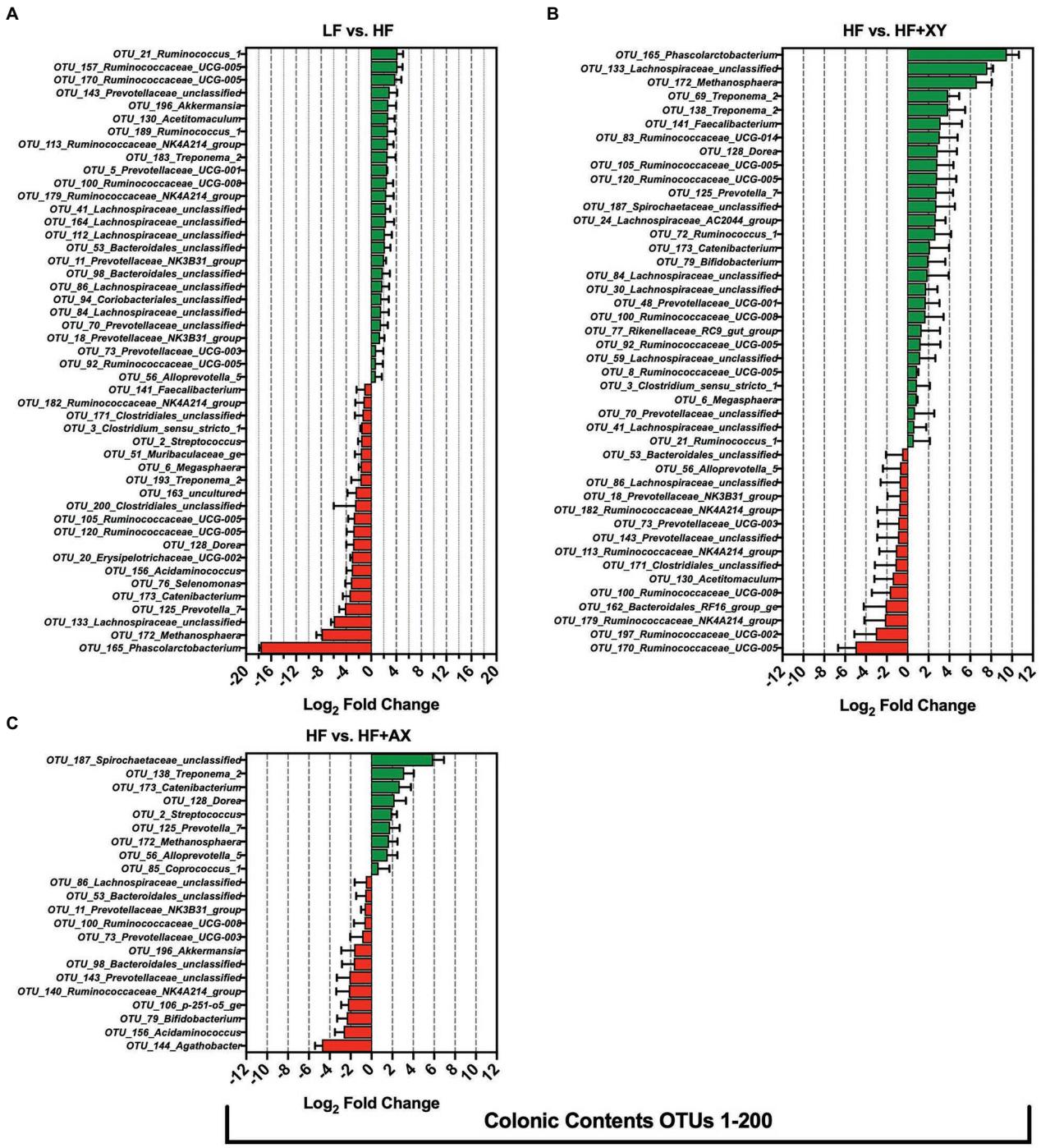

FIGURE 6 | The Log_2 fold change difference between **(A)** LF vs. HF, **(B)** HF vs. HF+XY, and **(C)** HF vs. HF+AX or OTUs with a contrast value of $Q < 0.05$ from the 200 most abundant OTUs among treatments present in the colonic contents.

abundance of seven OTUs in the colonic mucosa (**Figure 7C**): *OTU_189_Desulfovibrio*, *OTU_149_Treponema_2*, *OTU_182_Lachnospiraceae_unclassified*, *OTU_176_Treponema_2*, *OTU_136_Rikenellaceae_RC9_gut_group*, *OTU_147_Muribaculaceae_unclassified*, and *OTU_97_Subdoligranulum*.

PICRUSt2 Targeted Gene Characterizations

Relative to LF, HF increased the abundance of predicted gene counts for propionate kinase, L-lactate dehydrogenase, acetate-CoA ligase [adenosine diphosphate (ADP)-forming],

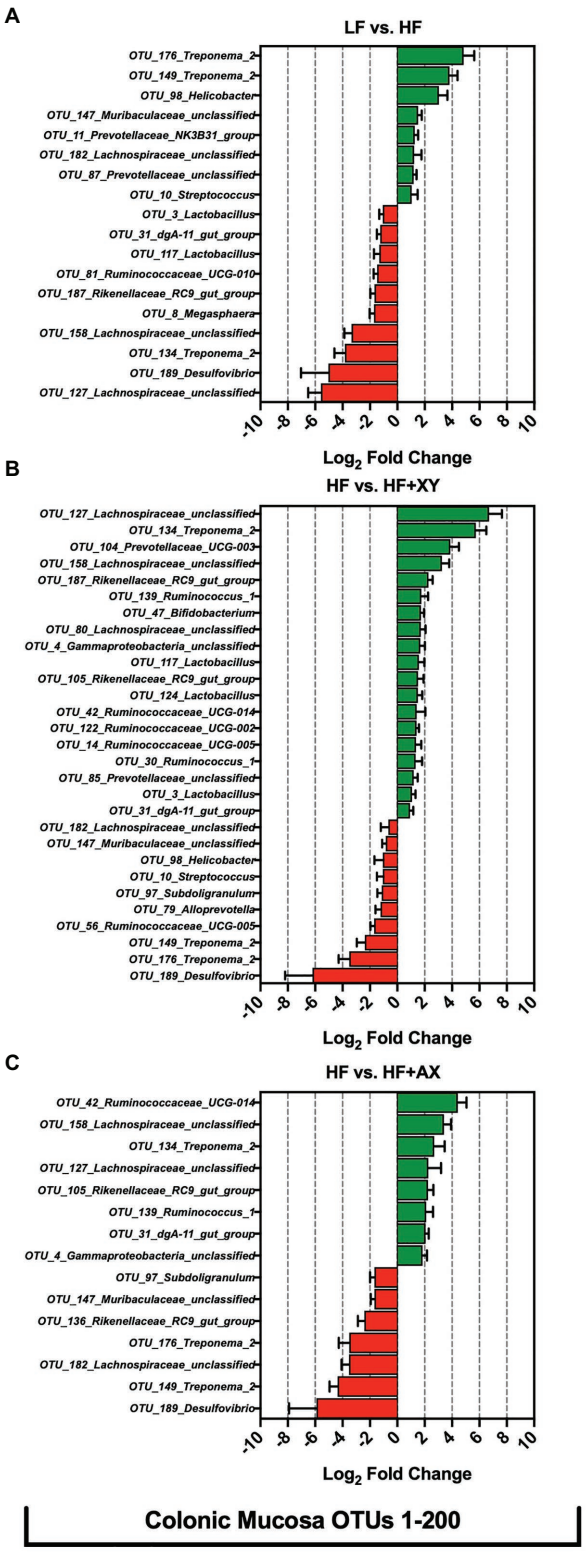

FIGURE 7 | The Log_2 fold change difference between **(A)** LF vs. HF, **(B)** HF vs. HF+XY, and **(C)** HF vs. HF+AX for OTUs with a contrast value of $Q < 0.05$ from the 200 most abundant OTUs among treatments present in the colonic mucosa.

and phosphoketolase in the cecal contents (**Figure 8A**; $Q < 0.05$). The addition of xylanase to HF increased predicted gene counts for acetate kinase, phosphate acetyltransferase, endo-1,4-beta-xylanase, acetate CoA-transferase, xylose isomerase, L-lactate dehydrogenase, and xylulose kinase ($Q < 0.05$). Compared to HF, HF+AX increased the abundance of predicted gene counts for phosphate acetyltransferase and L-lactate dehydrogenase ($Q < 0.05$).

In the cecal mucosa, relative to LF, HF increased predicted gene counts for acetate-CoA ligase (ADP-forming), propionate CoA-transferase, phosphoketolase, and propionate kinase (**Figure 8B**; $Q < 0.05$). Compared to HF, HF+XY increased xylan 1,4-β-xylosidase, succinate-CoA ligase (ADP-forming), xylulose kinase, acetate-CoA ligase (ADP-forming), oligosaccharide reducing-end xylanase, phosphoketolase, and non-reducing end alpha-L-arabinofuranosidase predicted gene counts in the cecal mucosa ($Q < 0.05$). The addition of AXOS to HF increased acetate-CoA ligase (ADP-forming), oligosaccharide reducing-end xylanase, and alpha-galactosidase predicted gene counts in the cecal mucosa.

In the colonic contents, relative to LF, HF increased predicted gene counts for propionate CoA-transferase, acetate-CoA ligase (ADP-forming), L-lactate dehydrogenase, and succinyl-CoA:acetate CoA-transferase (**Figure 8C**; $Q < 0.05$). The addition of xylanase to HF increased predicted gene counts for non-reducing end alpha-L-arabinofuranosidase, phosphoketolase, oligosaccharide reducing-end xylanase, and butyrate-acetoacetate CoA-transferase in the colonic contents ($Q < 0.05$). Likewise, compared to HF, HF+AX pregulated acetate-CoA ligase (ADP-forming), phosphoketolase, and non-reducing end alpha-L-arabinofuranosidase predicted gene counts in colonic content ($Q < 0.05$).

In the colonic mucosa, compared to LF, HF has a greater abundance of predicted gene counts for propionate kinase, glucuronoarabinoxylan endo-1,4-beta-xylanase, and endo-1,4-beta-xylanase (**Figure 8D**; $Q < 0.05$). Relative to HF, HF+XY increased xylose isomerase, butyrate-acetoacetate CoA-transferase, xylulose kinase, L-lactate dehydrogenase, succinyl-CoA:acetate CoA-transferase, propionate kinase, and endo-1,4-beta-xylanase predicted gene counts in the colonic mucosa ($Q < 0.05$). Compared to HF, HF+AX increased acetate-CoA ligase (ADP-forming), propionate CoA-transferase, and propionate kinase predicted gene counts in the colonic mucosa ($Q < 0.05$).

DISCUSSION

In swine nutrition, there has been a renewed interest in the beneficial aspects of DF, and particularly, its ability to modulate microbiota and gut health (Jha et al., 2019). However, the DF found in swine diets is often insoluble and poorly fermented by the hindgut microbiota, and often stems from corn and corn co-products (Gutierrez et al., 2013). Arabinoxylans encompass nearly half of the DF found in corn and several corn co-products (Jaworski et al., 2015). Corn-based arabinoxylans are poorly fermented due to the degree of interaction with other plant components, arabinose substitutions, abundant phenolic cross linkages, and lignification (Bach Knudsen, 2014). One strategy that may improve the fermentability of corn-based

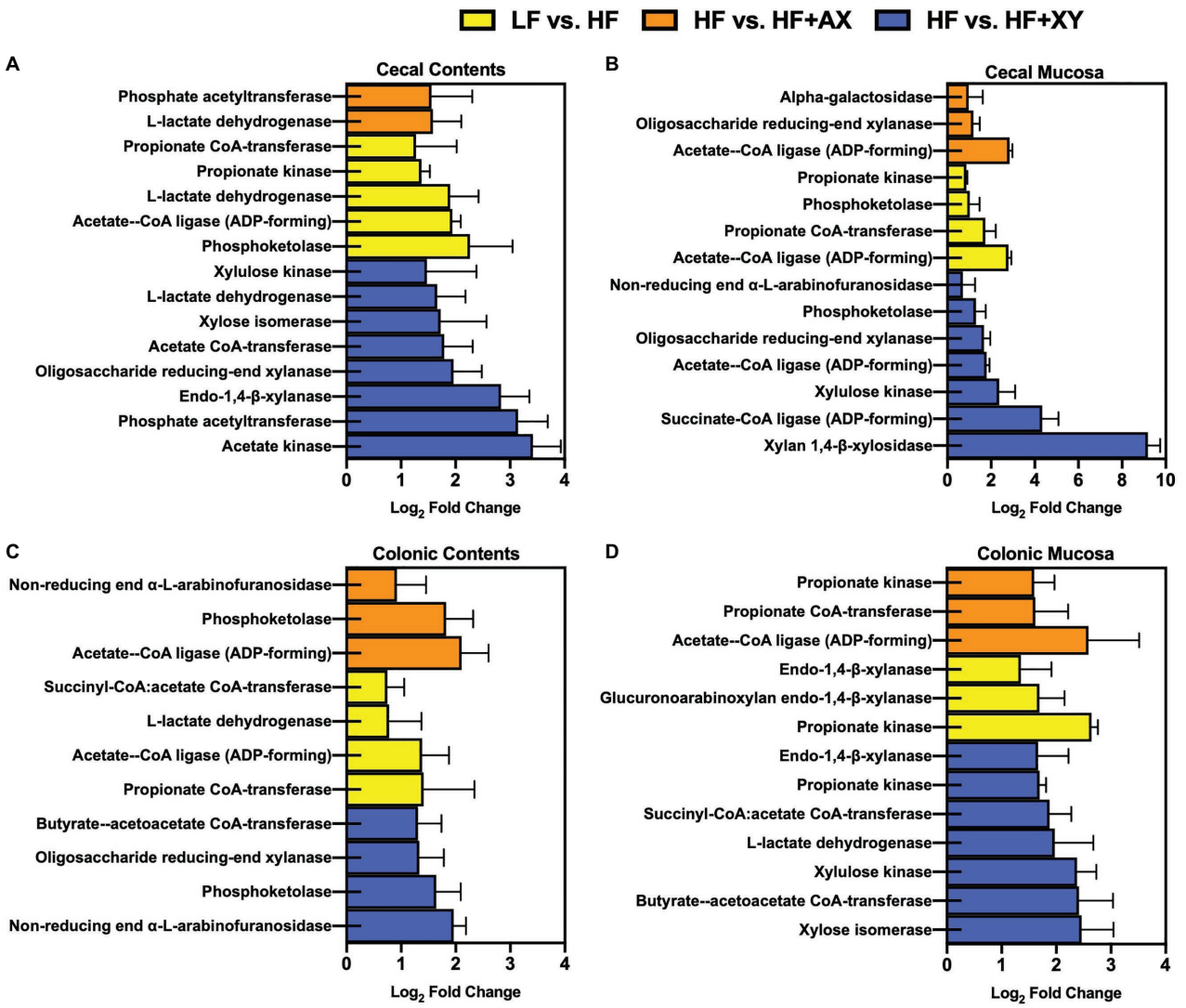

FIGURE 8 | The Log_2 fold change between LF vs. HF, HF vs. HF+XY, and HF vs. HF+AX for the PICRUSt2 significantly different predicted gene counts for enzymes associated with bacterial arabinoxylan degradation, xylose metabolism, or SCFA metabolism found in the **(A)** cecal contents, **(B)** cecal mucosa, **(C)** colonic contents, and **(D)** colonic mucosa.

arabinoxylans is to include xylanase into the diet. Xylanase hydrolyzes the β-(1-4) glycosidic bonds of arabinoxylans, and potentially releases AXOS, and more fragmented and depolymerized arabinoxylans (Dodd and Cann, 2009; Pedersen et al., 2015). Thus, it is logical that xylanase supplementation may improve DF fermentation, as the greater the degree and rate of depolymerization of DF, the faster and more efficiently it can be fermented by microbiota (Varel and Yen, 1997). Moreover, there is increasing evidence in poultry that AXOS can invoke a stimbiotic MOA that modulates microbial communities to support fiber degradation beyond what is feasible from fermentation of AXOS alone (González-Ortiz et al., 2019). The aim of this research was to characterize the modulation of the hindgut microbiota due to increased corn-based fiber, xylanase, or directly supplemented AXOS in pigs fed corn-based diets for 46 days. It was hypothesized that the addition of xylanase or AXOS to a diet high in DF would modulate intestinal microbial communities to support greater fiber degradation through a stimbiotic MOA.

The overall composition of microbial phyla and families observed in the cecum are comparable to what has been defined as "core microbiota" in pigs through a meta-analysis conducted by Holman et al. (2017). This is also the case for the overall composition of microbial phyla observed in the colon, with the exception of the increased prevalence of *Spirochaetes*. However, *Spirochaetes* have been observed at a similar relative abundance in the colon of pigs raised under commercial conditions (De Rodas et al., 2018). Similar to what Holman et al. (2017) observed, *Bacteroidetes* has an increased prevalence in the mucosa, and *Firmicutes* were more dominant in the contents of the large intestine.

At the family level, among all locations, *Prevotellaceae*, *Ruminococcaceae*, and *Lachnospiraceae* were the three most dominant families present, but when further classified into genera there were unique differences among which genera prevailed at each location. Moreover, the microbial genera characterized herein are typically present in the cecum and colon of commercially raised pigs (De Rodas et al., 2018; Wang et al., 2019). Intriguingly, within this study, there appears to be two discriminant shifts in microbial composition among dietary treatments: those due to increased DF (LF vs. HF), and those due to the addition of xylanase to HF (HF vs. HF+XY).

Relative to a typical corn-soybean meal basal diet (LF), HF increased measures of α-diversity and microbial richness in the cecal contents and mucosa, and colonic contents. These differences in microbial diversity and the modulation of cecal and colonic microbiota by HF, are likely a result of increased DF in the ileal digesta entering the large intestine. The HF treatment had a 30% addition of corn bran without solubles, which increased the NDF content of the diet by nearly 3-fold compared to LF. Moreover, LF had increased ileal digestibility of both DM and NDF in a related study (Petry et al., 2019b), and thus, would have less NDF entering the hindgut to be utilized as a substrate for microbiota. It has been established that diets enriched with DF promote microbial diversity in the large intestine of humans (Sonnenburg et al., 2016; Makki et al., 2018). Moreover, the increase in microbial diversity by HF is in agreement with Liu et al. (2018) who observed increased in the Shannon index in fecal microbiota from nursery pigs fed corn bran at an inclusion rate of 5%.

Within the cecal contents, HF increased the abundance of *Ruminococcaceae_UCG-005*, and in general, microbes in the *Ruminococcaceae* family are known to degrade and metabolize complex plant carbohydrates (Biddle et al., 2013; Chatellard et al., 2016). Moreover, HF increased the prevalence of *Treponema_2* in the cecal mucosa and contents. While little is known about *Treponema_2* in the swine microbiota, in ruminants, *Treponema* is known to increase in concert with cellulolytic bacteria such as *Ruminococcaceae_UCG-005* (Karri et al., 2016; Xie et al., 2018). This is further supported by the drastic increase in *Treponema_2* by HF in the colonic mucosa, and the modulation of *Prevotellaceae*. In contrast, relative to LF, HF decreased *Turicibacter* and *Lactobacillus* in the cecal contents, and *Megasphaera* and *Streptococcus* in the mucosa. *Turicibacter*, although there is limited information about this genus, has been found to increase in humans who consume low fiber diets (Gomez-Arango et al., 2018) and is positively correlated with increased body weight in pigs (Wang et al., 2019). Indeed, LF is lower in DF than HF, and pigs fed LF had increased BW in a related study (Petry et al., 2020a). The reduction is *Megasphaera* by HF, or inversely, a greater abundance of *Megasphaera* in LF, is in agreement with research that suggest pigs with greater feed efficiency, such as LF, have a greater abundance of *Megasphaera* (Tan et al., 2018; Petry et al., 2020a). In the colonic contents and mucosa, HF increased the abundance of *Ruminococcus_1*, and at the OTU level, *Ruminococcus_1* was increased in the cecal contents and mucosa. The increased abundance of *Ruminococcus_1* could be a result of increased mucin production as species within the *Ruminococcus* genus are prolific degraders of the polyglycans found in mucins (Crost et al., 2018). Furthermore, the abrasiveness of insoluble DF can increase mucin production in the gastrointestinal tract (Montagne et al., 2004; Agyekum and Nyachoti, 2017).

Across all locations, HF increased the abundance of various OTUs from the *Lachnospiraceae*, *Ruminococcaceae*, and *Prevotellaceae* families. Many species within these families have the potential to ferment diverse and complex polysaccharides (Biddle et al., 2013; Meehan and Beiko, 2014; Chen et al., 2017). Moreover, the increase in predicted gene counts for enzymes associated with propionate production by HF support the degradation of DF by *Prevotellaceae* (Chen et al., 2017). However, in Petry et al. (2019b, 2020b), compared to LF, HF had reduced SCFA concentrations and NDF digestibility in cecal and colonic contents. Interestingly, a study by Quan et al. (2018) found pigs with poor feed efficiency had a greater abundance of *Lachnospiraceae*, *Ruminococcaceae*, and *Prevotellaceae* families in the cecum and colon compared to more feed efficient pigs fed the same corn-soybean meal-based diet. It is plausible that these families are less efficient at fermenting DF, compared to the microbial communities that were more abundant in LF.

Supplementing xylanase to HF increased all measures of α-diversity in the cecal content, and HF+XY had the greatest Chao1 index among treatments in the colonic mucosa. Including a carbohydrase blend that contained xylanase in wheat bran, and soybean hull-based swine diets increased the Chao1 and Shannon indices of ileal digesta and feces (Zhang et al., 2018a). However, Zhang et al. (2018b) observed no differences in the Shannon and Simpson indices of cecal contents from pigs fed a corn distiller's dried grains with solubles (DDGS)-based diet supplemented with xylanase with a similar dietary adaptation time. These opposing results are potentially due to the recalcitrant nature of corn DDGS to xylanase hydrolysis (Abelilla and Stein, 2019), whereas, corn-bran appears to be more susceptible to xylanase (Petry et al., 2020a).

Directly supplementing AXOS did not alter α-diversity measurements in the colonic contents, with the exception of greater Simpson and Chao1 indices than LF and HF+XY, but not HF. Moreover, HF+AX did not modulate microbial communities to the same degree, or in a similar manner, to HF+XY. This is counterintuitive to what has been observed in poultry, and the prebiotic-like effect of AXOS supplementation in humans (Grootaert et al., 2007; Morgan et al., 2019; Bautil et al., 2020). It is plausible that AXOS produced *in situ* by xylanase differs in composition and degrees of polymerization due to the intrinsic complexities of corn-based arabinoxylans. Moreover, pigs, compared to poultry, have a longer intestine relative to their body weight (Moran, 1982). Thus, it is reasonable to speculate that the AXOS in HF+AX could have been fermented in the small intestine, and unable to modulate hindgut microbiota. Xylanase also has the potential to degrade arabinoxylans across the gastrointestinal tract, and continually produce soluble AXOS throughout the large intestine.

The most recently proposed MOA of xylanase suggests the *in situ* produced AXOS stimulates gastrointestinal microbiota to digest DF to a greater degree than the fermentation of

AXOS alone (Bedford, 2018). This was later coined as a "stimbiotic" or "stimbiotic mechanism" by González-Ortiz et al. (2019). Compared to HF, HF+XY increased predicted genes of microbial enzymes associated with pentose metabolism and arabinoxylan degradation in cecal contents, cecal mucosa, and colonic mucosa (**Figure 8**). These findings would suggest xylanase does indeed stimulate a fiber-fermenting microbiome in the large intestine of the pig. Moreover, within cecal and colonic contents, HF+XY increased the abundance of several OTUs within the *Lachnospiraceae* and *Ruminococcaceae* families to a greater degree than their modulation by HF alone. Genomic investigation into the metabolic capacities of *Lachnospiraceae* and *Ruminococcaceae* suggest these microbial communities are able to metabolize xylose and produce microbial carbohydrases (Biddle et al., 2013). These data, in conjunction with the improved cecal digestibility of NDF observed by Petry et al. (2019b), further support the premise that xylanase elicits a stimbiotic MOA. Likewise, the upregulation of xylan 1,4-β-xylosidase and alpha-L-arabinofuranosidase predicted gene counts within the cecal mucosa also suggest liberated AXOS are being fermented within the cecum. This is further supported by the findings of Petry et al. (2020b), who observed HF+XY increased both the absolute concentration and molar proportion of acetate in the cecum.

Interestingly, xylanase across locations increased *Lactobacillus*, *Bifidobacterium*, and *Faecalibacterium* at either the genus or OTU level. The increased abundance of *Lactobacillus* and *Bifidobacterium* by xylanase has also been observed in poultry (Vahjen et al., 1998; González-Ortiz et al., 2020). The increased prevalence of these microbial communities implies HF+XY promoted beneficial cross feeding that would favor acetate and butyrate production in the large intestine (Zeybek et al., 2020). Several species within the *Lactobacillus* genus have the capacity to utilize more polymerized and complex AXOS, and this often results in the production of small AXOS, lactate, and acetate (Immerzeel et al., 2014; McLaughlin et al., 2015). *Bifidobacterium* are likely feeding on the short AXOS liberated by exogenous xylanase, *Lactobacillus*, and other fibrolytic microbiota (Rivière et al., 2014). The increase in *Lactobacillus* and *Bifidobacterium* would also explain the increase in predicted gene counts for oligosaccharide reducing-end xylanase in the cecal contents, cecal mucosa, and colonic mucosa (Grootaert et al., 2007; Moura et al., 2007). Moreover, *Bifidobacterium* have the capacity to metabolize pentoses through the bifid shunt pathway which ultimately results in the production of acetate (Rivière et al., 2016). This would explain the increase in cecal acetate production observed by Petry et al. (2020b), and the rise in *Faecalibacterium* in the cecal mucosa. *Faecalibacterium*, whose only known species is *Faecalibacterium prausnitzii*, is an acetate-consuming and butyrate-producing bacterium that does not utilize carbohydrates efficiently and requires acetate for optimal proliferation (Falony et al., 2006; Miquel et al., 2014). The increase in *Faecalibacterium* in colonic contents by HF+XY may also explain the increase in molar proportion of butyrate reported by Petry et al. (2020b).

Butyrate is the preferential energy source for colonocytes and is a potent modulator of gastrointestinal health (Bedford and Gong, 2018). Moreover, butyrate aids in the control of enteric pathogens, reduces inflammation, and mitigates reactive oxygen species (Bach Knudsen et al., 2018). The butyrate produced from the metabolic cross-feeding of AXOS by *Lactobacillus*, *Bifidobacterium*, and *Faecalibacterium* may potentially explain the reductions in finishing pig mortality often observed when xylanase is used in commercial pork production (Zier-Rush et al., 2016). Moreover, in recent years, there have been several studies that observed xylanase modulates gastrointestinal health, immune function, oxidative stress, and intestinal morphology of pigs (Tiwari et al., 2018; Chen et al., 2020; Petry et al., 2020b). Potentially, these health benefits are a consequence of the aforementioned microbial modulation by xylanase.

CONCLUSION

Diets with higher DF increase microbial diversity in the large intestine and favor microbial communities that degrade complex carbohydrates and mucins. However, HF also reduced microbial communities found in abundance in the microbiome of more feed efficient pigs. Supplementing xylanase in HF further increased microbial diversity in cecal contents and colonic mucosa and favored microbial communities that produce microbial carbohydrases and ferment AXOS. Of particular interest, HF+XY increased the abundance of *Lactobacillus*, *Bifidobacterium*, and *Faecalibacterium* across the large intestine. These genera are known to work cooperatively to produce butyrate and may explain the unexpected health benefits commonly observed with xylanase supplementation in pigs. These data support the recently proposed stimbiotic MOA of xylanase. Compared to xylanase, AXOS did not elicit a similar response in hindgut microbiota. It is likely this oligosaccharide differs in composition from that produced by xylanase or may have been fermented in the small intestine. These data warrant further investigation into the stimbiotic potential of xylanase.

DATA AVAILABILITY STATEMENT

The datasets presented in this study can be found in online repositories. The name of the repository and accession number can be found below: National Center for Biotechnology Information (NCBI) BioProject, https://www.ncbi.nlm.nih.gov/, PRJNA667518.

ETHICS STATEMENT

The animal study was reviewed and approved by the Institutional Animal Care and Use Committee at Iowa State University (IACUC #9-17-8613-S), and followed the guidelines for the ethical and humane use of animals for research according to the Guide for the Care and Use of Agricultural Animals in Research and Teaching (FASS, 2010).

AUTHOR CONTRIBUTIONS

AP, NH, MB, and JP designed the experiment. AP performed the experiment, collected data, and conducted DNA extractions. AP and LK performed the bioinformatics and statistical analysis of the 16S rDNA sequencing data. SS-E contributed to the concept of microbial sequencing data analysis and results interpretation. JP was the principal investigator, who supervised all aspects of the study. All authors contributed to the article and approved the submitted version.

FUNDING

Financial support for this research was provided by AB Vista Feed Ingredients and by the Agriculture and Food Research Initiative Competitive grant no. 2016-38420-25496 from the United States Department of Agriculture National Institute of Food and Agriculture.

ACKNOWLEDGMENTS

We would like to thank Iowa Corn Processors, DSM, and Ajinomoto Heartland, Inc. for providing in-kind contributions to the Applied Swine Nutrition program at Iowa State University.

SUPPLEMENTARY MATERIAL

The Supplementary Material for this article can be found online at: https://www.frontiersin.org/articles/10.3389/fmicb.2021.619970/full#supplementary-material

REFERENCES

Abelilla, J. J., and Stein, H. H. (2019). Degradation of dietary fiber in the stomach, small intestine, and large intestine of growing pigs fed corn-or wheat-based diets without or with microbial xylanase. *J. Anim. Sci.* 97, 338–352. doi: 10.1093/jas/sky403

Acosta, J. A., Stein, H. H., and Patience, J. F. (2020). Impact of increasing the levels of insoluble fiber and the method of diet formulation on measures of energy and nutrient digestibility in growing pigs. *J. Anim. Sci.* 98:skaa130. doi: 10.1093/jas/skaa130

Agyekum, A. K., and Nyachoti, C. M. (2017). Nutritional and metabolic consequences of feeding high-fiber diets to swine: a review. *Engineering* 3, 716–725. doi: 10.1016/J.ENG.2017.03.010

Bach Knudsen, K. E. (2014). Fiber and nonstarch polysaccharide content and variation in common crops used in broiler diets. *Poult. Sci.* 93, 2380–2393. doi: 10.3382/ps.2014-03902

Bach Knudsen, K. E., Lærke, H. N., Hedemann, M. S., Nielsen, T. S., Ingerslev, A. K., Gundelund Nielsen, D. S., et al. (2018). Impact of diet-modulated butyrate production on intestinal barrier function and inflammation. *Nutrients* 10:1499. doi: 10.3390/nu10101499

Barbera, P., Kozlov, A. M., Czech, L., Morel, B., Darriba, D., Flouri, T., et al. (2019). EPA-ng: massively parallel evolutionary placement of genetic sequences. *Syst. Biol.* 68, 365–369. doi: 10.1093/sysbio/syy054

Bautil, A., Verspreet, J., Buyse, J., Goos, P., Bedford, M. R., and Courtin, C. M. (2020). Arabinoxylan-oligosaccharides kick-start arabinoxylan digestion in the aging broiler. *Poult. Sci.* 99, 2555–2565. doi: 10.1016/j.psj.2019.12.041

Bedford, M. R. (2018). The evolution and application of enzymes in the animal feed industry: the role of data interpretation. *Br. Poult. Sci.* 59, 486–493. doi: 10.1080/00071668.2018.1484074

Bedford, A., and Gong, J. (2018). Implications of butyrate and its derivatives for gut health and animal production. *Anim. Nutrit.* 4, 151–159. doi: 10.1016/j.aninu.2017.08.010

Bengtsson-Palme, J., Metaxa, F. A., Parsers, F. A., and Metaxa, F. A. (2020). Tag: HMMER.

Biddle, A., Stewart, L., Blanchard, J., and Leschine, S. (2013). Untangling the genetic basis of fibrolytic specialization by Lachnospiraceae and Ruminococcaceae in diverse gut communities. *Diversity* 5, 627–640. doi: 10.3390/d5030627

Caporaso, J. G., Ackermann, G., Apprill, A., Bauer, M., Berg-Lyons, D., and Betley, J., (2018). EMP 16S Illumina amplicon protocol. Available at: http://www.earthmicrobiome.org/protocols-and-standards/16s (Accessed August 1, 2019).

Caspi, R., Billington, R., Fulcher, C. A., Keseler, I. M., Kothari, A., Krummenacker, M., et al. (2018). The MetaCyc database of metabolic pathways and enzymes. *Nucleic Acids Res.* 46, D633–D639. doi: 10.1093/nar/gkx935

Chatellard, L., Trably, E., and Carrère, H. (2016). The type of carbohydrates specifically selects microbial community structures and fermentation patterns. *Bioresour. Technol.* 221, 541–549. doi: 10.1016/j.biortech.2016.09.084

Chen, T., Long, W., Zhang, C., Liu, S., Zhao, L., and Hamaker, B. R. (2017). Fiber-utilizing capacity varies in Prevotella- versus Bacteroides-dominated gut microbiota. *Sci. Rep.* 7:2594. doi: 10.1038/s41598-017-02995-4

Chen, H., Zhang, S., and Kim, S. W. (2020). Effects of supplemental xylanase on health of the small intestine in nursery pigs fed diets with corn distillers' dried grains with solubles. *J. Anim. Sci.* 98:skaa185. doi: 10.1093/jas/skaa185

Crost, E. H., Le Gall, G., Laverde-Gomez, J. A., Mukhopadhya, I., Flint, H. J., and Juge, N. (2018). Mechanistic insights into the cross-feeding of *Ruminococcus gnavus* and *Ruminococcus bromii* on host and dietary carbohydrates. *Front. Microbiol.* 9:2558. doi: 10.3389/fmicb.2018.02558.

Czech, L., Barbera, P., and Stamatakis, A. (2020). Genesis and Gappa: processing, analyzing and visualizing phylogenetic (placement) data. *Bioinformatics* 36, 3263–3265. doi: 10.1093/bioinformatics/btaa070

De Rodas, B., Youmans, B. P., Danzeisen, J. L., Tran, H., and Johnson, T. J. (2018). Microbiome profiling of commercial pigs from farrow to finish. *J. Anim. Sci.* 96, 1778–1794. doi: 10.1093/jas/sky109

Dodd, D., and Cann, I. K. O. (2009). Enzymatic deconstruction of xylan for biofuel production. *Bioenergy* 1, 2–17. doi: 10.1111/j.1757-1707.2009.01004.x

Douglas, G. M., Maffei, V. J., Zaneveld, J. R., Yurgel, S. N., Brown, J. R., Taylor, C. M., et al. (2020). PICRUSt2 for prediction of metagenome functions. *Nat. Biotechnol.* 38, 685–688. doi: 10.1038/s41587-020-0548-6

Falony, G., Vlachou, A., and Verbrugghe, K., and De Vuyst, L. (2006). Cross-feeding between *Bifidobacterium longum BB536* and acetate-converting, butyrate-producing colon bacteria during growth on oligofructose. *Appl. Environ. Microbiol.* 72:7835–7841. doi: 10.1128/AEM.01296-06

FASS (2010). *Guide for the care and use of agricultural animals in research and teaching. 3rd Edn*. Champaign, IL: Federation of Animal Science Societies, 169.

Gomez-Arango, L. F., Barrett, H. L., Wilkinson, S. A., Callaway, L. K., McIntyre, H. D., Morrison, M., et al. (2018). Low dietary fiber intake increases Collinsella abundance in the gut microbiota of overweight and obese pregnant women. *Gut Microbes* 9, 189–201. doi: 10.1080/19490976.2017.1406584

González-Ortiz, G., Gomes, G. A., Dos Santos, T. T., and Bedford, M. R. (2019). "New strategies influencing gut functionality and animal performance" in *The value of fibre: Engaging the second brain for animal nutrition*. eds. G. Gonzalez-Ortiz, M. R. Bedford, K. E. Bach Knudsen, C. Courtin and H. L. Classen (Wageningen, The Netherlands: Wageningen Academic Publishers), 233–254.

González-Ortiz, G., Olukosi, O. A., Jurgens, G., Apajalahti, J., and Bedford, M. R. (2020). Short-chain fatty acids and ceca microbiota profiles in broilers and turkeys in response to diets supplemented with phytase at varying

concentrations, with or without xylanase. *Poult. Sci.* 99, 2068–2077. doi: 10.1016/j.psj.2019.11.051

Grootaert, C., Delcour, J. A., Courtin, C. M., Broekaert, W. F., Verstraete, W., and Van de Wiele, T. (2007). Microbial metabolism and prebiotic potency of arabinoxylan oligosaccharides in the human intestine. *Trends Food Sci. Technol.* 18, 64–71. doi: 10.1016/j.tifs.2006.08.004

Gutierrez, N. A., Kerr, B. J., and Patience, J. F. (2013). Effect of insoluble-low fermentable fiber from corn-ethanol distillation origin on energy, fiber, and amino acid digestibility, hindgut degradability of fiber, and growth performance of pigs. *J. Anim. Sci.* 91, 5314–5325. doi: 10.2527/jas.2013-6328

Holman, D. B., Brunelle, B. W., Trachsel, J., and Allen, H. K. (2017). Meta-analysis to define a core microbiota in the swine gut. *mSystems* 2, e00004–e00017. doi: 10.1128/mSystems.00004-17

Immerzeel, P., Falck, P., Galbe, M., Adlercreutz, P., Karlsson, E. N., and Stålbrand, H. (2014). Extraction of water-soluble xylan from wheat bran and utilization of enzymatically produced xylooligosaccharides by *Lactobacillus*, *Bifidobacterium* and *Weissella* spp. *LWT-Food Sci. Tech.* 56, 321–327. doi: 10.1016/j.lwt.2013.12.013

Jaworski, N. W., Lærke, H. N., Bach Knudsen, K. E., and Stein, H. H. (2015). Carbohydrate composition and in vitro digestibility of dry matter and nonstarch polysaccharides in corn, sorghum, and wheat and coproducts from these grains. *J. Anim. Sci.* 93, 1103–1113. doi: 10.2527/jas.2014-8147

Jensen, B. B., and Jørgensen, H. (1994). Effect of dietary fiber on microbial activity and microbial gas production in various regions of the gastrointestinal tract of pigs. *Appl. Environ. Microbiol.* 60, 1897–1904. doi: 10.1128/AEM.60.6.1897-1904.1994

Jha, R., Fouhse, J. M., Tiwari, U. P., Li, L., and Willing, B. P. (2019). Dietary fiber and intestinal health of monogastric animals. *Front. Vet. Sci.* 6:48. doi: 10.3389/fvets.2019.00048

Karri, S., Vadela, M. B., Gutta, M., Onteru, S. K., and Gundi, V. A. K. B. (2016). Role of fiber and non fibrolytic bacteria in feed digestion in bovine rumen—an overview. *Int. J. Pharm. Biol. Sci.* 6, 207–211.

Kim, B. R., Shin, J., Guevarra, R., Lee, J. H., Kim, D. W., Seol, K. H., et al. (2017). Deciphering diversity indices for a better understanding of microbial communities. *J. Microbiol. Biotechnol.* 27, 2089–2093. doi: 10.4014/jmb.1709.09027

Kozich, J. J., Westcott, S. L., Baxter, N. T., Highlander, S. K., and Schloss, P. D. (2013). Development of a dual-index sequencing strategy and curation pipeline for analyzing amplicon sequence data on the MiSeq Illumina sequencing platform. *Appl. Environ. Microbiol.* 79, 5112–5120. doi: 10.1128/AEM.01043-13

Liu, P., Zhao, J., Wang, W., Guo, P., Lu, W., Wang, C., et al. (2018). Dietary corn bran altered the diversity of microbial communities and cytokine production in weaned pigs. *Front. Microbiol.* 9:2090. doi: 10.3389/fmicb.2018.02090

Louca, S., and Doebeli, M. (2018). Efficient comparative phylogenetics on large trees. *Bioinformatics* 34, 1053–1055. doi: 10.1093/bioinformatics/btx701

Makki, K., Deehan, E. C., Walter, J., and Bäckhed, F. (2018). The impact of dietary fiber on gut microbiota in host health and disease. *Cell Host Microbe* 23, 705–715. doi: 10.1016/j.chom.2018.05.012

McLaughlin, H. P., Motherway, M. O. C., Lakshminarayanan, B., Stanton, C., Ross, R. P., Brulc, J., et al. (2015). Carbohydrate catabolic diversity of bifidobacteria and lactobacilli of human origin. *Int. J. Food Microbiol.* 203, 109–121. doi: 10.1016/j.ijfoodmicro.2015.03.008

Meehan, C. J., and Beiko, R. G. (2014). A phylogenomic view of ecological specialization in the *Lachnospiraceae*, a family of digestive tract-associated bacteria. *Genome Biol. Evol.* 6, 703–713. doi: 10.1093/gbe/evu050

Miquel, S., Martín, R., Bridonneau, C., Robert, V., Sokol, H., Bermúdez-Humarán, L. G., et al. (2014). Ecology and metabolism of the beneficial intestinal commensal bacterium *Faecalibacterium prausnitzii*. *Gut Microbes* 5, 146–151. doi: 10.4161/gmic.27651

Montagne, L., Piel, C., and Lallès, J. P. (2004). Effect of diet on mucin kinetics and composition: nutrition and health implications. *Nutr. Rev.* 62, 105–114. doi: 10.1111/j.1753-4887.2004.tb00031.x

Moran, E. T. (1982). *Comparative nutrition of fowl and swine: The gastrointestinal systems*. Guelph, Ontario, Canada: University of Guelph.

Morgan, N. K., Keerqin, C., Wallace, A., Wu, S. B., and Choct, M. (2019). Effect of arabinoxylo-oligosaccharides and arabinoxylans on net energy and nutrient utilization in broilers. *Anim. Nutrit.* 5, 56–62. doi: 10.1016/j.aninu.2018.05.001

Moura, P., Barata, R., Carvalheiro, F., Gírio, F., Loureiro-Dias, M. C., and Esteves, M. P. (2007). In vitro fermentation of xylo-oligosaccharides from corn cobs autohydrolysis by Bifidobacterium and lactobacillus strains. *LWT-Food Sci. Technol.* 40, 963–972. doi: 10.1016/j.lwt.2006.07.013

Pedersen, M. B., Dalsgaard, S., Arent, S., Lorentsen, R., Knudsen, K. E. B., Yu, S., et al. (2015). Xylanase and protease increase solubilization of non-starch polysaccharides and nutrient release of corn-and wheat distillers dried grains with solubles. *Biochem. Eng. J.* 98, 99–106. doi: 10.1016/j.bej.2015.02.036

Petry, A. L., Huntley, N. F., Bedford, M. R., and Patience, J. F. (2019b). Xylanase improved the nutrient and energy digestibility of diets high in insoluble corn fiber fed to swine following a 36-d dietary adaptation period. *J. Anim. Sci.* 97(Suppl. 2), 216–217. doi: 10.1093/jas/skz122.381

Petry, A. L., Huntley, N. F., Bedford, M. R., and Patience, J. F. (2020a). Xylanase increased the energetic contribution of fiber and improved the oxidative status, gut barrier integrity, and growth performance of growing pigs fed insoluble corn-based fiber. *J. Anim. Sci.* 98:skaa233. doi: 10.1093/jas/skaa233

Petry, A. L., Huntley, N. F., Bedford, M. R., Schmitz-Esser, S., Koester, L., and Patience, J. F. (2020b). Can the fermentation of poorly fermentable and insoluble corn fiber be improved in the pig? – an investigation into the in vivo mode of action of xylanase. *J. Anim. Sci.* 98:207.

Petry, A. L., Masey O'Neill, H. V., and Patience, J. F. (2019). Xylanase, and the role of digestibility and hindgut fermentation in pigs on energetic differences among high and low energy corn samples. *J. Anim. Sci.* 97, 4293–4297. doi: 10.1093/jas/skz261

Petry, A. L., and Patience, J. F. (2020). Xylanase supplementation in corn-based swine diets: a review with emphasis on potential mechanisms of action. *J. Anim. Sci.* 98:skaa318. doi: 10.1093/jas/skaa318

Pruesse, E., Quast, C., Knittel, K., Fuchs, B. M., Ludwig, W., and Peplies, J. (2007). SILVA: a comprehensive online resource for quality checked and aligned ribosomal RNA sequence data compatible with ARB. *Nucleic Acids Res.* 35, 7188–7196. doi: 10.1093/nar/gkm864

Quan, J., Cai, G., Ye, J., Yang, M., Ding, R., Wang, X., et al. (2018). A global comparison of the microbiome compositions of three gut locations in commercial pigs with extreme feed conversion ratios. *Sci. Rep.* 8:4536. doi: 10.1038/s41598-018-22692-0

Rivière, A., Moens, F., Selak, M., Maes, D., Weckx, S., and De Vuyst, L. (2014). The ability of bifidobacteria to degrade arabinoxylan oligosaccharide constituents and derived oligosaccharides is strain dependent. *Appl. Environ. Microbiol.* 80, 204–217. doi: 10.1128/AEM.02853-13

Rivière, A., Selak, M., Lantin, D., Leroy, F., and De Vuyst, L. (2016). *Bifidobacteria* and butyrate-producing colon bacteria: importance and strategies for their stimulation in the human gut. *Front. Microbiol.* 7:979. doi: 10.3389/fmicb.2016.00979

Sonnenburg, E. D., Smits, S. A., Tikhonov, M., Higginbottom, S. K., Wingreen, N. S., and Sonnenburg, J. L. (2016). Diet-induced extinctions in the gut microbiota compound over generations. *Nature* 529, 212–215. doi: 10.1038/nature16504

Tan, Z., Wang, Y., Yang, T., Ao, H., Chen, S., Xing, K., et al. (2018). Differences in gut microbiota composition in finishing landrace pigs with low and high feed conversion ratios. *Antonie Van Leeuwenhoek* 111, 1673–1685. doi: 10.1007/s10482-018-1057-1

Tiwari, U. P., Chen, H., Kim, S. W., and Jha, R. (2018). Supplemental effect of xylanase and mannanase on nutrient digestibility and gut health of nursery pigs studied using both in vivo and in vitro models. *Anim. Feed Sci. Technol.* 245, 77–90. doi: 10.1016/j.anifeedsci.2018.07.002

Vahjen, W., Gläser, K., Schäfer, K., and Simon, O. (1998). Influence of xylanase-supplemented feed on the development of selected bacterial groups in the intestinal tract of broiler chicks. *J. Agric. Sci.* 130:4. doi: 10.1017/S0021859698005498

Varel, V. H., and Yen, J. T. (1997). Microbial perspective on fiber utilization by swine. *J. Anim. Sci.* 75, 2715–2722. doi: 10.2527/1997.75102715x

Wang, X., Tsai, T., Deng, F., Wei, X., Chai, J., Knapp, J., et al. (2019). Longitudinal investigation of the swine gut microbiome from birth to market reveals stage and growth performance associated bacteria. *Microbiome* 7:109. doi: 10.1186/s40168-019-0721-7

Weber, E. K., Patience, J. F., and Stalder, K. J. (2015). Wean-to-finish feeder space availability effects on nursery and finishing pig performance and total tract digestibility in a commercial setting when feeding dried distillers grains with solubles. *J. Anim. Sci.* 93, 1905–1915. doi: 10.2527/jas.2014-8136

Xie, X., Yang, C., Guan, L. L., Wang, J., Xue, M., and Liu, J. X. (2018). Persistence of cellulolytic bacteria *Fibrobacter* and *Treponema* after short-term corn

stover-based dietary intervention reveals the potential to improve rumen fibrolytic function. *Front. Microbiol.* 9:1363. doi: 10.3389/fmicb.2018.01363

Zeybek, N., Rastall, R. A., and Büyükkileci, A. O. (2020). Utilization of xylan-type polysaccharides in co-culture fermentations of *Bifidobacterium* and *Bacteroides* species. *Carbohydr. Polym.* 236:116076. doi: 10.1016/j.carbpol.2020.116076

Zhang, Y. J., Liu, Q., Zhang, W. M., Zhang, Z. J., Wang, W. L., and Zhuang, S. (2018a). Gastrointestinal microbial diversity and short-chain fatty acid production in pigs fed different fibrous diets with or without cell wall-degrading enzyme supplementation. *Livest. Sci.* 207, 105–116. doi: 10.1016/j.livsci.2017.11.017

Zhang, Z., Tun, H. M., Li, R., Gonzalez, B. J., Keenes, H. C., Nyachoti, C. M., et al. (2018b). Impact of xylanases on gut microbiota of growing pigs fed corn-or wheat-based diets. *Anim. Nutrit.* 4, 339–350. doi: 10.1016/j.aninu.2018.06.007

Zier-Rush, C. E., Groom, C., Tillman, M., Remus, J., and Boyd, R. D. (2016). The feed enzyme xylanase improves finish pig viability and carcass feed efficiency. *J. Anim. Sci.* 94:115. doi: 10.2527/msasas2016-244

Conflict of Interest: The authors declare that this study received funding from AB Vista. The funder had the following involvement with the study: AB Vista was involved in the conceptualization of the project and study design, and they provided the xylanase and AXOS used in this trial. MB was employed by AB Vista and contributed to the study design, and had a minor role in the decision to publish and the preparation of the manuscript.

The remaining authors declare that the research was conducted in the absence of any commercial or financial relationships that could be construed as a potential conflict of interest.

frontiers in Microbiology

ORIGINAL RESEARCH
published: 07 June 2021
doi: 10.3389/fmicb.2021.666940

Comparison of Gut Microbiota of Yaks From Different Geographical Regions

Wenwen Liu[1,2†], Qiang Wang[2†], Jiajia Song[2], Jinwei Xin[3,4], Songshan Zhang[1], Yuanhua Lei[1], Yuanli Yang[1], Peng Xie[1*] and Huayi Suo[2*]*

[1] Institute of Animal Sciences, Chinese Academy of Agricultural Sciences, Beijing, China, [2] College of Food Science, Southwest University, Chongqing, China, [3] State Key Laboratory of Hulless Barley and Yak Germplasm Resources and Genetic Improvement, Lhasa, China, [4] Institute of Animal Science and Veterinary, Tibet Academy of Agricultural and Animal Husbandry Sciences, Lhasa, China

Gut microbiota are closely linked to host health and adaptability to different geographical environments. However, information on the influence of different geographical conditions on the intestinal microbiota of yaks is limited. In this study, 18 yak fecal samples were collected from three regions of China, namely Shangri-la, Lhasa, and Yushu, and were analyzed via high-throughput sequencing. The alpha diversity, as measured by the Shannon, ACE, and Chao indices, was the highest in the Shangri-la samples. Principal coordinate analysis detected significant differences in the composition of the intestinal microbiota of yaks from different regions. A total of six phyla, 21 families, and 29 genera were identified in the fecal samples. The dominant phyla in the samples were Firmicutes and Bacteroidetes, and the most abundant family was Ruminococcaceae. In addition, *Ruminococcaceae_UCG-005* was the predominant genus and was more abundant in Yushu samples than in other samples. However, the predicted functional gene composition of the gut microbiota of yaks from different regions was similar. Our results revealed that geographical conditions influence the diversity and composition of the intestinal microbiota of yaks.

Keywords: high-throughput sequencing, gut microbiota, yak, diversity, geographical regions

OPEN ACCESS

Edited by:
Cristiano Gallina Moreira, São Paulo State University, Brazil

Reviewed by:
Elisa Borghi, University of Milan, Italy
Richard Agans, Independent Researcher, Dayton, OH, United States

***Correspondence:**
Jinwei Xin
xinjinwei80@163.com
Peng Xie
seulbird@163.com
Huayi Suo
birget@swu.edu.cn

† These authors have contributed equally to this work and share first authorship

Specialty section:
This article was submitted to Microbial Symbioses, a section of the journal Frontiers in Microbiology

Received: *11 February 2021*
Accepted: *12 May 2021*
Published: *07 June 2021*

Citation:
Liu W, Wang Q, Song J, Xin J, Zhang S, Lei Y, Yang Y, Xie P and Suo H (2021) Comparison of Gut Microbiota of Yaks From Different Geographical Regions. Front. Microbiol. 12:666940. doi: 10.3389/fmicb.2021.666940

INTRODUCTION

Yak (*Bos grunniens*) is a representative indigenous ruminant in the Qinghai-Tibetan Plateau, which is well adapted to live in environments of severe cold, poor foraging resources, high ultraviolet radiation, and low oxygen levels (Huang et al., 2012). Most yaks are found in South-Central Asia (China, Mongolia, Russia, and other countries) (Li et al., 2018). China houses approximately 14 million yaks belonging to 12 yak breeds, and most yaks are distributed in Qinghai, Yunnan, Tibet, and Gansu provinces (He et al., 2011; Wu, 2016). This population represents approximately 95% of the world's yak population (Zhu et al., 2018). Yaks also play vital roles in Qinghai-Tibetan Plateau agriculture as they provide milk, fur, meat, and transport for local herdsmen (Wiener et al., 2003). Yaks are associated with many harsh environmental conditions, such as low oxygen levels, low temperatures, and high altitudes, which limit the quality and availability of food (Wang et al., 2011; Zhou et al., 2017).

The environmental conditions in which yaks live vary greatly from region to region. For instance, Shangri-la is located in the northwest of Yunnan Province and the hinterland of the Qinghai-Tibet Plateau Hengduan mountain area and belongs to the temperate climate and plateau

climate zone. The average annual temperature of the Shangri-la plateau is approximately 5°C (Duan et al., 2019). Lhasa (Tibet) is located in the central and southern parts of the Qinghai-Tibet Plateau and has an alpine climate. The temperature here is markedly different between the day and nigh, and the day is long. Yaks also live in regions with hypoxia and sparse vegetation (Jia et al., 2018). Yushu (Qinghai Province) is located in the eastern part of the Qinghai-Tibet Plateau, where yaks live in areas with low oxygen partial pressure, large temperature differences between the day and night, intense radiation, and short grass growing period (Qin et al., 2019). In different regions, food availability is different for yaks. The diverse yak food include native grass, manually planted forage, and artificial forage supply. Hence, yaks have unique gut microbiota, which enables them to stay healthy and survive in harsh environments. Previous studies have shown that trillions of microbial cells, termed microbiota, living in the gastrointestinal tract (GIT), play an important role in host adaptation (Xin et al., 2019). Gastrointestinal microbiota are essential for immune response, GIT development, nutrient absorption, and metabolism in ruminants (Morgavi et al., 2015). Moreover, recent research has revealed that the complex microbiota of the rumen, particularly bacteria in the rumen, play a vital role in nutrient metabolism by providing energy and essential nutrients and converting plant fibers and proteins into microbial proteins and volatile fatty acids for the host (Wu et al., 2016). Microbial communities in mice have been found to modulate intestinal angiogenesis and bone mass density (Reinhardt et al., 2012; Sjögren et al., 2012). Furthermore, studies in mice have suggested that metabolic disorders are strongly linked to the composition of gut microbiota (Malmuthuge and Guan, 2016). For example, research on obesity has revealed that Rikenellaceae and Ruminococcaceae were more abundant in mice fed a high-fat diet, which is related to ingested diet, type 2 diabetes, and obesity (Kim et al., 2012). Thus, determining the diversity in gut microbiota of yaks will provide insights into their health and development.

High-throughput sequencing (HTS) technology is a general term applied to new genomic sequencing technologies, such as Illumina MiSeq, which can be done more inexpensively and faster than traditional approaches, making HTS a powerful tool for assessing microbial diversity (Pallen et al., 2010; Zhu et al., 2018). For instance, Zhou et al. (2016) used HTS technology to analyze microbial communities in the cecal tubes in Tibetan chickens and found that the gastrointestinal microbiota of Tibetan chickens from six different geographical environments diverged slightly. Zhao et al. (2018) found significant differences in the composition of the intestinal microbiota of Chinese rhesus macaques from six different geographical environments using MiSeq technology. In a study on the gut microbiota of obese individuals, Angelakis et al. (2019) used high-throughput 16S rRNA gene sequencing to reveal that there were significant differences in the intestinal microbiota of individuals having different geographical origins. Yang et al. (2020) used Illumina MiSeq to study the composition of *Bifidobacterium* communities and gastrointestinal microbiota of various individuals and found significant differences in the composition of microbial genera in samples grouped by region and age. Recent research in yaks demonstrated that the diversity of intestinal microbiota is significantly different in various parts of the rumen and varies with different feeding methods (Ren et al., 2020; Zhang X.-L. et al., 2020). However, to our knowledge, no research has been conducted to understand the effects of different geographical conditions on yak gut microbiota.

Considering the importance of the gut microbiome, this study compared the composition of microbiota of yaks from different regions. We characterized the microbial diversity of yaks from different regions and predicted microbial functions based on gene composition using HTS technology. The results of this study not only demonstrate that the gut microbiota of yaks are significantly affected by different geographical regions but also improve our understanding of the species composition of gut microbiota under different geographical conditions. Moreover, this study is the first to report a difference in the gut microbiota of yaks from different geographical regions, encountering different conditions.

MATERIALS AND METHODS

Animals and Fecal Sample Collection

Eighteen adult male yaks were sampled from three different geographical regions of China, namely Lhasa (Tibet Autonomous Region), Yushu (Qinghai Province), and Shangri-la (Yunnan Province). For each region, stool samples were collected from six yaks from a single group that exclusively grazed on natural pastures in the summer. After each yak defecated, the fresh fecal sample was immediately transferred into sterile tubes using sterile gloves and spoons. The tubes were then frozen in liquid nitrogen and transported to the laboratory on dry ice. The samples were stored at −80°C until further analysis. The sampling sites of this study are shown in **Figure 1**.

DNA Extraction, PCR Amplification, and Sequencing

Microbial genomic DNA was extracted from fecal samples using a FastDNA^{TM} Fecal Kit (MP Biomedicals, Santa Ana, CA, United States) according to the manufacturer's protocol (Shanks et al., 2011). The V3–V4 hypervariable regions of the bacterial 16S rRNA genes were PCR-amplified using the forward primer 338F (5′-ACTCCTACGGGAGGCAGCAG-3′) and reverse primer 806R (5′-GGACTACHVGGGTWTCTAAT-3′). PCR reactions contained 4 μL of 5 × FastPfu Buffer, 2 μL of 2.5 mM dNTPs, 0.8 μL of each primer (5 μM), 0.4 μL of FastPfu polymerase, and 10 ng of template DNA in a volume of 20 μL. Cycling parameters included initial denaturation at 95°C for 3 min, followed by 20 cycles of denaturation at 95°C for 30 s, annealing at 55°C for 30 s, and elongation at 72°C for 30 s, and final elongation for 10 min at 72°C. PCR products were recovered by electrophoresis using 2% agarose gels. Subsequently, the recovered PCR products were purified using an AxyPrep DNA Gel Extraction Kit (Axygen Biosciences, Union City, CA, United States) and eluted with Tris–HCl. The concentration of the purified PCR products was checked using electrophoresis in 2% agarose gels and quantified using QuantiFluor^{TM}-ST (Promega, Madison, WI, United States). Illumina paired-end sequencing libraries were prepared using the purified PCR

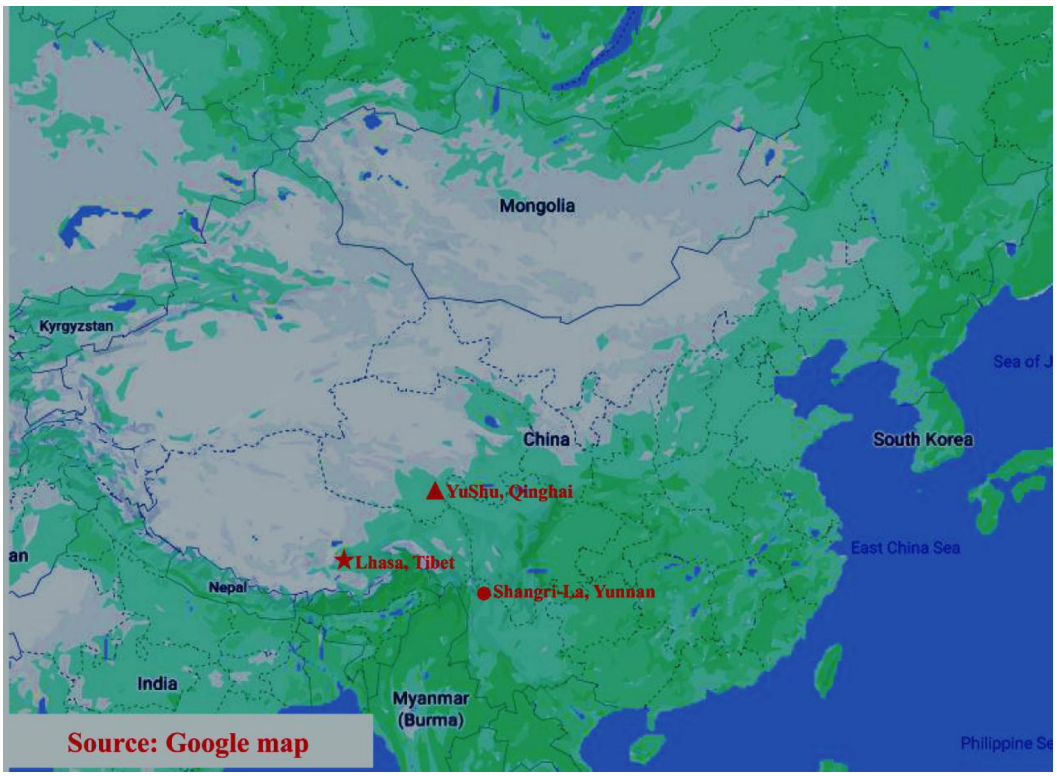

FIGURE 1 | Sampling sites in this research, including Lhasa, Yushu, and Shangri-la. The three sampling locations are represented by different shapes on the map. Triangle: Yushu (Qinghai Province); pentagon: Lhasa (Tibet Autonomous Region); circle: Shangri-La (Yunnan Province).

products according to the standard sample preparation protocol for the Illumina MiSeq platform (Illumina, San Diego, CA, United States). Thereafter, the libraries were sequenced using the Illumina MiSeq PE300 platform, and 2 × 300 bp PE reads were generated.

Data and Statistical Analysis

Clean reads were obtained by filtering the raw sequences using Trimmomatic. Paired-end reads were merged using Flash (V1.2.11). These sequences were grouped into operational taxonomic units (OTUs) based on 97% sequence identity using UPARSE (V7.0.1090). Each sequence was annotated by comparing the Ribosomal Database Project (RDP) classifier (V2.11)[1] against the SILVA (SSU123) database[2] using a comparison threshold of 70%. Alpha diversity was analyzed through three indices, namely Shannon, ACE, and Chao indices, and was calculated using mothur (V1.30.2)[3]. Principal coordinates analysis (PCoA) on weighted and unweighted UniFrac distance matrix was used for beta diversity analysis. The differences in the composition of gut microbiota among the three regions were detected by linear discriminant analysis effect size (LEfSe). PICRUSt 2 was used to predict the metabolic pathways of intestinal microbiota and investigate the functional differences in the microbial communities in samples from the three regions.

The R and SPSS (version 20.0) software packages were used for statistical analysis. Significant differences among groups were analyzed using one-way ANOVA, followed by Dunnett's *post hoc* test, and $p < 0.05$ was defined as significant.

RESULTS

Alpha Diversity of Microbial Communities in Yaks From Different Regions

A total of 160271 effective tags were generated from all the samples, including Lhasa 50507 reads, Shangri-la 52282 reads, and Yushu 57482 reads, with average read lengths of 436, 434, and 434 bp, respectively. Microbial diversity was analyzed using the Shannon diversity index, and richness was analyzed using Chao and ACE indices (**Figure 2**). The Shannon, ACE, and Chao indices were the highest in the Shangri-la samples (**Figures 2A–C**), suggesting that the diversity and richness of intestinal microbiota are the greatest for yaks from Shangri-la. The samples from Yushu had the lowest Shannon, ACE, and Chao indices. There were no significant differences in the Shannon, ACE, or Chao indices between the Lhasa and Yushu samples.

[1]https://sourceforge.net/projects/rdp-classifier/

[2]https://www.arb-silva.de/

[3]https://www.mothur.org/wiki/Download_mothur

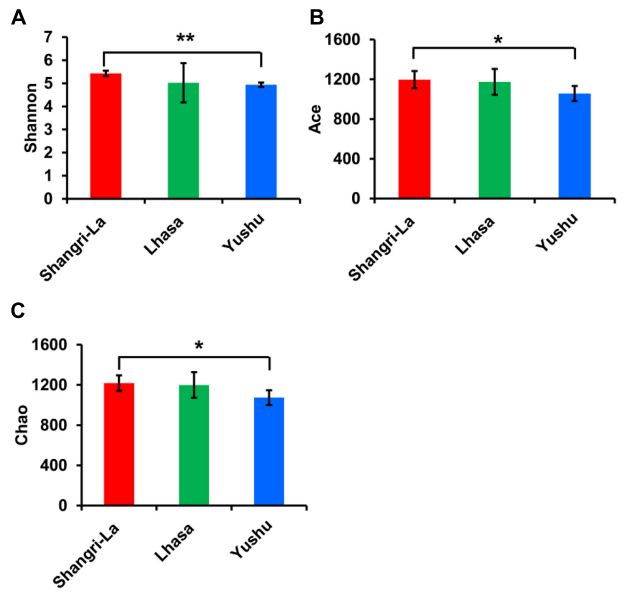

FIGURE 2 | Alpha diversity of gut bacteria among different places. **(A)** The Shannon index of each region. **(B)** The ACE index of each region. **(C)** The Chao index of each region. *indicates that differences between groups are significant, $p < 0.05$; **indicates that differences between groups are very significant, $p < 0.01$.

Beta Diversity of Microbial Communities in Yaks From Different Regions

Beta diversity was examined using PCoA. PCoA of the weighted (**Figure 3A**) and unweighted (**Figure 3B**) UniFrac distance matrices were carried out to reveal the differences in the bacterial community structure of the samples. The results of the PCoA showed distinct separation of samples from different regions based on the weighted UniFrac distance (Adonis: $R^2 = 0.4020$, $p = 0.001$) and unweighted UniFrac distance (Adonis: $R^2 = 0.3026$, $p = 0.001$). Furthermore, box plots of the first principal coordinate showed that samples from different regions were separated from each other (**Figures 3C,D**), revealing that yaks from each region host their own distinct gut microbiota.

Composition of Gut Microbiota of Yaks From Different Regions

Venn analysis (**Figure 4A**) showed that 1145 OTUs were shared among the three regions, indicating that Shangri-La, Lhasa, and Yushu had similar OTU distribution. However, some OTUs were unique to some regions; there were 110 unique OTUs in Shangri-la, 129 in Lhasa, and 123 in Yushu.

We detected six phyla (**Figure 4B** and **Supplementary Table 1**), in the samples from the three regions. These phyla accounted for more than 0.2% of the community abundance at the phylum level. The dominant phyla were Bacteroidetes, Firmicutes, Verrucomicrobia, and Proteobacteria. Firmicutes and Bacteroidetes were the most represented phyla across all three regions, accounting for 89.26, 94.24, and 90.30% of the sequences in the Shangri-La, Lhasa, and Yushu groups, respectively. The relative abundance of Verrucomicrobia, Proteobacteria, and Saccharibacteria were significantly different among the samples from the three regions (**Figure 5A**).

We detected taxa from 21 families (**Figure 4C**) in the samples. The dominant families in Shangri-la included Ruminococcaceae, Rikenellaceae, Prevotellaceae, and Lachnospiraceae, with relative abundances of 40.43, 9.97, 9.25, and 7.35%, respectively. In Lhasa, the dominant families were Ruminococcaceae (36.50%), Rikenellaceae (13.81%), Prevotellaceae (12.12%), Bacteroidales_BS11_gut_group (9.34%), and Bacteroidaceae (5.67%). In Yushu, the major families included Ruminococcaceae (47.11%), Rikenellaceae (15.19%), and Prevotellaceae (8.56%). The relative abundance of Lachnospiraceae and Bacteroidales_BS11_gut_group was significantly different among all the samples (**Figure 5B**).

We detected 29 genera (**Figure 4D**) in the samples. Of these, *Ruminococcaceae _UCG-005* (16.23%), *Rikenellaceae_RC9_gut_group* (5.21%), and *Ruminococcaceae _UCG-010* (10.96%) were the dominant genera in the Shangri-la samples. In the Lhasa samples, *Ruminococcaceae_UCG-005* (13.39%), *Rikenellaceae_RC9_gut_group* (9.48%), *norank _f__Bacteroidales_BS11_gut_group* (9.34%), *Ruminococcaceae _UCG-010* (6.09%), *Bacteroides* (5.67), and *Prevotellaceae_UCG-004* (5.15%) were dominant. In the Yushu samples, *Ruminococcaceae_UCG-005* (22.65%) was the most dominant genus, followed by *Rikenellaceae_RC9_gut_group* (9.00%) and *Prevotellaceae_UCG-004* (5.80%). The relative abundance of *Ruminococcaceae_UCG-005*, *norank _f__Bacteroidales_BS11_gut_group*, and *Ruminococcaceae_UCG-010* exhibited significant differences among the different sample regions (**Figure 5C**).

Linear discriminant analysis effect size revealed the relative abundance of the different bacterial taxa (from phylum to genus) in the samples from different regions (**Figure 6A**). Species with LDA scores >3 were considered as biological markers of the different groups (**Figure 6B**). The LEfSe results showed that 107 bacterial taxa were significantly enriched in the samples – 58, 27, and 22 enriched taxa were found in the Shangri-La, Lhasa, and Yushu samples, respectively. Signature gut microbes included Firmicutes, Clostridia, and *Ruminococcaceae_UCG-010* in the Shangri-La samples, Bacteroidetes in the Lhasa samples, and Ruminococcaceae in the Yushu samples.

Predicted Function and Metabolism of Gut Microbiota

PICRUSt 2 prediction of the metabolic pathways of gut microbiota based on 16S rRNA sequencing data revealed that pathways in metabolism had the highest relative abundance, accounting for 67.45, 68.32, and 67.81% of the identified pathways in the Shangri-La, Lhasa, and Yushu samples, respectively (**Table 1** and **Supplementary Table 2**). A total of 12 biochemical pathways were identified among metabolic functions (**Table 2**). Functions in carbohydrate metabolism, global and overview maps, and amino acid metabolism were enriched in all samples. Functions in amino acid metabolism were significantly

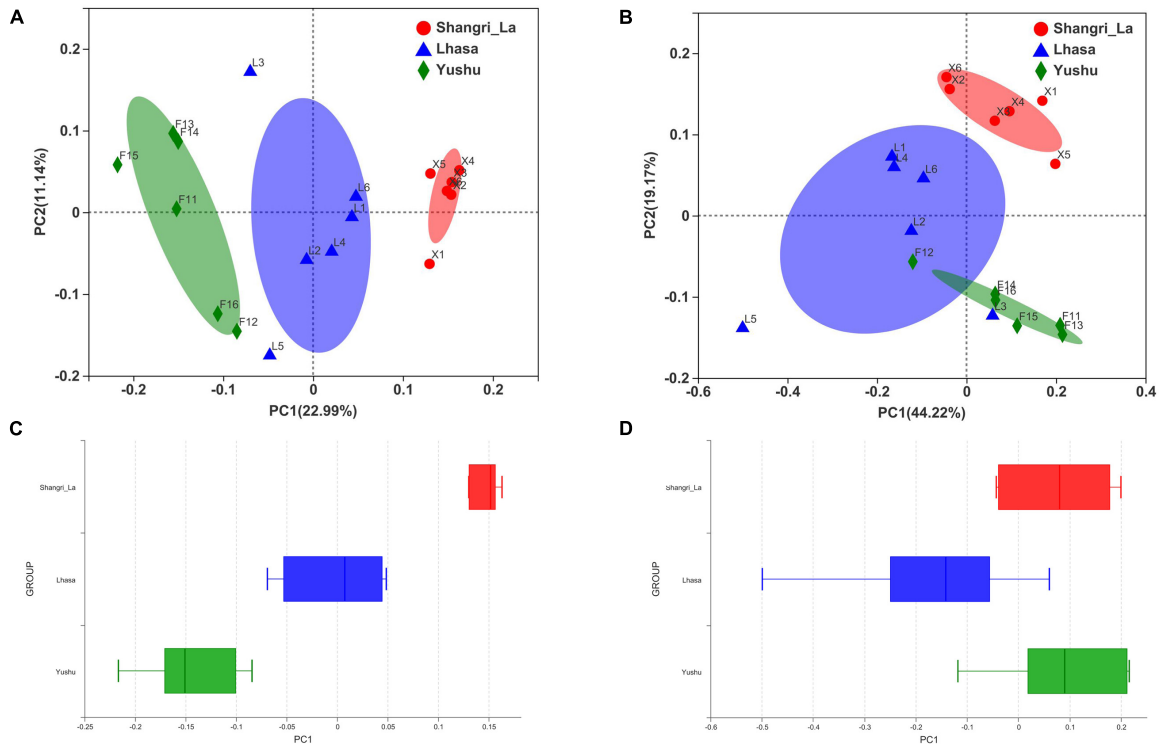

FIGURE 3 | Principal coordinates analysis (PCoA) of gut microbiota between different regions. **(A)** PCoA results based on unweighted UniFrac distance of bacterial communities from different regions. **(B)** PCoA results based on weighted UniFrac distance of bacterial communities from different regions. **(C)** The distinct separation of samples from different regions shown on the PCo1 axis based on weighted UniFrac distance. **(D)** The distinct separation of samples from different regions shown on the PCo1 axis based on unweighted UniFrac distance.

higher in Yushu samples than in samples from the other regions ($p < 0.05$).

Other functional roles in the microflora of the samples included cellular processes, organismal systems, environmental information processing, human diseases, and genetic information processing (**Table 3** and **Supplementary Table 3**). Additionally, pathways involved in replication and repair and translation were predominant in samples from each region. There were significant differences in the abundance of pathways related to infectious diseases: bacterial in the samples ($p < 0.05$). The functional roles in membrane transport in samples from Shangri-La were significantly higher than in those from the other regions ($p < 0.05$). Functional roles in folding, sorting and degradation, drug resistance: antineoplastic, and cancers: specific types in samples from Shangri-La were significantly lower than in those from the other regions ($p < 0.05$). The abundance of functional pathways for cell motility, cell growth and death, the digestive system, cellular community – prokaryotes, environmental adaptation, signal transduction, the nervous system, and aging in the samples from Lhasa were significantly different from those in samples from the other regions ($p < 0.05$). Human diseases from the immune diseases and endocrine and metabolic diseases pathways were significantly different in samples from Yushu than in those from other regions ($p < 0.05$).

DISCUSSION

Alpha diversity is the measure of species diversity in an area and is represented by the Chao, Shannon, and ACE indices. Beta diversity represents the regional differences in species composition, which can provide valuable information about how the microbiota differ (Wang et al., 2020). To better understand the diversity in gut microbiota of yaks from different regions, we analyzed our data using the Shannon, ACE, and Chao indices as well as PCoA. The Shannon, ACE, and Chao indices revealed significant differences in the diversity of gut microbiota between samples from Shangri-la and Yushu. The samples from Shangri-la had higher Shannon, ACE, and Chao indices than those from Lhasa and Yushu. Additionally, analysis of beta diversity revealed a distinct separation between samples from different regions. This may be due to increasing environmental radiation from temperate regions to high-altitude cold regions, which is accompanied by a shift in the vegetation that may cause regional variations in the diet of yaks. It is also probable that the high ultraviolet levels, low temperature, and low oxygen levels in the Qinghai-Tibetan Plateau habitats affect the diversity of yak bacterial communities (Li and Zhao, 2015). In conclusion, the diversity of the intestinal microbiota of yaks is closely related to geographical location and conditions.

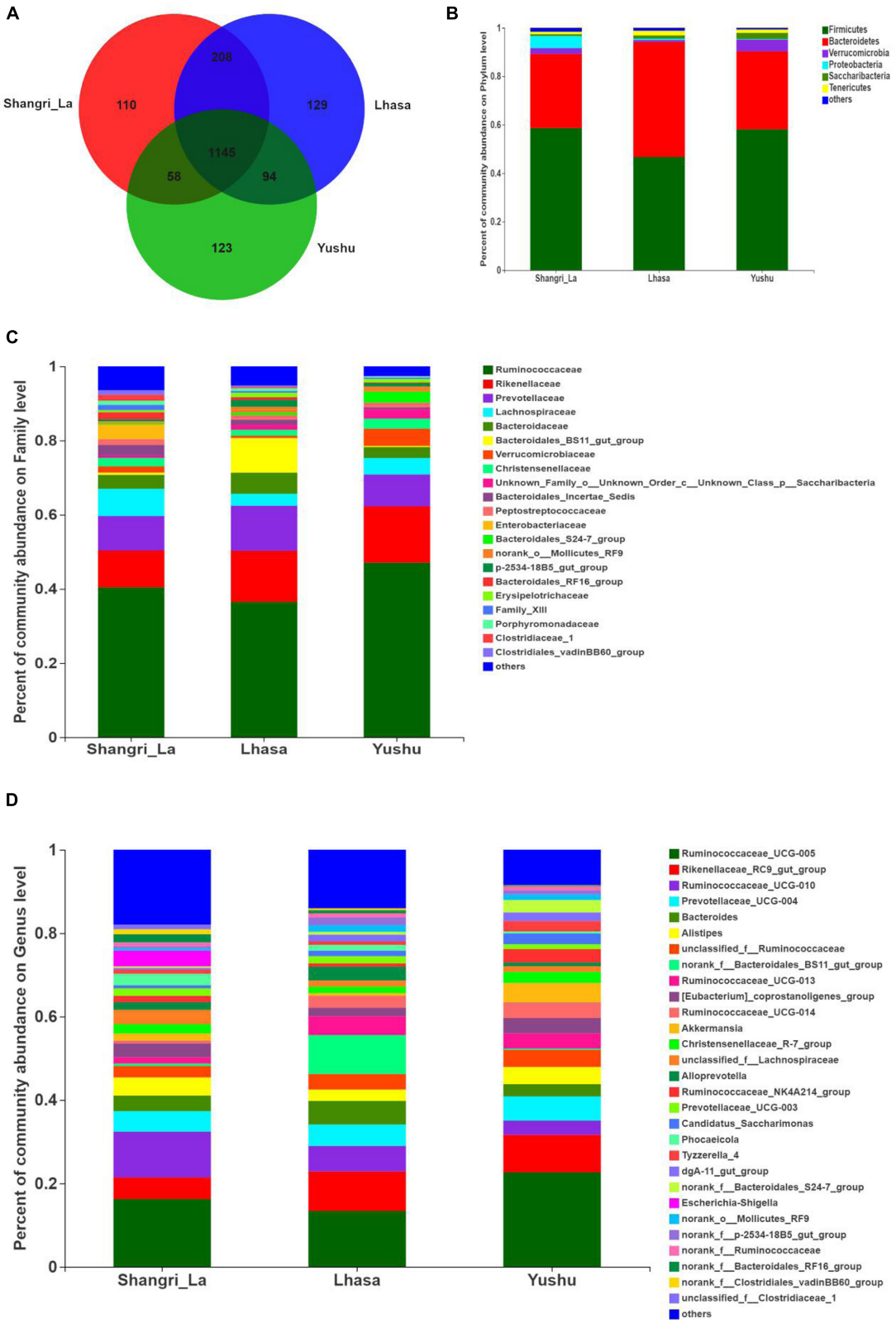

FIGURE 4 | Composition of gut microbiota of yaks from different regions. **(A)** Venn analysis. **(B)** Relative abundance of community at the phylum level. **(C)** Relative abundance of community at the family level. **(D)** Relative abundance of community at the genus level.

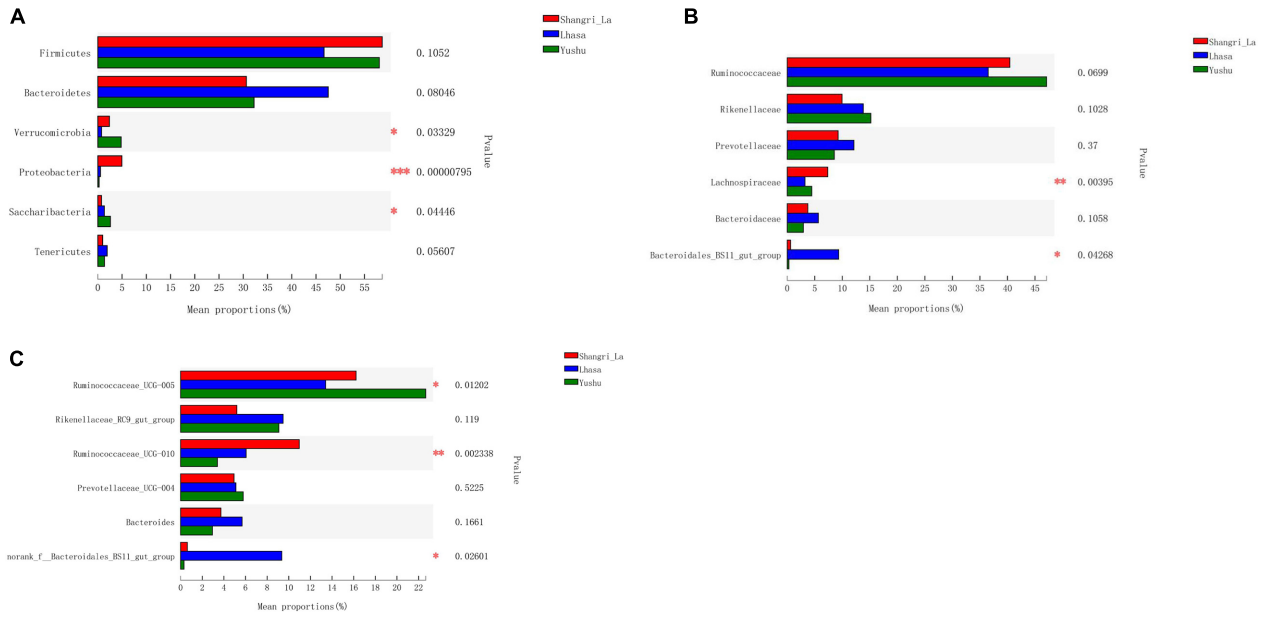

FIGURE 5 | Statistical comparison of the relative abundance of yak gut bacteria among different regions. **(A)** Comparison of dominant phyla in the Shangri-la, Lhasa, and Yushu groups. **(B)** Comparison of dominant families in the Shangri-la, Lhasa, and Yushu groups. **(C)** Comparison of dominant genera in the Shangri-la, Lhasa, and Yushu groups.

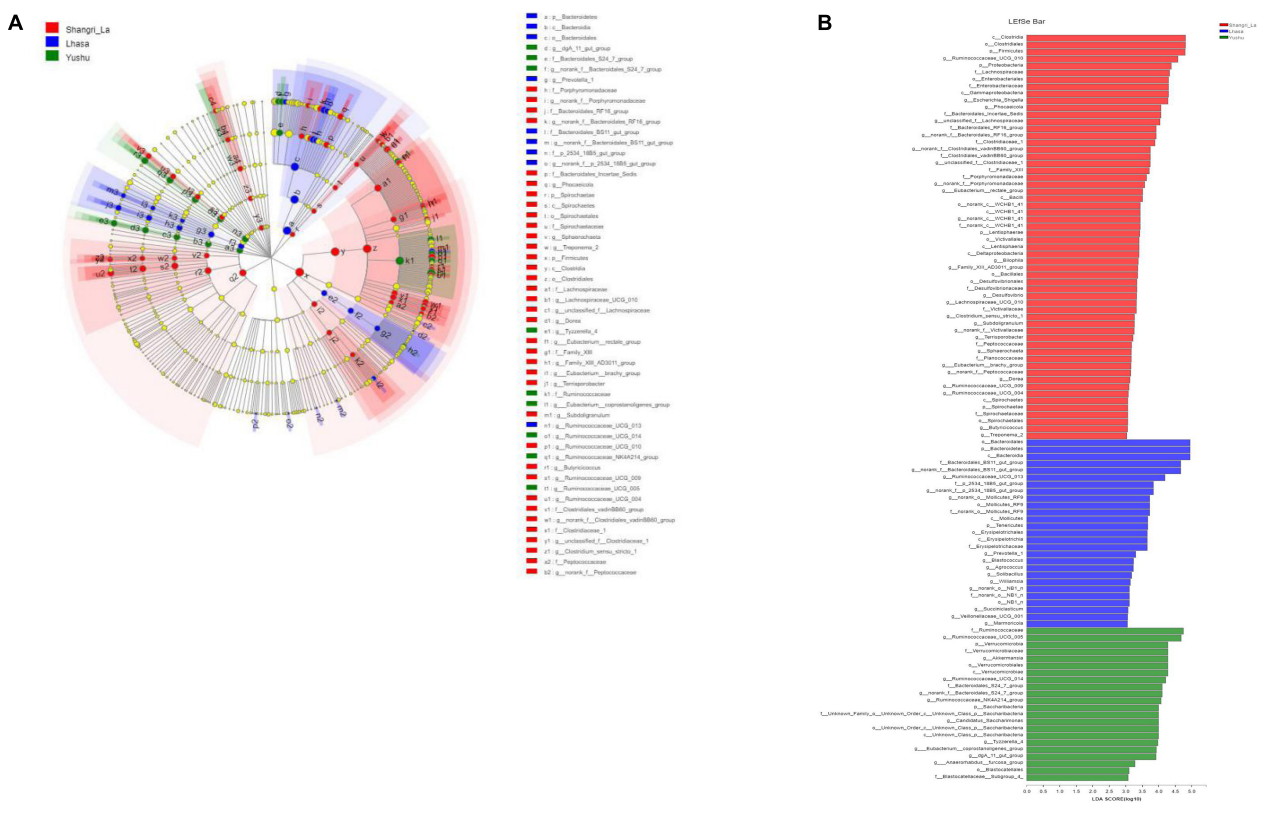

FIGURE 6 | LEfSe analysis of gut microbiota. **(A)** Linear discriminant analysis (LDA) effect size (LEfSe) conducted on the intestinal microbiota of yaks from different regions ($p < 0.05$, LDA > 3). Different colors and sizes of nodes indicate microbial groups with significant differences and enriched species abundance. Light yellow nodes indicate groups with no significant difference. **(B)** LEfSe for three regions.

TABLE 1 | The predicted functional composition (%) of the microbiota of yaks from different regions.

Functions	Shangri-La (n = 6)	Lhasa (n = 6)	Yushu (n = 6)
Cellular processes	6.07 ± 0.19^{a}	5.63 ± 0.34^{b}	5.98 ± 0.22^{a}
Environmental information processing	7.14 ± 0.29^{a}	6.19 ± 0.52^{b}	6.58 ± 0.32^{b}
Genetic information processing	12.86 ± 0.09^{b}	13.31 ± 0.57^{a}	13.18 ± 0.14^{ab}
Human diseases	4.17 ± 0.03^{a}	4.20 ± 0.05^{a}	4.15 ± 0.09^{a}
Metabolism	67.45 ± 0.52^{b}	68.32 ± 0.38^{a}	67.81 ± 0.56^{ab}
Organismal systems	2.31 ± 0.03^{a}	2.35 ± 0.08^{a}	2.29 ± 0.03^{a}

Letters$^{(a,b)}$ indicate significant differences within the same row ($p < 0.05$).

TABLE 2 | Predicted functional composition (%) of microbiota relating to metabolism.

Metabolic pathway	Shangri-La (n = 6)	Lhasa (n = 6)	Yushu (n = 6)
Amino acid metabolism	10.41 ± 0.05^{c}	10.58 ± 0.16^{b}	10.75 ± 0.07^{a}
Biosynthesis of other secondary metabolites	1.94 ± 0.05^{b}	2.02 ± 0.05^{a}	1.97 ± 0.06^{ab}
Carbohydrate metabolism	14.27 ± 0.21^{a}	14.15 ± 0.10^{ab}	13.99 ± 0.13^{b}
Energy metabolism	6.40 ± 0.07^{b}	6.54 ± 0.13^{a}	6.39 ± 0.07^{b}
Global and overview maps	12.84 ± 0.14^{b}	12.79 ± 0.41^{b}	13.20 ± 0.09^{a}
Glycan biosynthesis and metabolism	2.37 ± 0.21^{a}	2.63 ± 0.34^{a}	2.37 ± 0.19^{a}
Lipid metabolism	2.86 ± 0.02^{a}	2.92 ± 0.07^{a}	2.86 ± 0.06^{a}
Metabolism of cofactors and vitamins	6.17 ± 0.07^{a}	6.20 ± 0.09^{a}	6.15 ± 0.10^{a}
Metabolism of other amino acids	1.79 ± 0.03^{ab}	1.85 ± 0.11^{a}	1.76 ± 0.03^{b}
Metabolism of terpenoids and polyketides	1.47 ± 0.01^{b}	1.55 ± 0.09^{a}	1.50 ± 0.02^{ab}
Nucleotide metabolism	5.89 ± 0.05^{ab}	6.06 ± 0.25^{a}	5.85 ± 0.02^{b}
Xenobiotics biodegradation and metabolism	1.06 ± 0.01^{a}	1.03 ± 0.07^{a}	1.01 ± 0.02^{a}

Letters$^{(a,b,c)}$ indicate significant differences within the same row ($p < 0.05$).

TABLE 3 | Percentage composition of other functional genes of the microbiota of yaks from different regions.

Functions	Shangri-La (n = 6)	Lhasa (n = 6)	Yushu (n = 6)
Cellular processes			
Cell motility	1.58 ± 0.15^{a}	1.26 ± 0.26^{b}	1.56 ± 0.18^{a}
Cell growth and death	0.93 ± 0.03^{b}	1.01 ± 0.06^{a}	0.94 ± 0.04^{b}
Transport and catabolism	0.35 ± 0.05^{a}	0.41 ± 0.07^{a}	0.35 ± 0.05^{a}
Cellular community – eukaryotes	0.00 ± 0.00^{a}	0.00 ± 0.00^{a}	0.00 ± 0.00^{a}
Cellular community – prokaryotes	3.21 ± 0.12^{a}	2.92 ± 0.21^{b}	3.13 ± 0.14^{a}
Environmental information processing			
Signal transduction	2.83 ± 0.11^{a}	2.58 ± 0.14^{b}	2.75 ± 0.10^{a}
Membrane transport	4.30 ± 0.18^{a}	3.61 ± 0.39^{b}	3.84 ± 0.22^{b}
Signaling molecules and interaction	0.00 ± 0.00^{a}	0.00 ± 0.00^{a}	0.00 ± 0.00^{a}
Genetic information processing			
Replication and repair	4.76 ± 0.02^{b}	4.96 ± 0.25^{a}	4.87 ± 0.04^{ab}
Translation	5.49 ± 0.06^{b}	5.71 ± 0.26^{a}	5.64 ± 0.07^{ab}
Transcription	0.26 ± 0.00^{a}	0.26 ± 0.01^{a}	0.26 ± 0.01^{a}
Folding, sorting and degradation	2.34 ± 0.02^{b}	2.39 ± 0.07^{a}	2.40 ± 0.02^{a}
Human diseases			
Cancers: Overview	0.64 ± 0.01^{a}	0.66 ± 0.03^{a}	0.65 ± 0.02^{a}
Cardiovascular diseases	0.27 ± 0.00^{ab}	0.26 ± 0.02^{b}	0.28 ± 0.00^{a}
Immune diseases	0.05 ± 0.00^{a}	0.05 ± 0.01^{a}	0.04 ± 0.00^{b}
Infectious diseases: Parasitic	0.03 ± 0.00^{b}	0.05 ± 0.03^{a}	0.04 ± 0.01^{ab}
Drug resistance: Antimicrobial	1.55 ± 0.02^{a}	1.48 ± 0.07^{b}	1.49 ± 0.02^{ab}
Infectious diseases: Bacterial	0.70 ± 0.01^{a}	0.67 ± 0.03^{b}	0.64 ± 0.00^{c}
Drug resistance: Antineoplastic	0.36 ± 0.00^{b}	0.38 ± 0.01^{a}	0.39 ± 0.01^{a}
Endocrine and metabolic diseases	0.33 ± 0.00^{b}	0.32 ± 0.01^{b}	0.34 ± 0.00^{a}
Neurodegenerative Diseases	0.15 ± 0.01^{b}	0.18 ± 0.02^{a}	0.16 ± 0.02^{ab}
Cancers: Specific types	0.09 ± 0.00^{b}	0.11 ± 0.01^{a}	0.10 ± 0.01^{a}
Infectious diseases: Viral	0.01 ± 0.00^{a}	0.03 ± 0.01^{a}	0.03 ± 0.01^{a}
Substance dependence	0.00 ± 0.00^{a}	0.00 ± 0.00^{a}	0.00 ± 0.00^{a}
Organismal systems			
Circulatory system	0.00 ± 0.00^{a}	0.00 ± 0.00^{a}	0.00 ± 0.00^{a}
Environmental adaptation	0.21 ± 0.00^{a}	0.20 ± 0.01^{b}	0.20 ± 0.00^{a}
Endocrine system	0.86 ± 0.01^{a}	0.89 ± 0.04^{a}	0.86 ± 0.01^{a}
Digestive system	0.05 ± 0.01^{b}	0.07 ± 0.02^{a}	0.05 ± 0.01^{b}
Excretory system	0.04 ± 0.00^{ab}	0.03 ± 0.01^{b}	0.05 ± 0.00^{a}
Immune system	0.44 ± 0.01^{a}	0.43 ± 0.01^{a}	0.44 ± 0.01^{a}
Nervous system	0.29 ± 0.01^{a}	0.27 ± 0.01^{b}	0.29 ± 0.01^{a}
Aging	0.42 ± 0.01^{b}	0.45 ± 0.03^{a}	0.40 ± 0.01^{b}
Development	0.00 ± 0.00^{a}	0.00 ± 0.00^{a}	0.00 ± 0.00^{a}

Letters$^{(a,b,c)}$ indicate significant differences within the same row ($p < 0.05$).

Venn diagrams have often been used to determine the number of common and unique microbial species in samples, and can intuitively represent similarities and overlaps in species from different environments (Shade and Handelsman, 2012). In this study, Venn analysis and relevant abundance analysis revealed that core microbiota, as well as a quantity of unique microbiota, were present in the samples from each region; only some bacteria were significantly different between samples from different regions. A total of six phyla, 21 families, and 29 genera were detected in the samples from the three regions. We found that Firmicutes and Bacteroidetes were the dominant phyla in all the samples. In previous studies, these two phyla were found to be dominant in the gut microbiota of yaks (Liu et al., 2019; Ma et al., 2019), pikas (Li et al., 2019), goats (Lei et al., 2018), and sheep (Cui et al., 2019), indicating that they may be essential components of the mammalian intestinal microbiota (Fan et al., 2020). Firmicutes and Bacteroidetes are important for the digestion of proteins and carbohydrates (Spence et al., 2006). Our results suggest that the high abundance of Firmicutes

and Bacteroidetes found in yaks is possibly related to high energy consumption in cold environments (Zhang L. et al., 2020). We also found that the abundance of Verrucomicrobia, Proteobacteria, and Saccharibacteria were significantly different in the microbiota of yaks from different regions, which may be related to host diet and physiology (Kurilshikov et al., 2017). Studies have revealed that a lower abundance of Verrucomicrobia is correlated with increased fiber intake (Li et al., 2016). Yaks from Lhasa have a higher fiber intake than those from the other two regions. Ruminococcaceae, which is known to play an important role in cellulose and starch degradation (Jindou et al., 2006; Ze et al., 2012), was the most dominant family found in the microbiota of yaks from all three regions. The relative abundance of Ruminococcaceae was higher in the Yushu samples than in the other samples. This may be due to a high lignin and cellulose content in the diet of yaks from Yushu. The genus *Ruminococcaceae_UCG-005* belongs to the Ruminococcaceae family and is also important for cellulose digestion. It was predominant in all three regions. Therefore, the composition of the yak gut microbiome depends on the geographical region and corresponding conditions.

Gut microbiota have an important effect on the host's immune development, absorption, degradation of nutrients, and enzyme metabolism (Martin et al., 2010). Hence, it is essential to better understand the mechanisms that adapt the gut to different environments. Our PICRUSt2 analysis revealed that the functional gene composition of yak intestinal microbes was similar in yaks from the three regions; similar results were found for the bifidobacterial community of Chinese human subjects from different regions (Yang et al., 2020). Microbial communities often show incredible taxonomic diversity, however, their functional compositions are not directly related to taxonomic diversity because some similar gene functions are encoded by many concomitant but taxonomically distinct microbes (Louca et al., 2018). We found that the functional gene composition of the gut microbiota of yaks from different geographical regions was similar.

CONCLUSION

This study is the first to analyze the intestinal microbiota of yaks from three different geographical regions in China using high-throughput sequencing. The results indicate that the diversity and composition of the yak gut microbiota are related to the geographical regions. However, there were no significant differences in the functional gene composition of the microbiota of yaks from the different regions. Our findings provide a basis for studying the association between the intestinal flora of yaks and their adaptation to different geographical environments. Our study also lays the foundation for further exploring probiotic resources in the Qinghai-Tibetan Plateau.

DATA AVAILABILITY STATEMENT

The datasets presented in this study can be found in online repositories. The names of the repository/repositories and accession number(s) can be found below: NCBI (accession: PRJNA717166).

AUTHOR CONTRIBUTIONS

HS: conceptualization. WL: methodology. JX, SZ, YL, and YY: resources. QW: writing – original draft preparation. JS: writing – review and editing. JX, HS, and PX: supervision, project administration, and funding acquisition. All authors have read and agreed to the published version of the manuscript.

FUNDING

This work was supported by the Key Research and Development Projects in Tibet: Preservation of Characteristic Biological Germplasm Resources and Utilization of Gene Technology in Tibet (Grant No. XZ202001ZY0016N) and National Key R&D Program of China (2018YFD0502300).

SUPPLEMENTARY MATERIAL

The Supplementary Material for this article can be found online at: https://www.frontiersin.org/articles/10.3389/fmicb.2021.666940/full#supplementary-material

REFERENCES

Angelakis, E., Bachar, D., Yasir, M., Musso, D., Djossou, F., Melenotte, C., et al. (2019). Comparison of the gut microbiota of obese individuals from different geographic origins. *N. Microb. New Infect.* 27, 40–47. doi: 10.1016/j.nmni.2018.11.005

Cui, X., Wang, Z., Yan, T., Chang, S., Wang, H., and Hou, F. (2019). Rumen bacterial diversity of Tibetan sheep (Ovis aries) associated with different forage types on the Qinghai-Tibetan Plateau. *Can. J. Microb.* 65, 859–869. doi: 10.1139/cjm-2019-0154

Duan, Y. L., Miao, H. S., Liao, D. F., Kou, M. L., Li, Z. H., Wang, Z., et al. (2019). The serologic investigation and viral isolation of bluetongue virus in Shangri-La in Southwest China. *Transbound. Emerg. Dis.* 66, 2353–2361. doi: 10.1111/tbed.13292

Fan, Q., Wanapat, M., Yan, T., and Hou, F. (2020). Altitude influences microbial diversity and herbage fermentation in the rumen of yaks. *BMC Microb.* 20:1–13.

He, S., Ma, Y., Wang, J., Li, Q., Yang, X., Tang, S., et al. (2011). Milk fat chemical composition of yak breeds in China. *J. Food Composit. Anal.* 24, 223–230. doi: 10.1016/j.jfca.2010.07.008

Huang, X. D., Tan, H. Y., Long, R., Liang, J. B., and Wright, A.-D. G. (2012). Comparison of methanogen diversity of yak (Bos grunniens) and cattle (*Bos taurus*) from the Qinghai-Tibetan plateau. China. *BMC Microb.* 12:237. doi: 10.1186/1471-2180-12-237

Jia, Y., Yang, X., Zhang, C., Yang, S., Li, M., Xu, W., et al. (2018). Cryosurvival and pregnancy rates: One-step protocol for freezing–thawing Shangri-la Yak (Bos grunniens) Embryos. *Reproduct. Domest. Anim.* 53, 1168–1175. doi: 10.1111/rda.13222

Jindou, S., Borovok, I., Rincon, M. T., Flint, H. J., Antonopoulos, D. A., Berg, M. E., et al. (2006). Conservation and divergence in cellulosome architecture between two strains of Ruminococcus flavefaciens. *J. Bacteriol.* 188, 7971–7976. doi: 10.1128/jb.00973-06

Kim, K.-A., Gu, W., Lee, I.-A., Joh, E.-H., and Kim, D.-H. (2012). High fat diet-induced gut microbiota exacerbates inflammation and obesity in mice via the TLR4 signaling pathway. *PLoS One* 7:e47713. doi: 10.1371/journal.pone.0047713

Kurilshikov, A., Wijmenga, C., Fu, J., and Zhernakova, A. (2017). Host genetics and gut microbiome: challenges and perspectives. *Trends Immunol.* 38, 633–647. doi: 10.1016/j.it.2017.06.003

Lei, Y., Zhang, K., Guo, M., Li, G., Li, C., Li, B., et al. (2018). Exploring the spatial-temporal microbiota of compound stomachs in a pre-weaned goat model. *Front. Microbiol.* 9:1846.

Li, H., Zhou, R., Zhu, J., Huang, X., and Qu, J. (2019). Environmental filtering increases with elevation for the assembly of gut microbiota in wild pikas. *Microb. Biotechnol.* 12, 976–992. doi: 10.1111/1751-7915.13450

Li, K., Mehmood, K., Zhang, H., Jiang, X., Shahzad, M., Dong, X., et al. (2018). Characterization of fungus microbial diversity in healthy and diarrheal yaks in Gannan region of Tibet Autonomous Prefecture. *Acta Trop.* 182, 14–26. doi: 10.1016/j.actatropica.2018.02.017

Li, L., and Zhao, X. (2015). Comparative analyses of fecal microbiota in Tibetan and Chinese Han living at low or high altitude by barcoded 454 pyrosequencing. *Sci. Rep.* 5:14682.

Li, X., Guo, J., Ji, K., and Zhang, P. (2016). Bamboo shoot fiber prevents obesity in mice by modulating the gut microbiota. *Sci. Rep.* 6:32953.

Liu, C., Wu, H., Liu, S., Chai, S., Meng, Q., and Zhou, Z. (2019). Dynamic alterations in yak rumen Bacteria community and Metabolome characteristics in response to feed type. *Front. Microb.* 10:1116.

Louca, S., Polz, M. F., Mazel, F., Albright, M. B., Huber, J. A., O'Connor, M. I., et al. (2018). Function and functional redundancy in microbial systems. *Nat. Ecol. Evol.* 2, 936–943. doi: 10.1038/s41559-018-0519-1

Ma, L., Xu, S., Liu, H., Xu, T., Hu, L., Zhao, N., et al. (2019). Yak rumen microbial diversity at different forage growth stages of an alpine meadow on the Qinghai-Tibet Plateau. *PeerJ.* 7:e7645. doi: 10.7717/peerj.7645

Malmuthuge, N., and Guan, L. L. (2016). Gut microbiome and omics: a new definition to ruminant production and health. *Anim. Front.* 6, 8–12. doi: 10.2527/af.2016-0017

Martin, R., Nauta, A., Ben Amor, K., Knippels, L., Knol, J., and Garssen, J. (2010). Early life: gut microbiota and immune development in infancy. *Benefic. Microb.* 1, 367–382. doi: 10.3920/bm2010.0027

Morgavi, D. P., Rathahao-Paris, E., Popova, M., Boccard, J., Nielsen, K. F., and Boudra, H. (2015). Rumen microbial communities influence metabolic phenotypes in lambs. *Front. Microb.* 6:1060.

Pallen, M. J., Loman, N. J., and Penn, C. W. (2010). High-throughput sequencing and clinical microbiology: progress, opportunities and challenges. *Curr. Opin. Microb.* 13, 625–631. doi: 10.1016/j.mib.2010.08.003

Qin, X., Zhang, Y.-A., Du, M., Song, R., and Sun, Z. (2019). "Correlation Analysis and Body-Weight Estimation of Yak Traits in Yushu Prefecture," in *Proceeding of the International Conference on Harmony Search Algorithm*, (Berlin: Springer), 235–243. doi: 10.1007/978-3-030-31967-0_27

Reinhardt, C., Bergentall, M., Greiner, T. U., Schaffner, F., Östergren-Lundén, G., Petersen, L. C., et al. (2012). Tissue factor and PAR1 promote microbiota-induced intestinal vascular remodelling. *Nature* 483, 627–631. doi: 10.1038/nature10893

Ren, Q., Si, H., Yan, X., Liu, C., Ding, L., Long, R., et al. (2020). Bacterial communities in the solid, liquid, dorsal, and ventral epithelium fractions of yak (Bos grunniens) rumen. *MicrobiologyOpen* 9:e963.

Shade, A., and Handelsman, J. (2012). Beyond the Venn diagram: the hunt for a core microbiome. *Environ. Microb.* 14, 4–12. doi: 10.1111/j.1462-2920.2011.02585.x

Shanks, O. C., Kelty, C. A., Archibeque, S., Jenkins, M., Newton, R. J., McLellan, S. L., et al. (2011). Community structures of fecal bacteria in cattle from different animal feeding operations. *Appl. Environ. Microb.* 77, 2992–3001. doi: 10.1128/aem.02988-10

Sjögren, K., Engdahl, C., Henning, P., Lerner, U. H., Tremaroli, V., Lagerquist, M. K., et al. (2012). The gut microbiota regulates bone mass in mice. *J. Bone Mineral Res.* 27, 1357–1367. doi: 10.1002/jbmr.1588

Spence, C., Wells, W. G., and Smith, C. J. (2006). Characterization of the primary starch utilization operon in the obligate anaerobe *Bacteroides* fragilis: regulation by carbon source and oxygen. *J. Bacteriol.* 188, 4663–4672. doi: 10.1128/jb.00125-06

Wang, H., Long, R., Liang, J. B., Guo, X., Ding, L., and Shang, Z. (2011). Comparison of nitrogen metabolism in yak (Bos grunniens) and indigenous cattle (*Bos taurus*) on the Qinghai-Tibetan Plateau. *Asian-Austr. J. Anim. Sci.* 24, 766–773. doi: 10.5713/ajas.2011.10350

Wang, J., Ding, C., Tao, J., Jiang, X., Heino, J., Ding, L., et al. (2020). Damming affects riverine macroinvertebrate metacommunity dynamics: Insights from taxonomic and functional beta diversity. *Sci. Total Environ.* 2020:142945. doi: 10.1016/j.scitotenv.2020.142945

Wiener, G., Jianlin, H., and Ruijun, L. (2003). Origins, domestication and distribution of yak. *Yak* 2003, 1–16.

Wu, G. D., Compher, C., Chen, E. Z., Smith, S. A., Shah, R. D., Bittinger, K., et al. (2016). Comparative metabolomics in vegans and omnivores reveal constraints on diet-dependent gut microbiota metabolite production. *Gut* 65, 63–72. doi: 10.1136/gutjnl-2014-308209

Wu, J. (2016). The distributions of Chinese yak breeds in response to climate change over the past 50 years. *Anim. Sci. J.* 87, 947–958. doi: 10.1111/asj.12526

Xin, J., Chai, Z., Zhang, C., Zhang, Q., Zhu, Y., Cao, H., et al. (2019). Comparing the microbial community in four stomach of dairy cattle, yellow cattle and three yak herds in Qinghai-Tibetan Plateau. *Front. Microb.* 10:1547.

Yang, B., Yan, S., Chen, Y., Ross, R. P., Stanton, C., Zhao, J., et al. (2020). Diversity of gut microbiota and bifidobacterial community of chinese subjects of different ages and from different regions. *Microorgan.* 8:1108. doi: 10.3390/microorganisms8081108

Ze, X., Duncan, S. H., Louis, P., and Flint, H. J. (2012). Ruminococcus bromii is a keystone species for the degradation of resistant starch in the human colon. *ISME J.* 6, 1535–1543. doi: 10.1038/ismej.2012.4

Zhang, L., Jiang, X., Li, A., Waqas, M., Gao, X., Li, K., et al. (2020). Characterization of the microbial community structure in intestinal segments of yak (Bos grunniens). *Anaerobe* 61:102115. doi: 10.1016/j.anaerobe.2019.102115

Zhang, X.-L., Xu, T.-W., Wang, X.-G., Geng, Y.-Y., Liu, H.-J., Hu, L.-Y., et al. (2020). The Effect of Transitioning between Feeding Methods on the Gut Microbiota Dynamics of Yaks on the Qinghai–Tibet Plateau. *Animals* 10:1641. doi: 10.3390/ani10091641

Zhao, J., Yao, Y., Li, D., Xu, H., Wu, J., Wen, A., et al. (2018). Characterization of the gut microbiota in six geographical populations of Chinese rhesus macaques (*Macaca mulatta*), implying an adaptation to high-altitude environment. *Microb. Ecol.* 76, 565–577. doi: 10.1007/s00248-018-1146-8

Zhou, J., Zhong, C., Liu, H., Degen, A., Titgemeyer, E., Ding, L., et al. (2017). Comparison of nitrogen utilization and urea kinetics between yaks (Bos grunniens) and indigenous cattle (*Bos taurus*). *J. Anim. Sci.* 95, 4600–4612. doi: 10.2527/jas2017.1428

Zhou, X., Jiang, X., Yang, C., Ma, B., Lei, C., Xu, C., et al. (2016). Cecal microbiota of Tibetan Chickens from five geographic regions were determined by 16S rRNA sequencing. *Microbiologyopen* 5, 753–762. doi: 10.1002/mbo3.367

Zhu, Y., Cao, Y., Yang, M., Wen, P., Cao, L., Ma, J., et al. (2018). Bacterial diversity and community in Qula from the Qinghai–Tibetan Plateau in China. *PeerJ.* 6:e6044. doi: 10.7717/peerj.6044

Conflict of Interest: The authors declare that the research was conducted in the absence of any commercial or financial relationships that could be construed as a potential conflict of interest.

frontiers in Microbiology

ORIGINAL RESEARCH
published: 02 July 2021
doi: 10.3389/fmicb.2021.663945

Selenium Yeast Dietary Supplement Affects Rumen Bacterial Population Dynamics and Fermentation Parameters of Tibetan Sheep (*Ovis aries*) in Alpine Meadow

Xiongxiong Cui[1†], *Zhaofeng Wang*[1†], *Yuhui Tan*[1], *Shenghua Chang*[1], *Huiru Zheng*[2], *Haiying Wang*[2], *Tianhai Yan*[3], *Tsedan Guru*[4] *and Fujiang Hou*[1*]

[1] State Key Laboratory of Grassland Agro-ecosystems, Key Laboratory of Grassland Livestock Industry Innovation, Ministry of Agriculture and Rural Affairs, College of Pastoral Agriculture Science and Technology, Lanzhou University, Lanzhou, China, [2] School of Computing, Ulster University, Antrim, United Kingdom, [3] Sustainable Agri-Food Sciences Division, Agriculture Branch, Agri-Food and Biosciences Institute, Hillsborough, United Kingdom, [4] Animal Husbandry Science and Technology Demonstration Park of Maqu County, Gannan, China

OPEN ACCESS

Edited by:
Yvonne Vallès,
The University of the West Indies, Cave Hill, Barbados

Reviewed by:
Yan Tu,
Feed Research Institute (CAAS), China
Jinzhen Jiao,
Chinese Academy of Sciences, China

***Correspondence:**
Fujiang Hou
cyhoufj@lzu.edu.cn

[†]*These authors have contributed equally to this work*

Specialty section:
This article was submitted to Microbial Symbioses, a section of the journal Frontiers in Microbiology

Received: *04 February 2021*
Accepted: *31 May 2021*
Published: *02 July 2021*

Citation:
Cui X, Wang Z, Tan Y, Chang S, Zheng H, Wang H, Yan T, Guru T and Hou F (2021) Selenium Yeast Dietary Supplement Affects Rumen Bacterial Population Dynamics and Fermentation Parameters of Tibetan Sheep (Ovis aries) in Alpine Meadow. Front. Microbiol. 12:663945. doi: 10.3389/fmicb.2021.663945

Selenium (Se) deficiency is a widespread and seasonally chronic phenomenon observed in Tibetan sheep (*Ovis aries*) traditionally grazed on the Qinghai–Tibet Plateau (QTP). Effects of the dietary addition of Se-enriched yeast (SeY) on the bacterial community in sheep rumen and rumen fermentation were evaluated with the aim of gaining a better understanding of the rumen prokaryotic community. Twenty-four yearling Tibetan rams [initial average body weight (BW) of 31.0 ± 0.64 kg] were randomly divided into four treatment groups, namely, control (CK), low Se (L), medium Se (M), and high Se (H). Each group comprised six rams and was fed a basic diet of fresh forage cut from the alpine meadow, to which SeY was added at prescribed dose rates. This feed trial was conducted for over 35 days. On the final day, rumen fluid was collected using a transesophageal sampler for analyzing rumen pH, NH_3-N content, volatile fatty acid (VFA) level, and the rumen microbial community. Our analyses showed that NH_3-N, total VFA, and propionate concentrations in the M group were significantly higher than in the other groups ($P < 0.05$). Both the principal coordinates analysis (PCoA) and the analysis of similarities revealed that the bacterial population structure of rumen differed among the four groups. The predominant rumen bacterial phyla were found to be Bacteroidetes and Firmicutes, and the three dominant genera in all the samples across all treatments were *Christensenellaceae* R7 group, *Rikenellaceae* RC9 gut group, and *Prevotella* 1. The relative abundances of *Prevotella* 1, *Rikenellaceae* RC9 gut group, *Ruminococcus* 2, *Lachnospiraceae* XPB1014 group, *Carnobacterium*, and Hafnia-*Obesumbacterium* were found to differ significantly among the four treatment groups ($P < 0.05$). Moreover, Tax4fun metagenome estimation revealed that gene functions and metabolic pathways associated with carbohydrate and other amino acids were overexpressed in the rumen microbiota of SeY-supplemented sheep. To conclude, SeY significantly affects the abundance of rumen bacteria and ultimately affects the rumen microbial fermentation.

Keywords: Tibetan sheep, selenium, Qinghai-Tibet plateau, bacterial communities, high-throughput sequencing, grazing, alpine meadow selenium, rumen bacterial communities

INTRODUCTION

Rumen, a digestive organ that differentiates uminants from other mammals, is the most efficient natural fermentation system. In this organ, microorganisms ferment and degrade forage fibers and convert them into digestible proteins and volatile fatty acids (VFAs, the primary energy source for ruminants) for digestion and absorption (Dai et al., 2015). Rumen microorganisms are vital for ruminant nutrition as they are directly associated with the animal's diet (Puniya et al., 2015). The rumen microbial community predominantly consists of bacteria, in addition to fungi, protozoa, and a small number of phages (Miller et al., 2012), with each microorganism in a dynamic balance of competition and coordination. Several studies have shown that rumen microorganisms are closely linked to the ruminant livestock production efficiency and provide the host with as much as 65–75% of its energy requirement through anaerobic fermentation (Jewell et al., 2015; Chen et al., 2020). The rumen microbial community structure is affected by factors such as host type, health, and diet, and consequently, it varies across different regions and seasons (Yáñez-Ruiz et al., 2015).

In case the diet is nutritionally insufficient, supplying the rumen microorganisms with nutritional supplements is an appropriate practice to improve the feed conversion efficiency. Pino and Heinrichs (2016) reported that dietary minerals affect the rumen microorganism activity by affecting the rate of dilution of rumen digesta and eventually the rumen osmotic pressure. Gut health, trace element nutrition, and gut microbiome community structure are closely interdependent (Zhang et al., 2015; Faulkner et al., 2017; Biscarini et al., 2018; Ishaq et al., 2019). Research on this complex relationship between microelements and rumen microorganisms is ongoing since many decades. Selenium (Se) is an essential microelement for all life forms and plays a crucial role in livestock productivity (Białek and Czauderna, 2019). Several studies have examined the role of Se administration in improving the rumen efficiency and livestock production. Results of both *in vivo* and *in vitro* culture experiments have shown that Se supplementation promotes the rumen microorganism populations and improves the rumen's digestive efficiency (Shi et al., 2011). Naziroglu et al. (1997) reported that 0.3 mg/kg of Se simultaneously and effectively stimulates the production of total volatile fatty acid (TVFA), acetate, propionate, and butyrate in the rumen. A study by Miltko et al. (2016) reported that the administration of Se-enriched yeast (SeY) supplement increases the production of straight-chain and iso-branched-chain VFA in the rumen of Corriedale lambs. Morsy et al. (2019) evaluated the effect of oral administration of SeY in combination with vitamin E (SYPE) on rumen fermentation in Barki goats and observed an increase in the production of short-chain fatty acids, particularly of propionic acid. Another study showed that both selenized yeast and selenate increase the levels of acetate, propionate, butyrate, valerate, isobutyrate, and isovalerate in the rumen (Białek and Czauderna, 2019). Therefore, organic Se in the form of SeY has a good application prospect because it is safer and more efficient than inorganic Se (Kišidayová et al., 2014). Previous studies have shown that Se plays a role in improving the rumen function; however, its role in rumen microbial community metabolism remains poorly understood. Supplementation of sheep with sodium selenite or selenized yeast affects the population structure of rumen ciliate protozoa, with *Ophryoscolex* being the most Se-sensitive genus (Mihaliková et al., 2005). Although studies have been published on the biochemistry of ruminant Se nutrition, literature on the associated microbiological aspects is scarce.

The Qinghai–Tibet Plateau (QTP), with an average altitude of 4,500 m, is the world's highest plateau that accounts for one-quarter of China's landmass and offers one of the most extreme environments for livestock grazing (Thompson et al., 2000). The cold temperature- and hypoxia-resistant Tibetan sheep (*Ovis aries*) are the main source of income for local herders, providing them with precious resources, such as milk, meat, and fur and wool clothing, and dung as fertilizer and fuel (Zhao et al., 2011). The current population of ∼50 million Tibetan sheep extensively grazes in alpine meadows, ranging in altitude between 3,000 and 5,000 m (Zhou et al., 2015). The rumen microflora of the Tibetan sheep are affected by the harsh high-altitude environment, host type, age, and diet, and a greater percentage of novel species belongs to the phylum Firmicutes than that found in the rumen of lowland sheep (Huang et al., 2017). Microflora community comparisons between Tibetan sheep and Yak revealed that the α-diversity indices for the Tibetan sheep are significantly lower than those for Yak, with the rumen fungal community being affected by the host type (Guo et al., 2020). Han et al. (2020) reported that the rumen bacterial community of adult ewes is more diverse than that of rams and yearling ewes. Rumen bacterial diversity analysis of the Tibetan sheep through sequencing indicated the predominance of the phylum Firmicutes, with the remaining sequences belonging to Bacteroidetes, Proteobacteria, Actinobacteria, and unclassified operational taxonomic units (OTUs) (Huang et al., 2017). In our previous study, Bacteroidetes and Firmicutes were identified as the predominant rumen microbial phyla in the yearling Tibetan sheep, whereas the rumen of oat hay fed sheep was found to have a higher proportion of Proteobacteria and novel bacteria than the native pasture-fed sheep (Cui et al., 2019).

The Se content in plant-based diet of herbivore can vary remarkably across different regions (Surai and Fisinin, 2014). The soils of many regions of the world are low in Se; therefore, the majority of grazing animals in these areas receive insufficient dietary Se for their optimum health and performance, leading occasionally to clinical Se deficiency (Schrauzer and Surai, 2009). More than two-thirds of China's pastoral land is Se deficient, and hence, grazing livestock are unable to meet their dietary Se requirement from forage alone (Tashi et al., 2005; Xia et al., 2005). Research have shown that Se deficiency is widespread in Yak and Tibetan sheep of the QTP, often resulting in muscle atrophy, white muscle disease, and loss of animal production (Standing Committee on Agriculture, SCA, 1990; Xiong et al., 2018). Hence, correct feeding and management are essential to ensure the health and productivity of Tibetan sheep. Yet Tibetan herders typically follow the traditional grazing management model, in which the sheep continuously graze all year-round without Se supplementation. Moreover, the effect of Se deficiency on ruminants has received little attention so far. Although our previous study showed that SeY could benefit Tibetan sheep by

improving nitrogen metabolism and nutrient digestibility (Wang et al., 2019), the effect of Se dose rates on rumen fermentation parameters and microbial communities is still unknown.

Considering these Se deficiency-related livestock health and performance problems in the QTP, in the present study, we evaluated the effects of Se dietary supplement administered as SeY on rumen fermentation and bacterial community structure. The results of this study will broaden our understanding of rumen bacterial diversity and provide a scientific reference for determining appropriate SeY supplement dose rates to improve the Tibetan sheep production.

MATERIALS AND METHODS

Diet and Livestock Management

Feeding trials were conducted over a 35-day period from July to September (i.e., during warm season) at the Animal Husbandry Science and Technology Demonstration Park, Maqu County (N35° 58′, E101° 53′), Gansu Province, China. Twenty-four yearling Tibetan rams in good body condition [mean body weight (BW): 31.0 ± 0.64 kg] were selected from local pasture as test animals. These were divided randomly into four treatment groups, each of six rams, and fed a basic diet of fresh forage cut from alpine meadow, to which SeY was added at prescribed dose rates: control [CK: 0.00 g SeY/kg dry matter (DM)], low Se (L: 0.09g SeY/kg DM), medium Se (M: 0.18g SeY/kg DM), and high Se (H: 0.36g SeY/kg DM); taking into account the Se contents of the native pasture, the actual Se contents of the four diets were providing 0.023, 0.223, 0.423, and 0.823 mg Se/kg forage DM, respectively.

The trial period included 7 days in penned groups for acclimation and 28 days of formal experimentation. Each sheep was fed in a separate cage, with free access to water, and freshly cut native pasture was fed at 9:00 a.m., 11:00 a.m., 2:00 p.m., and 5:00 p.m. Each day, the forage being chopped into 5- to 10-cm lengths. Dominant pasture families were *Cyperaceae* (24.4%), *Poaceae* (18.6%), *Ranunculaceae* (17.8%), *Compositae* (17.2%), *Liliaceae* (4.1%), and *Fabaceae* (3.1%). SeY supplement (Angel Yeast Co., Ltd., of Hubei, China) was added evenly to this forage and fed once a day at 8:30 a.m. The chemical contents of native pasture and SeY specific parameters are listed in **Table 1**.

The Ethics and Animal Welfare Committee of Lanzhou University authorized all animal experimental procedures (file no: 2012-1 and 2012-2).

TABLE 1 | The chemical contents of diets [as dry matter (DM) basis] and selenium-enriched yeast (SeY) specific parameters.

Diets		SeY	
DM	35.8%	Appearance properties	Light yellow powder
Organic matter	89.9%	Selenium content	0.2%
Crude protein	7.3%	Drying weightlessness	≤6%
Neutral detergent fiber	59.3%	Ash	≤9%
Acid detergent fiber	32.7%	Relevant substances	≥85%
Ether extract	3.0%	Heavy metals	<3 ppm
Ash	10.0%		
Selenium (mg/kg)	0.023		

Sample Collection

On the final day of the experiment, and 2 h after feeding, a 10-ml sample of rumen fluid was obtained from each sheep using a transesophageal sampler, after first discarding the initial 50 ml to minimize contamination by oral saliva. Each sample was immediately sealed in a centrifuge tube and frozen at −20°C for subsequent analysis.

Analysis of Rumen Fermentation Products

The pH of rumen fluid samples was measured using a digital PB-21 pH meter (Sartorius, Germany). NH_3-N concentration was determined according to a colorimetric method using visible-light spectrophotometry (Agilent Cary 60 UV-Vis Spectrophotometer, USA). Volatile fatty acids were separated and quantified by gas chromatography (Focus GC AI 3000 Thermo Finnigan analyzer). One-microliter preprocessed sample was injected using a split (20:1) and using a Thermo Scientific AI 3000 autosampler (USA) on a Thermo Scientific TRACE 1300 Gas Chromatograph (USA). Injector and detector temperatures were both set at 200°C. Initial column temperature was 45°C, and the rate of temperature rise was set at 20°C/min. At 150°C, column temperature was held for 8 min, followed by further heating at 60°C rise/min until 185°C, where it was held for 1 min. The carrier gas used was nitrogen (purity: 99.99%; flow rate: 40.0 ml N_2/min).

DNA Extraction, Polymerase Chain Reaction Amplification, and Sequencing

Each sample was thawed separately and centrifuged at 4°C, and then 200 μl of the supernatant was taken for further analysis. CTAB method was used to extract total rumen microbial genomic DNA. Atomic spectrophotometry and 1% agarose gel electrophoresis were used to evaluate DNA concentration and purity. The universal prokaryote primers F336 and 806R were used to amplify the V3–V4 region of 16S rRNA. Polymerase chain reaction (PCR) amplification was carried out in a 20-μl reaction system. The PCR procedure consists of an initial step at 95°C for 2 min, followed by 30 cycles (95°C for 30 s, 55°C for 30 s, 72°C for 30 s), and a final extension at 72°C for 5 min. PCR expansion products of each sample were then mixed and detected by 2% agarose gel electrophoresis. Each PCR sample had two replicates for pyrosequencing. Sequencing of each PCR product (∼200 ng) was done by Novogene Bioinformatics Technology (Beijing, China) using the lon S5™ XL platform.

Sequence Analysis

Raw pyrosequencing single-end reads (400/600 bp) were assigned to samples sorted with barcodes and quality trimmed by FLASH 1.2.7 and QIIME 1.8.0 (Caporaso et al., 2010). The raw reads were spliced and filtered to obtain the high-quality clean reads following the quality controlled procedure and referenced against

the SILVA database (Edgar et al., 2011; Martin, 2011; Quast et al., 2012). Sequence analyses was clustered by UPARSE into OTUs based on 97% similarity (Edgar, 2013). A representative sequence for each OTU was screened, based on the mothur algorithm and using the SILVA database to further annotate taxonomic information (Quast et al., 2012). To identify the dominant species within each sample and determine the phylogenetic relationships between OTUs, taxonomic information was obtained, and the number of communities present in each sample was counted at each level of classification. Multiple sequence alignment was conducted and normalized using MUSCLE 3.8.31 (Edgar, 2004).

Statistical Analysis

For each bacterial community sample, species (OTU) richness and diversity were estimated using the ACE (abundance based coverage estimator), Sobs (observed species richness), and Chao 1 (species richness) indices; Shannon and Simpson indices (species diversity); and Good's coverage index (sequencing depth). Bacterial community structure of each group was then visualized by principal coordinates analysis (PCoA) based on Bray–Curtis dissimilarity matrices using R software (version 2.15.3). An ecologically organized heatmap of the top 35 most abundant genus was created using R software. All these index analyses were based on normalized data, calculated with QIIME 1.8.0 and displayed with R software. Based on the 16S rRNA gene sequence, the Tax4Fun microbial community function prediction used the SILVA database to classify OTU species, query the 16S copy number of each species (OTU) according to its NCBI genome annotation, and standardize the OTUs. Finally, the linear relationship between the SILVA classification and Kyoto Encyclopedia of Genes and Genomes (KEGG) database prokaryotic classification realized the prediction of the microbial community function (Aßhauer et al., 2015). The ruminal fermentation parameters and the α-diversity indices were analyzed using a completely randomized design by one-way analysis of variance (IBM SPSS Statistics 25.0). The Kruskal–Wallis rank sum test was used to compare the bacteria relative abundances between the four treatments using IBM SPSS Statistics 25.0. Significant difference value was set at $P < 0.05$.

RESULTS

Rumen Fermentation Parameters

Rumen fermentation parameters are shown in **Table 2**. NH_3-N, TVFA, and propionate concentrations in the M group were significantly higher than those in the other groups ($P < 0.05$). Acetate concentration and acetate-to-propionate ratio were both highest in the M group, which also had the lowest isobutyrate concentration ($P < 0.05$). Butyrate concentration was significantly higher in CK group ($P < 0.05$). There was no significant difference between the isovalerate, valerate concentrations, and pH of all four treatment groups ($P > 0.05$).

Bacterial Species Diversity

16S rRNA gene sequencing of all rumen fluid samples generated a total of 1,831,848 high-quality sequences with an average of 76,327 ± 1,517 [mean ± standard deviation (*SD*), $n = 24$] per sample. Nucleotide sequence identity was divided between reads into separate OTUs, based on a 97% similarity threshold, to obtain 5,032 OTUs. The sample rarefaction curves in **Supplementary Figure 1** reached the plateau period, indicating that the sequencing volume is sufficient to contain most of the microbial information in the sample. From the Good's coverage index, coverage of each sample reached 0.99, which reflected that sampling quality was sufficient in all the samples. **Table 3** shows that there was no significant difference in species diversity between all four treatment groups ($P > 0.05$).

Comparison of Bacterial Community Composition and OTUs Between Treatments

Rumen fluid flora analyses indicated that 23 phyla were present in all samples. The predominant phyla in all four treatment groups according to phylum assignment results are listed in **Supplementary Table 1**. The most abundant phylum was Firmicutes (CK 51.88%, L 52.51%, M 44.09%, and H 57.89%, respectively), the secondary phylum, Bacteroidetes (CK 35.64%, L 33.41%, M 42.25%, and H 31.57%, respectively), and the tertiary phylum, Proteobacteria (CK 8.36%, L 8.65%, M 9.42%, and H 5.69%, respectively) (**Figure 1A**). The most differentially abundant bacterial phylum in the four groups was Synergistetes (CK 0.14%, L 1.34%, M 0.55%, and H 0.45%, respectively), and the relative abundance of Synergistetes decreased with SeY additive level ($P < 0.05$) (**Supplementary Table 1**). At the family level, *Ruminococcaceae* (17.22%), *Christensenellaceae* (13.13%), *Rikenellaceae* (12.38%), and *Prevotellaceae* (12.29%) were the dominant families; other families included *Lachnospiraceae* (7.74%), *Bacteroidales* BS11 gut group (6.43%), *Enterobacteriaceae* (6.20%), *Clostridiaceae* 1 (3.19%), *Erysipelotrichaceae* (2.72%), and *Porphyromonadaceae* (1.60%) (**Figure 1B**).The difference in relative abundances of *Lachnospiraceae* was statistically significant ($P < 0.05$) (**Supplementary Table 2**). At the genus level, 274 genera were detected in all the samples, of which the 15 most abundant genera were found in the four groups (average relative abundance of >1% for at least one group) in the Tibetan sheep rumen, presented in **Supplementary Table 3**. The three dominant genera in all groups were *Christensenellaceae* R7 group (CK 14.28%, L 8.71%, M 11.98 %, and H 16.16%, respectively), *Rikenellaceae* RC9 gut group (CK 7.8%, L 13.95%, M 12.72%, and H 9.2%, respectively), and *Prevotella* 1 (CK 14.35%, L 5.29%, M 12.84%, and H 7.9%, respectively) (**Figure 1C**).

The differences in relative abundance of *Christensenellaceae* R-7 group, *Ruminococcus* 2, *Lachnospiraceae XPB1014 group*, *Carnobacterium*, *Prevotella 1*, *Dysgonomonas*, and Hafnia-*Obesumbacterium* in various groups were statistically significant ($P < 0.05$) (**Supplementary Table 3**). In order to provide clarity and visualization, a heatmap showed the top 35 genera (**Figure 2**). Based on heatmap, the results showed that the abundances of *Saccharofermentans*, *Peptoclostridium*, *Yersinia* [Eubacterium] *coprostanoligenes* group, *Acinetobacter*, and *Erysipelotrichaceae* UCG-004 were higher in the CK group than in the groups receiving Se supplement. However, the

TABLE 2 | Influence of Selenium dose rate on rumen fermentation parameters in Tibetan sheep.

Rumen fluid analyses[2]	Treatments[1]				SEM	*P*-value
	CK	L	M	H		
pH	6.40	6.39	6.42	6.33	0.05	0.938
NH_3-N (mg/dl)	17.70[a]	19.01[a]	22.49[b]	18.66[a]	0.18	0.001
TVFA (mmol/L)	29.74[a]	30.26[a]	32.87b[b]	31.23[b]	0.35	0.001
Acetate (%)	68.19[a]	68.12[a]	68.21[a]	69.73[b]	0.23	0.02
Propionate (%)	18.64[a]	19.74[b]	20.05[b]	18.41[a]	0.20	0.001
Isobutyrate (%)	2.11[a]	2.10[a]	2.00[a]	1.87[b]	0.34	0.046
Butyrate (%)	5.78[a]	6.30[b]	6.60[b]	7.18[c]	0.10	0.001
Isovalerate (%)	1.88	1.95	1.92	1.87	0.06	0.97
Valerate (%)	0.58	0.54	0.54	0.54	0.01	0.545
Acetate/propionate	3.66[a]	3.46[b]	3.41[b]	3.79[a]	0.04	0.001

[1]CK, L, M, and H: treatment groups supplemented with SeY at 0 (control), 0.09 (low), 0.18 (medium), and 0.36 (high) g/kg dry matter, respectively.
[2]NH_3-N: ammonia nitrogen; TVFA: total volatile fatty acids.
[a,b,c]Within rows, means without a common superscript differ ($P \leq 0.05$).

TABLE 3 | Operational taxonomic unit count and diversity estimation from sequencing analysis and based on the 16S rRNA gene libraries.

Item	Treatments[1]				SEM	*P*-value
	CK	L	M	H		
Observed species	1,341	1,332	1,341	1,321	15.03	0.249
Shannon	7.16	7.62	7.29	7.42	0.08	0.189
Simpson	0.96	0.98	0.97	0.97	0.01	0.277
Chao 1	1,571	1,543	1,578	1,575	21.16	0.942
ACE	1,603	1,556	1,589	1,600	18.52	0.818
Good's coverage	0.99	0.99	0.99	0.99	0.00	0.192

[1]CK, L, M, and H: treatment groups supplemented with SeY at 0 (control), 0.09 (low), 0.18 (medium), and 0.36 (high) g/kg dry matter, respectively.

low-level Se (L group) intake correlated positively with the abundance of *Ruminococcus* 2, *Roseburia*, *Carnobacterium*, *Desemzia*, *Fretibacterium*, and *Ruminococcaceae* UCG-005; the medium level Se (M group) intake correlated positively with the abundance of *Prevotellaceae* UCG-001, *Dysgonomonas*, and *Prevotellaceae* UCG-003; and the high-level Se (H group) intake correlated positively with the abundance of *Lachnospiraceae* XPB1014 group, *Pseudomonas*, *Butyrivibrio* 2, and unidentified *Bacteroidales* BS11 gut group. In all samples, a total of 4,150 OTUs were calculated. The number of OTUs shared among the four groups was 1,664, and the number of OTUs specific to the CK, L, M, and H groups was 473, 246, 152, and 308, respectively (**Figure 3**).

Se and Rumen Bacterial Community Dynamics

Principal coordinates analysis analyses based on Bray–Curtis dissimilarity matrices showed that rumen bacterial communities at four groups gathered together by their ration treatment and separated (**Figure 4**). The results of analysis of similarities strengthen the tendency of the difference of community structure of the four groups (CK-L: $P = 0.005$; CK-M: $P = 0.038$; CK-H: $P = 0.009$; L-M: $P = 0.029$; L-H: $P = 0.004$; M-H: $P = 0.015$).

Tax4Fun Prediction of Functional and Metabolic Capabilities

Forty-four functional pathways were identified based on the predicted metagenomes at the level 2 KEGG orthologs (KO) and their corresponding pathways (**Figure 5**). In this functional profile, the overall functional structure of the bacterial community identified using rumen fluid samples was found to be dominated by the following KEGG pathway-related processes: metabolism (carbohydrates, amino acids, nucleotides, and energy); genetic information processing (translation, replication, and repair); and environmental information processing (membrane transport and signal transduction). Regarding cellular processes in prokaryotes, the genes responsible for cellular motility and transport and catabolism pathways were found to be dominant. The genes related to human diseases and organismal system pathways were also predicted. Other KEGG pathways in the inferred functional profile of bacterial communities in rumen fluid could not be classified, although these pathways were principally related to metabolism, genetic information processing, and cellular processes and signaling. Eleven pathways showed significant differences among the CK, L, M, and H groups ($P < 0.05$) (**Supplementary Table 4**).

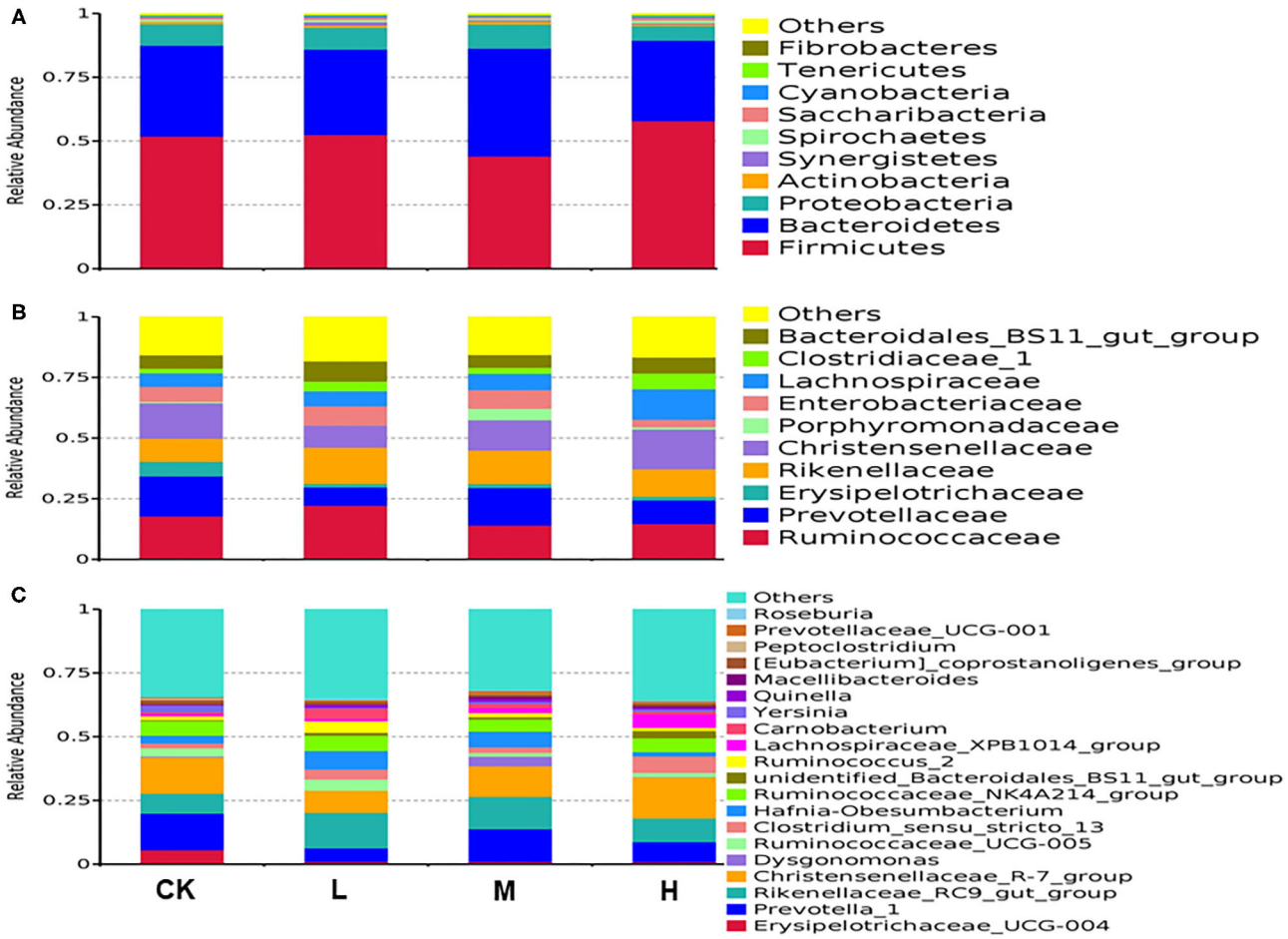

FIGURE 1 | Relative abundance of operational taxonomic units agglomerated of bacterial taxa averaged under phylum level for **(A)**, family level for **(B)**, and genera level for **(C)** at the four SeY doses (mg SeY/kg dry matter) (CK, 0; L, 0.09; M, 0.18; H, 0.36). The color-coded bar plot shows the average bacterial phylum, family, and genus distributions level of the nutritional diets sampled. CK, control; L, low Se, M, medium Se; H, high Se.

DISCUSSION

Biodiversity metrics evaluate the sustainability and productivity within numerous ecosystems, and the diversity of the gut intestinal microbiota is closely related to health, metabolic ability, and stability of animals (Fan et al., 2020). In this study, the bacteria diversity index of Tibetan sheep was not found to vary significantly between the groups receiving SeY supplement and the CK group, suggesting that Se-supplemented diets do not affect the diversity of rumen bacterial community in Tibetan sheep. A study on growing Beagle puppies reported that the α-diversity index of the gut bacterial community is not affected by the Se source (sodium selenite or SeY) (Pereira et al., 2020), which is consistent with our results.

Dietary changes play an important role in altering the composition of rumen microbial communities. However, regardless of the diet composition, Firmicutes and Bacteroidetes were reported to be the dominant phyla in the rumen (Jami et al., 2013), indicating that these bacteria play an important role in the rumen function and ecology of ruminants. In this study, the dominant phyla were Firmicutes and Bacteroidetes, and the finding is consistent with those of several studies on herbivores (Rubino et al., 2017; Cui et al., 2019). The dominant microbial community in the rumen of ruminants is not static and may be adjusted dynamically based on the conventional dominant bacterial group with changes in the feed type (McCann et al., 2016). Therefore, the investigation of rumen microorganisms is usually performed under specific dietary conditions (Clemmons et al., 2019). A previous study showed that members of the Bacteroidetes phylum are mainly responsible for protein hydrolysis and carbohydrate degradation, whereas those belonging to the phylum Firmicutes play an important role in energy utilization (Wu et al., 2011; Chen et al., 2015). In this study, we identified that the diet supplemented with a medium level of SeY may be more suitable for the survival of the phylum Bacteroidetes, whereas a high level of SeY may be more suitable for the survival of the phylum Firmicutes. The trend of increase in the relative abundance of Bacteroides and

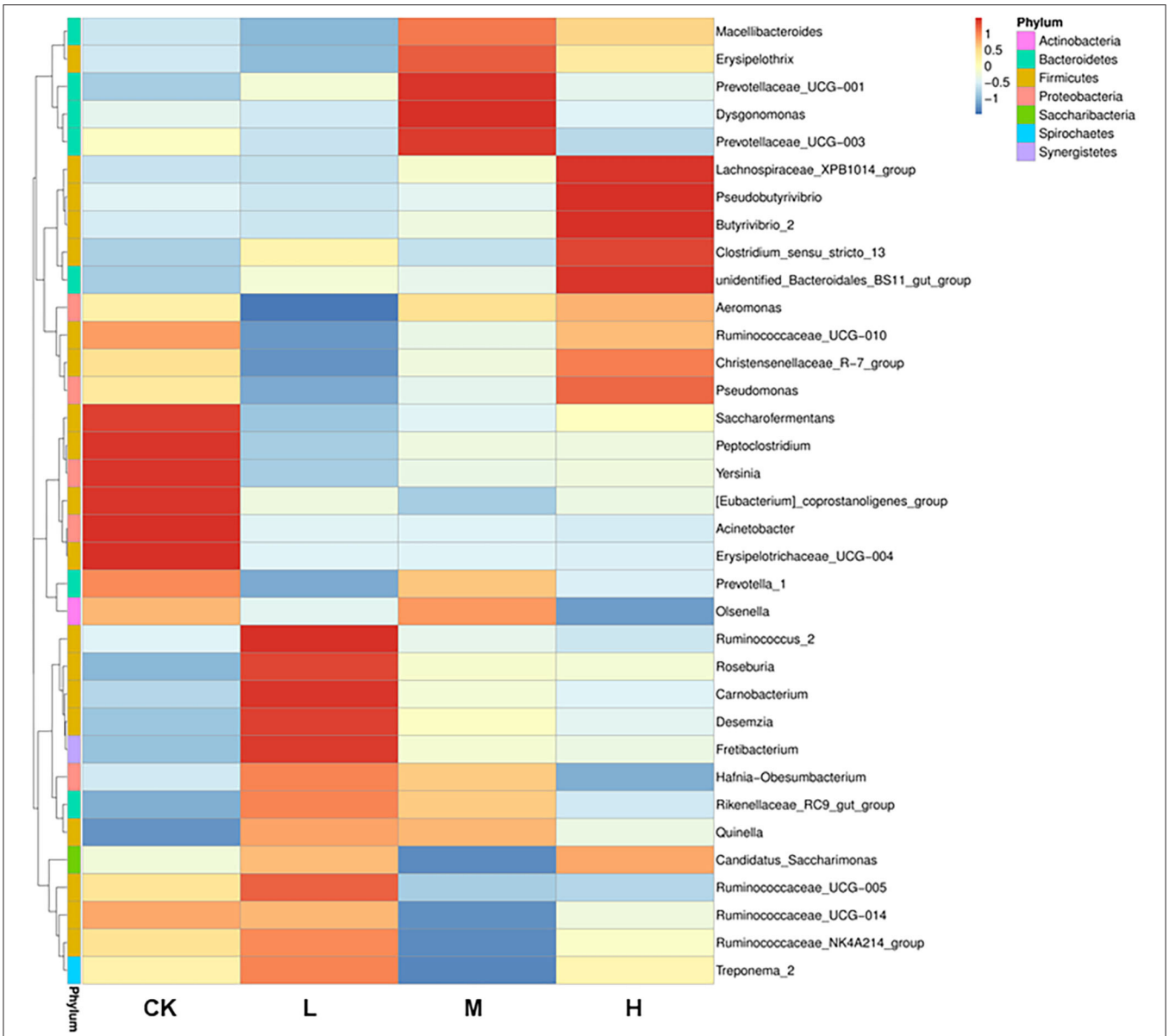

FIGURE 2 | Heatmap analysis of 35 shared prokaryotic community genera of all Tibetan sheep, as determined by the relative abundance of each shared genera through sequencing platform. The vertical direction is the sample information, and the horizontal direction is the species annotation information. The left cluster tree is the species clustering tree; the middle heatmap corresponds to the value of each row of the relative abundance of species after the standardized treatment of the *Z*-score.

Bacteroidetes/Firmicutes indicated that a medium level of SeY may improve the protein and carbohydrate utilization rate of native pasture. Interestingly, when SeY was included as a dietary supplement, the abundance of Synergistetes (an uncommon bacterial phylum) was influenced by the increasing dietary SeY-supplement level. Synergistetes are found under diverse anaerobic environments including soils, wastewater treatment systems, and human oral cavity, although they are not regular members in the rumen (Godon et al., 2005). According to a report, Synergistetes have diversified by exploiting the same type of metabolic niche under different habitats (Hugenholtz et al., 2010). We speculate that Synergistetes are mainly responsible for Se utilization in the rumen; however, this assumption requires further investigation. At the family level, the relative abundance of *Lachnospiraceae* increased with an increase in the SeY supplementation level. A previous study showed that *Lachnospiraceae* plays an essential role in producing beneficial metabolites for the host, with some members exhibiting strong hydrolyzing activities (Sagheddu et al., 2016). Many *Lachnospiraceae* species are associated with the production of butyrate, which assists in maintaining a healthy ruminant intestinal environment (Louis and Flint, 2009).

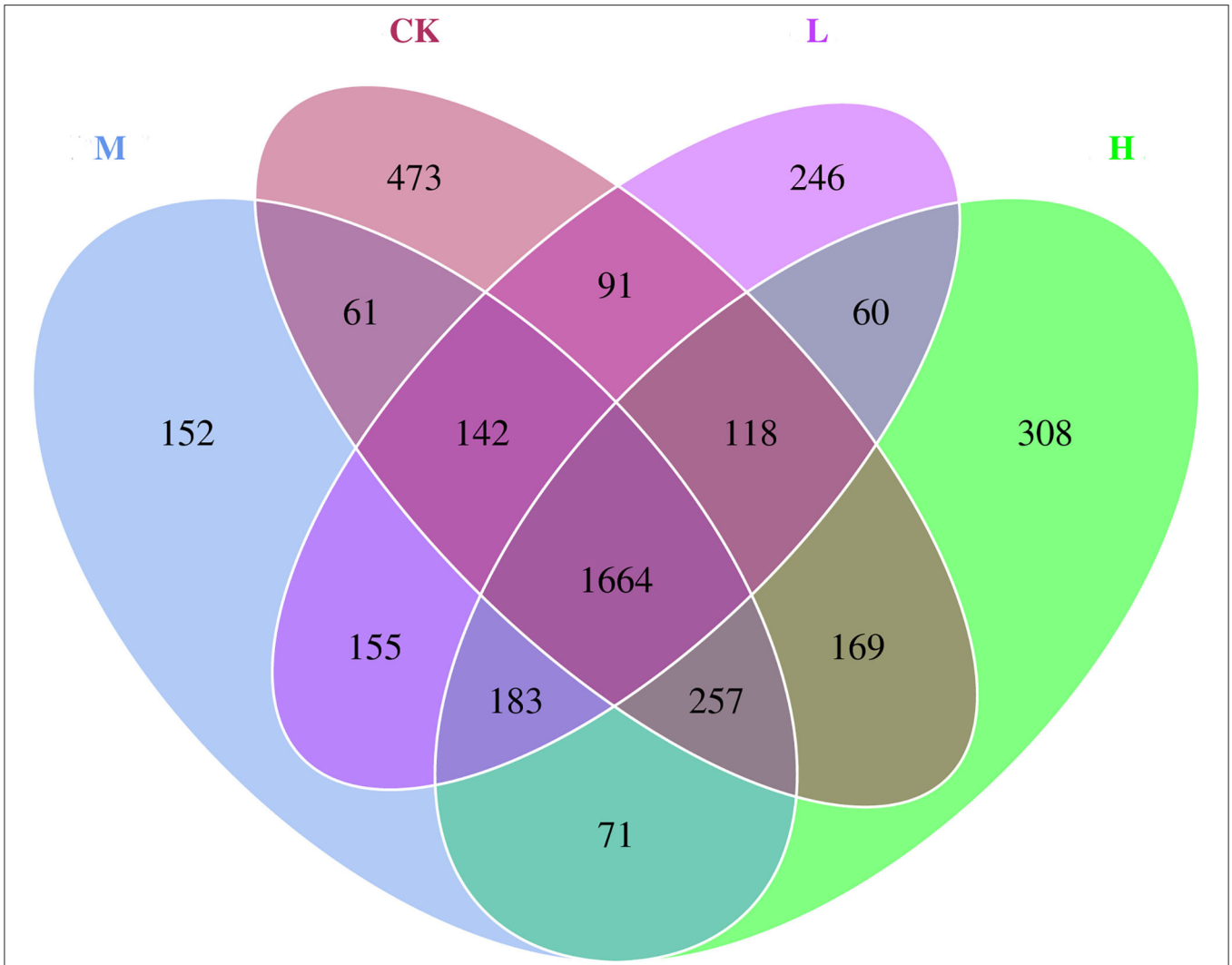

FIGURE 3 | Microbial diversity Venn diagram of rumen bacteria of Tibetan sheep at the four SeY doses (mg SeY/kg dry matter) (CK, 0; L, 0.09; M, 0.18; H, 0.36). CK, control; L, low Se, M, medium Se; H, high Se.

Meehan and Beiko (2014) showed that *Lachnospiraceae* species are involved in preventing colon cancer. In this feeding trial, the relative abundance of the species belonging to the family *Lachnospiraceae* was found increased with SeY-supplemented level. We speculate that this SeY supplementation-induced response could possibly help Tibetan sheep improve their health and metabolic capability.

Importantly, at the genus level, the abundance of *Christensenellaceae* R7 group, *Ruminococcus* 2, *Lachnospiraceae* XPB1014 group, *Carnobacterium*, *Prevotella 1*, *Dysgonomonas*, and *Hafnia*-Obesumbacterium showed clearly distinct responses to dietary Se supplementation; however, the predominant OTU in the rumen microbiome in all the four treatments was the *Christensenellaceae* R7 group. A study showed that *Christensenellaceae* are associated with a lean host phenotype of human (Goodrich et al., 2014). Our previous study reported that dietary supplementation of SeY could improve the food conversion ratio of Tibetan sheep and that there is a quadratic relationship between the SeY supplementation level and food conversion ratio, wherein a high Se dose rate is not beneficial for sheep growth (Wang et al., 2019). *Christensenellaceae* R7 may play an important role in the degradation of hemicellulose and cellulose (Dai et al., 2015). In this study, the abundance of *Christensenellaceae* R7 showed a decreasing to increasing trend with an increase in dietary SeY supplementation. This result supports the hypothesis that dietary supplementation with high amounts of SeY increases the *Christensenellaceae* R7 abundance, which may be disadvantageous in promoting the growth of Tibetan sheep, whereas supplementing the diet with low or medium amounts of SeY may be beneficial in promoting their growth and development. The *Ruminococcaceae* family plays an important role in mucosa associated in colon and cellulose degradation of mammals (Nava and Stappenbeck, 2011). The *Ruminococcus* genus consists of two types of

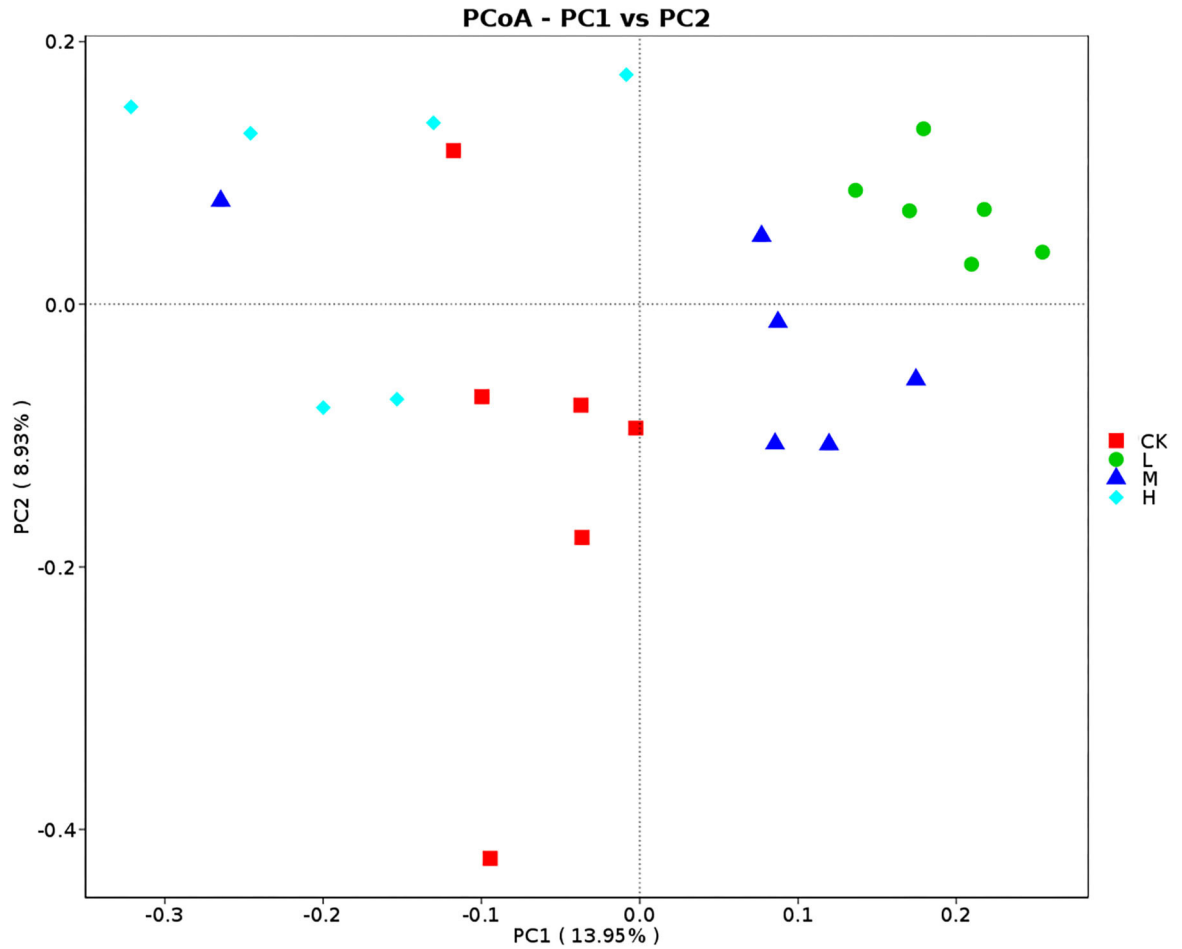

FIGURE 4 | PCoA (Bray–Curtis) of rumen bacteria in Tibetan sheep at the four SeY doses (mg SeY/kg dry matter) (CK, 0; L, 0.09; M, 0.18; H, 0.36). CK, control; L, low Se, M, medium Se; H, high Se.

powerful fiber-degrading bacteria that can break down fibers into hemicellulase and cellulose through rumen fermentation, and cellulose can be further degraded to VFAs (Jami and Mizrahi, 2012). Therefore, the abundance of *Ruminococcus* may affect the energy utilization efficiency to support Tibetan sheep adapted to harsh conditions of the QTP environment. In the process of adapting to the low-SeY and medium-SeY diets, the abundance of *Ruminococcus* 2 first increased and eventually decreased in the high-SeY diet group, indicating that SeY supplementation might affect cellulose digestion, VFA production, and energy utilization efficiency. Reduction in these bacterial populations in the high-SeY group might reduce the Tibetan sheep's ability to degrade plant cellulose and energy utilization efficiency. The proportion of the *Lachnospiraceae* XPB 1014 group was higher in the rumen of Tibetan sheep in the high-SeY group than in the rumen of those in other groups, indicating that the genus *Lachnospiraceae* XPB 1014 has different SeY sensitivities. *Carnobacteria* are ubiquitous lactic acid bacteria isolated from different habitats and can catabolize a wide range of carbohydrates. Their importance as probiotic cultures in the food and aquaculture breeding industry has been established (Leisner et al., 2007). A study showed that some *Carnobacterium* members are mainly responsible for humoral and cellular immune responses of various hosts (Kim and Austin, 2006). In the present study, the relative abundance of *Carnobacterium* significantly increased in the rumen of Tibetan sheep that were fed a diet supplemented with medium level of SeY, indicating that such a diet may improve the utilization of dietary carbohydrates and immune capacity. The *Prevotellaceae* family is a metabolically and genetically diverse microbial population in the rumen that possesses the ability to degrade lignocellulosic feedstock (Bi et al., 2018). Moreover, the *Prevotellaceae* family is also involved in pectin and protein metabolism (Schnorr et al., 2014). For ruminants, *Prevotellaceae* plays an important role in degrading oligopeptides (Walker et al., 2003). Proteins as a nitrogen source are essential for the growth of *Prevotella* 1. A correlation analysis revealed that *Prevotella* 1 plays an important role in the metabolism of amino acids in the rumen (Xue et al., 2020). In our study, the abundance of the genus *Prevotella* 1 was found to be affected by SeY-supplemented

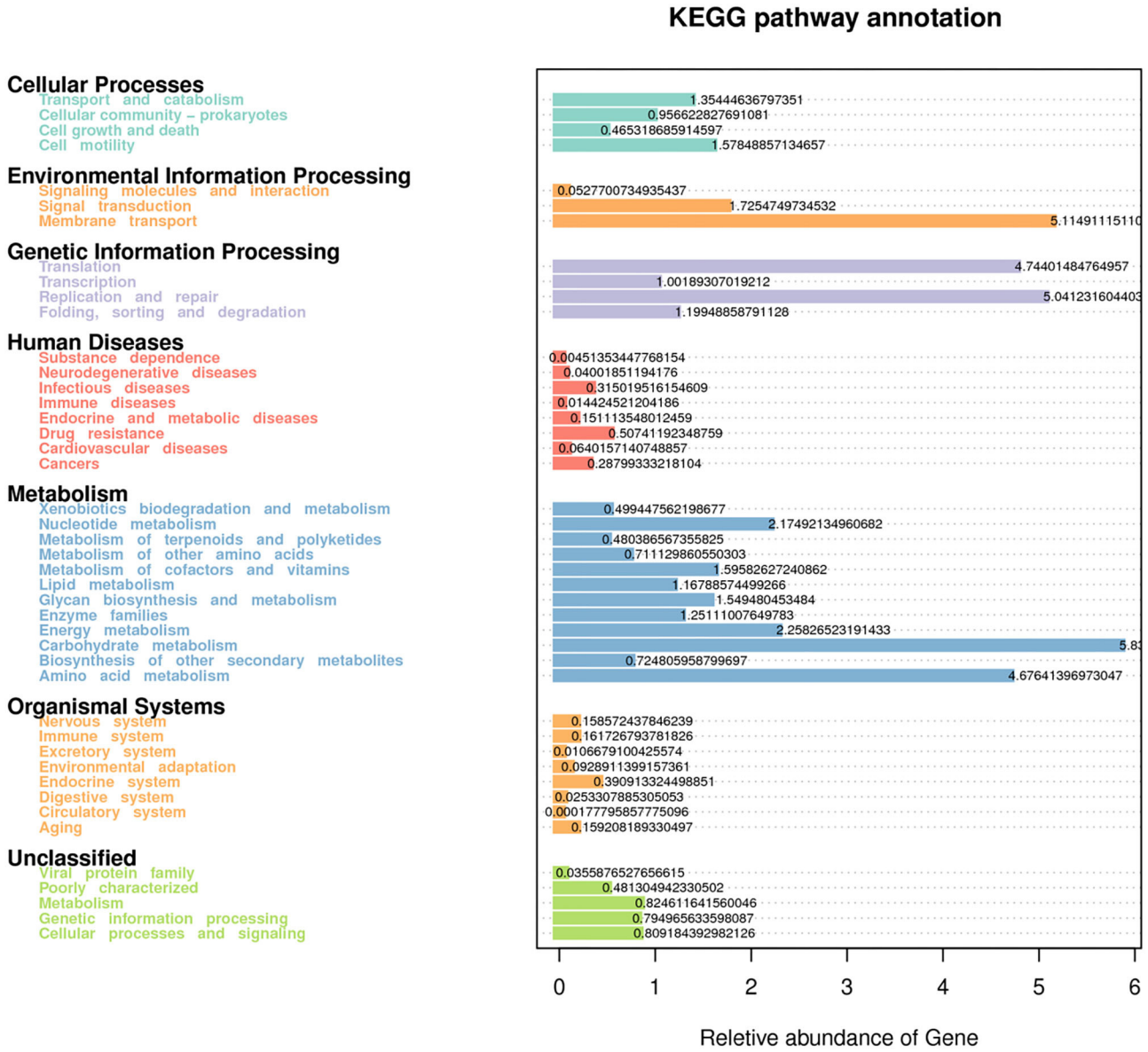

FIGURE 5 | Predictive functional analysis using Tax4Fun tool, showing relative abundance of assigned KEGG identity to the pathways of metabolisms at subsystem levels (KO_2).

level. On the basis of the aforementioned experimental results, we conclude that SeY supplementation affects the fermentation of feed, cellulose degradation, and protein metabolism in the rumen of Tibetan sheep and significantly improves when medium amounts of this nutrient are administered as a supplement. This conclusion is supported by the finding of our previous study on digestive and metabolic of Tibetan sheep by SeY supplementation (Wang et al., 2019). Proteobacteria play a crucial role in rumen metabolism, especially in the digestion of soluble carbohydrates, biofilm formation, and fermentation (Pitta et al., 2016). In addition, the abundance of an uncommon potentially pathogenic genus belonging to phylum Proteobacteria, Hafnia-*Obesumbacterium*, in the rumen of Tibetan sheep was found to differ significantly among all the four treatment groups ($P < 0.05$). Some species of Hafnia-*Obesumbacterium* have been detected in frog droppings (Tong et al., 2020), distal intestinal lumen of rainbow trout (Lyons et al., 2017), and human gut (Ramos-Vivas, 2020) but have been rarely reported in rumen fluids of sheep. The relationship between the ruminants and Hafnia-*Obesumbacterium* remains poorly understood and deserves further investigation.

In addition to variations in Tibetan sheep rumen microbiomes, VFA levels varied considerably in response to SeY among all the four treatment groups. Changes in rumen microflora affect VFA production, which eventually affects the efficiency of nutrient utilization (Hernandez-Sanabria

et al., 2012). Volatile fatty acid levels produced during rumen fermentation can be considered an important index of rumen fermentation, and the type of rumen fermentation affects the energy utilization rate and energy reserve site (Cone and Becker, 2012). Volatile fatty acids are largely absorbed across the host's ruminal epithelium, which play an essential role in ruminant immunity and growth (Fan et al., 2020). Acetate is the main precursor of milk fat synthesis in ruminants, whereas propionate is an important glucose precursor (Allen, 2014). Thus, propionate-type fermentation is more conducive to the fattening of livestock. In this study, significantly higher levels of propionate and TVFA were observed in the M group ($P < 0.01$). This increase in the propionate concentration resulted in an increase in the TVFA concentration and a decrease in the ratio of acetate to propionate. This result showed that supplementation of Tibetan sheep with a medium level of SeY might lead to more efficient transportation and absorption of VFAs than the CK group. Our previous digestive and metabolic experiments had also shown that a medium Se dose rate (0.4 mg/kg DM) improves nitrogen metabolism and nutrient digestibility, which are beneficial for the growth and development of young Tibetan sheep (Wang et al., 2019). Shi et al. (2011) reported that the addition of 3 g nano-Se/kg forage DM to the basic diet of sheep increases the TVFA concentration in their rumen. A study by Farzaliev (1981) reported that the addition of 0.1 mg Na_2SeO_3/kg BW to the high energy diet of young bulls increases VFA and propionate levels and reduces the acetate content. Isoacids (such as isobutyrate and isovalerate) are branched-chain VFAs produced by the oxidative deamination of branched-chain amino acids in the rumen, and the levels of branched-chain VFA correlate with the extent of protein fermentation (Hino and Russell, 1985). These iso-VFAs are required for the normal growth and activity of rumen cellulolytic bacteria (Wolin et al., 1997). In this study, we showed that a high SeY dose rate decreases the iso-VFA levels, suggesting that a high SeY dose inhibits the deamination activity and protein fermentation in the rumen of Tibetan sheep. Rumen bacteria can metabolize inorganic Se by allowing the binding of Se to their own protein. Inorganic Se has been shown to promote rumen bacterial reproduction *in vitro* (Kim et al., 1997). Organic Se used in this study also supports these conclusions. Dietary protein is the main source of rumen NH_3-N, and its concentration is affected by the degradation and absorption rates of rumen nitrogen, which reflect the rate of nitrogen use by the rumen microorganisms. The present study indicated that SeY supplementation affects the efficiency of conversion of dietary nitrogen into microbial nitrogen that improves significantly when medium doses of SeY are administered, which could be attributable to variations in rumen microflora in the Tibetan sheep with different levels of SeY. This result is supported the finding of our previous study on nitrogen metabolism of Tibetan sheep by SeY supplementation (Wang et al., 2019).

As expected, the prediction analysis of the bacterial community function showed differences among each treatment group. Rumen bacterial communities are capable of adapting to a vast range of ruminant diets, which clearly shows the significance of the rumen microbial ecosystem in providing ruminant nutritional needs. The Tax4Fun prediction tool helped in deriving metabolic pathways at the subsystem level, revealing the potential of SeY use for regulating the rumen microbial population structure and function in Tibetan sheep. Diet usually plays a major role in shaping the rumen microbial community structure. However, to achieve optimum results by dietary intervention, genetic differences among livestock should also be considered (Carmody et al., 2015). Functional prediction analysis revealed that the function of the rumen bacteria varies among the SeY-supplemented groups and the CK group. Our data of Tax4Fun gene function estimation indicate that the relative abundances of carbohydrate metabolism and metabolism of other amino acids were significantly impacted by Se; those genes involved in energy metabolism and carbohydrate were enhanced in supplementing Se in diets of Tibetan sheep. Because of the inherently low nutrients available in partial native pasture, a good production of livestock cannot be guaranteed. Therefore, long-term supplementation of medium levels of SeY is a wise choice for improving the productivity for livestock. Administration of medium levels of Se as a booster to Tibetan sheep grazing on the natural grassland can prevent nutritional deficiencies in these sheep. In addition, SeY may widely affect the interaction among rumen microorganisms, although the mechanism of these interactions remains unclear. Therefore, other scientific methods such as metagenomics analysis are required to further understand the physiological characteristics of the rumen microbes in this species. Notably, we identified a large number of unclassified genera with unknown functions. Our finding suggests that Tibetan sheep may have a highly diverse intestinal microbiome, and further in-depth studies are required to investigate the microbiome diversity.

CONCLUSION

The addition of SeY in the diet changed the rumen microflora of Tibetan sheep, which eventually affected the levels of VFAs in the rumen fluid. Abundant variations in the rumen bacteria indicated that the addition of SeY to the diet exerts a positive effect on the rumen microbial community and metabolic function of Tibetan sheep. SeY can be used as a trace element supplement for grazing Tibetan sheep in alpine meadows on the QTP to improve rumen fermentation and microbial community structure. However, considering the risk of Se toxicity, we suggest that the dietary Se level of 0.4 mg/kg DM is optimum. Significant or extremely significant differences in bacterial abundance were observed with variations in SeY doses among different diets administered to the sheep, indicating that these microbial communities might have a specific function in rumen metabolism; however, further studies are required to determine their exact role. Future studies may reveal the characteristics of the microbial composition and population structure in the rumen environment of Tibetan sheep.

DATA AVAILABILITY STATEMENT

The datasets presented in this study can be found in online repositories. The names of the repository/repositories and

accession number(s) can be found below: https://www.ncbi.nlm.nih.gov/, PRJNA627580.

ETHICS STATEMENT

The animal study was reviewed and approved by The Ethics and Animal Welfare Committee of Lanzhou University authorized all animal experimental procedures (file No: 2012-1 and 2012-2).

AUTHOR CONTRIBUTIONS

Conceptualization: FH; Original draft preparation: XC; Interpretation participant: HZ, HW, and TY; Study conception and funding: FH; Literature search: ZW, XC, and SC; Experimental work and data collection: XC, YT, and TG; Conception, development, and implementation of computational methods: XC and ZW. All authors contributed to the article and approved the submitted version.

FUNDING

This research was funded by the Second Tibetan Plateau Scientific Expedition and Research: Grassland Ecosystem and Ecological Animal Husbandry (2019QZKK0302), the Program for Strategic Priority Research Program of the Chinese Academy of Sciences (XDA20100102), the National Natural Science Foundation of China (No. 31672472 and No. 31201821), and Innovative Research Team of Ministry of Education (IRT_17R50).

SUPPLEMENTARY MATERIAL

The Supplementary Material for this article can be found online at: https://www.frontiersin.org/articles/10.3389/fmicb.2021.663945/full#supplementary-material

REFERENCES

Allen, M. S. (2014). Drives and limits to feed intake in ruminants. *Animal. Prod. Sci.* 54,1513–1524. doi: 10.1071/AN14478

Aßhauer, K. P., Wemheuer, B., Daniel, R., and Meinicke, P. (2015). Tax4Fun: predicting functional profiles from metagenomic 16S rRNA data. *Bioinformatics*. 31, 2882–2884. doi: 10.1093/bioinformatics/btv287

Bi, Y. L., Zeng, S. Q., Zhang, R., Diao, Q. Y., and Tu, Y. (2018). Effects of dietary energy levels on rumen bacterial community composition in Holstein heifers under the same forage to concentrate ratio condition. *BMC Microbiol*. 18:69. doi: 10.1186/s12866-018-1213-9

Białek, M., and Czauderna, M. (2019). Composition of rumen-surrounding fat and fatty acid profile in selected tissues of lambs fed diets supplemented with fish and rapeseed oils, carnosic acid, and different chemical forms of selenium. *Livest. Sci.* 226, 122–132. doi: 10.1016/j.livsci.2019.06.013

Biscarini, F., Palazzo, F., Castellani, F., Masetti, G., Grotta, L., Cichelli, A., et al. (2018). Rumen microbiome in dairy calves fed copper and grape-pomace dietary supplementations: composition and predicted functional profile. *PLoS ONE.* 13:e0205670. doi: 10.1371/journal.pone.0205670

Caporaso, J. G., Kuczynski, J., Stombaugh, J., Bittinger, K., Bushman, F. D., Costello, E. K., et al. (2010). QIIME allows analysis of high-throughput community sequencing data. *Nat. Methods* 7, 335–336. doi: 10.1038/nmeth.f.303

Carmody, R. N., Gerber, G. K., Luevano, J. M., Gatti, D. M., Somes, L., Svenson, K. L., et al. (2015). Diet dominates host genotype in shaping the murine gut microbiota. *Cell Host Microbe.* 17, 72–84. doi: 10.1016/j.chom.2014.11.010

Chen, J., Harstad, O. M., Mcallister, T., Drsch, P., and Holo, H. (2020). Propionic acid bacteria enhance ruminal feed degradation and reduce methane production *in vitro*. *Acta Agric. Scand. A Anim. Sci.* 69, 169–175. doi: 10.1080/09064702.2020.1737215

Chen, Y. B., Lan, D. L., Tang, C., Yang, X. N., and Li, J. (2015). Effect of DNA extraction methods on the apparent structure of yak rumen microbial communities as revealed by 16S rDNA sequencing. *Pol. J. Microbiol.* 64, 29–36.

Clemmons, B. A., Voy, B. H., and Myer, P. R. (2019). Altering the gut microbiome of cattle: considerations of host-microbiome interactions for persistent microbiome manipulation. *Microb. Ecol.* 77, 523–536. doi: 10.1007/s00248-018-1234-9

Cone, J. W., and Becker, P. M. (2012). Fermentation kinetics and production of volatile fatty acids and microbial protein by starchy feedstuffs. *Anim. Feed. Sci. Technol.* 172, 34–41. doi: 10.1016/j.anifeedsci.2011.12.006

Cui, X. X., Wang, Z. F., Yan, T. H., Chang, S. H., Wang, H., and Hou, F. J. (2019). Rumen bacterial diversity of Tibetan sheep (*Ovis aries*) associated with different forage types on the Qinghai-Tibetan Plateau. *Can. J. Microbiol.* 65, 859–869. doi: 10.1139/cjm-2019-0154

Dai, X., Tian, Y., Li, J., Luo, Y., Liu, D., Zheng, H., et al. (2015). Metatranscriptomic analyses of plant cell wall polysaccharide degradation by microorganisms in the cow rumen. *Appl. Environ. Microbiol.* 81, 1375–1386. doi: 10.1128/AEM.03682-14

Edgar, R. C. (2004). "MUSCLE: multiple sequence alignment with improved accuracy and speed," in *Computational Systems Bioinformatics Conference, CSB 2004* (Stanford, CA: IEEE), 16–19. doi: 10.1109/CSB.2004.120

Edgar, R. C. (2013). UPARSE: highly accurate OTU sequences from microbial amplicon reads. *Nat. Method.* 10, 996–998. doi: 10.1038/nmeth.2604

Edgar, R. C., Haas, B. J., Clemente, J. C., Quince, C., and Knight, R. (2011). UCHIME improves sensitivity and speed of chimera detection. *Bioinformatics* 27, 2194–2200. doi: 10.1093/bioinformatics/btr381

Fan, Q., Wanapat, M., Yan, T., and Hou, F. (2020). Altitude influences microbial diversity and herbage fermentation in the rumen of yaks. *BMC Microbiol.* 20:370. doi: 10.1186/s12866-020-02054-5

Farzaliev, V. J. Z. (1981). Rumen fermentation in young animals affected by fat and selenium [bulls, buffalo calves]. *Zhivotnovodstv*. Moscow.

Faulkner, M. J., Wenner, B. A., Solden, L. M., and Weiss, W. P. (2017). Source of supplemental dietary copper, zinc, and manganese affects fecal microbial relative abundance in lactating dairy cows. *J. Dairy Sci.* 100, 1037–1044. doi: 10.3168/jds.2016-11680

Godon, J. J., Morinière, J., Moletta, M., Gaillac, M., Bru, V., and Delgènes, J. P. (2005). Rarity associated with specific ecological niches in the bacterial world: the 'Synergistes' example. *Environ. Microbiol.* 7, 213–224. doi: 10.1111/j.1462-2920.2004.00693.x

Goodrich, J. K., Di Rienzi, S. C., Poole, A. C., Koren, O., Walters, W. A., Caporaso, J. G., et al. (2014). Conducting a microbiome study. *Cell.* 158, 250–262. doi: 10.1016/j.cell.2014.06.037

Guo, W., Wang, W. W., Bi, S. S., Long, R. J., Ullah, F., Shafiq, M., et al. (2020). Characterization of anaerobic rumen fungal community composition in yak, Tibetan sheep and small tail han sheep grazing on the Qinghai-Tibetan Plateau. *Animals* 10:144. doi: 10.3390/ani10010144

Han, X. P., Liu, H. J., Hu, L. Y., Ma, L., Xu, S. X., and Zhao, N., et al. (2020). Impact of sex and age on the bacterial composition in rumen of Tibetan sheep in Qinghai China. *Livest. Sci.* 238:104030. doi: 10.1016/j.livsci.2020.104030

Hernandez-Sanabria, E., Goonewardene, L. A., Wang, Z., Durunna, O. N., Moore, S. S., and Guan, L. L. (2012). Impact of feed efficiency and diet on adaptive variations in the bacterial community in the rumen fluid of cattle. *Appl. Environ. Microb.* 78, 1203–1214. doi: 10.1128/AEM.05114-119

Hino, T., and Russell, J. B. (1985). Effect of reducing-equivalent disposal and NADH/NAD on deamination of amino acids by intact rumen

microorganisms and their cell extracts. *Appl. Environ. Microbiol.* 50:1368. doi: 10.1016/0141-4607(85)90029-0

Huang, J. Q., Li, Y. J., and Luo, Y. Z. (2017). Bacterial community in the rumen of Tibetan sheep and Gansu alpine fine-wool sheep grazing on the Qinghai-Tibetan Plateau, China. *J. Gen. Appl. Microbiol.* 63, 122–130. doi: 10.2323/jgam.2016.08.003

Hugenholtz, P., Hooper, S. D., and Kyrpides, N. C. (2010). Focus: synergistetes. *Environ. Microbiol.* 11, 1327–1329. doi: 10.1111/j.1462-2920.2009.01949.x

Ishaq, S. L., Page, C. M., Yeoman, C. J., Murphy, T. W., Emon, M. L. V., and Stewart, W. C. (2019). Zinc AA supplementation alters yearling ram rumen bacterial communities but zinc sulfate supplementation does not. *J. Anim. Sci.* 97, 687–697. doi: 10.1093/jas/sky456

Jami, E., Israel, A., Kotser, A., and Mizrahi, I. (2013). Exploring the bovine rumen bacterial community from birth to adulthood. *ISME J.* 7, 1069–1079. doi: 10.1038/ismej.2013.2

Jami, E., and Mizrahi, I. (2012). Composition and similarity of bovine rumen microbiota across individual animals. *PLoS ONE* 7:e33306. doi: 10.1371/journal.pone.0033306

Jewell, K. A., McCormick, C. A., Odt, C. L., Weimer, P. J., and Suen, G. (2015). Ruminal bacterial community composition in dairy cows is dynamic over the course of two lactations and correlates with feed efficiency. *Appl. Environ. Microbiol.* 81, 4697–4710. doi: 10.1128/AEM.00720-15

Kim, D. H., and Austin, B. (2006). Cytokine expression in leucocytes and gut cells of rainbow trout, *Oncorhynchus mykiss* Walbaum, induced by probiotics. *Vet. Immunol. Immunopathol.* 114, 297–304. doi: 10.1016/j.vetimm.2006.08.015

Kim, J., Soest, P. J. V., and Combs, G. F. (1997). Studies on the effects of selenium on rumen microbial fermentation *in vitro*. *Biol. Trace. Elem. Res.* 56:2032213. doi: 10.1007/BF02785393

Kišidayová, S., Mihaliková, K., Siroka, P., Cobanová, K., and Váradyová, Z. (2014). Effects of inorganic and organic selenium on the fatty acid composition of rumen contents ofsheep and the rumen bacteria and ciliated protozoa. *Anim. Feed Sci. Technol.* 193, 51–57. doi: 10.4028/www.scientific.net/KEM.493-494.231

Leisner, J. J., Laursen, B. G., Prévost, H., Drider, D., and Dalgaard, P. (2007). Carnobacterium: positive and negative effects in the environment and in foods. *FEMS Microbiol. Rev.* 31, 592–613. doi: 10.1111/j.1574-6976.2007.00080.x

Louis, P., and Flint, H. J. (2009). Diversity, metabolism and microbial ecology of butyrate-producing bacteria from the human large intestine. *FEMS Microbiol. Lett.* 294, 1–8. doi: 10.1111/j.1574-6968.2009.01514.x

Lyons, P. P., Turnbull, J. F., Dawson, K. A., and Crumlish, M. (2017). Phylogenetic and functional characterization of the distal intestinal microbiome of rainbow trout *Oncorhynchus mykiss* from both farm and aquarium settings. *J. Appl. Microbiol.* 122, 347–363. doi: 10.1111/jam.13347

Martin, M. (2011). Cutadapt removes adapter sequences from high-throughput sequencing reads. *Embnet. J.* 17:1. doi: 10.14806/ej.17.1.200

McCann, J. C., Luan, S., Cardoso, F. C., Derakhshani, H., Khafipour, E., and Loor, J. J. (2016). Induction of Subacute ruminal acidosis affects the ruminal microbiome and epithelium. *front. microbiol.* 7:701. doi: 10.3389/fmicb.2016.00701

Meehan, C. J., and Beiko, R. G. (2014). a phylogenomic view of ecological specialization in the Lachnospiraceae, a family of digestive tract-associated Bacteria. *Genome Biol. Evol.* 6, 703–713. doi: 10.1093/gbe/evu050

Mihaliková, K., Grešáková, L., BoldiŽárová, K., Faix, Š., Leng, L., and Kišidayová, S. (2005). The effects of organic selenium supplementation on the rumen ciliate population in sheep. *Folia Microbiol.* 50, 353–356. doi: 10.1007/BF02931418

Miller, M. E. B., Yeoman, C. J., Chia, N., Tringe, S. G., Angly, F. E., Edwards, R. A., et al. (2012). Phage–bacteria relationships and crispr elements revealed by a metagenomic survey of the rumen microbiome. *Environ. Microbiol.* 14, 207–227. doi: 10.1111/j.1462-2920.2011.02593.x

Miltko, R., Rozbicka-Wieczorek, J. A., Wiesyk, E., and Czauderna, M. (2016). The influence of different chemical forms of selenium added to the diet including carnosic acid, fish oil and rapeseed oil on the formation of volatile fatty acids and methane in the rumen, and fatty acid profiles in the rumen content and muscles of lambs. *Acta. Vet. Beograd.* 66, 373–391. doi: 10.1515/acve-2016-0032

Morsy, A. S., El-zaiat, H. M., Saber, A. M., Anwer, M. M., and Sallam, S. M. (2019). Impact of organic selenium and vitamin E on rumen fermentation, milk production, feed digestibility, blood parameters and parasitic response of lactating goats. *J. Agric. Sci. Technol.* 21, 1793–1806.

Nava, G. M., and Stappenbeck, T. S. (2011). Diversity of the autochthonous colonic microbiota. *Gut Microbes.* 2, 99–104. doi: 10.4161/gmic.2.2.15416

Naziroglu, M., Aksakal, M., Cay, M., and Celik, S. (1997). Effects of vitamin E and selenium on some rumen parameters in lambs. *Acta Vet. Hung.* 45, 447–456. doi: 10.1016/S0093-691X(97)00016-2

Pereira, A. M., Pinna, C., Biagi, G., Stefanelli, C., Maia, M. R. G., Matos, E., et al. (2020). Supplemental selenium source on gut health: insights on fecal microbiome and fermentation products of growing puppies. *FEMS. Microbiol. Ecol.* 96:fiaa212. doi: 10.1093/femsec/fiaa212

Pino, F., and Heinrichs, A. J. (2016). Effect of trace minerals and starch on digestibility and rumen fermentation in diets for dairy heifers. *J. Dairy Sci.* 99, 2797–2810. doi: 10.3168/jds.2015-10034

Pitta, D. W., Pinchak, W. E., Indugu, N., Vecchiarelli, B., Sinha, R., and Fulford, J. D. (2016). Metagenomic analysis of the rumen microbiome of steers with wheat-induced frothy bloat. *Front. Microbiol.* 7:689. doi: 10.3389/fmicb.2016.00689

Puniya, A. K., Singh, R., and Kamra, D. N. (2015). *Rumen Microbiology: From Evolution to Revolution*. New Delhi: Springer, India. doi: 10.1007/978-81-322-2401-3

Quast, C., Pruesse, E., Yilmaz, P., Gerken, J., Schweer, T., Yarza, P., et al. (2012). The SILVA ribosomal RNA gene database project: improved data processing and web-based tools. *Nucleic. Acids. Res.* 41, D590–D596. doi: 10.1093/nar/gks1219

Ramos-Vivas, J. (2020). Microbiology of Hafnia alvei. *Enferm. Infecc. Microbiol. Clin.* 1, 1–6. doi: 10.1016/j.eimc.2020.02.001

Rubino, F., Carberry, C., M., Waters, S., Kenny, D., McCabe, M. S., et al. (2017). Divergent functional isoforms drive niche specialisation for nutrient acquisition and use in rumen microbiome. *ISME. J.* 11, 932–944. doi: 10.1038/ismej.2016.172

Sagheddu, V., Patrone, V., Miragoli, F., Puglisi, E., and Morelli, L. (2016). Infant early gut colonization by lachnospiraceae: high frequency of *Ruminococcus gnavus*. *Front. Pediatr.* 4:57. doi: 10.3389/fped.2016.00057

Schnorr, S. L., Candela, M., Rampelli, S., Centanni, M., Consolandi, C., Basaglia, G., et al. (2014). Gut microbiome of the Hadza hunter-gatherers. *Nat. Commun.* 5:3654. doi: 10.1038/ncomms4654

Schrauzer, G. N., and Surai, P. F. (2009). Selenium in human and animal nutrition: Resolved and unresolved issues. A partly historical treatise in commemoration of the fiftieth anniversary of the discovery of the biological essentiality of selenium, dedicated to the memory of Klaus Schwarz (1914–1978) on the occasion of the thirtieth anniversary of his death. *Crit. Rev. Biotechnol.* 29, 2–9. doi: 10.1080/07388550902728261

Shi, L., Xun, W., Yue, W., Zhang, C., Ren, Y., Liu, Q., et al. (2011). Effect of elemental nano-selenium on feed digestibility, rumen fermentation, and purine derivatives in sheep. *Anim. Feed. Sci. Technol.* 163, 136–142. doi: 10.1016/j.anifeedsci.2010.10.016

Standing Committee on Agriculture, SCA (1990). *Feeding Standards for Australian Livestock. Ruminants*. Melbourne, Australia, CSIRO Publishing.

Surai, P. F., and Fisinin, V. I. (2014). Selenium in poultry breeder nutrition: an update. *Anim. Feed. Sci. Technol.* 191, 1–15. doi: 10.1016/j.anifeedsci.2014.02.005

Tashi, N., Luo, X., Yu, S., and Judson, G. (2005). A *Survey of the Mineral Status of Livestock in the Tibet Autonomous Region of China*. Working Papers 118371, Australian Centre for International Agricultural Research.

Thompson, L. G., Yao, T., Mosley-Thompson, E., Davis, M. E., Henderson, K. A., and Lin, P. N. (2000). A high-resolution millennial record of the South Asian monsoon from himalayan ice cores. *Science* 289:1916. doi: 10.1126/science.289.5486.1916

Tong, Q., Cui, L. Y., Du, X. P., Hu, Z. F., Bie, J., Xiao, J. H., et al. (2020). Comparison of gut microbiota diversity and predicted functions between healthy and diseased *Rana dybowskii*. *Front. Microbiol.* 11:2096. doi: 10.3389/fmicb.2020.02096

Walker, N. D., McEwan, N. R., and Wallace, R. J. (2003). Cloning and functional expression of dipeptidyl peptidase IV from the ruminal bacterium prevotella albensis m384t. *Microbiology* 149, 2227–2234. doi: 10.1099/mic.0.26119-0

Wang, Z. F., Tan, Y. H., Cui, X. X., Chang, S. H., Xiao, X., Yan, T. H., et al. (2019). Effect of different levels of selenium yeast on the antioxidant status, nutrient digestibility, selenium balances and nitrogen metabolism of Tibetan

sheep in the Qinghai-Tibetan Plateau. *Small. Ruminant. Res.* 180, 63–69. doi: 10.1016/j.smallrumres.2019.10.001

Wolin, M. J., Miller, T. L., and Stewart, C. S. (1997). "Microbe–microbe interactions," in *The Rumen Microbial Ecosystem,* eds P. N. Hobson and C. S. Stewart (London: Blackie Academic and Professional Press), 467–491.

Wu, G. D., Chen, J., Hoffmann, C., Bittinger, K., Chen, Y. Y., and Keilbaugh, S. A. (2011). Linking long-term dietary patterns with gut microbial enterotypes. *Science* 334, 105–108. doi: 10.1126/science.1208344

Xia, Y., Hill, K. E., Byrne, D. W., Xu, J., and Burk, R. F. (2005). Effectiveness of selenium supplements in a low-selenium area of China. *Am. J. Clin. Nutr.* 81, 829–834. doi: 10.1093/ajcn/81.4.829

Xiong, X., Lan, D., Li, J., Lin, Y., and Li, M. (2018). Selenium supplementation during *in vitro* maturation enhances meiosis and developmental capacity of yak oocytes. *Anim. Sci.* 89, 298–306. doi: 10.1111/asj.12894

Xue, M. Y., Sun, H. Z., Wu, X. H., Liu, J. X., and Guan, L. L. (2020). Multi-omics reveals that the rumen microbiome and its metabolome together with the host metabolome contribute to individualized dairy cow performance. *Microbiome.* 8:64. doi: 10.1186/s40168-020-00819-8

Yáñez-Ruiz, D. R., Abecia, L., and Newbold, C. J. (2015). Manipulating rumen microbiome and fermentation through interventions during early life: a review. *Front. Microbiol.* 6:1133. doi: 10.3389/fmicb.2015.01133

Zhang, T. T., Zhao, G. Y., Zheng, W. S., Niu, W. J., and Lin, S. X. (2015). Effects of rare earth element lanthanum on rumen methane and volatile fatty acid production and microbial flora *in vitro*. *J. Anim. Physiol. Anim. Nutr.* 99, 442–448. doi: 10.1111/jpn.12251

Zhao, Y., Zhao, E., Zhang, N., and Duan, C. (2011). Mitochondrial DNA diversity, origin, and phylogenic relationships of three Chinese large-fat-tailed sheep breeds. *Trop. Anim. Health. Prod.* 43:1405. doi: 10.1007/s11250-011-9869-2

Zhou, J. W., Guo, X. S., Degen, A. A., Zhang, Y., Liu, H., Mi, J. D., et al. (2015). Urea kinetics and nitrogen balance and requirements for maintenance in Tibetan sheep when fed oat hay. *Small. Ruminant. Res.* 129, 60–68. doi: 10.1016/j.smallrumres.2015.05.009

Conflict of Interest: The authors declare that the research was conducted in the absence of any commercial or financial relationships that could be construed as a potential conflict of interest.

frontiers in Microbiology

ORIGINAL RESEARCH
published: 08 July 2021
doi: 10.3389/fmicb.2021.696588

A High Starch Diet Alters the Composition of the Intestinal Microbiota of Largemouth Bass *Micropterus salmoides*, Which May Be Associated With the Development of Enteritis

Xiaoli Huang[1†], Liang Zhong[1†], Qin Kang[1†], Sha Liu[1], Yang Feng[2], Yi Geng[2], Defang Chen[1], Yangping Ou[2], Shiyong Yang[1], Lizi Yin[2] and Wei Luo[1]*

[1] Department of Aquaculture, College of Animal Science & Technology, Sichuan Agricultural University, Chengdu, China, [2] Department of Basic Veterinary, College of Veterinary Medicine, Sichuan Agricultural University, Chengdu, China

OPEN ACCESS

Edited by:
Yvonne Vallès, The University of the West Indies, Cave Hill, Barbados

Reviewed by:
Darrell W. Cockburn, Pennsylvania State University (PSU), United States
Satya P. Singh, Saurashtra University, India

***Correspondence:**
Defang Chen
chendf_sicau@126.com

† These authors have contributed equally to this work and share first authorship

Specialty section:
This article was submitted to Microbial Symbioses, a section of the journal Frontiers in Microbiology

Received: *17 April 2021*
Accepted: *11 June 2021*
Published: *08 July 2021*

Citation:
Huang X, Zhong L, Kang Q, Liu S, Feng Y, Geng Y, Chen D, Ou Y, Yang S, Yin L and Luo W (2021) A High Starch Diet Alters the Composition of the Intestinal Microbiota of Largemouth Bass Micropterus salmoides, Which May Be Associated With the Development of Enteritis. Front. Microbiol. 12:696588. doi: 10.3389/fmicb.2021.696588

Starch is an inexpensive feed ingredient that has been widely used in fish feed. However, starch utilization by carnivorous fish is limited and excess starch is detrimental to the health of the organism. High starch diets often lead to liver damage, but the effects on the intestine are often overlooked. Therefore, in this study, two isonitrogenous and isolipidic semi-pure diets (NC: 0% α-starch, HC: 22% α-starch) were formulated and fed to largemouth bass (*Micropterus salmoides)* for 45 days. The effects of the high starch diet on the intestine of largemouth bass were comprehensively investigated by intestinal microbiota, histopathology, ultrastructural pathology, and enzymology analyses. Feeding the HC diet did not affect the growth of largemouth bass during the experimental period. However, the high starch diet led to a reduction in the diversity and abundance of intestinal microbiota in largemouth bass, with a significant increase in the abundance of harmful bacteria (*Aeromonas*) and a decrease in the abundance of beneficial bacteria (*Clostridium*, *Lactobacillus,* and *Bifidobacterium*). Feeding the HC diet caused the development of enteritis, with goblet cell hyperplasia, epithelial necrosis and detachment and inflammatory cell infiltration, and leading to enlarged apical openings and mitochondrial damage in goblet cells. Long-term feeding of the HC diet inhibited intestinal α-amylase activity. changes in the intestinal microbiota, such as an increase in *Aeromonas* and a decrease in *Clostridium*, *Lactobacillus*, and *Bifidobacterium*, may be closely related to the development of enteritis. Therefore, adding these beneficial bacteria as probiotics may be an effective way to prevent damage to the intestine of largemouth bass from a high carbohydrate diet. Our results suggest reducing the amount of starch added to the largemouth bass diets. This study provides a reference for protecting the largemouth bass gut during modern intensive culture.

Keywords: high starch diet, intestinal microbiota, enteritis, intestinal diseases, *Micropterus salmoides*

INTRODUCTION

Starch is a carbohydrate and is a source of nutrition for most animals. Due to its low cost, starch is widely used in various fish feeds. It has been reported that adding the appropriate amount of starch to the diet stimulates protein-sparing action (Li et al., 2020), improves feed adhesion and facilitates feed production (Zhang et al., 2020c), reduces environmental pollution (Asaduzzaman et al., 2010), and improves fish growth performance (Zhou et al., 2015). However, fish live in water where it is almost impossible to ingest plant starch; therefore, fish have very limited digestion, absorption, and metabolism of starch, particularly carnivorous fish (Stone, 2003). Previous studies have reported that long-term consumption of high starch feed by carnivorous fish leads to the accumulation of glycogen and fat in the liver (Zhang Y.M. et al., 2020) and to hyperglycemia (Kamalam et al., 2017), which can seriously affect the growth of farmed fish and even lead to death.

The intestines are one of the most important organs of aquatic animals, and they play an important role in a variety of physiological functions such as digestion and absorption of nutrients, and endocrine and immune activities (Banić et al., 2018). A large number of intestinal microbiota inhabit the intestines of animals, which affects health and nutrition in a variety of ways, such as enhancing metabolic capacity of the host, protecting the host from pathogens, and regulating gastrointestinal development (Bäckhed et al., 2005). A balanced intestinal microbiota is a prerequisite for normal physiological functioning. However, the intestinal microbiota is susceptible to changes in the external environment, of which the composition of the diet is one of the most important factors (Salonen and de Vos, 2014). The abundance and diversity of intestinal microbiota decreased significantly in the rice field eel (*Monopterus albus*) fed a high-fat diet (Peng et al., 2019). Falcinelli et al. (2017) reported that zebrafish intestinal microbiota is altered when the fish are fed a high-fat diet. Similar to a high-fat diet, high starch intake leads to disturbances in the intestinal microbiota of juvenile golden pompano (*Trachinotus ovatus*) and increases the abundance of harmful bacteria (Zhao et al., 2020). Therefore, a balanced intestinal microbiota is essential for the body, and when this balance is disturbed, it can lead to a variety of intestinal diseases, such as inflammatory bowel disease (IBD; Manichanh et al., 2012) or Cohn's disease (Li et al., 2012) in mammals, and enteritis in grass carp (*Ctenopharyngodon idellus*) (Tuan et al., 2018) and sturgeon (Huang et al., 2020).

The largemouth bass (*Micropterus salmoides*) is a typical carnivore that is widely farmed around the world as a commercially valuable fish, with an annual production of more than 470,000 tons in China (Fisheries and Fisheries Administration, 2020). However, largemouth bass do not use starch efficiently, and excessive starch intake damages normal organ structure and function. Adding 25% carbohydrate to the diet results in a significant decrease in survival and a significant increase in blood glucose levels and liver vacuolation in largemouth bass (Amoah et al., 2008). It has also been reported that adding 20% starch restricts growth, and enhances oxidative damage in the liver and the accumulation of liver glycogen in largemouth bass (Lin et al., 2018). Zhang et al. (2020b) reported that adding only 15% starch results in significant whitening of the liver, a significant increase in hepatic vacuolization, and disturbances in hepatic glucose metabolism. However, the effects of high starch on the intestine are often overlooked. Therefore, this study aimed to systematically investigate the effects of starch intake on the intestine of largemouth bass. The results of this study are intended to provide a reference for protecting the intestines of cultured largemouth bass.

MATERIALS AND METHODS

Experimental Diets

Two isonitrogenous (49% crude protein) and isolipidic (9% crude lipid) semi-purified diets were formulated to contain different levels of α-starch, such as the NC (0% α-cassava starch) and HC (22% α-cassava starch) diets, respectively (**Table 1**). Fish meal, casein, and soybean protein concentrate were used as the protein sources, and soybean oil and soybean lecithin were used as the lipid sources. All dry ingredients were crushed and sifted through 280 μm mesh, weighed according to the ratio and mixed manually for 10 min. The mixed ingredients were transferred to a pelletizer and processed into 2 mm diameter pellets. All diets were air-dried at room temperature (23–30°C) and stored at −20°C until use.

Feeding Trial and Experimental Conditions

Eighty healthy juvenile largemouth bass (initial length 9.23 ± 0.46 cm, initial weight 7.20 ± 1.15 g) were obtained from a commercial farm in Chengdu, Sichuan, China. The fish were acclimated and fed the NC diet for 2 weeks in plastic tanks. At the start of the experiment, the fish were fasted for 24 h and grouped after anesthesia with MS-222. The 80 fish were randomly distributed into two groups, containing a control group (fed the NC, 0% starch) and the experimental group (fed the HC, 22% starch). The dietary treatments were randomly assigned to three replicates. The daily diet was fed at 8% of body weight, the amount of which was divided into two parts on average and fed daily at 9:00 and 18:00 for 45 days. The daily amount of the diet offered to the fish was adjusted every 15 days by weighing the total weight of the fish in each tank.

During the experiment, the water was changed twice daily with advanced aeration. Water temperature was 24.9 ± 1.0°C, dissolved oxygen was >6 mg L^{-1}, pH was 7–8, and ammonia-nitrogen was almost zero. The photoperiod was 12L:12D, with lights on from 8:00 to 20:00. Fish mortality was observed and recorded every day.

All animal handling procedures were approved by the Animal Care and Use Committee of Sichuan Agricultural University, following the guidelines for animal experiments of Sichuan Agricultural University, under permit number DY-2019202033.

Chemical Analysis

The chemical composition analyses of the diets were conducted by standard methods (AOAC, 2005). Crude protein was

TABLE 1 | Formulation and proximate chemical composition of the trial diets.

Ingredients	Starch level in diets (g.kg^{-1})	
	NC	HC
Fish meal[a]	490	490
Casein[a]	130	130
Soybean protein concentrate[a]	60	60
Soybean oil[a]	30	30
Soybean lecithin[a]	20	20
Yeast extract[a]	8	8
$Ca(H_2PO_4)_2$[a]	10	10
Choline chloride[a]	3	3
Vitamin mixture[b]	8	8
Mineral mixture[c]	5	5
Carboxymethyl cellulose[a]	15	15
Lysine[a]	1	1
α-Cassava starch[a]	220	0
Zeolite powder[a]	0	220
Proximate compositions (g. kg^{-1}, dry matter)		
Crude protein	490	491
Crude lipid	82	91
Ash	301	103
Starch	13	224

[a]*Supplied by Chengdu Sanwang Feed Ltd (Chengdu, China).*
[b]*Vitamin Premix (mg kg^{-1} diet): vitamin A, 32.00; vitamin D3, 16.00; vitamin E, 351.83; vitamin K3, 30.03; vitamin C, 3288.80; vitamin B1, 19.77; vitamin B2, 60.00; vitamin B6, 36.43; vitamin B12, 24.00; niacinamide, 80.80; calcium pantothenate, 75.10; folic acid, 6.73; inositol, 329.90; biotin, 32.00;* L*-carnitine, 102.03.*
[c]*Mineral mix (mg kg^{-1} diet): $FeSO_4$ (Fe), 70.33; $MgSO_4$ (Mg), 351.33; $CuSO_4$ (Cu), 8.00; $ZnSO_4$ (Zn), 99.70; $MnSO_4$ (Mn), 19.50; $CoCl_2$ (Co), 19.37; Ca $(IO_3)_2$ (I), 50.17; Na_2SeO_3 (Se), 4.00.*

determined using the Kjeldahl method (N × 6.25) (Kjeltec 2,300, FOSS, Hilleroed, Denmark). Crude lipid was determined by petroleum ether extraction (without acid hydrolysis) using Soxtec (Soxtec 2,055, FOSS, Denmark). Ash was determined by combusting at 550°C to constant weight in a muffle furnace (Shenyang Energy-saving Electric Furnace Factory, Shenyang, China). Starch content was analyzed by spectrophotometry (spectropolarimeter CP225D, Sartorius, Goettingen, Germany). Intestinal trypsin, α-amylase, lipase, and total protein were assayed using commercial kits (Nanjing Jiancheng Bioengineering Institute, Nanjing, China).

Sample Collection

The fish were sampled 30 and 45 days after the feeding trial began. All fish were anesthetized with MS-222 before sampling and were weighed and measured for body length and intestinal length. The intestinal length was measured from the stomach-intestine junction to the posterior end of the intestine. Five fish were used for histopathological and ultrastructural pathological observations and ten fish were used to determine intestinal digestive enzyme activity during each of the two sampling periods. However, an additional nine fish were sampled at 45 days for high-throughput sequencing of the intestinal microbiota 16s rRNA of sequences.

Histopathological Examination

The five fish sampled after 30 and 45 days were fixed in 10% neutral buffered formalin. After 2 days of fixation, the fish were trimmed into cassettes, dehydrated through graded ethanol solutions, cleared in xylene, and embedded in paraffin wax. Sections of 4 μm were prepared and mounted on slides for hematoxylin and eosin (H&E) and Alcian blue-periodic acid Schiff (AB-PAS) staining, respectively. The slides were examined under an optical microscope after staining. The number of goblet cells was measured in 6–8 well-oriented villi.

The degree of intestinal cell hyperplasia, necrosis and detachment of epithelial cells, inflammatory cell infiltration, and necrosis of the lamina propria was scored with reference to the modified grade scoring system established by Baums et al. (2013). Histological changes were assessed using a score ranging from 1 to 7, depending on the extent of the lesion: (1) unchanged; (3) mild; (5) moderate; and (7) severe.

Electron Microscopy

Fresh intestinal tissue was placed in fixative (2.5% glutaraldehyde in pH 7.4 cacodylate buffer). The intestinal tissues were washed three times in PBS and post-fixed in 1% osmium tetroxide. The samples were dehydrated through ascending concentrations of alcohol and post-embedded in Araldite. Cross-oriented ultra-thin sections were cut and stained with uranyl acetate and lead citrate. Images were acquired on a HITACHI HT7700 transmission electron microscope (Tokyo, Japan).

High-Throughput Sequencing of the Intestinal Microbiota 16s rRNA

Collection of Intestinal Contents

At the end of the trial, the intestinal contents of nine largemouth bass from each treatment were sampled. The ventral surface of the fish was opened to expose the peritoneal cavity under sterile conditions. Thereafter, the entire intestine was excised, and rinsed several times in 0.65% sterile saline. The intestinal contents were collected in a sterile Eppendorf tube. The samples were kept on ice for less than 2 h and then stored at −80°C, pending analysis.

DNA Extraction and Purification

Genomic DNA was extracted from the intestinal contents using a bacterial DNA isolation kit (Foregene Company, Limited, China), according to the manufacturer's instructions. After extraction, the genomic DNA was detected by 1% agarose gel electrophoresis. Samples were used for polymerase chain reaction (PCR) amplification with the forward primer (338F: 5′- ACTCCTACGGGAGGCAGCAG-3′) and the reverse primer (806R: 5′- GGACTACHVGGGTWTCTAAT-3′). The PCR product was detected by 2% agarose gel electrophoresis and purified with the AxyPrep DNA Gel Extraction Kit (Axygen, Corning, NY, United States), quantified using the QuantiFluorTM-ST Blue Fluorescence

System (Promega, Beijing, China), and subjected to next-generation sequencing.

Sequencing, Processing and Analysis

Sequencing of the 16S rDNA was performed on an Illumina Miseq PE300 platform (Illumina, San Diego, CA, United States) by Meiji Bioinformatics Technology Company, Limited (Shanghai, China). The library was constructed for the V3–V4 amplicons, and paired-end (PE) sequencing was performed on the MiSeq system. The sequencing data were uploaded to the Sequence Read Archive at the National Center for Biotechnology Information (Accession number PRJNA730220). Based on the overlapping relationship between PE reads, pairs of reads were merged into a sequence using Flash software. Raw fastq files were demultiplexed, quality-filtered with the following criteria: (i) the 300 bp reads were truncated at any site receiving an average quality score <20 in a 50 bp sliding window, discarding the truncated reads <50 bp, (ii) splicing pairs of reads into a sequence based on the overlapping relationship between PE reads, assembling only sequences with an overlap of more than 10 bp, (iii) the maximum mismatch ratio allowed in the overlap region of a spliced sequence was 0.2, after removing non-conforming sequences, and (iv) exact barcode matching and two nucleotide mismatches in primer matching were removed (Zhou et al., 2016). The remaining sequences were clustered into operational taxonomic units (OTUs) with a similarity cutoff of 97%, and the OTU taxonomic analysis was performed using the Usearch pipeline[1] (Zhang Y.M. et al., 2020). Each OTU was compared with the 16s rRNA database (Silva), using a BLAST analysis to obtain species classification information. A species composition analysis was conducted using Circos software. Species with a relative abundance rate of <0.01 in all samples were classified as "others." The Shannon and Simpson indexes were used to assess community diversity, and the Ace and Chao indexes were used to assess community richness. The Venn diagram was prepared and the alpha diversity analysis was performed with Mothur[2] (Zhang et al., 2020c). An effect size analysis (LEfSe) was performed to characterize the microbial differences between the two groups, such as a linear discriminant analysis (LDA). The non-parametric factorial Kruskal–Wallis rank-sum test was used to detect significant differences between assigned taxa, and the LDA was used to quantify the effect size of each feature with an alpha value of <0.05 (Zhang et al., 2020c).

Statistical Analysis

All data are expressed as mean ± standard deviation. The experimental data were first tested for homogeneity of variance, using one-way analysis of variance. Non-normal data were subjected to the non-parametric Games-Howell test. Statistical analyses were performed using IBM SPSS 20.0 software (IBM Corp., Armonk, NY, United States), and a P-value < 0.05 was considered significant.

[1]http://drive5.com/uparse/

[2]https://www.mothur.org/wiki/Download_mothur

RESULTS

The Effects of High Dietary Starch on Growth Performance of Largemouth Bass

The growth performance of largemouth bass during the experiment is shown in **Figure 1**. The results showed no significant differences in weight, body length, or intestinal length between the two treatment groups after 30 and 45 days, respectively, but these indicators were significantly higher on day 45 than on day 30 ($P < 0.001$) (**Figures 1A–C**). Interestingly, the intestinal body ratio of fish fed the NC diet was significantly higher on day 30 than that of fish fed the HC ($P < 0.05$), but an opposite trend was detected at 45 days (**Figure 1D**).

High Starch Feed Alters the Intestinal Microbiota Composition of Largemouth Bass

The effect of a high starch diet on the intestinal microbiota of largemouth bass was examined by 16S high-throughput sequencing. A total of 279,431 high-quality valid sequences were obtained with an average sequence length of 417 bp (**Supplementary Table 1**). In total, 650 OTUs were identified in the two groups of six samples, with 97% similarity. These OTUs belonged to 425 genera, 251 families, 159 orders, 65 classes, and 29 phyla. The rarefaction curve of all samples was flat (**Supplementary Figure 1**), indicating that all samples were sequenced.

The results of the alpha diversity analysis showed that fish fed the NC diet had higher diversity and richness values of the intestinal microbiota than the fish fed the HC diet (**Supplementary Table 2**). A total of 194 OTUs were shared by fish fed both levels of starch, and fish fed the NC diet contained 284 unique OTUs, and those fed the HC diet only 172 OTUs (**Figure 2A**), suggesting that the high starch diets led to reduced OTU counts in the intestinal microbiota of largemouth bass. These results indicate that the high starch diet reduced the diversity and richness of the largemouth bass intestinal microbiota.

Proteobacteria, Firmicutes, Fusobacteria, Actinobacteria, and Bacteroidetes were identified as the dominant phyla in fish fed both diets, but their relative abundance differed between the two groups. The abundance of Fusobacteria increased in fish fed the HC diet, whereas the abundance of Proteobacteria and Firmicutes decreased in fish fed the HC diet compared to the fish fed the NC diet (**Figure 2B**). *Ralstonia*, *Cetobacterium*, *Mycoplasma*, *Clostridium sensu* stricto, and Peptostreptococcaceae were the top five dominant genera in fish fed the NC diet, while *Cetobacterium*, *Ralstonia*, *Mycoplasma*, *Plesiomonas*, and *Rhodococcus* were dominant in fish fed the HC diet (**Figure 2C**). Four species were identified in both groups, namely, *Ralstonia pickettii*, *Plesiomonas shigelloides*, *Rhodococcus erythropolis*, and *Acinetobacter johnsonii* (**Figure 2D**). These results suggest that the intestinal microbiota of largemouth bass was affected by the high starch diet.

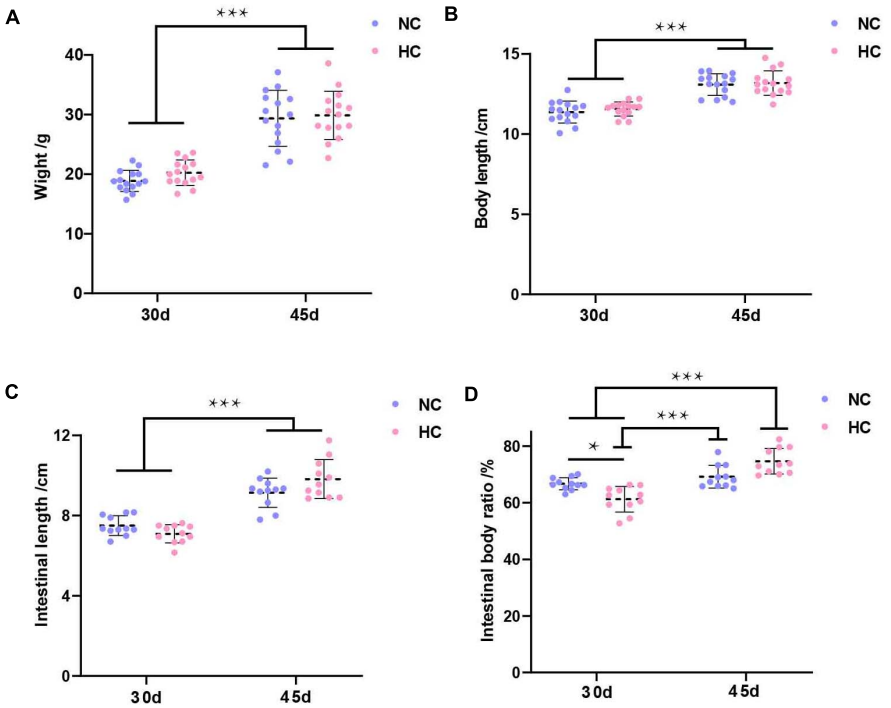

FIGURE 1 | Growth performance of largemouth bass **(A–D)** Weight, body length, intestinal length, and intestinal body ratio of largemouth bass after 30 and 45 days, respectively (*$P < 0.05$; ***$P < 0.001$. NC: 0% α-starch diet, HC: 22% α-starch diet).

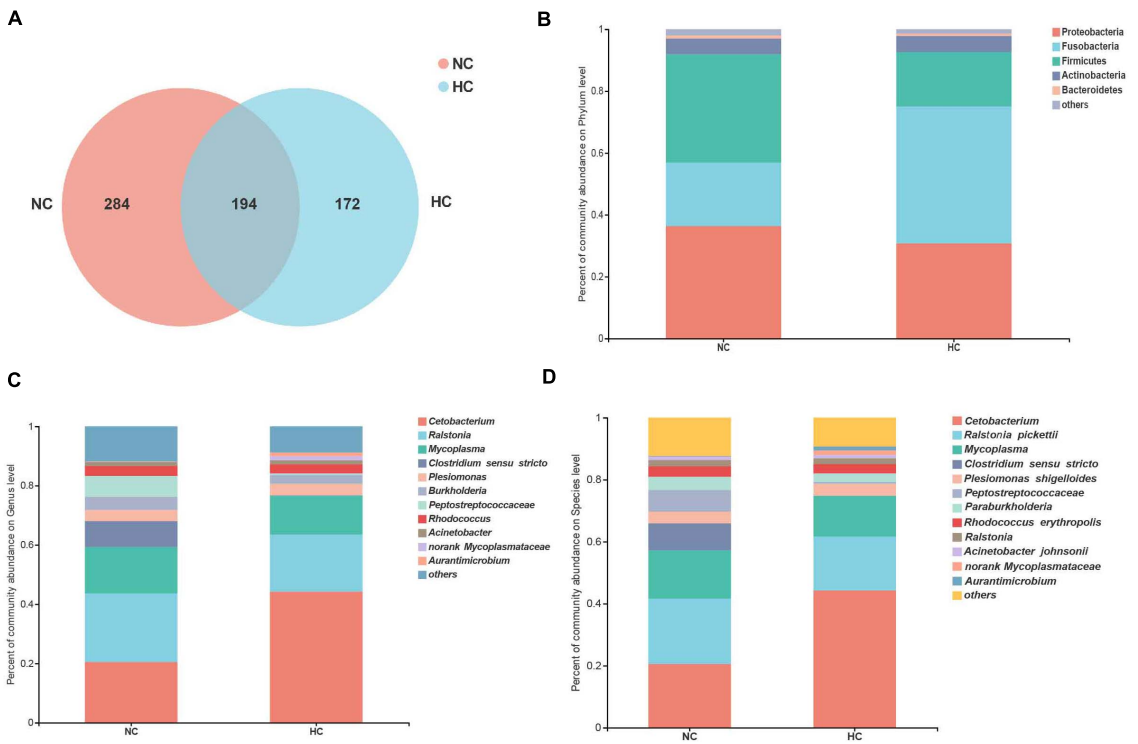

FIGURE 2 | Analysis of the composition of the intestinal microbiota of largemouth bass fed the NC and HC diets. **(A)** Venn diagram of unique and shared OTUs. **(B–D)** intestinal microbiota composition at the phylum, genus, and species levels, respectively (NC: 0% α-starch diet, HC: 22% α-starch diet).

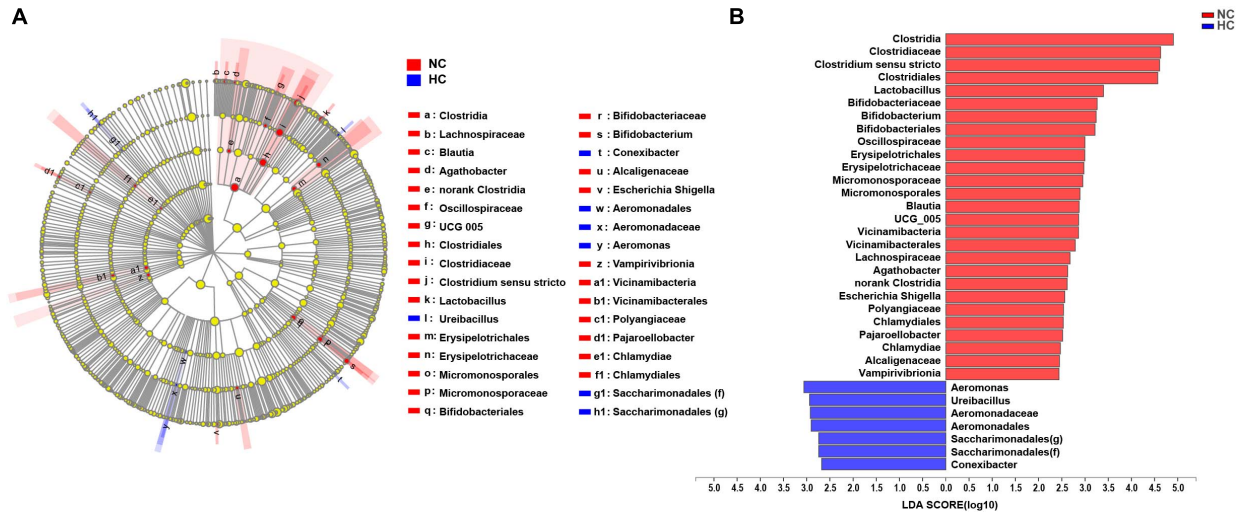

FIGURE 3 | LEfSe analysis of the differences in the intestinal microbiota of largemouth bass fed two diets **(A)** Taxonomic representation of differences in the intestinal microbiota of largemouth bass treated with the NC or HC diets. The concentric circles from the inside out represent the different taxonomic classes (phylum to genus). The different colored nodes indicate differences in intestinal microbiota (red represents a significantly higher abundance of intestinal microbiota in the NC treatment than in the HC treatment, while blue represents the opposite, and yellow indicates no significant difference). The size of each node indicates the abundance of intestinal microbiota. **(B)** Histogram of linear discriminant analysis (LDA) scores for differential abundance of the intestinal microbiota.

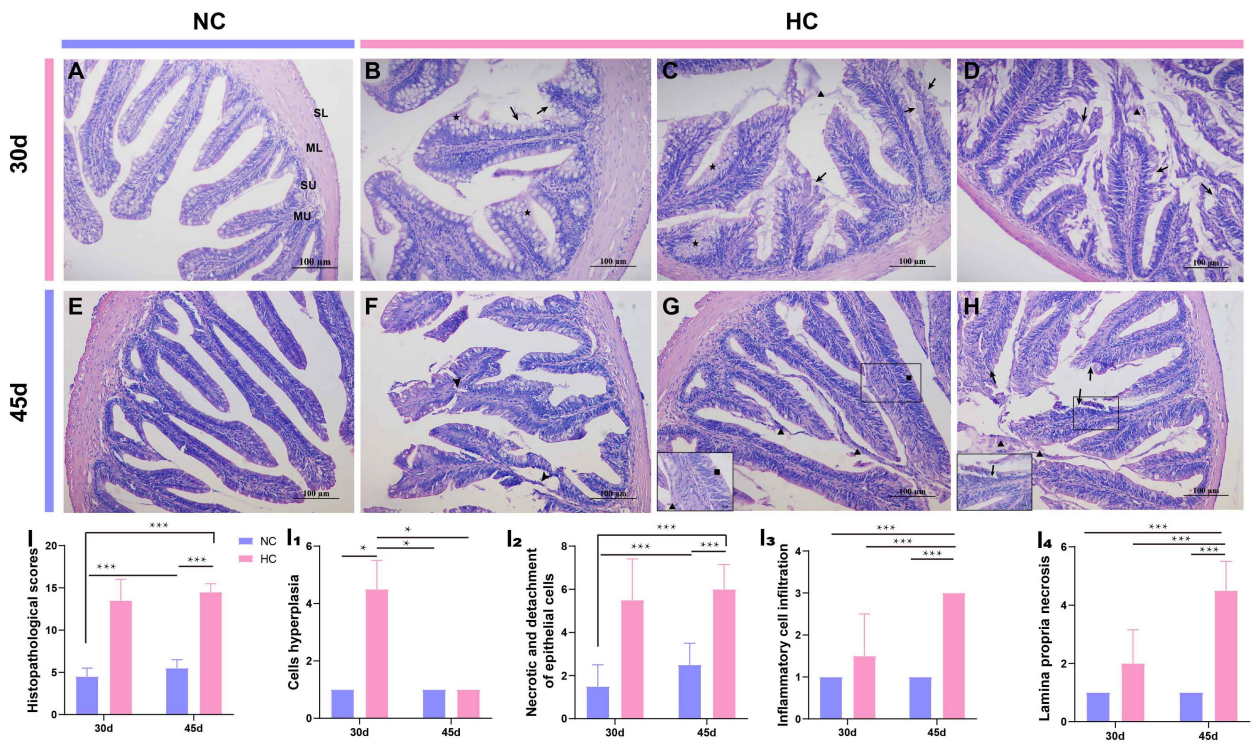

FIGURE 4 | Histopathological observations of the largemouth bass intestine (H&E staining) **(A)** The intestines of the NC-fed fish were undamaged at 30 days, with an intact mucous layer (MU), submucosal layer (SU), muscle layer (ML), and serosa layer (SL); **(B–D)** Proliferation of mucus cells (pentagram), increased mucus secretion (triangles), and loss of epithelial cells were detected in the intestines of fish fed the HC diet for 30 days (arrow); **(E)** The intestines of NC-fed fish at 45 days; **(F–H)** the intestines of fish fed the HC diet for 45 days; intestinal villi broken (arrowhead), mucus secreted (triangles), and epithelial cells shed (arrow), respectively; **(I)** Total intestinal histopathological score; **(I_1–I_4)** the histopathological scores for cell hyperplasia, necrosis, and detachment of epithelial cells, inflammatory cell infiltration, and necrosis of the lamina propria, respectively (*$P < 0.05$, ***$P < 0.001$. NC: 0% α-starch diet, HC: 22% α-starch diet).

The High Starch Diets Reduce the Relative Abundance of Beneficial Intestinal Bacteria in Largemouth Bass

A LEfSe LDA analysis was performed to further analyze the differences in intestinal microbiota composition between fish fed the NC and the HC diets. The results revealed significant differences in the intestinal microbiota of largemouth bass fed the NC and the HC diets (**Figure 3**). The relative abundance of order *Aeromonadales*, family Aeromonadaceae, Saccharimonadales (f), genus *Aeromonas*, *Ureibacillus*, *Saccharimonadales* (g), *Conexibacter* in the intestinal microbiota of fish fed the HC diet increased significantly compared to fish fed the NC diet; however, the relative abundance of class Clostridia, Vicinamibacteria, Chlamydiae, Vampirivibrionia, Micromonosporales, order Clostridiales, Bifidobacteriales, Erysipelotrichales, Micromonosporales, Vicinamibacterales, norank Clostridia, Chlamydiales, family Clostridiaceae, Bifidobacteriaceae, Oscillospiraceae, Erysipelotrichaceae, Micromonosporaceae, Lachnospiraceae, Polyangiaceae, Alcaligenaceae, genus *Clostridium sensu* stricto, *Lactobacillus*, *Bifidobacterium*, *Blautia*, UCG 005, *Agathobacter*, *Escherichia Shigella*, and *Pajaroellobacter* decreased significantly. This result suggests that the high starch diets changed the intestinal microbiota of largemouth bass, increasing the relative abundance of harmful bacteria (*Aeromonas*) and decreasing the relative abundance of beneficial bacteria (*Clostridium sensu* stricto, *Lactobacillus*, and *Bifidobacterium*) in the intestine.

A High Starch Diet Induces Enteritis in Largemouth Bass

Numerous studies have shown that changes in the intestinal microbiota are closely related to the development of intestinal diseases (Sokol et al., 2006; Li et al., 2012). In this study, the high starch diets caused changes in the intestinal microbiota, but it was not known whether the intestine was diseased. Therefore, further observations of the changes in intestinal tissues of largemouth bass were used to determine whether intestinal diseases developed. H&E staining was used to investigate the changes in intestinal histology of largemouth bass. The results showed that after 30 and 45 days, fish fed the NC diet had a healthy intestine with an intact mucous layer (MU), submucosal layer (SU), muscle layer (ML), serosa layer (SL), and a smooth intestinal mucosa (**Figures 4A,E**); however, fish fed the HC diet developed significant damage to the intestine. A large proliferation of goblet cells in the intestinal mucosa of HC-fed fish, an increase in mucus secretion, a large amount of mucus adhering to the intestinal villi, damage to the intestinal mucosa, and necrosis and shedding of epithelial cells were observed after 30 days (**Figures 4B–D**). At 45 days, the proliferation of goblet cells decreased, but necrosis of the lamina propria, the intestinal villi ruptured, the layer of intestinal villi cells increased, and inflammatory cells infiltrated, while shedding epithelial cells and secreted mucus were still visible in the intestinal lumen (**Figures 4F–H**). According to the intestinal histopathological score, feeding the HC diet caused obvious damage to the largemouth bass intestine, which appeared to be moderate to severe necrotizing enteritis due to the increase in the number of goblet cells and mucus secretion and accompanied by shedding of necrotic epithelial cells and infiltration of inflammatory cells (**Figures 4I–I$_4$**).

Alcian blue-periodic acid Schiff staining was used to further observe the changes in the intestinal goblet cells of largemouth bass fed the high starch diet. The results showed that the number of intestinal goblet cells was significantly higher in fish fed the HC diet than in fish fed the NC diet for 30 days (**Figures 5A–C,G**). The number of goblet cells was significantly lower at 45 days than at 30 days, and the number did not differ from that of fish fed the NC diet, but a large amount of mucus was visible in the intestinal lumen (**Figures 5D–F,G**). This may be related to the self-adaptive regulation by the organism.

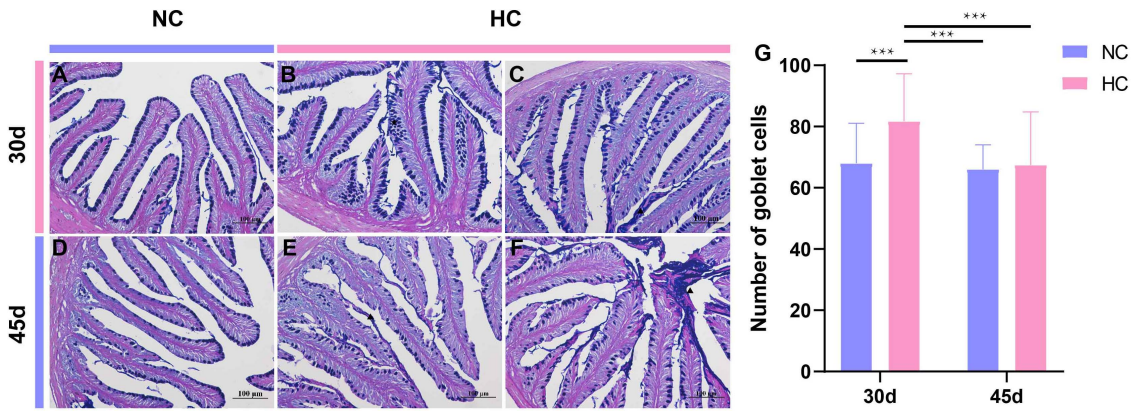

FIGURE 5 | Intestinal goblet cells observations of the largemouth bass intestine (AB-PAS staining) **(A)** The number and distribution of intestinal goblet cells in fish fed the NC diet for 30 days; **(B,C)** proliferation of goblet cells (pentagram), increased mucus secretion (triangles) of fish fed the HC diet for 30 days; **(D)** number and distribution of intestinal goblet cells in NC-fed fish after 45 days; **(E,F)**, the number of goblet cells decreased in HC-fed fish at 45 days, and a large amount of mucus was secreted into the intestinal lumen (triangle); **(G)** number of intestinal goblet cells in largemouth bass fed the NC and HC diets for 30 and 45 days (***$P < 0.001$. NC: 0% α-starch diet, FC: 22% α-starch diet).

Organelle changes in the intestinal cells that occurred during the 45 days were further observed by transmission electron microscopy. The cell structure of fish fed the NC diet was intact and the striated border at the top of the cells was visible (**Figure 6A**), while the intestinal goblet cells of fish fed the HC diet were filled with mucoprotein (**Figure 6B**). Some goblet cells had enlarged apical openings (**Figure 6C**), and some intracellular mitochondrial cristae were broken or had disappeared, vacuolated, or contained unidentified membranous structures (**Figure 6D**). This was similar to the histopathological observations that a large amount of mucus was present in the intestinal lumen of fish fed the HC diet. These results suggest that a high starch diet could cause significant damage to the largemouth bass intestine.

The High Starch Diets Alter Largemouth Bass Intestinal Digestive Function

The changes in the intestinal microbiota and the development of enteritis affect the digestive function of the intestine (Buts et al., 1999). Therefore, three common intestinal digestive enzymes were tested. As shown in **Figure 5**, no significant differences in trypsin or lipase activities were observed in either treatment group after 30 and 45 days (**Figures 7A,B**). However, the pattern of change in α-amylase activity was different. Amylase activity was significantly higher after 30 days in fish fed the HC diet than in fish fed the NC diet ($P < 0.05$), but the opposite trend was observed at 45 days. In addition, the α-amylase activity of the fish fed the HC diet for 30 days was significantly higher than that after 45 days ($P < 0.05$) (**Figure 7C**). This result suggests that largemouth bass adapt to a high starch diet by increasing intestinal amylase activity within 30 days, but if fed a high starch diet for a long time, they may not be able to effectively digest and absorb the starch.

DISCUSSION

The intestinal microbiota is an important component of the intestinal immune barrier and is closely related to various diseases, such as inflammation, non-alcoholic fatty liver, and obesity (Boulange et al., 2016). The intestinal microbiota is symbiotic in the intestine and can be affected by food (Flint et al., 2014). Numerous studies have found that a high-carbohydrate diet alters the intestinal microbiota. Feeding of juvenile rainbow trout (*Oncorhynchus mykiss*) with high carbohydrate induced intestinal microbiota disorders, with a significant increase in the relative abundance of *Aeromonas* sp., *Shewanella* sp., and γ-Proteobacteria (Geurden et al., 2014). Analysis of the intestinal microbiota of Chinese perch (*Siniperca chuatsi*) fed high starch showed a significant increase in the abundance of Tenericutes and a significant decrease in Fusobacteria (Zhang et al., 2020a). Largemouth bass fed a high starch diet developed disrupted intestinal microbiota with reduced abundance of intestinal probiotics (*Lactobacillus*) and increased abundance of potentially pathogenic intestinal bacteria (e.g., *Brevundimonas* and *Ralstonia*), which led to reduced intestinal acetate and butyrate concentrations, and impaired intestinal function (Zhou et al., 2020). In the present study, the high starch diet reduced the diversity and abundance of intestinal microbiota in largemouth bass, while the abundance of beneficial bacteria, such as *Clostridium*, *Lactobacillus*, and *Bifidobacterium* decreased. *Clostridium* is an important butyrate producing genus in the intestinal tract of animals (Vital et al., 2014). Butyrate is thought to improve the morphology of intestinal villus tissue, increase the activity of intestinal digestive enzymes, prevent intestinal diseases, and promote the growth of fish (Abdel-Latif et al., 2020). *Lactobacillus* and *Bifidobacterium* have been used as probiotics in fish, as they protect intestinal epithelial cells from damage and enhance disease resistance (Maji et al., 2016; Cavalcante et al., 2020; Ljubobratovic et al., 2020). Thus, the decrease in the abundance of *Clostridium*, *Lactobacillus*, and *Bifidobacterium* led to insufficient butyrate synthesis and probiotics and may induce enteritis in largemouth bass.

As one of the most important carbohydrates, starch is widely used in aquatic animal feeds, as it is considered one of the most inexpensive and readily available feed ingredients. However, most fish, particularly carnivorous fish, cannot efficiently use starch and chronic overconsumption leads to metabolic disorders and tissue damage or death (Tian et al., 2012; Wade et al., 2020). The activities of intestinal antioxidant enzymes, the length of the intestinal villi, and the thickness of the intestinal wrinkled were significantly reduced in *Oreochromis niloticus* fed a high carbohydrate diet (Xu, 2017). Ding et al. (2020) reported that intestinal villi of snakehead (*Channa argus*) became sparse and short as the carbohydrate content of the diet was increased (13–19%), and the intestinal villi were injured and shed at 19% carbohydrate content. In the present study, the

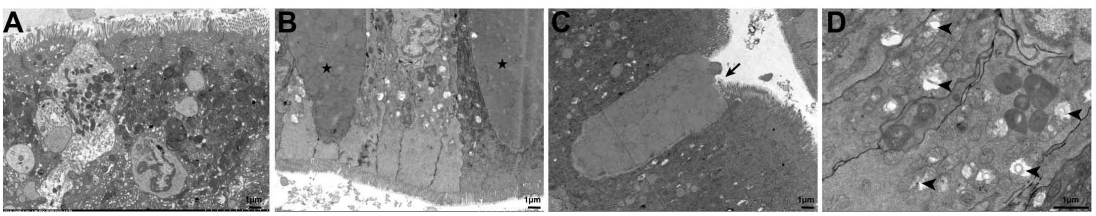

FIGURE 6 | Ultrastructural pathology of the largemouth bass intestine after 45 days of feeding the two diets. **(A)** The intestinal cells of largemouth bass fed the NC diet were structurally intact and undamaged; **(B–D)** the intestinal cells of largemouth bass fed the HC diet. Mucoprotein-filled goblet cells (pentagram), goblet cells with enlarged apical openings (arrow), mitochondria with broken cristae, vacuolated, and unidentified membranous structures (arrowhead) were observed.

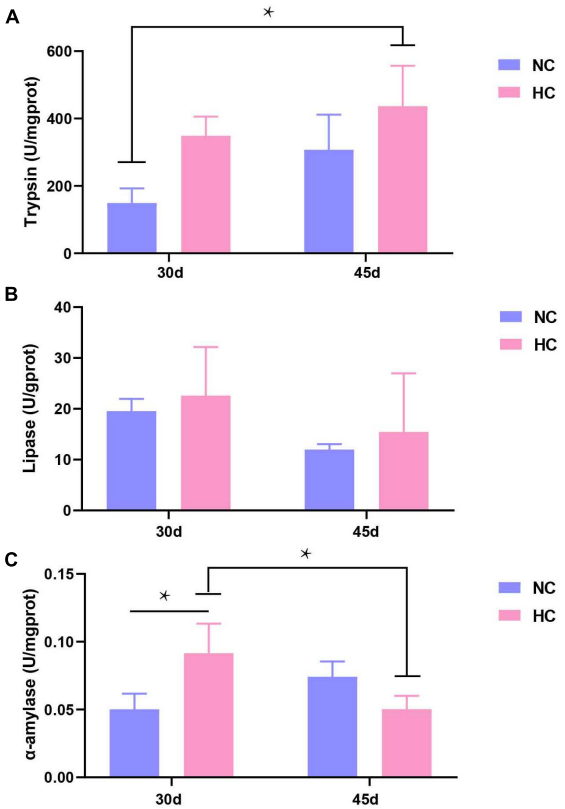

FIGURE 7 | Intestinal digestive enzyme activities of largemouth bass **(A–C)** Trypsin, lipase, and α-amylase activity after 30 and 45 days, respectively (*$P < 0.05$. NC: 0% α-starch diet, FC: 22% α-starch diet).

intestines of largemouth bass developed moderate to severe necrotizing enteritis with an increase in the number of goblet cells and mucus secretion accompanied by shedding of necrotic epithelial cells and infiltration by inflammatory cells. These observations suggest that a high starch diet could damage the intestines of fish.

Trypsin, lipase, and α-amylase are the most important digestive enzymes in the intestine. α-Amylase metabolizes starch by breaking α-1,4-glycosidic bonds and facilitating digestion and absorption (Kim et al., 1999). In fish, α-amylase is mainly synthesized and secreted by the hepatopancreas (Ou, 2018) and is released by the intestinal mucosa to perform its physiological functions (Zhou, 2012). High protein and carbohydrate diets inhibit α-amylase activity (Xie et al., 2015; Hu et al., 2018). In the present study, long-term intake of the high starch diets resulted in reduced α-amylase activity. Largemouth bass that consumed high starch content developed damage to the hepatopancreas and insufficient α-amylase secretion. The changes in the intestinal microbiota affected the integrity of the intestinal mucosa, which affected the release of amylase and its attachment to the intestinal mucosa, leading to reduced α-amylase activity. However, more detailed interactions between the microbiota and the intestinal digestive enzymes need to be investigated in future studies.

CONCLUSION

This study demonstrated that a high starch diet reduced the diversity and abundance of the intestinal microbiota in largemouth bass. The abundance of beneficial bacteria decreased, which may be associated with the development of enteritis. Our results illustrate the effects of a high starch diet on the intestines of largemouth bass. Intestinal health can be protected by adding probiotics to replace bacteria lost in this study (such as *Clostridium*, *Lactobacillus,* and *Bifidobacterium*). Therefore, our results provide a reference for conserving the intestinal microbiota of largemouth bass during modern intensive culture.

DATA AVAILABILITY STATEMENT

The datasets presented in this study can be found in online repositories. The names of the repository/repositories and accession number(s) can be found below: Sequence Read Archive (SRA) at the National Center for Biotechnology Information (NCBI) (accession number PRJNA730220).

ETHICS STATEMENT

All animal handling procedures were approved by the Animal Care and Use Committee of Sichuan Agricultural University, following the guidelines of animal experiments of Sichuan Agricultural University, under permit number DY-2019202033.

AUTHOR CONTRIBUTIONS

XH, LZ, QK, and DC contributed to conception and design of the study and article writing and revision. LZ wrote the first draft of the manuscript. SL performed the statistical analysis. YF organized the database. YG, YO, SY, LY, and WL wrote sections of the manuscript. All authors contributed to manuscript revision, read, and approved the submitted version.

FUNDING

This work was supported by Open Topic of the Key Laboratory of Freshwater Fisheries Healthy Farming of the Ministry of Agriculture and Rural Affairs (No. ZJK202004) and the double support plan of Sichuan Agricultural University (NO.1921993230).

ACKNOWLEDGMENTS

We thank all the authors for stimulating discussions and support.

SUPPLEMENTARY MATERIAL

The Supplementary Material for this article can be found online at: https://www.frontiersin.org/articles/10.3389/fmicb.2021.696588/full#supplementary-material

REFERENCES

Abdel-Latif, H., Dawood, M., Menanteau-Ledouble, S., and El-Matbouli, M. (2020). Benefits of dietary butyric acid, sodium butyrate, and their protected forms in aquafeeds: a review. *Rev. Fish. Sci. Aquacult.* 28, 1–28. doi: 10.1080/23308249.2020.1758899

Amoah, A., Coyle, S., Webster, C., Durborow, R., Bright, L., and Tidwell, J. (2008). Effects of graded levels of carbohydrate on growth and survival of largemouth bass, *Micropterus salmoides*. *J. World Aquacult. Soc.* 39, 397–405. doi: 10.1111/j.1749-7345.2008.00168.x

AOAC (2005). *Official Methods of Analysis of Association of Official Analytical Chemists*, 15th Edn. ed. B. Kenesseth Helrick.

Asaduzzaman, M., Wahab, M., Verdegem, M., Adhikary, R., Rahman, S., Azim, E., et al. (2010). Effects of carbohydrate source for maintaining a high C:N ratio and fish driven re-suspension on pond ecology and production in periphyton based freshwater prawn farming systems. *Aquaculture* 301, 37–46.

Bäckhed, F., Ley, R., Sonnenburg, J., Peterson, D., and Gordon, J. (2005). Host-bacterial mutualism in the human intestine. *Science* 307, 1915–1920. doi: 10.1126/science.1104816

Banić, M., Urek, M. C., and Prka, L. (2018). "Intestinal function," in *Gastrointestinal Complications of Diabetes: A Comprehensive Guide*, eds M. Duvnjak and L. Smirčić-Duvnjak (Cham: Springer International Publishing), 103–113.

Baums, C. G., Hermeyer, K., Leimbach, S., Adamek, M., Czerny, C. P., Hörstgen-Schwark, G., et al. (2013). Establishment of a model of *Streptococcus iniae* Meningoencephalitis in Nile Tilapia (*Oreochromis niloticus*). *J. Comp. Pathol.* 149, 94–102. doi: 10.1016/j.jcpa.2012.10.003

Boulange, C., Neves, A. L., Chilloux, J., Nicholson, J., and Dumas, M.-E. (2016). Impact of the gut microbiota on inflammation, obesity, and metabolic disease. *Genome Med.* 8, 1–12. doi: 10.1186/s13073-016-0303-2

Buts, J. P., Keyser, N. D., Marandi, S., Hermans, D., Sokal, E. M., Chae, Y., et al. (1999). *Saccharomyces boulardii* upgrades cellular adaptation after proximal enterectomy in rats. *Gut* 45, 89–96. doi: 10.1136/gut.45.1.89

Cavalcante, R. B., Telli, G. S., Tachibana, L., Dias, D. D., Oshiro, E., Natori, M. M., et al. (2020). Probiotics, prebiotics and synbiotics for Nile tilapia: growth performance and protection against *Aeromonas hydrophila* infection. *Aquacult. Rep.* 17:100343. doi: 10.1016/j.aqrep.2020.100343

Ding, X. Q., Yao, L., Hou, Y., Hou, Y. B., Wang, G. L., Fan, J. H., et al. (2020). Effects of different carbohydrate levels in puffed feed on digestive tract morphological function and liver tissue structure of snakeheads (*Channa argus*). *Aquacult. Res.* 51, 1–12. doi: 10.1111/are.14402

Falcinelli, S., Rodiles, A., Hatef, A., Picchietti, S., Cossignani, L., Merrifield, D., et al. (2017). Dietary lipid content reorganizes gut microbiota and probiotic *L. rhamnosus* attenuates obesity and enhances catabolic hormonal milieu in zebrafish. *Sci. Rep.* 7:5512. doi: 10.1038/s41598-017-05147-w

Fisheries and Fisheries Administration (2020). *China Fisheries Statistical Yearbook*. Beijing: China Agriculture Press.

Flint, H., Duncan, S., and Louis, P. (2014). Links between diet, gut microbiota composition and gut metabolism. *Proc. Nutr. Soc.* 74, 1–10. doi: 10.1017/S0029665114001463

Geurden, I., Elisabeth, P.-J., Veron, V., Cerezo, T., Mazurais, D., Zambonino-Infante, J., et al. (2014). High or low dietary carbohydrate: protein ratios during first-feeding affect glucose metabolism and intestinal microbiota in juvenile rainbow trout. *J. Exp. Biol.* 217, 3396–3406. doi: 10.1242/jeb.106062

Hu, Y., Chen, Y., Zhang, D., Chen, T., Liu, B., and Gao, Q. (2018). Effects of different dietary carbohydrate and protein levels on growth, intestinal digestive enzymes and serum indexes in large-size grass carp (*Ctenopharyngodon idella*). *J. Fish. China* 42, 777–786. doi: 10.11964/jfc.20170510849

Huang, X., Zhong, L., Fan, W., Feng, Y., Xiong, G., Liu, S., et al. (2020). Enteritis in hybrid sturgeon (*Acipenser schrenckii*♂ × *Acipenser baeri*♀) caused by intestinal microbiota disorder. *Aquacult. Rep.* 18:100456. doi: 10.1016/j.aqrep.2020.100456

Kamalam, B. S., Médale, F., and Panserat, S. (2017). Utilisation of dietary carbohydrates in farmed fishes: new insights on influencing factors, biological limitations and future strategies. *Aquaculture* 290, 3–27. doi: 10.1016/j.aquaculture.2016.02.007

Kim, J., Cha, S.-S., Kim, K., Kim, T.-J., Ha, N.-C., Oh, S.-T., et al. (1999). Crystal structure of a maltogenic amylase provides insights into a catalytic versatility. *J. Biol. Chem.* 274, 26279–26286. doi: 10.1074/jbc.274.37.26279

Li, M., Hu, F. C., Qiao, F., Du, Z. Y., and Zhang, M. L. (2020). Sodium acetate alleviated high-carbohydrate induced intestinal inflammation by suppressing MAPK and NF-κB signaling pathways in Nile tilapia (*Oreochromis niloticus*). *Fish Shellfish Immunol.* 98, 758–765. doi: 10.1016/j.fsi.2019.11.024

Li, Q., Wang, C., Tang, C., Li, N., and Li, J. (2012). Molecular-phylogenetic characterization of the microbiota in ulcerated and non-ulcerated regions in the patients with Crohn's disease. *PLoS One* 7:e34939. doi: 10.1371/journal.pone.0034939

Lin, S.-M., Shi, C.-M., Mu, M.-M., Chen, Y.-J., and Luo, L. (2018). Effect of high dietary starch levels on growth, hepatic glucose metabolism, oxidative status and immune response of juvenile largemouth bass, *Micropterus salmoides*. *Fish Shellfish Immunol.* 78, 121–126. doi: 10.1016/j.fsi.2018.04.046

Ljubobratovic, U., Kosanovic, D., Demeny, F. Z., Krajcsovics, A., Vukotic, G., Stanisavljevic, N., et al. (2020). The effect of live and inert feed treatment with lactobacilli on weaning success in intensively reared pike-perch larvae. *Aquaculture* 516:734608. doi: 10.1016/j.aquaculture.2019.734608

Maji, U. J., Mohanty, S., Mahapatra, A. S., and Maiti, N. K. (2016). Diversity and probiotic potentials of putative lactic acid bacteria for application in freshwater aquaculture. *Turkish J. Fish. Aquat. Sci.* 16, 805–818. doi: 10.4194/1303-2712-v16_4_07

Manichanh, C., Borruel, N., Casellas, F., and Guarner, F. (2012). The gut microbiota in IBD. *Nat. Rev. Gastroenterol. Hepatol.* 9, 599–608. doi: 10.1038/nrgastro.2012.152

Ou, H. (2018). *Effects of Different Feed on Digestive Enzyme and Intestinal Morphologic Structure of Micropterus salmoides*. Ph. D. Thesis. Shanghai: Shanghai Ocean University.

Peng, M., Xue, J., Hu, Y., Wen, C., Hu, B., Jian, S., et al. (2019). Disturbance in the homeostasis of intestinal microbiota by a high-fat diet in the rice field eel (*Monopterus albus*). *Aquaculture* 502, 347–355. doi: 10.1016/j.aquaculture.2018.12.062

Salonen, A., and de Vos, W. M. (2014). "Impact of diet on human intestinal microbiota and health," in *Annual Review of Food Science and Technology*, Vol. 5, eds M. P. Doyle and T. R. Klaenhammer (Palo Alto: Annual Reviews), 239–262.

Sokol, H., Seksik, P., Rigottier-Gois, L., Lay, C., Lepage, P., Podglajen, I., et al. (2006). Specificities of the fecal microbiota in inflammatory bowel disease. *Inflamm. Bowel Dis.* 12, 106–111. doi: 10.1097/01.MIB.0000200323.38139.c6

Stone, D. A. J. (2003). Dietary carbohydrate utilization by fish. *Rev. Fish. Sci.* 11, 337–369. doi: 10.1080/10641260390260884

Tian, L. X., Liu, Y. J., Yang, H. J., Liang, G. Y., and Niu, J. (2012). Effects of different dietary wheat starch levels on growth, feed efficiency and digestibility in grass carp (*Ctenopharyngodon idella*). *Aquacult. Int.* 20, 283–293. doi: 10.1007/s10499-011-9456-6

Tuan, T., Zhang, J., Xiong, F., Wang, G.-T., Li, W., and Wu, S. (2018). Altered gut microbiota associated with intestinal disease in grass carp (*Ctenopharyngodon idellus*). *World J. Microbiol. Biotechnol.* 34:71. doi: 10.1007/s11274-018-2447-2

Vital, M., Howe, A., and Tiedje, J. (2014). Revealing the bacterial butyrate synthesis pathways by analyzing (Meta) genomic Data. *mBio* 5:e00889-14. doi: 10.1128/mBio.00889-14

Wade, N. M., Trenkner, L. H., Viegas, I., Tavares, L. C., Palma, M., Skiba-Cassy, S., et al. (2020). Dietary starch promotes hepatic lipogenesis in barramundi (*Lates calcarifer*). *Br. J. Nutr.* 124, 363–373. doi: 10.1017/s0007114520001051

Xie, D., Xu, S., Wang, S., You, C., and Li, Y. (2015). Cloning, tissue expression, and nutritional regulation of the α-amylase gene in the herbivorous marine teleost *Siganus canaliculatus*. *Aquaculture* 454, 229–236. doi: 10.1016/j.aquaculture.2015.12.031

Xu, X. X. (2017). *Effects of High Carbohydrate Levels in the Dietary on Growth Properties, Glucose and Lipid Metabolisms, Intestinal Health and Immune Performance of GIFT, Oreochromis niloticus Shanghai. Ph. D. Thesis*. Shanghai: Shanghai Ocean University.

Zhang, Y., Liang, X.-F., He, S., Chen, X., Wang, J., Li, J., et al. (2020a). Effects of high carbohydrate diet-modulated microbiota on gut health in chinese perch. *Front. Microbiol.* 11:575102.

Zhang, Y., Xie, S., Wei, H., Zheng, L., Liu, Z., Fang, H., et al. (2020b). High dietary starch impaired growth performance, liver histology and hepatic glucose metabolism of juvenile largemouth bass, *Micropterus salmoides*. *Aquacult. Nutr.* 26, 1083–1095. doi: 10.1111/anu.13066

Zhang, Y., Xu-Fang, L., Shan, H., Xu, C., Jie, W., Jiao, L., et al. (2020c). Effects of high carbohydrate diet-modulated microbiota on gut health in Chinese perch. *Front. Microbiol.* 11:575102. doi: 10.3389/fmicb.2020.575102

Zhang, Y. M., Guo, T. Y., Liu, Z. L., Fang, H. H., Zheng, L., Xie, J., et al. (2020). High dietary starch inclusion impairs growth and antioxidant status, and alters liver organization and intestinal microbiota in largemouth bass *Micropterus salmoides*. *Aquacult. Nutr.* 26, 1806–1821. doi: 10.1111/anu.13131

Zhao, W., Xie, J., Fang, H.-H., Liu, Y.-J., Tian, L.-X., and Niu, J. (2020). Effects of corn starch level on growth performance, antioxidant capacity, gut morphology and intestinal microflora of juvenile golden pompano, *Trachinotus ovatus*. *Aquaculture* 524, 735197. doi: 10.1016/j.aquaculture.2020.735197

Zhou, C., Ge, X., Niu, J., Lin, H., Huang, Z., and Tan, X. (2015). Effect of dietary carbohydrate levels on growth performance, body composition, intestinal and hepatic enzyme activities, and growth hormone gene expression of juvenile golden pompano, *Trachinotus ovatus*. *Aquaculture* 437, 390–397. doi: 10.1016/j.aquaculture.2014.12.016

Zhou, H. (2012). *The Effect of Feed Carbohydrates on the Digestive Function and Tissue Structure of Channa argus*. Ph. D. Thesis. Zhejiang: Zhejiang University.

Zhou, S. S., Xu, J., Zhu, H., Wu, J., Xu, J. D., Yan, R., et al. (2016). Gut microbiota-involved mechanisms in enhancing systemic exposure of ginsenosides by coexisting polysaccharides in ginseng decoction. *Sci. Rep.* 6:22474. doi: 10.1038/srep22474

Zhou, Y. L., He, G. L., Jin, T., Chen, Y. J., and Lin, S. M. (2020). High dietary starch impairs intestinal health and microbiota of largemouth bass, *Micropterus salmoides*. *Aquaculture* 534:736261. doi: 10.1016/j.aquaculture.2020.736261

Conflict of Interest: The authors declare that the research was conducted in the absence of any commercial or financial relationships that could be construed as a potential conflict of interest.

frontiers in Microbiology

ORIGINAL RESEARCH
published: 20 July 2021
doi: 10.3389/fmicb.2021.701081

Feeding Systems and Host Breeds Influence Ruminal Fermentation, Methane Production, Microbial Diversity and Metagenomic Gene Abundance

*Rajaraman Bharanidharan[1], Chang Hyun Lee[2], Krishnaraj Thirugnanasambantham[3,4], Ridha Ibidhi[3], Yang Won Woo[5], Hong-Gu Lee[6], Jong Geun Kim[3,7] and Kyoung Hoon Kim[3,7]**

[1] Department of Agricultural Biotechnology, College of Agriculture and Life Sciences, Seoul National University, Seoul, South Korea, [2] Cargill Agri Purina Inc., Technology Application Center, Pyeongchang, South Korea, [3] Department of Ecofriendly Livestock Science, Institute of Green Bio Science and Technology, Seoul National University, Pyeongchang, South Korea, [4] Pondicherry Centre for Biological Science and Educational Trust, Tamil Nadu, India, [5] GN Food Ltd., R&D Team, Seoul, South Korea, [6] Department of Animal Science and Technology, SangHa Life Science College, Konkuk University, Seoul, South Korea, [7] Department of International Agricultural Technology, Graduate School of International Agricultural Technology, Seoul National University, Pyeongchang, South Korea

OPEN ACCESS

Edited by:
Yvonne Vallès, The University of the West Indies, Cave Hill, Barbados

Reviewed by:
Fenja Klevenhusen, Bundesanstalt für Risikobewertung (BfR), Germany
Yanfen Cheng, Nanjing Agricultural University, China

***Correspondence:**
Kyoung Hoon Kim
khhkim@snu.ac.kr

Specialty section:
This article was submitted to Microbial Symbioses, a section of the journal Frontiers in Microbiology

Received: *27 April 2021*
Accepted: *28 June 2021*
Published: *20 July 2021*

Citation:
Bharanidharan R, Lee CH, Thirugnanasambantham K, Ibidhi R, Woo YW, Lee H-G, Kim JG and Kim KH (2021) Feeding Systems and Host Breeds Influence Ruminal Fermentation, Methane Production, Microbial Diversity and Metagenomic Gene Abundance. Front. Microbiol. 12:701081. doi: 10.3389/fmicb.2021.701081

Our previous research revealed the advantages of separate feeding (SF) systems compared to total mixed ration (TMR) in terms of ruminal methane (CH_4) production. The purpose of this experiment was to confirm the advantage of SF as a nutritional strategy for CH_4 mitigation, and to determine the effects of different feeding systems (TMR and SF) on the rumen microbiome and associated metagenome of two different breeds and on CH_4 emissions. We randomly allocated four Holstein (305 ± 29 kg) and four Hanwoo steers (292 ± 24 kg) to two groups; the steers were fed a commercial concentrate with tall fescue (75:25) as TMR or SF, in a crossover design (two successive 22-day periods). Neither feeding systems nor cattle breeds had an effect on the total tract digestibility of nutrients. The TMR feeding system and Hanwoo steers generated significantly more CH_4 ($P < 0.05$) and had a higher yield [g/d and g/kg dry matter intake (DMI)] compared to the SF system and Holstein steers. A larger rumen acetate:propionate ratio was observed for the TMR than the SF diet ($P < 0.05$), and for Hanwoo than Holstein steers ($P < 0.001$), clearly reflecting a shift in the ruminal H_2 sink toward CH_4 production. The linear discriminant analysis (LDA) effect size (LEfSe) revealed a greater abundance ($\alpha < 0.05$ and LDA > 2.0) of operational taxonomic units (OTUs) related to methanogenesis for Hanwoo steers compared to Holstein steers. Kendall's correlation analysis revealed wide variation of microbial co-occurrence patterns between feeding systems, indicating differential H_2 thermodynamics in the rumen. A metagenome analysis of rumen microbes revealed the presence of 430 differentially expressed genes, among which 17 and 27 genes exhibited positive and negative associations with CH_4 production, respectively ($P < 0.001$). A strong interaction between feeding system and breed was observed for microbial and metagenomic abundance. Overall, these results suggest that the TMR feeding system produces more CH_4, and that Hanwoo cattle

are higher CH_4 emitters than SF diet and Holstein cattle, respectively. Interestingly, host-associated microbial interactions differed within each breed depending on the feeding system, which indicated that breed-specific feeding systems should be taken into account for farm management.

Keywords: Hanwoo, TMR, rumen, methane, metagenome, microbial network

INTRODUCTION

Some dietary interventions have the potential to reduce ruminal CH_4 emissions with little negative impact on the animals. One strategy involves the use of different cattle feeding systems, such as separate feeding (SF) and total mixed ration (TMR) feeding with concentrate and forage. A review by Beigh et al. (2017) also clarified the advantages of TMR over conventional SF systems in ruminants. Compared to SF, TMR has a stabilising effect on rumen pH, and also has positive effects on dry matter intake (DMI), milk fat content (Phipps et al., 1984), nutrient use efficiency (Lailer et al., 2005), total milk production (Reddy and Reddy, 1983), and microbial protein synthesis (Liu et al., 2015) in dairy cattle. TMR feeding was also reported to have various advantages in beef production, in terms of precision, efficiency and convenience, which are believed to improve overall on-farm productivity (Moya et al., 2014). The practice of TMR feeding in beef cattle production has increased gradually, and is now used in about 20% of beef cattle farms in Korea. This has led to an increase in research on its effects on ruminal fermentation, animal performance and carcass quality in Hanwoo (Korean native cattle) steers (Lee et al., 2010; Kim et al., 2011; Chung et al., 2017). However, the effects of the TMR and SF systems on ruminal CH_4 mitigation have not been studied extensively in either dairy or beef cattle. One early study compared TMR and SF silage-based diets for maintenance-level feeding of lactating Holstein cows, and found no differences in CH_4 emissions between the feeding systems (Holter et al., 1977). Our previous studies of Holstein steers, with an average daily gain (ADG) of 0.65 kg, revealed higher CH_4 emissions with the TMR than SF system (Lee et al., 2016; Bharanidharan et al., 2018). However, further studies are needed to validate the effects of these feeding systems on CH_4 production in beef cattle.

The extensive livestock production system in Korea has contributed to an increase in atmospheric CH_4 concentrations, with a reported 3.89 $MtCO_2$ eq/y derived from enteric fermentation; this accounted for 50% of total CH_4 emissions (7.81 $MtCO_2$ eq/y) in Korea from the agricultural sector in 2018 (FAOSTAT, 2021). In the first quarter of 2021, Korea had around 3.33 million beef cattle, with Hanwoo accounting for 3.16 million head and Holstein accounting for the remainder (Korean Statistical Information Service (KOSIS), 2021). Studies have suggested that host breeds provide different environments for the microbial ecosystem in the rumen, and may influence the microbial composition and CH_4 emissions (Duthie et al., 2017; De Mulder et al., 2018; Olijhoek et al., 2018; Islam et al., 2021). A comparison of the whole-genome sequence between Hanwoo and Holstein steers also revealed huge differences in the copy number variation regions (CNVR) between the two breeds (Choi et al., 2014), which could influence the rumen microbial composition (Benson et al., 2010). Furthermore, studies have provided direct evidence of the genetic influence of the host animal on CH_4 production by ruminal microbes, thereby allowing the breeding of low-emitting animals through genetic selection (Roehe et al., 2016; Zhang et al., 2020). However, there have been no studies directly comparing CH_4 emissions and rumen microbiomes between the Hanwoo and Holstein breeds with the diet held constant.

A better understanding of the contributions of Korean indigenous breeds to the microbial metagenome and variation in CH_4 emissions will enable identification of metagenomic markers and the development of an optimal feeding system, both of which will reduce ruminal emissions. The present study was performed to clarify the effects of different feeding systems (TMR and SF), as well as differences in metabolites and microbiota, between the rumens of Hanwoo and Holstein steers, and their interactions with CH_4 emissions, fermentation characteristics and the microbial metagenome using next-generation sequencing.

MATERIALS AND METHODS

All experimental animals were obtained from the animal farm of Seoul National University. The methods and protocols for all experiments involving animals were approved by the Committee for the Institutional Animal Care and Use of Seoul National University (SNU-160105-1), and performed in accordance with relevant guidelines and regulations.

Experimental Animals and Diet

Four Holstein and four Hanwoo steers [initial body weights (BWs) of 305 ± 29 and 292 ± 24 kg, respectively] were allocated to two adjacent pens fitted with Calan doors. Four steers of each breed were offered commercial concentrate and tall fescue hay (75:25, on a DM basis) as either TMR or SF for two consecutive 22-day periods in a crossover design. All animals were adapted for 30 days to the experimental diet (TMR), and to the Calan doors, before the experiment. Each experimental period included 14 days of diet adaptation in the pen, 3 days of metabolic adaptation in a respiratory chamber, 2 days of CH_4 measurements, 2 days of grab faecal sampling and 1 day of rumen fluid sampling. The diets (**Table 1**) were provided at 2.1% BW twice daily (at 09:00 and 18:00) and the animals had unrestricted access to water in both the pen and respiratory chamber. The DM intake was recorded daily, both in the pen and in the chamber. The TMR diet was prepared by blending commercial concentrate and chopped tall fescue hay every 7 days

TABLE 1 | Ingredients and chemical composition of the basal diet used in the experiment.

Ingredient composition, % DM	
Concentrate	
Broken corn	1.0
Wheat	12.8
Sodium bicarbonate	0.6
Rice bran	5.0
Salt	0.2
Molasses	2.0
Ammonium chloride	0.1
CMS	1.1
Corn flake	15.0
DDGS	7.2
Soybean Hull	1.4
Amaferm^{TM}	0.1
Corn gluten feed	15.0
Limestone	2.5
Palm kernel meal	11.0
Mineral-vitamin mixture[a]	0.2
Roughage	
Tall fescue hay	25.0
Chemical composition, % DM	
OM	93.3
CP	12.9
EE	4.4
aNDFom[b]	38.3
ADFom[c]	19.0
GE, MJ/kg	18.0

CMS, condensed molasses soluble; DDGS, dried distiller's grains with solubles. Amaferm^{TM}, fermentation extract of Aspergillus oryzae (Biozyme Enterprises Inc., MO, United States); CP, crude protein; EE, ether extract; GE, gross energy; OM, organic matter.

[a]Nutrients per kg of additive (Grobic-DC; Bayer HealthCare, Leverkusen, Germany): Vit. A, 2,650,000 IU; Vit. D3, 530,000 IU; Vit. E, 1,050 IU; Niacin, 10,000 mg; Mn, 4,400 mg; Zn, 4,400 mg; Fe, 13,200 mg; Cu, 2,200 mg; I, 440 mg; Co, 440 mg.

[b]Neutral detergent fibre assayed with a heat stable amylase and expressed exclusive of residual ash.

[c]Acid detergent fibre excluding residual ash.

during the experimental period. The prepared TMR diet was then packed in vinyl bags in quantities of 20 kg and stored for feeding to the animals. In the SF system, tall fescue hay was provided first, followed by concentrate pellet with flaked corn 40 min later, to avoid an unnecessary drop in pH during initial ruminal fermentation compared to the TMR diet. The BW of the animals was measured at both the beginning and end of each period to determine the ADG. The offered feed samples were collected at the beginning of the experimental period. The refused feed samples were collected daily when the animals were placed in the chamber. Both samples were packed and stored at −20°C until being analysed for DM content and the composition of other chemicals as described previously (Bharanidharan et al., 2018). The particle size of the offered feed in both the TMR and SF diets was determined using a Penn State particle separator according to the technique of Kononoff et al. (2003).

Enteric CH_4 Measurement, Digestion Trial, and Rumen Sampling

Methane production was measured using four open-circuit whole-body respiratory chambers, as described previously (Bharanidharan et al., 2018), with a ventilation rate of 700 L/min maintained throughout the experiment. The apparent total tract digestibility of nutrients in steers was studied using chromic oxide (Cr_2O_3) as an external marker, which was top-dressed twice daily at 0.2% of the daily feed amount throughout the experiment. On day 20, a faecal grab sample (100 g fresh weight) was collected from the rectum of each animal 30 min before feeding, and at 1, 3, 5, and 7 h post-feeding. On day 21, faeces were collected 30 min before feeding, and at 2, 4, 6, and 8 h post-feeding. Samples were frozen at −20°C until analysis. The samples were then composited by day and period for each steer prior to analysis of the digestibility of nutrients, as described previously (Bharanidharan et al., 2018). Ruminal fluid samples were collected before feeding (0 h), and at 1.5 and 3 h post-feeding, on day 22 of each period using a stomach tube (Oriental Dream, Hwaseong, Korea). The samples were filtered through four layers of muslin cloth. After immediately measuring pH using a Seven Easy pH meter (Mettler-Toledo, Schwerzenbach, Switzerland), ruminal fluid was centrifuged at 12,000 × g for 10 min (Smart 15; Hanil Science Industrial, Gimpo, South Korea). The supernatant was transferred to a 50-mL centrifuge tube and stored at −20°C for determination of ammonia-nitrogen (NH_3-N) and volatile fatty acid (VFA) concentrations using the methods described previously (Bharanidharan et al., 2018). For microbial analysis, rumen fluid samples collected 3-h post-feeding were snap frozen in liquid nitrogen and then stored at −80°C until DNA extraction.

16SrRNA Gene Sequencing, Bioinformatics, and Statistical Analyses

The genomic DNA was extracted from 16 rumen samples (four per feeding system per breed) and a V4 sequencing library was constructed and sequenced for paired-end 250-bp reads using the Illumina MiSeq system (Illumina, San Diego, CA, United States). The primers and methods were described previously (Bharanidharan et al., 2018). The raw Illumina MiSeq reads were demultiplexed according to the barcodes and the sequences were quality-filtered based on the quality control process of Quantitative Insights Into Microbial Ecology (QIIME, version 1.9.0)[1]. The quality control conditions were as follows: read truncation: the raw read was truncated from the first low-quality base site with a maximum of three consecutive low-quality base calls (Phred Q < 20) allowed; and length filtering: to delete reads of continuous high quality (Phred $Q \geq 20$), with a base length <70% of the read length. Non-overlapping regions, chimeric sequences and singletons were discarded. Each read was screened for operational taxonomic unit (OTU) picking using UCLUST embedded within QIIME 1.9.0, with reference to the Greengenes database (gg_otus-13_8-release, 97% nucleotide identity). The resulting OTU table was rarefied across samples to a depth of 10,000 reads based on the mean values of 10 iterations using the QIIME platform. All statistical analyses were performed on samples obtained from the same depth. Microbial community diversity was estimated in terms of the Chao1, Shannon, and Simpson indices using PAST software (Hammer et al., 2001).

[1]http://qiime.org/index.html

Determination of core and unique taxa was accomplished based on the abundance and prevalence (two-parameter) cut-offs across all the samples, using the inbuilt algorithm in Calypso software (Zakrzewski et al., 2017). Any taxa found to be ubiquitous (>90% occurrence across all samples) were defined as "core taxa" in the rumen, whereas those prevalent only in particular sample groups were defined as "unique taxa." To identify bacterial lineages and other parameters that differentiated Hanwoo and Holstein cattle given the TMR or SF diet, we performed a principal component analysis (PCA) in the R software environment (R Development Core Team, Vienna, Austria) using the prcomp package; the results were visualised three-dimensionally using the pca3d package (Weiner, 2019). To identify robust microbial biomarkers for the two breeds, we calculated the linear discriminant analysis (LDA) effect size (LEfSe; Segata et al., 2011) using the Galaxy web application[2]. The OTU counts in each sample were used as the input for the LEfSe analysis. Differences among classes were determined using the Kruskal–Wallis test, at a significance level of $P < 0.05$ and with a threshold LDA score of 2.0. Feeding system was included as a subclass. The LEfSe subclasses were analysed using the Wilcoxon rank sum test, with $P < 0.05$ again taken to indicate significance. Relationships among microbes in the rumens of Hanwoo and Holstein steers given the TMR and SF diets were evaluated using Kendall's correlation analysis, and a correlation plot was constructed using PAST software. To predict the molecular functions of each sample based on 16S rRNA data, we used the online version of the Phylogenetic Investigation of Communities by Reconstruction of Unobserved States (PICRUSt) bioinformatics software package (Langille et al., 2013), hosted on the Galaxy platform[2]. We used the Kyoto Encyclopaedia of Genes and Genomes (KEGG) database (Kanehisa and Goto, 2000) to predict the metagenome of our samples, based on OTU data obtained from rarefied 16S rRNA gene sequences using PICRUSt. The functions and products of the genes of interest were also obtained from the KEGG database. Differences between breeds given the TMR or SF diet in terms of the predicted molecular functions of bacterial communities were determined using a canonical correspondence analysis (CCA) in Calypso software. The non-parametric Kendall rank correlation coefficient was calculated to test the correlations among CH_4 production, fermentation characteristics, bacterial communities, gene abundance and functional pathways in the rumen, using the corr.test function of the R psych package (Revelle, 2018). The resulting correlation matrix was visualised as a heatmap using the heatmap.2 function in the gplots R package (Warnes et al., 2015).

Daily CH_4 emission, total tract digestibility, microbial diversity, gene abundance and functional abundance data were analysed using the MIXED procedure in SAS software (SAS Institute, Cary, NC, United States). The fixed effects in the model included breed, feeding system; their interaction effect was also analysed. Random effects, including period and animal, were nested within treatments. Ruminal fermentation characteristics were subjected to repeated measures analysis using the SAS PROC MIXED function (Littell et al., 1998). Appropriate covariance structures were obtained based on the Akaike information criterion. Means were calculated using the LSMEANS function, where each animal was considered as an experimental unit. $P < 0.05$ was taken to indicate significant differences according to treatment, and $0.05 < P < 0.1$ was considered to indicate a trend toward significance.

[2]https://huttenhower.sph.harvard.edu/galaxy

RESULTS

Effects of Feeding System and Host Breed on Enteric CH_4 Production and Fermentation

The TMR diet had a higher percentage (99.5%) of particles <1.18 mm in size than the SF diet, whereas the SF diet had a higher percentage (72%) of particles in the size range of 19–8 mm than the TMR diet ($P < 0.05$) (**Table 2**). However, DM and organic matter (OM) intake did not vary between feeding systems (**Table 3**). Similarly, no feed sorting was observed in the SF diet. Holstein steers had higher DMI than Hanwoo steers in the chamber (**Table 3**). In addition, there were significant ($P < 0.05$) interactions between breed and feeding system for DM, OM, and gross energy (GE) intake (**Table 3**) in the chamber. Holstein steers had a greater ($P < 0.05$) ADG than Hanwoo steers (**Table 3**). Although there was no effect on apparent total tract nutrient digestibility ($P > 0.05$; **Table 3**), TMR feeding resulted in greater CH_4 production (g/day) and CH_4 yield per unit of OM, neutral detergent fibre and GE intake than the SF diet in both Holstein and Hanwoo steers ($P < 0.05$; **Table 4**). Hanwoo steers had a higher CH_4 yield than Holstein steers ($P < 0.005$).

The mean concentration of total ruminal VFA did not differ between the experimental treatments ($P > 0.05$; **Table 5**). The steers given the TMR diet had a lower ruminal pH than those given the SF diet ($P = 0.069$), and the proportion of acetate was higher in the rumen fluid of steers given the TMR diet ($P < 0.01$). The proportions of butyrate and isobutyric acid did not vary between feeding systems ($P > 0.05$), whereas the proportions of valerate and isovaleric acid were lower in steers given the TMR than SF diet ($P = 0.001$). Hanwoo steers had a lower propionate and higher butyrate content than Holstein steers ($P < 0.001$). Similarly, the ratio of acetate to propionate in Hanwoo steers was greater than that in Holstein steers ($P < 0.05$). Ruminal NH_3-N concentrations did not vary significantly between feeding systems or breeds.

TABLE 2 | Feed Particle size distribution (%) in different feeding systems.

Particle size (% DM)	TMR	SF	*P*-value
>19 mm	13.8 ± 1.5	28.4 ± 1.9	0.034
19–8.0 mm	18.5 ± 1.2	64.5 ± 2.0	0.003
8.0–1.18 mm	29.1 ± 2.3	7.0 ± 0.4	0.004
<1.18 mm	38.6 ± 2.9	0.2 ± 0.6	0.004

Values are least square means ± standard deviation (n = 3 replications). DM, dry matter; SF, separate feeding; TMR, total mixed ration.

TABLE 3 | Least square means of body weight, nutrient intake and apparent total tract digestibility (%) of Hanwoo and Holstein steers fed by the TMR and SF systems.

Item	Hanwoo		Holstein		SEM	*P*-value		
	TMR	SF	TMR	SF		Breed	FS	Breed × FS
Initial BW, kg	297.2	292.7	305.2	338.2	26.9	–	–	–
Final BW, kg	313.7	297.2	338.2	367.2	29.9	–	–	–
ADG, kg/d	0.6	0.6	1.1	1.0	0.26	0.014	0.411	0.591
Intake (kg/d)								
DM	5.7	5.1	6.4	7.6	0.65	0.093	0.401	0.026
OM	5.3	4.6	6.0	6.9	0.60	0.093	0.841	0.031
NDF	2.2	1.9	2.5	2.7	0.28	0.161	0.540	0.058
ADF	1.1	0.9	1.2	1.3	0.15	0.184	0.736	0.073
CP	0.8	0.7	0.9	1.1	0.09	0.067	0.008	0.013
GEI, MJ/d	103.4	100.1	116.4	149.2	12.50	0.088	0.028	0.015
Digestibility (%)								
DM	50.2	40.1	52.8	53.9	5.07	0.127	0.466	0.319
OM	54.1	41.3	55.9	52.3	6.29	0.310	0.169	0.399
NDF	37.6	37.9	39.9	44.3	4.69	0.437	0.677	0.717
ADF	30.2	32.0	30.9	41.8	5.06	0.391	0.304	0.459
CP	41.9	34.0	43.0	51.6	6.14	0.132	0.954	0.181
GE	56.1	44.5	58.1	55.0	5.93	0.325	0.125	0.322

ADF, acid detergent fibre; ADG, average daily gain; BW, body weight; CP, crude protein; DM, dry matter; FS, feeding system; GEI, gross energy intake; NDF, neutral detergent fibre; OM, organic matter; SF, separate feeding; TMR, total mixed ration. Number of steers = 8.

TABLE 4 | Least square means of methane production recorded in Hanwoo and Holstein steers fed with TMR and SF diets over 24 h.

Item	Hanwoo		Holstein		SEM	*P*-value		
	TMR	SF	TMR	SF		Breed	FS	Breed × FS
CH_4, g/d	135.4	96.1	100.0	78.8	6.3	0.024	<0.0001	0.061
CH_4, g/kg DMI	23.9	19.5	15.7	10.9	1.2	0.001	0.021	0.853
CH_4, g/kg OMI	25.6	21.5	16.9	12.1	1.3	0.001	0.029	0.776
CH_4, g/kg DOM	47.9	32.7	30.6	20.7	2.6	0.001	0.004	0.325
CH_4, g/kg NDFI	62.4	55.2	41.1	30.5	4.5	0.003	0.091	0.680
CH_4, g/kg DNDF	177.1	114.3	109.7	74.5	16.2	0.006	0.010	0.412
MCR	7.4	5.5	4.9	3.1	0.4	0.001	0.009	0.894
EF	49.4	35.1	36.5	28.8	2.3	0.024	<0.0001	0.074

DMI, dry matter intake; DNDF, digestible NDF; DOM, digestible organic matter; EF, emission factor (CH_4 kg/head/yr); FS, feeding system; GEI, gross energy intake; MCR, metabolic conversion ratio (CH_4 energy expressed as %GEI); NDFI, neutral detergent fibre intake; OMI, organic matter intake; SF, separate feeding; TMR, total mixed ration.
Number of steers = 8.

Effects of Feeding System and Host Breed on Rumen Bacterial/Archaeal Richness, Diversity, Composition, and Core Microbiome

At a depth of 10,000 quality reads, an average of 806 OTUs (range: 503–907 OTUs) were generated (**Supplementary Figure 1**). There were no differences ($P > 0.05$) in richness or diversity indices between the feeding systems. Differences in alpha diversity metrics, including observed OTUs ($P < 0.05$), Chao1 index ($P = 0.083$) and Shannon index ($P < 0.05$), were detected between breeds, demonstrating greater richness and diversity in Hanwoo steers (**Figure 1** and **Supplementary Table 1**).

The relative abundance of the bacterial genus *Prevotella* (18.6–33.2%) was high in all samples (**Figure 2** and **Supplementary Table 2**). Similarly, the archaeal genus *Methanobrevibacter* (0.5–1.3%) was also abundant. The core microbiome across the different feeding systems and cattle breeds used in this study consisted of 49 identified and 37 unclassified genera, which together accounted for 98.74% of the total rumen microbial population (**Supplementary Figure 2**). When individual groups were analysed for core taxa, Holstein steers given the SF diet were found to possess a small, distinctive core microbiome, including three additional genera (*Acidaminococcus*, *Aequorivita*, and *B42*), which were found to be unique (**Supplementary Table 3**). Similarly, Acholeplasmatales unclassified and *Megasphaera* were identified as being unique to the Hanwoo steers and SF system, respectively.

The LEfSe analysis identified several OTUs that differed significantly between breeds ($P < 0.05$ and LDA > 2.0), indicating that they were robust biomarkers (**Figure 3**). The OTUs in the kingdom Archaea, phylum Euryarchaeota, families Methanomassiliicoccaceae and Methanobacteriaceae and the genera vadinCA11 and *Methanobrevibacter* were significantly more enriched in Hanwoo steers than Holstein steers. Several other families, including Spirochaetaceae, BS11 and Lachnospiraceae, were also identified as biomarkers in Hanwoo steers. A PCA biplot clustered all samples into two groups to explore the correlations with mean taxonomic annotation, CH_4 yield and other fermentation parameters (**Supplementary Figure 3**).

Effects of Feeding System and Host Breed on the Rumen Microbiome

Both feeding system and breed were found to have a significant effect on microbial composition at the phylum and genus levels ($P < 0.05$; **Table 6**). The feeding system × breed interaction effect on the rumen microbiome in relation to methanogenesis was significant ($P < 0.05$). Notably, the TMR system increased the archaea/bacteria ratio and abundances of the phylum Euryarchaeota and genus *Methanobrevibacter* in Hanwoo steers to a greater extent than in Holstein steers.

Co-occurrence of Rumen Microbes in Steers Varied by Feeding System and Host Breed

Strong associations of hydrogenotrophic *Methanobrevibacter* and methylotrophic *Methanosphaera* with *Butyrivibrio* were detected in Holstein steers given the TMR diet ($\tau = 1$, $P < 0.05$; **Figure 4B**). Strong associations were also detected between vadinCA11 and *Ruminococcus* ($\tau = 1$, $P < 0.05$) in TMR-fed Hanwoo steers (**Figure 4A**), and between pectinolytic *Sphaerochaeta* and vadinCA11 ($\tau = 1$, $P < 0.05$) in the TMR diet Holstein steers (**Figure 4B**). In contrast, in the SF Holstein steers (**Figure 4D**), we detected trends toward negative associations of *Methanobrevibacter* and vadinCA11 with *Anaerostipes*, *Coprococcus*, *Anaerovibrio*, *Prevotella*, *Pyramidobacter*, and *Succiniclasticum* ($\tau = -0.91$, $P = 0.063$). In SF Hanwoo steers (**Figure 4C**), negative associations were observed between

TABLE 5 | Effects of feeding system and host breed on ruminal fermentation characteristics[a].

Item	Hanwoo						Holstein						SEM	*P*-value		
	TMR			SF			TMR			SF				Breed	FS	Breed × FS
	0 h	1.5 h	3 h	0 h	1.5 h	3 h	0 h	1.5 h	3 h	0 h	1.5 h	3 h				
pH	7.0	6.7	6.6	6.9	6.7	6.7	6.9	6.5	6.2	6.9	6.7	6.6	0.17	0.162	0.028	0.247
Total VFA, mM	86.7	110.6	112.3	81.4	103.6	101.6	80.7	110.1	105.7	55.3	108.9	113.6	8.51	0.457	0.168	0.888
VFA,%																
Acetate	46.8	43.0	44.5	44.8	42.4	43.5	46.5	42.0	42.8	44.5	38.1	37.9	1.57	0.210	0.001	0.073
Propionate	23.5	26.4	25.4	22.8	25.3	24.7	28.2	28.8	28.4	30.3	36.5	37.5	2.28	<0.0001	0.041	0.009
Isobutyrate	1.9	1.7	1.5	2.3	1.8	1.7	1.9	1.8	1.6	2.3	1.5	1.3	0.18	0.647	0.356	0.083
Butyrate	24.3	25.1	24.9	25.8	26.0	26.0	19.6	22.8	22.9	17.8	18.5	18.2	2.26	0.001	0.255	0.035
Isovalerate	2.0	1.9	1.7	2.7	2.5	2.1	2.4	2.7	2.3	3.0	2.6	2.0	0.22	0.051	0.001	0.006
Valerate	1.6	2.0	1.9	1.7	2.1	2.0	1.4	1.9	1.9	2.1	2.9	3.0	0.27	0.015	0.000	0.002
Acetate:propionate	2.0	1.6	1.8	2.0	1.7	1.8	1.7	1.5	1.5	1.5	1.1	1.1	0.13	<0.0001	0.042	0.021
NH_3-N, mg/dL	7.8	18.1	13.4	10.6	17.6	11.5	6.9	19.3	13.2	4.0	11.4	8.9	2.45	0.096	0.081	0.068

FS, feeding system; SF, separate feeding; TMR, total mixed ration.
a Values are least square means with standard error.
Number of steers = 8.

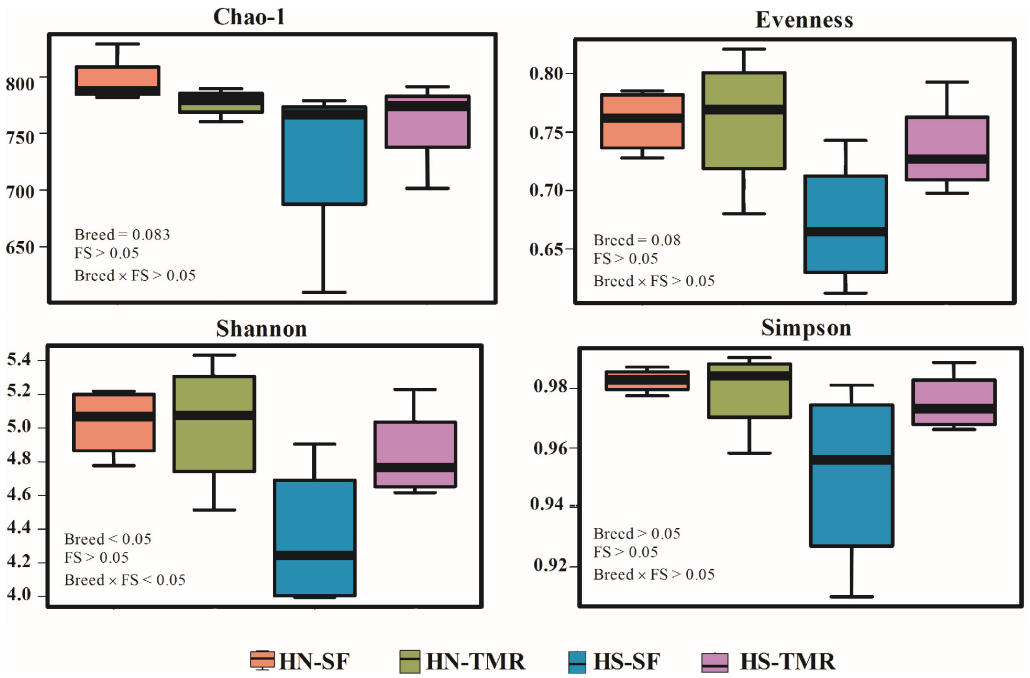

FIGURE 1 | Alpha diversity metrics of the bacterial/archaeal composition in the rumen of Hanwoo (HN) and Holstein (HS) steers fed a total mixed ration (TMR) or separate feed (SF) diet.

Methanobrevibacter and *Sharpea*, and between *Anaerostipes* and *Butyrivibrio* ($\tau = -1$, $P < 0.05$).

Predicted Molecular Functions of Steer Rumen Microbiota Varied by Feeding System and Host Breed

A total of 430 genes (**Supplementary Table 4**) and 49 gene families (**Supplementary Table 5**) differed between feeding systems or breeds ($P < 0.1$). The genes *pyruvate kinase* (*pyk*), K00873 ($P < 0.05$); *branched-chain amino acid transport system permease protein* (*livM*), K01998 ($P < 0.05$); *anaerobic carbon-monoxide dehydrogenase catalytic subunit* (*cooS*), K00198; and *F-type H^+-transporting ATPase subunits* (*atpA–G*), K02110 ($P = 0.053$) were abundant in the SF system. *Pyruvate ferredoxin oxidoreductase alpha subunit* (*porA*), K00169 ($P = 0.076$) and *cobalt/nickel transport system permease protein* (*cbiM*), K02007 ($P = 0.083$) were enriched in Hanwoo steers.

Pathways related to CH_4 metabolism ($P = 0.050$) and butanoate metabolism ($P < 0.05$) were enriched in the rumen of

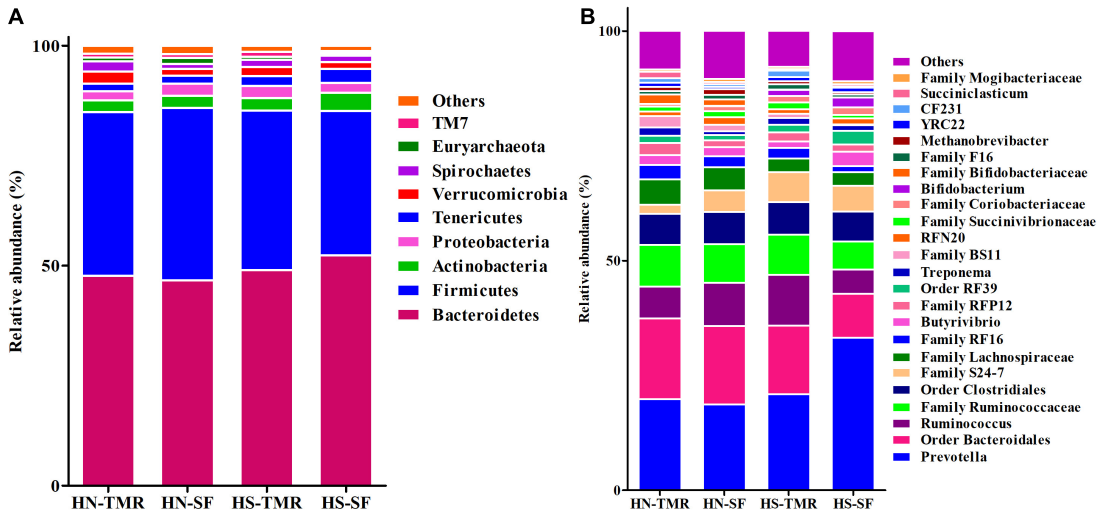

FIGURE 2 | Taxonomic profiles of the relative phylum-level **(A)** and genus-level **(B)** abundances of bacteria and archaea in both Hanwoo (HN) and Holstein (HS) steers fed by different feeding systems, with a classification criterion of >0.5% of the total sequence.

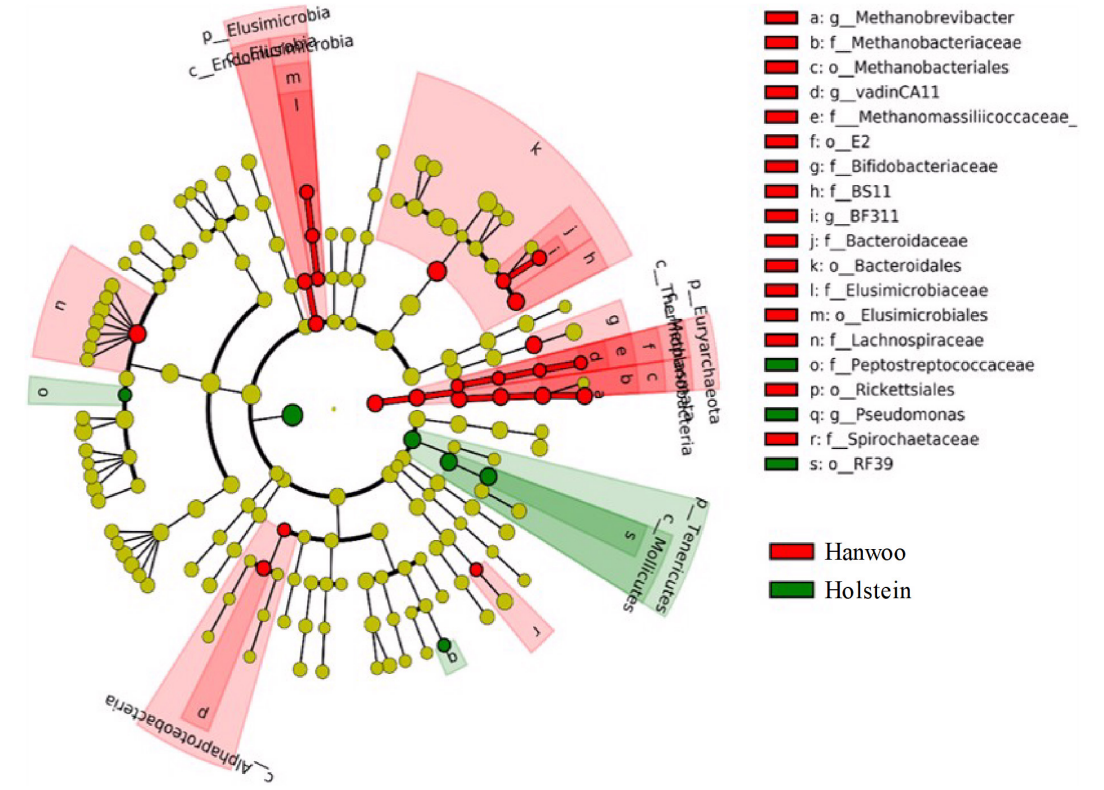

FIGURE 3 | LDA effect size (LEfSe) cladogram demonstrating taxonomic differences between the Hanwoo and Holstein breeds. Taxa enriched in the rumen of Holstein steers are indicated by a positive LDA score (green), while taxa enriched in the rumen of Hanwoo steers have a negative score (red). Only taxa meeting an LDA significance threshold of 2 and $P < 0.05$ are shown.

Hanwoo steers, whereas those related to the purine metabolism pathway ($P = 0.090$) were abundant in Holstein steers. CCA of the relative abundance values of KEGG pathways of genes from the rumen microbiota showed distinct clustering of Hanwoo and Holstein cattle given the TMR and SF diets, explaining 32% of the variance (**Figure 5**). Genes related to CH_4 metabolism ($P = 0.050$), pyruvate metabolism ($P = 0.069$), the bacterial secretion system ($P < 0.05$), and fatty acid biosynthesis

TABLE 6 | Relative abundance of taxa in the Hanwoo and Holstein steers fed by different feeding systems.

Classification	Total Sequences (%)				SEM	*P*-Value			Function
	Hanwoo		Holstein						
	TMR	SF	TMR	SF		Breed	FS	Breed × FS	
Archaea: Bacteria	0.010	0.014	0.007	0.005	0.003	0.022	0.787	0.041	
Phylum level									
Euryarchaeota	0.942	1.358	0.729	0.527	0.300	0.022	0.790	0.041	Hydrogenotrophic, H_2 (U)
Fibrobacteres	0.270	0.222	0.610	0.208	0.117	0.188	0.079	0.156	Cellulolytic, acetate, formate, lactate (P)
Planctomycetes	0.191	0.480	0.136	0.247	0.069	0.062	0.016	0.221	NH_3 oxidation, N_2 (P)
Synergistetes	0.045	0.044	0.012	0.026	0.008	0.011	0.472	0.153	Saccharolytic
Genus/family level									
Ruminococcus	6.945	9.381	11.037	5.320	2.024	0.994	0.433	0.067	Cellulolytic, acetate, formate, lactate (P)
Coriobacteriaceae	0.518	1.046	1.395	1.615	0.352	0.093	0.401	0.639	Acetate and lactate (P)
Bifidobacteriaceae	2.063	1.412	0.038	0.082	0.555	0.057	0.392	0.335	Acetate and lactate (P)
Methanobrevibacter	0.874	1.297	0.697	0.500	0.292	0.025	0.773	0.046	Hydrogenotrophic, H_2 (U)
CF231	1.026	0.618	1.367	0.264	0.382	0.975	0.256	0.094	Proteolytic, NH_3 (P)
Succiniclasticum	1.370	0.485	0.330	0.461	0.299	0.099	0.225	0.113	Succinate (U), propionate (P)
Christensenellaceae	0.385	0.436	0.388	0.148	0.194	0.453	0.326	0.045	Fibre degrader
Fibrobacter	0.270	0.222	0.610	0.208	0.117	0.188	0.079	0.156	VFA (P)
p-75-a5	0.240	0.360	0.449	0.170	0.065	0.886	0.244	0.009	Fibrolytic
Pirellulaceae	0.191	0.480	0.135	0.247	0.070	0.061	0.016	0.222	NH_3 oxidation, N_2 (P)
Lactobacillus	0.056	0.580	0.112	0.079	0.116	0.060	0.240	0.031	Lactate (P)
BF311	0.289	0.254	0.127	0.088	0.077	0.053	0.625	0.979	Lignocellulose digestion
Selenomonas	0.406	0.081	0.107	0.042	0.081	0.060	0.035	0.133	Acetate, propionate, formate, lactate (P)
Bulleidia	0.031	0.044	0.028	0.506	0.153	0.062	0.420	0.048	Acetate, lactate, succinate (P)
Anaerovibrio	0.253	0.057	0.077	0.052	0.041	0.031	0.012	0.039	Succinate, propionate (P)
Desulfovibrio	0.126	0.065	0.051	0.112	0.039	0.676	0.990	0.086	Sulphur oxidation
Clostridiaceae	0.062	0.114	0.067	0.081	0.016	0.506	0.030	0.163	Glucose assimilation
Lachnospira	0.012	0.010	0.002	0.266	0.095	0.083	0.398	0.062	Acetate, formate, lactate (P)
Bacteroides	0.014	0.134	0.090	0.009	0.037	0.483	0.674	0.051	VFA (P)
Enterobacteriaceae	0.025	0.081	0.041	0.035	0.025	0.372	0.536	0.077	N_2 fixation
Atopobium	0.020	0.046	0.026	0.046	0.008	0.738	0.020	0.717	Lactate (P)
Spirochaetaceae	0.053	0.042	0.028	0.008	0.016	0.014	0.053	0.535	Pectinolytic, Formate, acetate, lactate (P)
vadinCA11	0.052	0.040	0.015	0.013	0.007	0.007	0.420	0.472	Methylotrophic
Pseudomonas	0.011	0.018	0.018	0.070	0.015	0.025	0.282	0.030	Degrader
Dehalobacterium	0.031	0.052	0.026	0.007	0.024	0.400	0.910	0.078	H_2 oxidation
Peptostreptococcaceae	0.003	0.007	0.030	0.074	0.023	0.081	0.476	0.104	N.I.
Pyramidobacter	0.033	0.030	0.010	0.026	0.008	0.059	0.528	0.092	Iso-fatty acids (P)
Weissella	0.016	0.043	0.014	0.016	0.008	0.122	0.030	0.050	Lactate (P)
Leuconostoc	0.012	0.026	0.009	0.009	0.009	0.373	0.429	0.041	Lactate (P)

The table only includes taxa represented in >0.01% of the total sequences that tended to differ (0.05 < P < 0.1) and showed significant differences (P < 0.05).
FS, feeding system; N.I., no information; P, producer; SF, separate feeding; TMR, total mixed ration; U, utiliser; VFA, volatile fatty acids.
Data are least square means with standard error.
Number of steers = 8.

(P = 0.089) were enriched in Hanwoo steers given the SF diet compared to Holstein steers given the SF diet (**Figure 6**).

Association Between Microbial Gene Abundance and Steer Rumen CH_4 Production Varied by Feeding System and Host Breed

A total of 44 genes were strongly correlated with CH_4 production, of which 17 were positively correlated and 27 were negatively correlated (**Supplementary Table 6**). The relative abundances of genes associated with CH_4 production are presented as a heatmap, which clearly showed that most genes positively and negatively correlated with CH_4 emissions were enriched in TMR Hanwoo and SF Holstein cattle, respectively (**Figure 7**). The genes *pyruvate ferredoxin oxidoreductase gamma subunit* (porG), K00172 (τ = 0.50, P = 0.006); *trimethylamine-corrinoid protein* (mttC), K14084 (τ = 0.76, P < 0.001); cbiM, K02007 (τ = 0.39, P = 0.004); *V/A-type H^+/Na^+-transporting ATPase subunit* (atpA), K02117 (τ = 0.47, P = 0.001); pyk, K00873

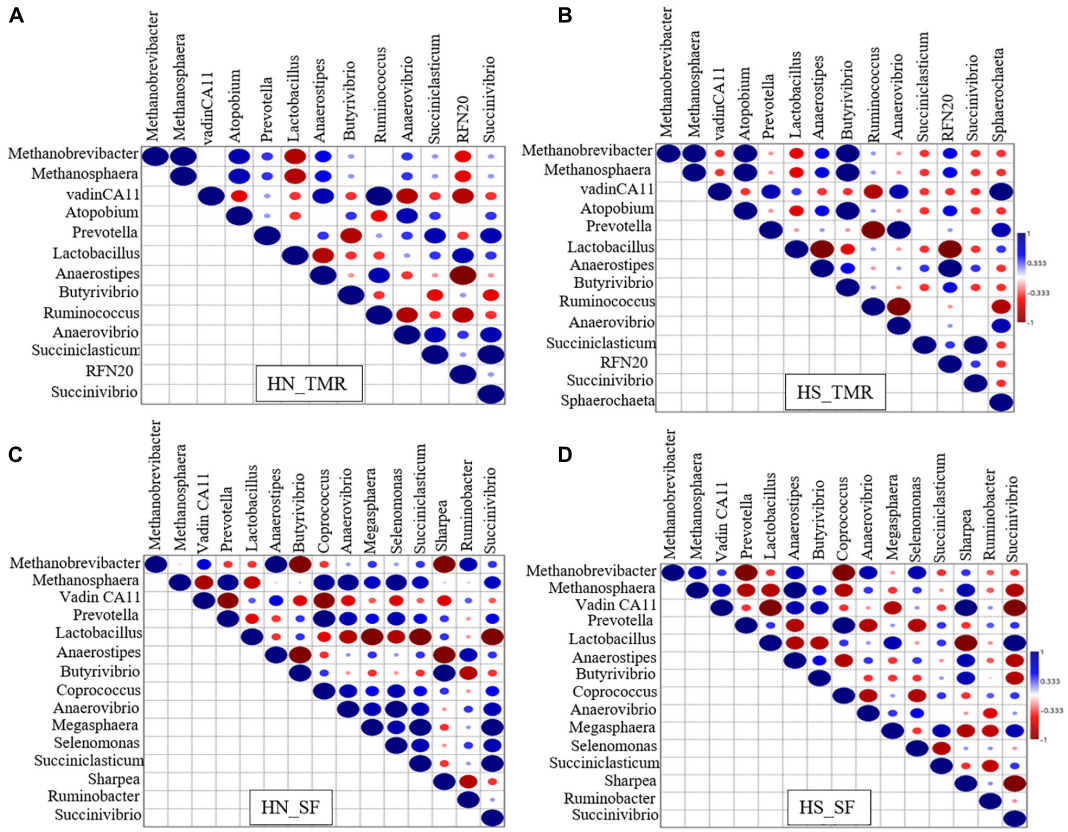

FIGURE 4 | Kendall rank correlation analysis of the co-occurrences of microbial lineages. **(A)** Hanwoo (HN) steers fed a total mixed ration (TMR) diet. **(B)** Holstein (HS) steers given TMR diet. **(C)** Hanwoo (HN) steers given separate feed (SF) diet. **(D)** Holstein (HS) steers given SF diet. The genera were included in the matrix if they had a relative abundance of at least 0.01% in at least one steer. Correlation strength is indicated by the intensity of the colour. The scale colours denote whether the correlation is positive (closer to 1, blue Spheres) or negative (closer to −1, red Spheres). Big sphere indicates that the correlation is significant ($P < 0.05$).

($\tau = -0.41$, $P = 0.003$); and *acetate kinase* (*ackA*), K00925 ($\tau = -0.46$, $P = 0.001$) were found to be involved in pyruvate/CH_4 metabolism, exhibiting significant associations with CH_4 yield. Among these genes, porG ($P = 0.076$) and cbiM ($P = 0.083$) were enriched in Hanwoo steers (**Figure 8**).

Association Among Rumen CH_4 Production, Microbial Abundance, Functional Abundance, and Metabolites

We detected associations ($P < 0.1$) among several variables (**Figure 9** and **Supplementary Tables 7, 8**). Notably, archaeal genera *Methanobrevibacter* ($\tau = 0.31$, $P = 0.094$), vadinCA11 ($\tau = 0.41$, $P < 0.05$) and the archaea:bacteria ratio ($\tau = 0.33$, $P = 0.078$) were positively associated with the CH_4 yield and CH_4 metabolism pathway. *Fibrobacter* ($\tau = -0.46$, $P < 0.05$), *Anaerovibrio* ($\tau = -0.51$, $P < 0.05$), *Selenomonas* ($\tau = -0.59$, $P < 0.005$) and *Succiniclasticum* ($\tau = -0.25$, $P = 0.077$) were negatively associated with the acetate:propionate ratio in the rumen. The CH_4 metabolism ($\tau = 0.43$, $P < 0.05$), purine metabolism (Kendall's $\tau = -0.42$, $P < 0.05$) and C_5 branched dibasic acid metabolism ($\tau = 0.47$, $P < 0.05$) pathways were associated with CH_4 yield.

DISCUSSION

Consistent with several previous reports, neither feeding system nor breed had any effect on total tract digestibility in the present study (Holter et al., 1977; Yan et al., 1998; Huuskonen et al., 2014). However, a recent study (Genís et al., 2021) reported increases in DM and CP digestibility in animals fed with the SF diet compared to the TMR diet using unprocessed long straw for which more than 70% of particles were >19 mm. However, this cannot be compared with the present study where the proportion of feed particles >19 mm was only 28%. Furthermore, in the present study, the ruminal pH of Holstein steer at 3 h post-TMR feeding was inconsistent with our previous study, which showed that the TMR diet helped to maintain ruminal pH (Bharanidharan et al., 2018). This may have been due to the 40-min delay in feeding of the concentrate to the SF animals, where the presence of sodium bicarbonate in the concentrate may have had a longer-duration stabilising effect on the rumen pH compared to TMR feeding. Furthermore, in the present study, rumen sampling was limited to 3 h, where the SF group may have experienced a further decrease in pH compared to the TMR diet in the later feeding period. In addition, in the TMR feeding system, feed particles <8 mm accounted for almost 70% of the total feed,

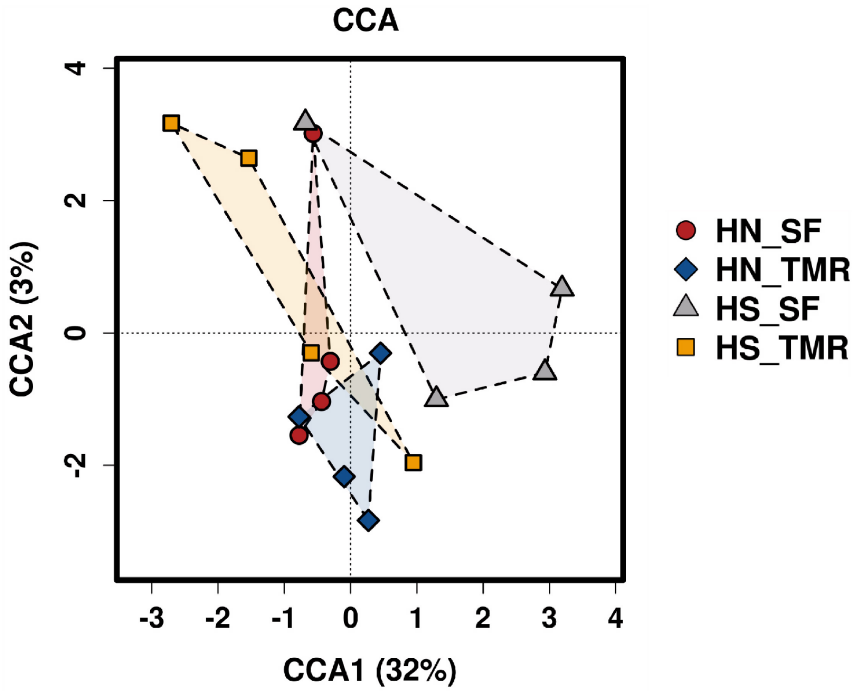

FIGURE 5 | Canonical correspondence analysis (CCA) of microbial functional diversity in the rumen of Hanwoo (HN) and Holstein (HS) steers fed a total mixed ration (TMR) or separate feed (SF) diet.

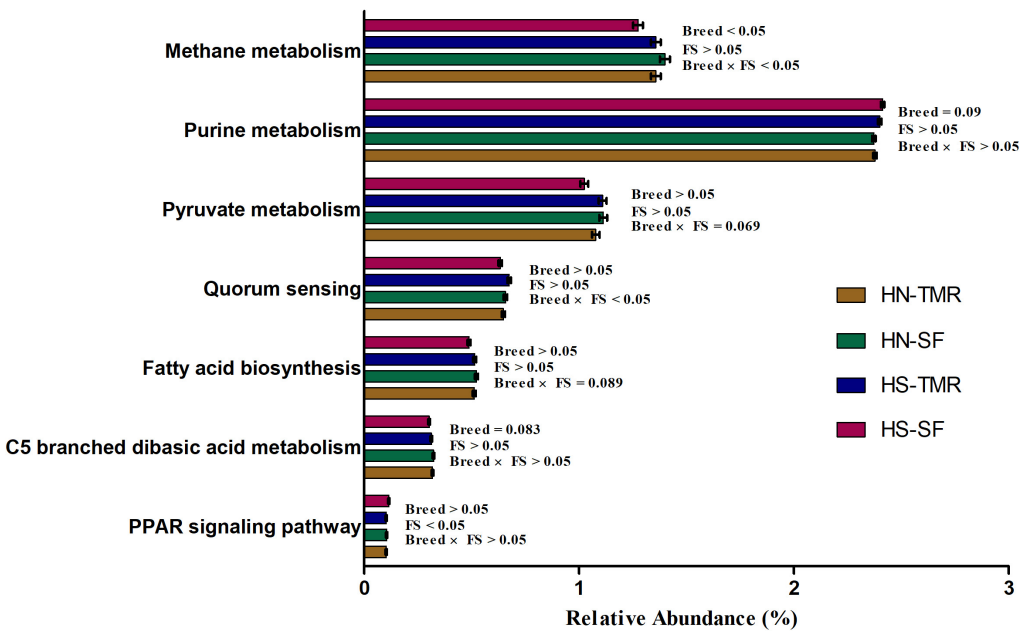

FIGURE 6 | Variations in important rumen microbial Kyoto Encyclopaedia of Genes and Genomes (KEGG) metabolic pathways related to methane emissions in Hanwoo (HN) and Holstein (HS) steers fed a total mixed ration (TMR) or separate feed (SF) diet.

which may have decreased the amount of time spent chewing and the ruminal pH during the initial phase of feeding (Krause et al., 2002). However, a recent study (Genís et al., 2021) noted no change in rumination or chewing activity between animals given the TMR and SF diets, although there were large variations in ruminal pH. Several studies have also reported no changes in ruminal pH in association with TMR feeding or feed particle size (Li et al., 2003; Schroeder et al., 2003; Liu et al., 2015).

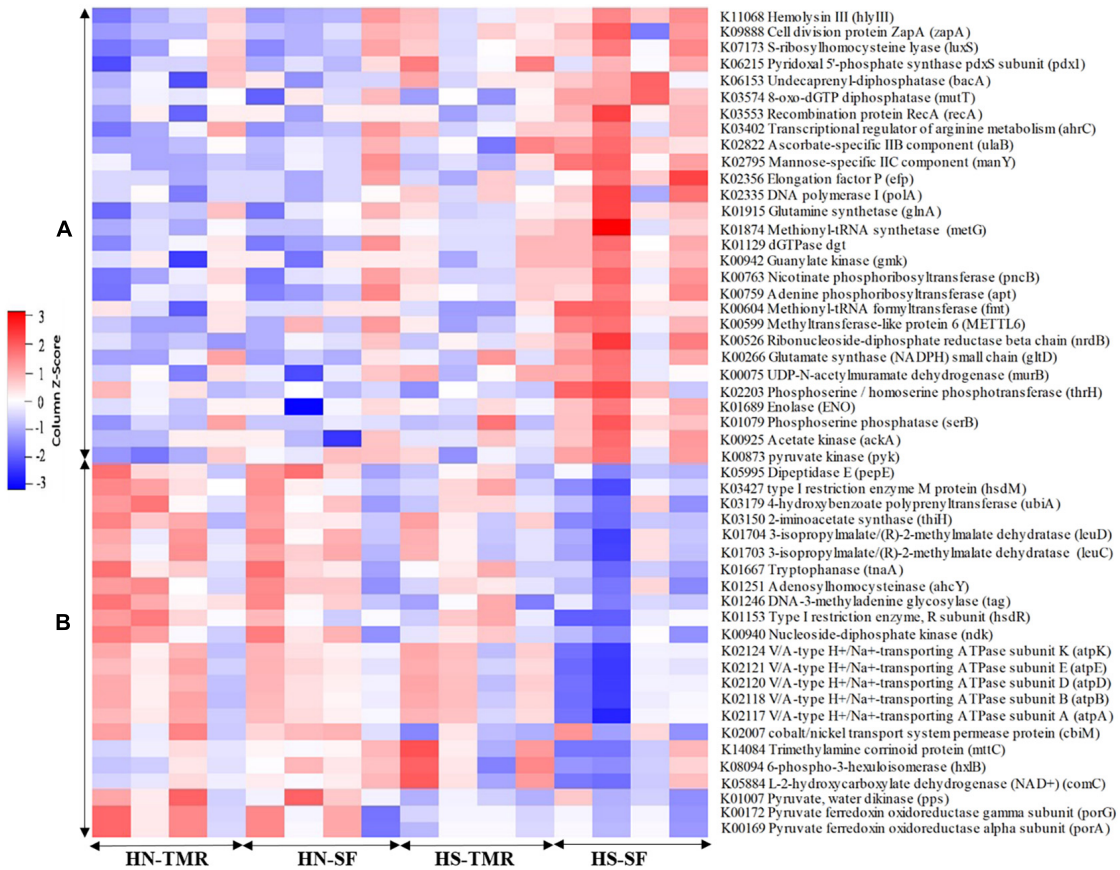

FIGURE 7 | Heatmap of the relative abundance of microbial genes negatively **(A)** and positively **(B)** associated with methane production, as identified by Kendall rank correlation analysis. The scale colours denote whether the abundance is high (closer to 1, red squares) or low (closer to −1, blue squares).

Nutrition, feeding management, and animal production strategies for reducing enteric CH_4 emissions may be more effective than strategies using feed additives as rumen modifiers (reviewed by Knapp et al., 2014). This is because a few rumen modifiers have been shown to be associated with adverse effects on rumen microbial fermentation, digestibility, residues in livestock products and adaptation to microbes on prolonged feeding at effective concentrations (reviewed by Honan et al., 2021). In this study, TMR feeding resulted in greater CH_4 production and yield, consistent with the findings of our previous study (Bharanidharan et al., 2018). This may be related to the larger and smaller proportions of acetate and propionate, respectively, in the TMR diet, suggesting that there were fewer beneficial hydrogenotrophic reactions in the TMR system (Moss et al., 2000). Our observations contradicted earlier reports (reviewed by Janssen, 2010) that smaller particle sizes and higher passage rates were associated with a higher rumen H_2 concentration, so that negative thermodynamic feedback reduces the production of H_2 by fermentative microbes, resulting in increased propionate formation and ultimately reduced CH_4 formation. Although the ruminal turnover rate was not evaluated in the present study, we postulated that the time lag between forage and concentrate feeding in the SF diet may have increased the feed passage rate compared to the TMR diet, thereby increasing propionate production and reducing CH_4 production (Janssen, 2010). However, the limited effects of passage rate on total tract digestibility in the present study could have been due to post-ruminal compensatory digestion (Hoover, 1978). The increased proportions of isovaleric acid and valerate in the rumen of steers with the SF diet were consistent with the results of a previous study suggesting increased ruminal protein digestion (Allison and Bryant, 1963). The effects of iso-fatty acids on the synthesis of branched-chain amino acids and microbial protein depends on a wide range of hydrogenation and carboxylation reactions, which probably affect methanogenesis (Bharanidharan et al., 2018). Numerous studies have reported advantages of iso-fatty acids, in terms of rumen microbial status (Liu et al., 2014), microbial protein synthesis (Kim et al., 2005), lactation performance (Liu et al., 2018), and nutrient utilisation (Misra and Thakur, 2001). Molecular analysis of the rumen contents of feedlot beef steers also revealed increased valerate concentrations in animals with improved feed efficiency (Guan et al., 2008). However, the lack of difference in ADG between feeding systems suggested a need for more studies focusing on the effects of the SF system on animal performance.

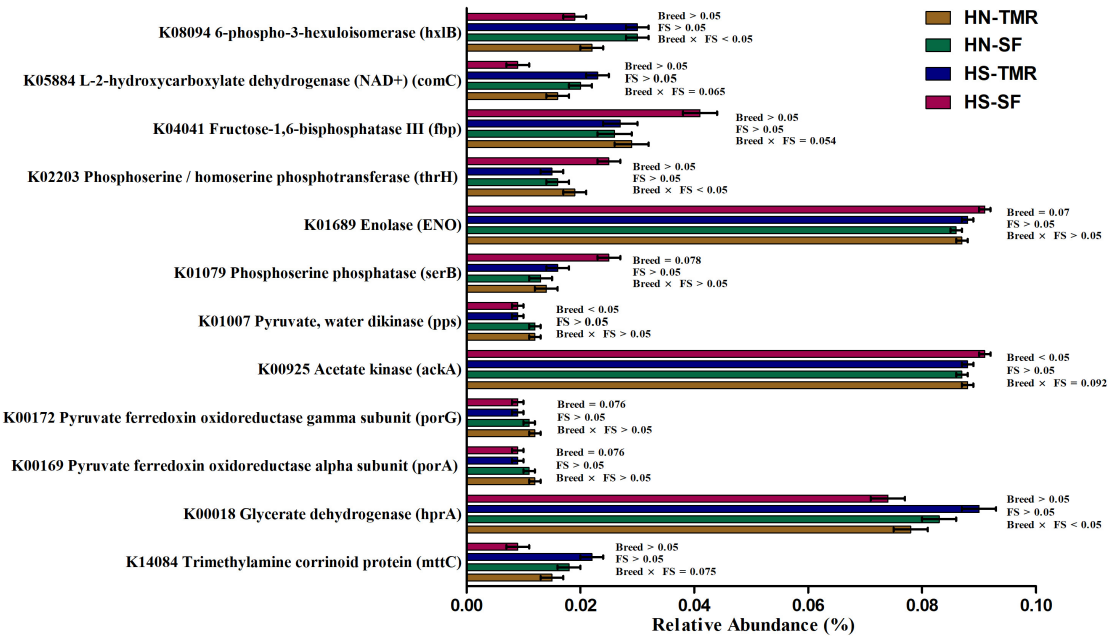

FIGURE 8 | The metagenomic abundance of key genes involved in the methane metabolism pathway that tend to differ ($0.05 < P < 0.1$) or were significantly different ($P < 0.05$) between Hanwoo (HN) and Holstein (HS) steers fed a total mixed ration (TMR) or separate feed (SF) diet.

The lower ADG observed in Hanwoo steers in the present study may have been related to the greater rumen microbial richness. An earlier study (Shabat et al., 2016) reported an association between greater microbial richness and inefficiency in cattle. Similarly, another study (Kang et al., 2005) suggested that Hanwoo steers may be inefficient when compared to Holstein steers, consistent with the results of this study. The robust rumen microbial biomarkers identified by LEfSe analysis in the present study indicated enrichment of several archaeal genera in Hanwoo steers compared to Holstein steers. This is consistent with a previous study (Lee et al., 2012), which reported a larger archaeal population in the rumen of Korean Hanwoo steers than Holstein dairy cows. We also detected a strong positive association of the archaea:bacteria ratio with CH_4 yield, which is regarded as a proxy for CH_4 emissions, regardless of cattle breed or diet (Wallace et al., 2015a; Auffret et al., 2018). In the present study, the most abundant archaeal taxa (*Methanobrevibacter*) was also positively associated with CH_4 yield, consistent with previous reports of its higher abundance in high CH_4 emitters (Wallace et al., 2015a; Auffret et al., 2018). The greater abundances of Methanomassiliicoccaceae and vadinCA11 in the rumen of Hanwoo steers indicated higher methylamine/methanol-mediated CH_4 production (Paul et al., 2012). A previous study (Lee et al., 2012) also noted a higher concentration of methylamine in the rumen of Hanwoo steers than Holstein dairy cows. This was further supported by the higher abundances of pectinolytic Lachnospiraceae (Dusková and Marounek, 2001) and Spirochaetaceae (Ziołecki and Wojciechowicz, 1980), which may increase methylamine/methanol concentrations *via* the fermentation of digested pectin (Schink and Zeikus, 1980). Furthermore, this hypothesis was supported by the positive associations among vadinCA11, *Sphaerochaeta* and CH_4 yield, and a recent study that revealed strong positive associations of *Sphaerochaeta* and BS11 with CH_4 production (Difford et al., 2018).

Although a difference in microbial abundance was observed between breeds in this study, the feeding system did not significantly influence the major rumen microbiome. However, it did affect minor genera, such as *Atopobium* and *Weissella*, which are efficient lactate producers (Zhou et al., 2004; Abriouel et al., 2015) enriched in the animals given the SF diet. Enrichment of the *lactyl-CoA dehydrogenase* (*lcdA*) gene has been observed in *Megasphaera* spp., in low CH_4 emitters that produce propionate from lactate *via* the acrylate pathway in the rumen (Counotte et al., 1981). Our core microbiome analysis only identified *Megasphaera* in steers given the SF diet, which may be related to their higher propionate content. Similarly, enrichment of lactate-producing *Sharpea* has been observed in the rumen of low CH_4-emitting sheep (Kamke et al., 2016). Intriguingly, in the present study, a strong negative association was detected between *Sharpea* and *Methanobrevibacter* in Hanwoo steers given the SF diet, suggesting competitive utilisation of H_2. Although increased CH_4 production in the TMR system may be related to an increased ruminal H_2 concentration, there were no differences in methanogen populations between the feeding systems. Similarly, the observed interaction between feeding system and breed for the total population of Euryarchaeota and *Methanobrevibacter* did not have a large influence on total CH_4 yield. Many studies have failed to detect correlations between overall methanogen abundance and CH_4 emissions (reviewed by Tapio et al., 2017). Therefore, further studies

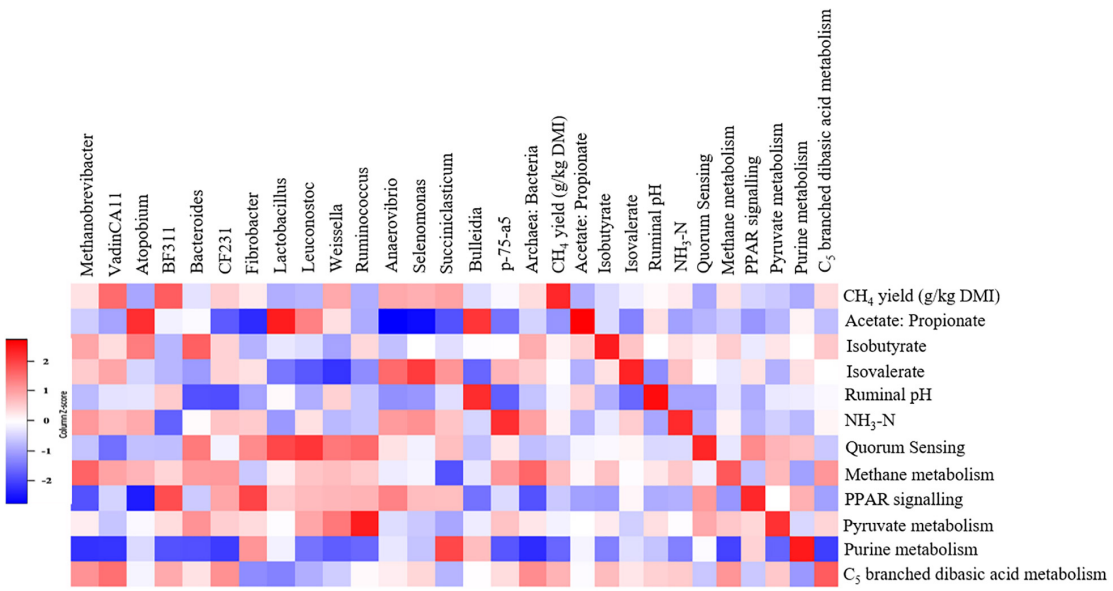

FIGURE 9 | Associations among methane yield, fermentation parameters, rumen microbes, and metabolic pathways in steers. The genera and metabolic pathways were included in the matrix if they were differentially abundant ($P < 0.1$) and had at least 0.01% relative abundance in at least one of the steers. Correlation strength is indicated by the intensity of the colour. The scale colours denote whether the correlation is positive (closer to 1, red squares) or negative (closer to −1, blue squares).

are needed to investigate other feeding variables, such as feeding behaviour (e.g., chewing activity), ruminal digestion and passage rate, which may provide a plausible explanation for the observed effects.

Despite the negligible differences in the microbiome, there were distinct microbial co-occurrences between the TMR and SF systems, which provided a plausible explanation for the observed differences in CH_4 production. For example, the genera *Anaerostipes*, *Coprococcus*, *Anaerovibrio*, *Prevotella* and *Succiniclasticum*, which are involved in propionate production (Strobel, 1992; Van Gylswyk, 1995; Kishimoto et al., 2006; Privé et al., 2013; Reichardt et al., 2014), were negatively associated with hydrogenotrophic *Methanobrevibacter* in the Holstein steers given the SF diet, which clearly demonstrated the low availability of H_2 for methanogenesis. The observed negative correlations of both *Anaerovibrio* and *Succiniclasticum* with the acetate:propionate ratio further supports this finding. *Megasphaera* and *Coprococcus* are more abundant in the rumen of efficient animals (Shabat et al., 2016), which may be related to the increased propionate and ADG in Holstein steers seen in the present study. Strong positive associations of the H_2-producing bacteria *Ruminococcus* and *Butyrivibrio*, with vadinCA11 and *Methanobrevibacter*, respectively, were observed in the TMR feeding system, indicating that methanogenesis was the major H_2 sink (Wolin et al., 1997).

Numerous studies have shown that microbes distributed in the rumen operate as an integrated system and have roles in the complex metabolic processes occurring within this ecosystem (Auffret et al., 2018; Wirth et al., 2018). The observed variations in H_2 thermodynamics associated with changes in microbial abundances, and co-occurrences in breeds or feeding systems, reflect the predicted metabolic processes. The positive associations among the relative contents of isovalerate in the rumen, C_5 branched dibasic acid metabolism pathway and CH_4 metabolism pathway with CH_4 yield clearly demonstrated a role of iso-fatty acids in CH_4 production, as discussed in our previous report (Bharanidharan et al., 2018). The large abundance of genes encoding branched-chain amino acid transport system permease protein subclasses, *livH* (K01997) and *livM* (K01998) in the rumen of steers given the SF diet may have aided transport of branched-chain amino acids (Belitsky, 2015), in accordance with the increased and decreased iso-fatty acid and CH_4 production in the rumen, respectively (Allison and Bryant, 1963). This hypothesis was supported by the associations among *Methanobrevibacter*, vadinCA11 and the C_5 branched dibasic acid metabolism pathway in the rumen. Similarly, genes involved in pyruvate metabolism were strongly associated with the CH_4 metabolism pathway, demonstrating their indirect roles in methanogenesis. The gene *ackA*, which produces acetyl phosphate by utilising acetate, and the genes *serB* and *thrH*, which produce serine by utilising H_2, were negatively associated with CH_4 production and enriched in low-emitting Holstein steers. In contrast, *porA* and *porG*, which are involved in acetyl-coA synthesis from pyruvate, leading to CO_2 and H_2 production, were positively associated with CH_4 production and were abundant in high-emitting Hanwoo steers. These results clearly explain the differential patterns of pyruvate metabolism, H_2 production and sinks between high- and low-emitting breeds detected in the present study. Similarly, Hanwoo steers showed abundant expression of cbiM, which helps to provide Ni to Ni-dependent methyl reductases and is correlated with methylamine/methanol-mediated CH_4

production. Although no association was detected with CH_4 yield, the gene *cooS*, which is involved in reductive acetogenesis (Wood et al., 1986), and *atpA–G*, which are involved in energy synthesis, were enriched in the SF system. All genes associated with methanogenesis in the present study were previously reported as potential metagenomic biomarkers of CH_4 emission or feed efficiency (Wallace et al., 2015b; Roehe et al., 2016; Auffret et al., 2018; Lima et al., 2019), and could be used for the genetic selection of low-emitting animals. However, genes such as *methyl-coenzyme M reductase alpha subunit* (*mcrA*), *formylmethanofuran dehydrogenase subunit B* (*fmdB*) and *formate dehydrogenase alpha subunit* (*fdhF*), which are directly involved in the final step of methanogenesis leading to CH_4 emission, were not identified in the present study. This could be attributed to the slightly higher (0.18 ± 0.04 SD) nearest sequence taxon index (NSTI) noted in the present study, thereby suggesting that functions based on 16S rRNA information have limitations, such that PICRUSt results should be interpreted with caution. Previous studies have also demonstrated weak correlations between the *mcr* gene and CH_4 emissions (Morgavi et al., 2012; Tapio et al., 2017). Gene expression analyses can improve understanding of complex methanogenic processes compared to microbial and gene abundance analyses (Shi et al., 2014). A strong interaction was observed between breed and feeding system in the L-*fuculokinase* (*fucK*) gene, K00879, which is involved in fucose metabolism and plays an important role in host–microbe interactions (Hooper et al., 1999; Pacheco et al., 2012). Similarly, *Ruminococcus* spp., which are involved in fucose metabolism (Hooper et al., 2002) and correlated with quorum sensing and the CH_4 metabolism pathway, also exhibited a similar feeding system × breed interaction. However, these interactions must be verified in a larger sample. Taken together, these results suggest that feeding systems differentially influence host–microbe interactions in different breeds, and therefore influence the rumen fermentation pattern and CH_4 formation to some extent. Therefore, breed-specific feeding systems should be selected with caution.

CONCLUSION

Comprehensive knowledge of bacterial/archaeal community composition and metabolic function is important for understanding their relationships with the host, and to develop feeding strategies to control CH_4 emissions. In this study, we described the rumen microbial community and its associated functions in Holstein and Hanwoo steers provided with the same diet, under the same management conditions, to identify compositional changes that might underlie the marked differences in CH_4 production between these breeds. This study is the first to show that Hanwoo cattle are higher CH_4 emitters than Holstein steers, as supported by the greater abundance of bacterial/archaeal genera and genes involved in CH_4 metabolism in Hanwoo cattle. We also demonstrated that, compared to TMR feeding, the SF system can reduce ruminal CH_4 emissions, regardless of cattle breed. Similarly, genetic factors interacted with the feeding system, leading to divergent effects in the rumen, and therefore to large differences in microbial gene abundance, but with little effect on CH_4 production. Wide variation in microbial co-occurrence patterns was observed in accordance with feeding system and breed, indicating different patterns of H_2 thermodynamics in the rumen. The results of this study provide insight into the complex bacterial interactions occurring in the rumen, and may facilitate appropriate selection of strategies for modulating bacterial functions to reduce CH_4 emissions. Specific microbial genes associated with CH_4 can be used to develop molecular tools, facilitating the breeding of low CH_4-emitting animals.

DATA AVAILABILITY STATEMENT

The datasets generated for this study can be found in online repositories. The name of the repository (NCBI) and accession number (PRJNA725944) can be found in the following link: https://www.ncbi.nlm.nih.gov/sra/PRJNA725944.

ETHICS STATEMENT

The animal study was reviewed and approved by the Committee for the Institutional Animal Care and Use of Seoul National University (SNU-160105-1).

AUTHOR CONTRIBUTIONS

RB and KK designed and conceptualised the experiment. RB, CL, KT, RI, and YW performed the management of steers and sample collection. RB performed the operation of respiratory chamber, data curation, performed microbial data processing, bioinformatics, statistical analyses, visualisation, and wrote the first draft of the manuscript including tables and figures. RB, CL, and YW performed the laboratory analyses. RB, H-GL, JK, and KK revised the first draft of the manuscript including tables and figures. All authors contributed to the final manuscript revision, read and approved the final manuscript.

FUNDING

The present study was supported by the Korea Institute of Planning and Evaluation for Technology in Food, Agriculture, Forestry and Fisheries (IPET); the Ministry of Agriculture, Food and Rural Affairs, South Korea (research project no. 314081-2).

SUPPLEMENTARY MATERIAL

The Supplementary Material for this article can be found online at: https://www.frontiersin.org/articles/10.3389/fmicb.2021.701081/full#supplementary-material

REFERENCES

Abriouel, H., Lerma, L. L., Casado Muñoz, M. D. C., Montoro, B. P., Kabisch, J., Pichner, R., et al. (2015). The controversial nature of the *Weissella* genus: technological and functional aspects versus whole genome analysis-based pathogenic potential for their application in food and health. *Front. Microbiol.* 6:1197. doi: 10.3389/fmicb.2015.01197

Allison, M. J., and Bryant, M. P. (1963). Biosynthesis of branched-chain amino acids from branched-chain fatty acids by rumen bacteria. *Arch. Biochem. Biophys.* 101, 269–277. doi: 10.1016/S0003-9861(63)80012-0

Auffret, M. D., Stewart, R., Dewhurst, R. J., Duthie, C. A., Rooke, J. A., Wallace, R. J., et al. (2018). Identification, comparison, and validation of robust rumen microbial biomarkers for methane emissions using diverse *Bos taurus* breeds and basal diets. *Front. Microbiol.* 8:2642. doi: 10.3389/fmicb.2017.02642

Beigh, Y. A., Ganai, A. M., and Ahmad, H. A. (2017). Prospects of complete feed system in ruminant feeding: a review. *Vet. World* 10, 424–437. doi: 10.14202/vetworld.2017.424-437

Belitsky, B. R. (2015). Role of branched-chain amino acid transport in *Bacillus subtilis* CodY activity. *J. Bacteriol.* 197, 1330–1338. doi: 10.1128/JB.02563-14

Benson, A. K., Kelly, S. A., Legge, R., Ma, F., Low, S. J., Kim, J., et al. (2010). Individuality in gut microbiota composition is a complex polygenic trait shaped by multiple environmental and host genetic factors. *Proc. Natl. Acad. Sci. U.S.A.* 107, 18933–18938. doi: 10.1073/pnas.1007028107

Bharanidharan, R., Arokiyaraj, S., Kim, E. B., Lee, C. H., Woo, Y. W., Na, Y., et al. (2018). Ruminal methane emissions, metabolic, and microbial profile of Holstein steers fed forage and concentrate, separately or as a total mixed ration. *PLoS One* 13:e0202446. doi: 10.1371/journal.pone.0202446

Choi, J. W., Liao, X., Stothard, P., Chung, W. H., Jeon, H. J., Miller, S. P., et al. (2014). Whole-genome analyses of Korean native and Holstein cattle breeds by massively parallel sequencing. *PLoS One* 9:e101127. doi: 10.1371/journal.pone.0101127

Chung, C. S., Cho, W. K., Jang, I. S., Lee, S. S., and Moon, Y. H. (2017). Effects of feeding system on growth performance, plasma biochemical components and hormones, and carcass characteristics in Hanwoo steers. *Asian Austr. J. Anim. Sci.* 30, 1117–1123. doi: 10.5713/ajas.17.0166

Counotte, G. H., Prins, R. A., Janssen, R. H., and Debie, M. J. (1981). Role of *Megasphaera* elsdenii in the fermentation of dl-[2-C]lactate in the Rumen of dairy cattle. *Appl. Environ. Microbiol.* 42, 649–655. doi: 10.1128/aem.42.4.649-655.1981

De Mulder, T., Peiren, N., Vandaele, L., Ruttink, T., De Campeneere, S., Van de Wiele, T., et al. (2018). Impact of breed on the rumen microbial community composition and methane emission of Holstein Friesian and Belgian Blue heifers. *Livest. Sci.* 207, 38–44. doi: 10.1016/j.livsci.2017.11.009

Difford, G. F., Plichta, D. R., Løvendahl, P., Lassen, J., Noel, S. J., Højberg, O., et al. (2018). Host genetics and the rumen microbiome jointly associate with methane emissions in dairy cows. *PLoS Genet.* 14:e1007580. doi: 10.1371/journal.pgen.1007580

Dusková, D., and Marounek, M. (2001). Fermentation of pectin and glucose, and activity of pectin-degrading enzymes in the rumen bacterium *Lachnospira multiparus*. *Lett. Appl. Microbiol.* 33, 159–163. doi: 10.1046/j.1472-765x.2001.00970.x

Duthie, C. A., Haskell, M., Hyslop, J. J., Waterhouse, A., Wallace, R. J., Roehe, R., et al. (2017). The impact of divergent breed types and diets on methane emissions, rumen characteristics and performance of finishing beef cattle. *Animal* 11, 1762–1771. doi: 10.1017/S1751731117000301

FAOSTAT (2021). *Food and Agriculture Organization of the United Nations Statistical Database*. Available online at: http://www.fao.org/faostat/en/#data/GT (accessed April 27, 2021).

Genís, S., Verdú, M., Cucurull, J., and Devant, M. (2021). Complete feed versus concentrate and straw fed separately: effect of feeding method on eating and sorting behavior, rumen acidosis, and digestibility in crossbred Angus bulls fed high-concentrate diets. *Anim. Feed Sci. Technol.* 273:114820. doi: 10.1016/j.anifeedsci.2021.114820

Guan, L. L., Nkrumah, J. D., Basarab, J. A., and Moore, S. S. (2008). Linkage of microbial ecology to phenotype: correlation of rumen microbial ecology to cattle's feed efficiency. *FEMS Microbiol. Lett.* 288, 85–91. doi: 10.1111/j.1574-6968.2008.01343.x

Hammer, D. A. T., Ryan, P. D., Hammer, Ø, and Harper, D. A. T. (2001). *Past: Paleontological Statistics Software Package for Education and Data Analysis*. Available online at: https://palaeo-electronica.org/2001_1/past/issue1_01.htm (accessed July 22, 2018).

Holter, J. B., Urban, W. E., Hayes, H. H., and Davis, H. A. (1977). Utilization of diet components fed blended or separately to lactating cows. *J. Dairy Sci.* 60, 1288–1293. doi: 10.3168/JDS.S0022-0302(77)84024-1

Honan, M., Feng, X., Tricarico, J. M., and Kebreab, E. (2021). Feed additives as a strategic approach to reduce enteric methane production in cattle: modes of action, effectiveness and safety. *Anim. Prod. Sci.* doi: 10.1071/AN20295

Hooper, L. V., Midtvedt, T., and Gordon, J. I. (2002). How host-microbial interactions shape the nutrient environment of the mammalian intestine. *Annu. Rev. Nutr.* 22, 283–307. doi: 10.1146/annurev.nutr.22.011602.092259

Hooper, L. V., Xu, J., Falk, P. G., Midtvedt, T., and Gordon, J. I. (1999). A molecular sensor that allows a gut commensal to control its nutrient foundation in a competitive ecosystem. *Proc. Natl. Acad. Sci. U.S.A.* 96, 9833–9838. doi: 10.1073/PNAS.96.17.9833

Hoover, W. H. (1978). Digestion and absorption in the hindgut of ruminants. *J. Anim. Sci.* 46, 1789–1799. doi: 10.2527/jas1978.4661789x

Huuskonen, A., Pesonen, M., and Joki-Tokola, E. (2014). Effects of supplementary concentrate level and separate or total mixed ration feeding on performance of growing dairy bulls. *Agric. Food Sci.* 23, 257–265. doi: 10.23986/afsci.46460

Islam, M., Kim, S.-H., Ramos, S. C., Mamuad, L. L., Son, A.-R., Yu, Z., et al. (2021). Holstein and jersey steers differ in rumen microbiota and enteric methane emissions even fed the same total mixed ration. *Front. Microbiol.* 12:601061. doi: 10.3389/fmicb.2021.601061

Janssen, P. H. (2010). Influence of hydrogen on rumen methane formation and fermentation balances through microbial growth kinetics and fermentation thermodynamics. *Anim. Feed Sci. Technol.* 160, 1–22. doi: 10.1016/j.anifeedsci.2010.07.002

Kamke, J., Kittelmann, S., Soni, P., Li, Y., Tavendale, M., Ganesh, S., et al. (2016). Rumen metagenome and metatranscriptome analyses of low methane yield sheep reveals a Sharpea-enriched microbiome characterised by lactic acid formation and utilisation. *Microbiome* 4:56. doi: 10.1186/s40168-016-0201-2

Kanehisa, M., and Goto, S. (2000). KEGG: kyoto encyclopedia of genes and genomes. *Nucleic Acids Res.* 28, 27–30.

Kang, S. W., Oh, Y. K., Choi, C. W., Kim, G.-H., and Son, Y. S. (2005). Study on comparison of growth performance, feed efficiency and carcass characteristics for holstein, Hanwoo and F1(Holstein ♀ X Hanwoo ♂) Steers. *J. Anim. Sci. Technol.* 47, 243–252. doi: 10.5187/jast.2005.47.2.243

Kim, K. H., Lee, S. S., and Kim, K. J. (2005). Effect of intraruminal sucrose infusion on volatile fatty acid production and microbial protein synthesis in sheep. *Asian Austr. J. Anim. Sci.* 18, 350–353. doi: 10.5713/ajas.2005.350

Kim, S. H., Alam, M. J., Gu, M. J., Park, K. W., Jeon, C. O., Ha, J. K., et al. (2011). Effect of total mixed ration with fermented feed on ruminal in vitro fermentation, growth performance and blood characteristics of Hanwoo steers. *Asian Austr. J. Anim. Sci.* 25, 213–223. doi: 10.5713/ajas.2011.11186

Kishimoto, A., Ushida, K., Phillips, G. O., Ogasawara, T., and Sasaki, Y. (2006). Identification of intestinal bacteria responsible for fermentation of gum arabic in pig model. *Curr. Microbiol.* 53, 173–177. doi: 10.1007/s00284-005-0219-3

Knapp, J. R., Laur, G. L., Vadas, P. A., Weiss, W. P., and Tricarico, J. M. (2014). Invited review: enteric methane in dairy cattle production: quantifying the opportunities and impact of reducing emissions. *J. Dairy Sci.* 97, 3231–3261. doi: 10.3168/jds.2013-7234

Kononoff, P. J., Heinrichs, A. J., and Buckmaster, D. R. (2003). Modification of the Penn State Forage and total mixed ration particle separator and the effects of moisture content on its measurements. *J. Dairy Sci.* 86, 1858–1863. doi: 10.3168/jds.S0022-0302(03)73773-4

Korean Statistical Information Service (KOSIS) (2021). *Number of Farms in Households and Animals in Heads by Type*. Available online at: http://kosis.kr/statHtml/statHtml.do?orgId=101&tblId=DT_1EO200&language=en&conn_path=I3 (accessed March 11, 2021).

Krause, K. M., Combs, D. K., and Beauchemin, K. A. (2002). Effects of forage particle size and grain fermentability in midlactation cows. II. Ruminal pH and

chewing activity. *J. Dairy Sci.* 85, 1947–1957. doi: 10.3168/jds.S0022-0302(02)74271-9

Lailer, P. C., Dahiya, S. S., and Chauhan, T. R. (2005). Complete feed for livestock concept, present status and future trend: a review. *Indian J. Anim. Sci.* 75, 84–91.

Langille, M. G. I., Zaneveld, J., Caporaso, J. G., McDonald, D., Knights, D., Reyes, J. A., et al. (2013). Predictive functional profiling of microbial communities using 16S rRNA marker gene sequences. *Nat. Biotechnol.* 31, 814–821. doi: 10.1038/nbt.2676

Lee, H. J., Jung, J. Y., Oh, Y. K., Lee, S. S., Madsen, E. L., and Jeon, C. O. (2012). Comparative survey of rumen microbial communities and metabolites across one caprine and three bovine groups, using bar-coded pyrosequencing and 1H nuclear magnetic resonance spectroscopy. *Appl. Environ. Microbiol.* 78, 5983–5993. doi: 10.1128/AEM.00104-12

Lee, S., Kim, Y., Oh, Y., and Kwak, W. (2010). Effects of feeding methods of total mixed ration on behavior patterns of growing Hanwoo Steers. *Asian Austr. J. Anim. Sci.* 23, 1469–1475. doi: 10.5713/ajas.2010.10100

Lee, Y., Bharanidharana, R., Park, J.-H., Jang, S. S., Yeo, J. M., Kim, W. Y., et al. (2016). Comparison of Methane Production of Holstein Steers Fed Forage and Concentrates Separately or As a TMR. *J. Korean Soc. Grassl. Forage Sci.* 36, 104–108. doi: 10.5333/kgfs.2016.36.2.104

Li, D. Y., Lee, S. S., Choi, N. J., Lee, S. Y., Sung, H. G., Ko, J. Y., et al. (2003). Effects of feeding system on rumen fermentation parameters and nutrient digestibility in Holstein steers. *Asian Austr. J. Anim. Sci.* 16, 1482–1486. doi: 10.5713/ajas.2003.1482

Lima, J., Auffret, M. D., Stewart, R. D., Dewhurst, R. J., Duthie, C. A., Snelling, T. J., et al. (2019). Identification of rumen microbial genes involved in pathways linked to appetite, growth, and feed conversion efficiency in cattle. *Front. Genet.* 10:701. doi: 10.3389/fgene.2019.00701

Littell, R. C., Henry, P. R., and Ammerman, C. B. (1998). Statistical analysis of repeated measures data using SAS procedures. *J. Anim. Sci.* 76, 1216–1231. doi: 10.2527/1998.7641216x

Liu, Q., Wang, C., Guo, G., Huo, W. J., Zhang, S. L., Pei, C. X., et al. (2018). Effects of branched-chain volatile fatty acids on lactation performance and mRNA expression of genes related to fatty acid synthesis in mammary gland of dairy cows. *Animal* 12, 2071–2079. doi: 10.1017/S1751731118000113

Liu, Q., Wang, C., Pei, C. X., Li, H. Y., Wang, Y. X., Zhang, S. L., et al. (2014). Effects of isovalerate supplementation on microbial status and rumen enzyme profile in steers fed on corn stover based diet. *Livest. Sci.* 161, 60–68. doi: 10.1016/J.LIVSCI.2013.12.034

Liu, Y. F., Sun, F. F., Wan, F. C., Zhao, H. B., Liu, X. M., You, W., et al. (2015). Effects of three feeding systems on production performance, rumen fermentation and rumen digesta particle structure of beef cattle. *Asian Austr. J. Anim. Sci.* 29, 659–665. doi: 10.5713/ajas.15.0445

Misra, A. K., and Thakur, S. S. (2001). Effect of dietary supplementation of sodium salt of Isobutyric acid on ruminal fermentation and nutrient utilization in a wheat straw based low protein diet fed to crossbred cattle. *Asian Austr. J. Anim. Sci.* 14, 479–484. doi: 10.5713/ajas.2001.479

Morgavi, D. P., Martin, C., Jouany, J.-P., and Ranilla, M. J. (2012). Rumen protozoa and methanogenesis: not a simple cause–effect relationship. *Br. J. Nutr.* 107, 388–397. doi: 10.1017/S0007114511002935

Moss, A. R., Jouany, J.-P., and Newbold, J. (2000). Methane production by ruminants: its contribution to global warming. *Ann. Zootech.* 49, 231–253. doi: 10.1051/animres:2000119

Moya, D., Holtshausen, L., Marti, S., Gibb, D. G., McAllister, T. A., Beauchemin, K. A., et al. (2014). Feeding behavior and ruminal pH of corn silage, barley grain, and corn dried distillers' grain offered in a total mixed ration or in a free-choice diet to beef cattle1. *J. Anim. Sci.* 92, 3526–3536. doi: 10.2527/jas.2013-7224

Olijhoek, D. W., Løvendahl, P., Lassen, J., Hellwing, A. L. F., Höglund, J. K., Weisbjerg, M. R., et al. (2018). Methane production, rumen fermentation, and diet digestibility of Holstein and Jersey dairy cows being divergent in residual feed intake and fed at 2 forage-to-concentrate ratios. *J. Dairy Sci.* 101, 9926–9940. doi: 10.3168/jds.2017-14278

Pacheco, A. R., Curtis, M. M., Ritchie, J. M., Munera, D., Waldor, M. K., Moreira, C. G., et al. (2012). Fucose sensing regulates bacterial intestinal colonization. *Nature* 492, 113–117. doi: 10.1038/nature11623

Paul, K., Nonoh, J. O., Mikulski, L., and Brune, A. (2012). Methanoplasmatales & thermoplasmatales-related archaea in termite guts and other environments, are the seventh order of methanogens. *Appl. Environ. Microbiol.* 78, 8245–8253. doi: 10.1128/AEM.02193-12

Phipps, R. H., Bines, J. A., Fulford, R. J., and Weller, R. F. (1984). Complete diets for dairy cows: a comparison between complete diets and separate ingredients. *J. Agric. Sci.* 103:171. doi: 10.1017/S0021859600043434

Privé, F., Kaderbhai, N. N., Girdwood, S., Worgan, H. J., Pinloche, E., Scollan, N. D., et al. (2013). Identification and characterization of three novel lipases belonging to families II and V from *Anaerovibrio lipolyticus* 5ST. *PLoS One* 8:e69076. doi: 10.1371/journal.pone.0069076

Reddy, D. N., and Reddy, M. R. (1983). The effect of feeding complete feeds on nutrient utilization and milk production on crossbred cows. *Indian J. Dairy Sci.* 36, 421–423.

Reichardt, N., Duncan, S. H., Young, P., Belenguer, A., McWilliam Leitch, C., Scott, K. P., et al. (2014). Phylogenetic distribution of three pathways for propionate production within the human gut microbiota. *ISME J.* 8, 1323–1335. doi: 10.1038/ismej.2014.14

Revelle, W. (2018). *psych: Procedures for Psychological, Psychometric, and Personality Research. R Package Version 1.8.4.* Available online at: https://CRAN.R-project.org/package=psych (accessed Sep 23, 2018).

Roehe, R., Dewhurst, R. J., Duthie, C. A., Rooke, J. A., McKain, N., Ross, D. W., et al. (2016). Bovine host genetic variation influences rumen microbial methane production with best selection criterion for low methane emitting and efficiently feed converting hosts based on metagenomic gene abundance. *PLoS Genet.* 12:e1005846. doi: 10.1371/journal.pgen.1005846

Schink, B., and Zeikus, J. G. (1980). Microbial methanol formation: a major end product of pectin metabolism. *Curr. Microbiol.* 4, 387–389. doi: 10.1007/BF02605383

Schroeder, M. M., Soita, H. W., Christensen, D. A., Khorasani, G. R., and Kennelly, J. J. (2003). Effect of total mixed ration particle size on rumen pH, chewing activity, and performance in dairy cows. *Asian Austr. J. Anim. Sci.* 16, 1755–1762. doi: 10.5713/ajas.2003.1755

Segata, N., Izard, J., Waldron, L., Gevers, D., Miropolsky, L., Garrett, W. S., et al. (2011). Metagenomic biomarker discovery and explanation. *Genome Biol.* 12:R60. doi: 10.1186/gb-2011-12-6-r60

Shabat, S., Sasson, G., Doron-Faigenboim, A., Durman, T., Yaacoby, S., Berg Miller, M. E., et al. (2016). Specific microbiome-dependent mechanisms underlie the energy harvest efficiency of ruminants. *ISME J.* 10, 2958–2972. doi: 10.1038/ismej.2016.62

Shi, W., Moon, C. D., Leahy, S. C., Kang, D., Froula, J., Kittelmann, S., et al. (2014). Methane yield phenotypes linked to differential gene expression in the sheep rumen microbiome. *Genome Res.* 24, 1517–1525. doi: 10.1101/gr.168245.113

Strobel, H. J. (1992). Vitamin B12-dependent propionate production by the ruminal bacterium Prevotella ruminicola 23. *Appl. Environ. Microbiol.* 58, 2331–2333. doi: 10.1128/aem.58.7.2331-2333.1992

Tapio, I., Snelling, T. J., Strozzi, F., and Wallace, R. J. (2017). The ruminal microbiome associated with methane emissions from ruminant livestock. *J. Anim. Sci. Biotechnol.* 8:7. doi: 10.1186/s40104-017-0141-0

Van Gylswyk, N. O. (1995). *Succiniclasticum ruminis* gen. nov., sp. nov., a ruminal bacterium converting Succinate to propionate as the sole energy-yielding mechanism. *Int. J. Syst. Bacteriol.* 45, 297–300. doi: 10.1099/00207713-45-2-297

Wallace, R. J., Rooke, J. A., Duthie, C.-A., Hyslop, J. J., Ross, D. W., McKain, N., et al. (2015a). Archaeal abundance in post-mortem ruminal digesta may help predict methane emissions from beef cattle. *Sci. Rep.* 4:5892. doi: 10.1038/srep05892

Wallace, R. J., Rooke, J. A., McKain, N., Duthie, C.-A., Hyslop, J. J., Ross, D. W., et al. (2015b). The rumen microbial metagenome associated with high methane production in cattle. *BMC Genom.* 16:839. doi: 10.1186/s12864-015-2032-0

Warnes, G. R., Bolker, B., Bonebakker, L., Gentleman, R., Huber, W., Liaw, A., et al. (2015). Various R programming tools for plotting data. *Compr. R. Arch. Netw.* 2, 1–66.

Weiner, J. M. (2019). *pca3d: Three Dimensional PCA Plots. R Package Version 0.10.1.* Available online at: https://cran.r-project.org/web/packages/pca3d/pca3d.pdf (accessed March 03, 2019).

Wirth, R., Kádár, G., Kakuk, B., Maróti, G., Bagi, Z., Szilágyi, Á, et al. (2018). The planktonic core microbiome and core functions in the cattle rumen by next generation sequencing. *Front. Microbiol.* 9:2285. doi: 10.3389/fmicb.2018.02285

Wolin, M. J., Miller, T. L., and Stewart, C. S. (1997). "Microbe-microbe interactions," in *The Rumen Microbial Ecosystem*, eds P. N. Hobson and C. S. Stewart (Dordrecht: Springer), 467–491. doi: 10.1007/978-94-009-1453-7_11

Wood, H. G., Ragsdale, S. W., and Pezacka, E. (1986). The acetyl-CoA pathway of autotrophic growth. *FEMS Microbiol. Lett.* 39, 345–362. doi: 10.1016/0378-1097(86)90022-4

Yan, T., Patterson, D. C., and Gordon, F. J. (1998). The effect of two methods of feeding the concentrate supplement to dairy cows of high genetic merit. *Anim. Sci.* 67, 395–403. doi: 10.1017/S1357729800032793

Zakrzewski, M., Proietti, C., Ellis, J. J., Hasan, S., Brion, M. J., Berger, B., et al. (2017). Calypso: a user-friendly web-server for mining and visualizing microbiome-environment interactions. *Bioinformatics* 33, 782–783. doi: 10.1093/bioinformatics/btw725

Zhang, Q., Difford, G., Sahana, G., Løvendahl, P., Lassen, J., Lund, M. S., et al. (2020). Bayesian modeling reveals host genetics associated with rumen microbiota jointly influence methane emission in dairy cows. *ISME J.* 14, 2019–2033. doi: 10.1038/s41396-020-0663-x

Zhou, X., Bent, S. J., Schneider, M. G., Davis, C. C., Islam, M. R., and Forney, L. J. (2004). Characterization of vaginal microbial communities in adult healthy women using cultivation-independent methods. *Microbiology* 150, 2565–2573. doi: 10.1099/mic.0.26905-0

Ziołecki, A., and Wojciechowicz, M. (1980). Small pectinolytic spirochetes from the rumen. *Appl. Environ. Microbiol.* 39, 919–922. doi: 10.1128/aem.39.4.919-922.1980

Conflict of Interest: CL and YW are employed by Cargill Agri Purina Inc., and GN Food Ltd., respectively.

The remaining authors declare that the research was conducted in the absence of any commercial or financial relationships that could be construed as a potential conflict of interest.

frontiers in Microbiology

PERSPECTIVE
published: 30 July 2021
doi: 10.3389/fmicb.2021.664257

Prenatal Depression, Breastfeeding, and Infant Gut Microbiota

*Nicole Rodriguez[1], Hein M. Tun[2], Catherine J. Field[3], Piushkumar J. Mandhane[1], James A. Scott[4] and Anita L. Kozyrskyj[1]**

[1] Department of Pediatrics, University of Alberta, Edmonton, AB, Canada, [2] HKU-Pasteur Research Pole, Li Ka Shing Faculty of Medicine, School of Public Health, The University of Hong Kong, Hong Kong, China, [3] Department of Agricultural, Food and Nutritional Science, University of Alberta, Edmonton, AB, Canada, [4] Dalla Lana School of Public Health, University of Toronto, Toronto, ON, Canada

Depressive symptoms are common during pregnancy and are estimated to affect 7–20% of pregnant women, with higher prevalence found in those with a prior history of depression, in ethnic minorities, and those with increased exposure to stressful life events. Maternal depression often remains undiagnosed, and its symptoms can increase adverse health risks to the infant, including impaired cognitive development, behavioral problems, and higher susceptibility to physical illnesses. Accumulating research evidence supports the association between maternal physical health elements to infant gut health, including factors such as mode of delivery, medication, feeding status, and antibiotic use. However, specific maternal prenatal psychosocial factors and their effect on infant gut microbiota and immunity remains an area that is not well understood. This article reviews the literature and supplements it with new findings to show that prenatal depression alters: (i) gut microbial composition in partially and fully formula-fed infants at 3–4 months of age, and (ii) gut immunity (i.e., secretory Immunoglobulin A) in all infants independent of breastfeeding status. Understanding the implications of maternal depression on the infant gut microbiome is important to enhance both maternal and child health and to better inform disease outcomes and management.

Keywords: prenatal depression, breastfeeding, birth mode, infant, gut microbiota, gut immunity

OPEN ACCESS

Edited by:
M. Pilar Francino, Fundación para el Fomento de la Investigación Sanitaria y Biomédica de la Comunitat Valenciana (FISABIO), Spain

Reviewed by:
Ravinder K. Nagpal, Florida State University, United States
Anne Lang Dunlop, Emory University, United States

****Correspondence:***
Anita L. Kozyrskyj
kozyrsky@ualberta.ca

Specialty section:
This article was submitted to Microbial Symbioses, a section of the journal Frontiers in Microbiology

Received: *04 February 2021*
Accepted: *23 June 2021*
Published: *30 July 2021*

Citation:
Rodriguez N, Tun HM, Field CJ, Mandhane PJ, Scott JA and Kozyrskyj AL (2021) Prenatal Depression, Breastfeeding, and Infant Gut Microbiota. Front. Microbiol. 12:664257. doi: 10.3389/fmicb.2021.664257

INTRODUCTION

The World Health Organization (WHO) lists depression as the leading cause of disease burden for women of reproductive age (Davalos et al., 2012). Depression before and after birth is often accompanied by symptoms of sadness and anxiety, anhedonia, appetite loss, sleep disturbance, confusion, and mood lability (Bernard-Bonnin et al., 2004). An estimated 18.4% of women experience prenatal depression, with 12.7% having major depressive episodes, and 13% experiencing postpartum depression. Women in their reproductive years are especially at high risk for major depression, with increased risk present during pregnancy or within the first 12 months post-delivery (Figueiredo et al., 2014). When left undetected, maternal depression results in reduced mother-child quality interactions, including reduced breastfeeding, impaired response

to the infant's hunger cues, and less contingent stimulation. Prenatal depression is a significant contributor to shorter breastfeeding duration (Dias and Figueiredo, 2015).

In addition to its negative impact on maternal health, prenatal depression can have long term consequences on children's physical and mental health, and cognitive and socio-emotional development (Bernard-Bonnin et al., 2004). Depression alters the intrauterine environment, including elevation in circulating cortisol, which can negatively affect the developing fetus (Lewis et al., 2015). Various epidemiological studies suggest the association of maternal depression and the development of a compromised infant immune system susceptible to illnesses including asthma, allergy, and other atopic diseases (Smejda et al., 2019). Fetal exposure to prenatal depression predicts elevated inflammatory biomarkers at age 25. Prenatal depression can also extend its influence to the critical "window of opportunity" during the infant's first year of life and the beginning stages of gut microbiota development when it is most sensitive to perturbation (van den Elsen et al., 2019).

Several factors have been identified as key to shaping early microbiota composition and function, including birth mode, antibiotic use, and infant nutrition (Milani et al., 2017). Next to birth mode, breastfeeding has the most critical influence in young infants. Breast milk shapes the gut microbiota composition of infants by providing nutrients for bacterial growth (Bravi et al., 2016; Moossavi et al., 2019). Infants who are partially breastfed and even those who receive small amounts of formula supplementation display significant shifts in their gut microbial composition (Forbes et al., 2018). Additionally, breastfeeding also shapes infant immune development to support oral tolerance induction and allergy prevention (van den Elsen et al., 2019).

Many studies support the importance of early-life factors, including maternal and infant factors, in establishing nascent gut microbiota that consequently contribute to infant nutrient acquisition, pathogen exclusion, immune system regulation, and other health and developmental outcomes. This brief review aims to present evidence from the literature that examines maternal prenatal depression's relationship with infant gut microbiota and immunity, taking into account maternal prenatal diet and infant diet.

PRENATAL DEPRESSION AFFECTS INFANT GUT MICROBIAL COMPOSITION DEPENDENT ON BREASTFEEDING

To understand the link between maternal depression, breastfeeding, and infant gut microbiota, it is essential to consider the decision-making process that women undergo when choosing to breastfeed. Breastfeeding behavior has two stages (Meedya et al., 2010). First is the *intention* or the decision to breastfeed, which is shaped by sociodemographic, clinical, and psychosocial factors; and second is *initiation*, which is dependent on the intention, as well as lactation coaching, birth mode, and perinatal complications. The overwhelming majority of women make decisions on whether to breast or formula feed during the prenatal period; intention is one of the strongest predictors of breastfeeding initiation (Bogen et al., 2010). A comprehensive systematic review revealed that prenatal depression may or may not reduce breastfeeding intention (Dias and Figueiredo, 2015). It does not appear to reduce breastfeeding initiation, pointing to the success of lactation coaching. However, depression during pregnancy predicts shorter breastfeeding duration. Hence, prenatal depression may make no difference on whether a woman intends to and/or initiates breastfeeding, but it is certainly a factor in whether she continues to breastfeed. Lastly, prenatal depression appears to have a more substantial impact on breastfeeding duration than postnatal depression (Dias and Figueiredo, 2015).

Building on previous studies of maternal perinatal depression and the infant gut microbiome (Zijlmans et al., 2015), we compared whole gut microbiota community composition in infants at mean age 3.7 months according to maternal depression status in the CHILD Cohort Study (**Box 1**). Differences were found in Bray-Curtis measure of microbial beta-diversity between infants of mothers with and without prenatal depression (**Figure 1** and **Table 1**; Beals, 1984). Notably, these observed gut microbial community differences were independent of breastfeeding status, and of many maternal and household factors known to influence infant gut microbiota, including breastfeeding difficulty. There were interactions in maternal mood differences according to breastfeeding status that will be discussed later. Further, infant gut microbial abundance differed according to maternal history of depression, classified as during pregnancy, in the past and never (**Figure 1** and **Table 2**). Gut bacteria in the families of the phylum, Firmicutes families – Erysipelotrichaceae, Lachnospiraceae, and Ruminococcaceae were more abundant in infants of mothers experiencing depression during pregnancy versus infants whose mothers never had depression and those with depression in the past. Based on pairwise comparisons of abundance, only Ruminococcaceae and Lachnospiraceae showed a statistically significant difference between all three depression categories ($p < 0.01$), including enrichment in infants whose mothers had depression in the past versus those who did not. These butyrate-producing bacteria are strict anaerobes that normally become more abundant in later infancy. Many have been found to be elevated in the gut of adults with depression and of mice following fecal transplantation from adults with depression, although not uniformly so (Barandouzi et al., 2020).

Interestingly, CHILD study infants born to women with prenatal or history of depression had significantly fewer Proteobacteria in their gut microbiota, specifically the Enterobacteriaceae, than infants whose mothers never had depression (**Table 2**). Typically, Proteobacteria peak in abundance during early infancy — a phenomenon called the "Proteobacteria bloom," and then slowly decline after the first 3 years of life as gut microbiota start to resemble that of an adult (Shin et al., 2015). This Proteobacterial bloom plays a crucial role in infant immune mechanisms, including homeostasis and tolerance to environmental pathogens, and prepares the infant gut for colonization by strict anaerobes in later infancy. As summarized by Campos-Rodríguez et al. (2013), evidence is accumulating from several studies that maternal prenatal

BOX 1 | Methods.

Study population

The present study involved a subsample of 996 term infants from three study sites (Edmonton, Vancouver, and Winnipeg) of the CHILD birth cohort (www.childstudy.ca). Mothers were mainly of Caucasian ethnicity (75.3%), between the ages of 30 and 34 (39.9%), and were generally healthy. One quarter of women reported depression during pregnancy or in the past. Most infants were born vaginally (74.7%), and 11.3% by elective and 14% by emergency cesarean section. At 3–4 months, 43.2% of infants were exclusively breastfed, including 29.4% exclusively breastfed since birth and 13.8% who briefly received formula in hospital. An additional 34.3% were partially breastfed and 22.4% were not breastfed at all. Cesarean delivery rates increased from 20 to 29% as exclusivity of breastfeeding declined, but were highest in exclusively breastfed infants receiving some formula after birth (31.5%).

Study measures

For the purposes of this study, the term breastfeeding is used to describe feeding the infant breast milk, whether at the breast or from the bottle. At 3 months postpartum, mothers completed questionnaires reporting on breastfeeding status and the introduction of formula. Breastfeeding status was classified into four groups as exclusive (breast milk only), exclusively breastfed after hospital, partial (breast milk and formula), and none (formula only). Patient chart reviews were used to classify infants into exclusively breastfed "after hospital" if they briefly received formula in hospital but were thereafter exclusively breastfed following hospital discharge. Breastfeeding status was determined for the same date as fecal sample collection. Candidate confounding factors were selected from a literature review. They included covariates such as mode of delivery, parity, gestational diabetes, infant sex, birth weight, and hospital-administered antibiotics to the mother or neonate that were obtained from hospital records. Mothers also completed standardized questionnaires during pregnancy and 3 months postpartum for information related to maternal characteristics such as race (Asian, Caucasian, First Nations, and Other), age, post-secondary education (Yes/No), smoking and pre-existing conditions (i.e., recurrent urinary tract infections) or other factors such as presence of siblings, pets in household or cleaning product usage. Additionally, the Healthy Eating Index was used to assess the quality of maternal diet (Guenther et al., 2013). Fecal stool samples were collected at a home visit at 3–4 months (mean ± SD: 3.7 ± 1.0) and were transported to the laboratory on ice and stored at −80°C until processing. DNA was extracted using the QIAamp DNA Stool Mini Kit (Qiagen Inc., Valencia, CA, United States). The 16S ribosomal RNA (rRNA) V4 region was amplified by primers 515f (TATGGTAATTGTGTGCCAGCMGCCGCGGTAA) and 806r (AGTCAGTCAGCCGGACTACHVGGGTWTCTAAT). PCR amplicons were pooled and multiplexed (48 or 96 samples per run) and sequenced on an Illumina MiSeq (San Diego, CA, United States) to generate 2 × 150 bp. The QIIME (v 1.8.0) platform was used to analyze 16S rRNA amplicon data (Desantis et al., 2006; Caporaso et al., 2010). Briefly, reads were assembled, demultiplexed and clustered at 97% using USEARCH (v 6.1). Taxonomic classification of sequence clusters was performed using the Greengenes reference database (v 13.8); non-bacterial sequences clustered at 97% similarity, and singletons were removed. The final dataset included a total of 265,095,597 sequences (median 235,623 per sample, range 13,134–833,392), corresponding to 939 unique OTUs. Data were rarefied to 13,000 sequences per sample and summarized at various taxonomic ranks.

Statistical analysis

Microbiota community structures were visualized using principal coordinate analysis (PCoA). Total microbial beta-diversity, measured by the Bray-Curtis method, was tested by permutational analysis of variance (PERMANOVA) with 999 permutations using the adonis function from the R "vegan" package (Anderson, 2001). To reduce confounding bias, covariates were added to models in a sequential order of most to least variance explained (i.e., F-model). Analyses were performed in R (version 3.3.3; R Development Core Team). Taxon median relative abundance was compared by non-parametric Kruskal–Wallis tests and *post hoc* Dunn's tests with false discovery rate (FDR) correction for multiple comparisons.

depression affects phylogenetic diversity of second trimester gut microbiota, and in turn, gut microbial colonization of offspring. More recently, Hu et al. (2019) found psychosocial stress during pregnancy, specifically anxiety, also to be associated with a less diverse microbial community in meconium (first stool) of the newborn (Hu et al., 2019). Since passage of meconium predates breastfeeding in many infants, their results point to a causal pathway for prenatal depression. It is striking then, that CHILD study results were consistent with theirs, on the correlation between higher pregnancy-related anxiety with lower levels of meconium Enterobacteriaceae. Further, a small study of longitudinally collected fecal samples after vaginal birth found enrichment with some enterobacterial genera but a reduction in other enterobacteria over the first 4 months of life when maternal stress, anxiety or cortisol levels were high in the last trimester of pregnancy; lactobacilli and bifidobacteria were also less abundant (Zijlmans et al., 2015). Thus, evidence is accumulating that prenatal depression disrupts healthy development of offspring gut microbiota months after birth. This process may be initiated by the transfer of a suboptimal maternal microbiome to the newborn, which may promote the same microbiota that are elevated in women with depression (Barandouzi et al., 2020).

Ample research supports the importance of breast milk to the establishment of gut microbiota (Williams et al., 2019) and provision of essential human milk oligosaccharides for microbial growth (Moossavi et al., 2019). Mother's milk also carries with it microbiota and metabolites derived from multiple sources, including the breast's surface, lactiferous ducts, or from the maternal gut (Dieterich et al., 2013). Within the first 6 months of life, breastfeeding is only second to birth mode as a substantial and independent determinant of gut microbial composition (Madan et al., 2016; Yang et al., 2019). Next to birth mode, breastfeeding status explained the next highest variation in community diversity (r-squared, 4.5%) in CHILD study infants at mean age 3.7 months (**Table 1**). Yet, independent of 15 adjusting covariates, including infant feeding status, prenatal depression ranked 4th to explain 0.5% of the variation in gut microbial diversity among all infants.

It is also important to know how prenatal depression impacts the gut microbiota of infants within feeding groups (e.g., exclusive, partial, and no breastfeeding). Similar gut microbial dysbiosis has been reported in 3–4 months old infants following maternal prenatal stress in the presence or absence of breastfeeding (Zijlmans et al., 2015). In the CHILD study, no gut microbiota compositional differences were found by maternal prenatal mood status in fully-breastfed infants at 3–4 months, in whom the major determinant of gut microbial diversity was birth mode (**Table 1**). In contrast, prenatal depression was associated with statistically significant changes to total microbial diversity of infants who were not exclusively breastfed (**Table 1**). Enrichment with Lachnospiraceae and Ruminococcaceae, and depletion of Enterobacteriaceae are characteristic of 3–4 months gut microbiota during partial or

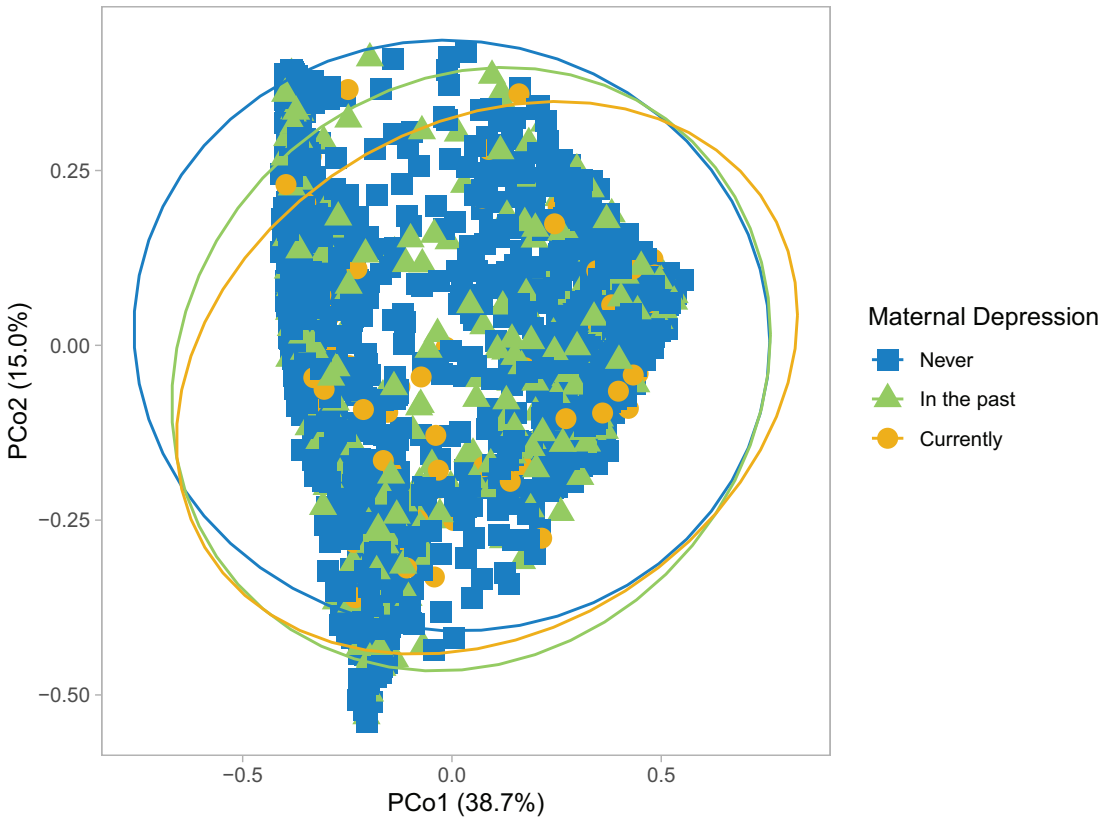

FIGURE 1 | Microbial community structure of infant gut microbiota according to maternal prenatal depression. Principal coordinate analysis performed using Bray-Curtis dissimilarity matrices.

full formula-feeding when compared to exclusive breastfeeding, and independent of birth mode (Forbes et al., 2018). Prenatal depression further enhanced the abundance of Lachnospiraceae and Ruminococcaceae in CHILD study infants (**Table 2**). Importantly, next to cesarean birth (r^2 up to 9.7%), prenatal depression ranked 2nd in explaining the variation in gut microbial diversity in the partially (1.1%) and fully formula-fed (2.7%) groups (**Table 1**).

Shifts in the normal development of infant gut microbiota, such as the premature depletion of Proteobacteria or enrichment of butyrate-producers, increase risk for gastrointestinal and allergic diseases, and future overweight (Milani et al., 2017; Forbes et al., 2018; Korpela and de Vos, 2018; Tun et al., 2018). There is a growing appreciation of signaling pathways of the "gut-brain axis" that involve gut microbiota. Since the prenatal and postnatal periods are important phases of development for both the brain and gut, significant potential exists for maternal distress to have long-term effects on both gut microbiota and neurodevelopment (Codagnone et al., 2019). In summary, human evidence is amassing on the detrimental impact of prenatal depression on gut microbiota in offspring. Since prenatal depression results in shorter breastfeeding duration, and because breastfeeding is a strong predictor of microbiome composition, the evidence implies that prenatal depression harms the infant gut microbiome by reducing duration of breastfeeding. In this section, we also pointed to the limited research on differential impacts of maternal depression according to breastfeeding status, which presents additional risk of adverse outcomes in infants not exclusively breastfed in early life.

PRENATAL DEPRESSION AFFECTS INFANT GUT IMMUNITY INDEPENDENT OF BREASTFEEDING

The early establishment of the infant gut microbiome has a significant influence on postnatal development of the gut mucosal immune system, and early infancy is a critical window of influence for both systems (Milani et al., 2017). The innate and adaptive immune systems both develop in concert with gut microbiota, and both are required to achieve host-gut microbiota homeostasis. Secretory IgA (sIgA) is a mucosal immunoglobulin of the adaptive immune system that acts as the first line of defense against invading pathogens by coating bacteria (Corthésy, 2013). It also binds to members of the gut microbiota, promoting homeostasis by preventing overgrowth by a single species. Since infants are unable to produce sIgA in significant amounts during the early days of postnatal life, they are highly dependent on their mother's breast milk as a source for sIgA (Maruyama et al., 2009). Suboptimal binding of Proteobacterial microbiota

TABLE 1 | Univariable and multivariable PERMANOVA analysis of infant gut microbiota at 3–4 months in the CHILD cohort.

	Univariable		Multivariable[a]	
	Pr(>F)[b]	R2[c]	Pr(>F)[b]	R2[c]
All infants[d]				
Prenatal depression	**0.001**	0.0057	**0.006**	0.0048
Birth mode	**0.001**	0.0523	**0.001**	0.0597
Breastfeeding status	**0.001**	0.0457	**0.001**	0.0448
Exclusive breastfeeding from birth up to 3–4 months				
Prenatal depression	0.706	0.0020	0.566	0.0031
Birth mode	**0.001**	0.0701	**0.001**	0.0759
Exclusive breastfeeding at 3–4 months but not in hospital after birth				
Prenatal depression	0.701	0.0043	0.633	0.0058
Birth mode	**0.001**	0.0756	**0.016**	0.0577
Partial breastfeeding at 3–4 months				
Prenatal depression	**0.003**	0.0133	**0.023**	0.0111
Birth mode	**0.001**	0.0602	**0.001**	0.05801
No breastfeeding at 3–4 months				
Prenatal depression	**0.040**	0.0116	**0.022**	0.0274
Birth mode	**0.001**	0.0510	**0.001**	0.0971

[a]Adjusted for maternal age, race, pre-pregnancy BMI, prenatal diet (healthy eating index/HEI), recurrent UTI, and smoking, birth mode, infant sex, antibiotics, length of hospital stay, BF difficulty medication, older siblings, dog in household, and study site.
[b]P-value corresponds to the beta-coefficient and is for each of the variables.
[c]R^2 value is specific to each of the covariates.
[d]Association of prenatal depression in all infants (i.e., not stratified by breastfeeding status at 3–4 months).
[e]Bolded values are statistically significant.

TABLE 2 | Median abundance of bacterial taxa in infant gut microbiota at 3–4 months according to reported status of maternal depression.

Taxon	Maternal prenatal depression				
	Never	In the past	Currently	pFDR	Pairwise pFDR
Actinobacteria	12.74	11.94	9.48		
Actinomycetaceae	0.21	0.09	0.33		
Bifidobacteriaceae	11.99	11.23	8.74		
Coriobacteriaceae	0.42	0.50	0.37		
Micrococcaceae	0.12	0.11	0.04		
Bacteroidetes	29.46	32.46	33.15		
Bacteroidaceae	26.62	30.34	28.36		
Porphyromonadaceae	2.17	1.56	2.16		
Firmicutes	28.28	30.83	33.72		
Clostridiaceae	4.21	4.05	2.02		
Enterococcaceae	0.16	0.16	0.10		
Erysipelotrichaceae	0.95	0.59	0.96		bc
Lachnospiraceae	8.01	8.71	9.81		abc
Ruminococcaceae	1.87	1.89	4.03	*	abc
Streptococcaceae	2.05	2.20	0.90		bc
Veillonellaceae	10.30	12.42	15.06		
Proteobacteria	27.38	22.40	20.28	*	ab
Enterobacteriaceae	25.67	20.14	18.42	*	ab
Pasteurellaceae	0.85	0.84	0.61		

*Taxa with median abundance >0% in 3–4 months microbiota. Overall comparisons by rank-based non-parametric Kruskal–Wallis test with FDR correction for multiple comparisons; *p < 0.01. Pairwise comparisons by Dunn's post hoc tests for multiple comparisons: [a]Never/In the past; [b]Never/Currently; [c]In the past/Currently.*

to sIgA has been associated with gastrointestinal conditions such as necrotizing enterocolitis in preterm infants, and even future allergic disease (Dzidic et al., 2017; Hornef and Torow, 2020).

Gut microbiota and sIgA binding are selective, such that several members of the Firmicutes (e.g., lactobacilli, Lachnospiraceae, and Ruminococcaceae) are preferentially bound to gut sIgA (Macpherson et al., 2018). Specific gut microbiota, like the lactobacilli, and their metabolites can also promote the infant's own production of sIgA by gut mucosal cells and increase sIgA binding to microbiota (Kukkonen et al., 2010;

Kim et al., 2016). Inverse associations between *Clostridium difficile* colonization and gut sIgA levels in young infants have been reported (Drall et al., 2019). As such, an imbalance in infant gut microbiota from the depletion (e.g., lactobacilli or enterobacteria) or enhancement of specific microbiota (e.g., members of the Lachnospiraceae) subsequent to prenatal depression has capacity to affect sIgA binding and/or production with further disruption to host-gut microbiota homeostasis. Animal experimental models have confirmed a causal association between psychological stress and adaptive gut immunity. When young mice are exposed to repeated restraint stress (stress due to immobilization), significantly lower intestinal sIgA levels and number of IgA-producing cells in intestinal mucosa are observed (Campos-Rodríguez et al., 2013). The natural stress experienced by mice when they change cages or social groups has also been found to lower fecal sIgA levels. Posited pathways for prenatal distress include greater transmission of glucocorticoids to the developing fetus that reduces the number of IgA-producing cells (Campos-Rodríguez et al., 2013; Lewis et al., 2015). Equally plausible are postnatal sIgA changes secondary to gut microbial dysbiosis from prenatal distress. More recently, restraint stress in a murine model raised the extent of gut IgA binding of microbiota like the Lachnospiraceae; this result was replicated in fecal samples from adults with irritable bowel syndrome, a condition often aggravated by stress (Rengarajan et al., 2020).

Kang et al. (2020) published the first human report regarding the independent association between maternal depressive symptomatology during pregnancy and compromised gut immunity in offspring. This recent study which examined infant fecal sIgA concentrations in relation to maternal depression trajectories, revealed that infants born to mothers in the prenatal trajectory (high depressive symptoms scores primarily during pregnancy) were twice more likely to have lower sIgA concentrations than infants of mothers with low symptom scores. At 4–8 months of age, the reduction in fecal sIgA concentrations among infants of mothers in the prenatal trajectory amounted to a large effect size of 0.53. Importantly, in the presence of prenatal depression, they were equally likely to be low in infants not breastfed, who fully depend on self-production of sIgA, and in exclusively breastfed infants. The latter results are consistent with previous findings by Kawano and Emori (2015) in which maternal psychological states affect immune properties of breast milk. This breast milk study demonstrated that women who scored highly on measures of anxiety, depression, and anger tended to have lower sIgA concentrations in their milk.

In summary, maternal depression during pregnancy can compromise offspring adaptive immunity through direct actions of cortisol on fetal development of IgA-producing cells and indirectly, through postnatal changes to infant gut microbiota and altered sIgA production or binding. Consequently, lowered gut sIgA concentrations or abundance of IgA-stimulating gut microbiota can impair microbe-sIgA interactions, increasing the risk of *C. difficile* colonization and allergic disease. Even if prenatal depression does not alter gut microbiota in exclusively breastfed infants (see above section), *in utero* action to reduce the number of IgA-producing cells has real potential to affect IgA-gut microbiota binding in exclusively breastfed infants. Finally, women experiencing distress have lowered sIgA amounts in breast milk and they are less likely to breastfeed for a longer duration.

PRENATAL DEPRESSION INFLUENCES THE INFANT'S GUT MICROBIOME INDEPENDENT OF PRENATAL DIET

To maintain a healthy pregnancy, adequate nutrition is needed to nourish both mother and fetus. A narrative review by Boutté et al. (2021) confirmed that worldwide, women with depression or stress during pregnancy eat an unhealthy diet, high on fat, and low in fruits and vegetables. Aspects of the prenatal diet related to fat consumption have been associated with changes to pregnancy and infant gut microbiota (Chu et al., 2016; Mandal et al., 2016). Notably, greater self-reported fruit intake during pregnancy has been linked to enhanced neurodevelopment in the CHILD study (Bolduc et al., 2016).

In the above-mentioned CHILD study, a "healthy" prenatal diet (i.e., an HEI score of above 80) was strongly associated with gut microbial diversity in infants at 3–4 months (r^2, 0.37%, p = 0.009). This univariate association remained only within non-breastfed infants, in whom prenatal diet explained a greater percentage of the variation in beta-diversity (r^2, 1.08%, p = 0.04). Prenatal diet associations with infant gut microbiota were lost altogether in multivariate models that included prenatal depression (**Table 1**). These results demonstrate that maternal depression influences the infant gut microbiome even following adjustment for prenatal diet quality. They also indicate that a healthy maternal prenatal diet is especially important to infants who are not breastfed, the benefits of which may be affected by depression during pregnancy.

CONCLUSION

Evidence is accumulating on the association between maternal prenatal depression and gut microbial diversity in early infancy. Characteristic of the altered gut microbial community structure and important to the infant's adaptive immunity are disruptions in the typical Proteobacterial bloom, and enrichment with microbiota in the families *Ruminococcaceae* and *Lachnospiraceae*. The latter is seen in infants who develop overweight. We reported new evidence that prenatal depression-related differences in microbial diversity are more likely to manifest in infants with partial or absence of breastfeeding. On the other hand, prenatal depression appears to affect sIgA independent of infant feeding type. Future study is needed to more fully characterize gut microbiota changes at the genus level, and to include viral and fungal, and other communities as well. This micro-level characterization also requires testing for metabolism end-products to determine the specific pathways by which maternal depression affects the infant gut microbiome/virome/mycobiome and future health.

Breastfeeding has many psychological benefits; our review suggests that breastfeeding can be protective against the impact of maternal depression on infant gut microbiota. It also emphasizes the importance of pregnancy depression screening to identify women at risk for breastfeeding cessation since type of infant feeding strongly influences gut microbial composition. The review also underscores the importance of prenatal counseling on depression and dietary intake to promote future gut health of the newborn. Finally, obtaining evidence on the detrimental impact of prenatal depression on infant gut microbiota is critical to inform strategies that identify and timely target women with depression during pregnancy, as their infants will benefit from breastfeeding coaching to prolong its duration.

ETHICS STATEMENT

The studies involving human participants were reviewed and approved by the University of Alberta Health Research Ethics Boards. Written informed consent to participate in this study was provided by the participants' legal guardian/next of kin.

AUTHOR CONTRIBUTIONS

AK contributed to the conception and design of the study. HT, CF, PM, and JS organized the database. NR wrote the first draft of the manuscript. All authors contributed to manuscript revision, read, and approved the submitted version.

FUNDING

The CHILD Cohort Study was initially funded by the Canadian Institutes of Health Research (CIHR) and Allergy, Genes and Environment Networks of Centres of Excellence (AllerGen NCE). Visit CHILD at childcohort.ca. This research was specifically funded by the CIHR Microbiome Initiative team grant #227312. These entities had no role in the design and conduct of the study, collection, management, analysis, and interpretation of the data, and preparation, review, or approval of the manuscript.

ACKNOWLEDGMENTS

We thank the CHILD Cohort Study (CHILD) participant families for their dedication and commitment to advancing health research. We also thank Forbes and Azad for their contribution to the data analysis and interpretation.

REFERENCES

Anderson, M. J. (2001). A new method for non-parametric multivariate analysis of variance. *Austral Ecol.* 26, 32–46. doi: 10.1111/j.1442-9993.2001.01070.pp.x

Barandouzi, Z. A., Starkweather, A. R., Henderson, W. A., Gyamfi, A., and Cong, X. S. (2020). Altered composition of gut microbiota in depression: a systematic review. *Front. Psychiatry* 11:541. doi: 10.3389/fpsyt.2020.00541

Beals, E. W. (1984). Bray-curtis ordination: an effective strategy for analysis of multivariate ecological data. *Adv. Ecol. Res.* 14, 1–55. doi: 10.1016/s0065-2504(08)60168-3

Bernard-Bonnin, A.-C., Canadian Paediatric, Society, Mental Health, Developmental Disabilities, and Committee. (2004). Maternal depression and child development. *Paediatr. Child Health* 9, 575–583. doi: 10.1093/pch/9.8.575

Bogen, D. L., Hanusa, B. H., Moses-Kolko, E., and Wisner, K. L. (2010). Are maternal depression or symptom severity associated with breastfeeding intention or outcomes? *J. Clin. Psychiatry* 71, 1069–1078. doi: 10.4088/JCP.09m05383blu

Bolduc, F. V., Lau, A., Rosenfelt, C. S., Langer, S., Wang, N., Smithson, L., et al. (2016). Cognitive enhancement in infants associated with increased maternal fruit intake during pregnancy: results from a birth cohort study with validation in an animal model. *EbioMedicine* 8, 331–340. doi: 10.1016/j.ebiom.2016.04.025

Boutté, A. K., Turner-McGrievy, G. M., Wilcox, S., Liu, J., Eberth, J. M., and Kaczynski, A. T. (2021). Associations of maternal stress and/or depressive symptoms with diet quality during pregnancy: a narrative review. *Nutr. Rev.* 79, 495–517. doi: 10.1093/nutrit/nuaa019

Bravi, F., Wiens, F., Decarli, A., Dal Pont, A., Agostoni, C., and Ferraroni, M. (2016). Impact of maternal nutrition on breast-milk composition: a systematic review. *Am. J. Clin. Nutr.* 104, 646–662. doi: 10.3945/ajcn.115.120881

Campos-Rodríguez, R., Godínez-Victoria, M., Abarca-Rojano, E., Pacheco-Yépez, J., Reyna-Garfias, H., Barbosa-Cabrera, R. E., et al. (2013). Stress modulates intestinal secretory immunoglobulin A. *Front. Int. Neurosci.* 7:86. doi: 10.3389/fnint.2013.00086

Caporaso, J. G., Kuczynski, J., Stombaugh, J., Bittinger, K., Bushman, F. D., Costello, E. K., et al. (2010). QIIME allows analysis of high-throughput community sequencing data. *Nat. Methods* 7, 335–336. doi: 10.1038/nmeth.f.303

Chu, D. M., Antony, K. M., Ma, J., Prince, A. L., Showalter, L., Moller, M., et al. (2016). The early infant gut microbiome varies in association with a maternal high-fat diet. *Genome Med.* 8:77. doi: 10.1186/s13073-016-0330-z

Codagnone, M. G., Stanton, C., O'Mahony, S. M., Dinan, T. G., and Cryan, J. F. (2019). Microbiota and neurodevelopmental trajectories: role of maternal and early-life nutrition. *Annals Nutrit. Metab.* 74(Suppl. 2), 16–27. doi: 10.1159/000499144

Corthésy, B. (2013). Multi-faceted functions of secretory IgA at mucosal surfaces. *Front. Immunol.* 4:185. doi: 10.3389/fimmu.2013.00185

Davalos, D. B., Yadon, C. A., and Tregellas, H. C. (2012). Untreated prenatal maternal depression and the potential risks to offspring: a review. *Arch. Women's Mental Health* 15, 1–14. doi: 10.1007/s00737-011-0251-1

Desantis, T. Z., Hugenholtz, P., Larsen, N., Rojas, M., Brodie, E. L., Keller, K., et al. (2006). Greengenes, a chimera-checked 16S rRNA gene database and workbench compatible with ARB. *Appl. Environ. Microbiol.* 72, 5069–5072. doi: 10.1128/aem.03006-05

Dias, C. C., and Figueiredo, B. (2015). Breastfeeding and depression: a systematic review of the literature. *J. Affect. Disord.* 171, 142–154. doi: 10.1016/j.jad.2014.09.022

Dieterich, C. M., Felice, J. P., O'Sullivan, E., and Rasmussen, K. M. (2013). Breastfeeding and health outcomes for the mother-infant dyad. *Pediatr. Clin. North Am.* 60, 31–48. doi: 10.1016/j.pcl.2012.09.010

Drall, K. M., Tun, H. M., Morales-Lizcano, N. P., Konya, T. B., Guttman, D. S., Field, C. J., et al. (2019). Clostridioides difficile colonization is differentially associated with gut microbiome profiles by infant feeding modality at 3-4 months of age. *Front. Immunol.* 10:2866. doi: 10.3389/fimmu.2019.02866

Dzidic, M., Abrahamsson, T. R., Artacho, A., Björkstén, B., Collado, M. C., Mira, A., et al. (2017). Aberrant IgA responses to the gut microbiota during infancy precede asthma and allergy development. *J. Allergy Clin. Immunol.* 139, 1017–1025.e14. doi: 10.1016/j.jaci.2016.06.047

Figueiredo, B., Canário, C., and Field, T. (2014). Breastfeeding is negatively affected by prenatal depression and reduces postpartum depression. *Psychol. Med.* 44, 927–936. doi: 10.1017/S0033291713001530

Forbes, J. D., Azad, M. B., Vehling, L., Tun, H. M., Konya, T. B., Guttman, D. S., et al. (2018). Association of exposure to formula in the hospital and subsequent

infant feeding practices with gut microbiota and risk of overweight in the first year of life. *JAMA Pediatr.* 172:e181161. doi: 10.1001/jamapediatrics.2018.1161

Guenther, P. M., Casavale, K. O., Reedy, J., Kirkpatrick, S. I., Hiza, H. A. B., Kuczynski, K. J., et al. (2013). Update of the healthy eating index: HEI-2010. *J. Acad. Nutrit. Dietetics* 113, 569–580. doi: 10.1016/j.jand.2012.12.016

Hornef, M. W., and Torow, N. (2020). 'Layered immunity' and the 'neonatal window of opportunity' - timed succession of non-redundant phases to establish mucosal host-microbial homeostasis after birth. *Immunology* 159, 15–25. doi: 10.1111/imm.13149

Hu, J., Ly, J., Zhang, W., Huang, Y., Glover, V., Peter, I., et al. (2019). Microbiota of newborn meconium is associated with maternal anxiety experienced during pregnancy. *Dev. Psychobiol.* 61, 640–649. doi: 10.1002/dev.21837

Kang, L. J., Vu, K. N., Koleva, P. T., Field, C. J., Chow, A., Azad, M. B., et al. (2020). Maternal psychological distress before birth influences gut immunity in mid-infancy. *Clin. Exp. Allergy* 50, 178–188. doi: 10.1111/cea.13551

Kawano, A., and Emori, Y. (2015). The relationship between maternal postpartum psychological state and breast milk secretory immunoglobulin a level. *J. Am. Psychiatr. Nurses Assoc.* 21, 23–30. doi: 10.1177/1078390314566882

Kim, M., Qie, Y., Park, J., and Kim, C. H. (2016). Gut microbial metabolites fuel host antibody responses. *Cell Host Microbe* 20, 202–214. doi: 10.1016/j.chom.2016.07.001

Korpela, K., and de Vos, W. M. (2018). Early life colonization of the human gut: microbes matter everywhere. *Curr. Opin. Microbiol.* 44, 70–78. doi: 10.1016/j.mib.2018.06.003

Kukkonen, K., Kuitunen, M., Haahtela, T., Korpela, R., Poussa, T., and Savilahti, E. (2010). High intestinal IgA associates with reduced risk of IgE-associated allergic diseases. *Pediatr. Allergy Immunol.* 21 (Pt 1), 67–73. doi: 10.1111/j.1399-3038.2009.00907.x

Lewis, A. J., Austin, E., Knapp, R., Vaiano, T., and Galbally, M. (2015). Perinatal maternal mental health, fetal programming and child development. *Healthcare (Basel, Switzerland)* 3, 1212–1227. doi: 10.3390/healthcare3041212

Macpherson, A. J., Yilmaz, B., Limenitakis, J. P., and Ganal-Vonarburg, S. C. (2018). IgA function in relation to the intestinal microbiota. *Annu. Rev. Immunol.* 36, 359–381. doi: 10.1146/annurev-immunol-042617-053238

Madan, J. C., Hoen, A. G., Lundgren, S. N., Farzan, S. F., Cottingham, K. L., Morrison, H. G., et al. (2016). Association of cesarean delivery and formula supplementation with the intestinal microbiome of 6-Week-Old infants. *JAMA Pediatr.* 170, 212–219. doi: 10.1001/jamapediatrics.2015.3732

Mandal, S., Godfrey, K. M., McDonald, D., Treuren, W. V., Bjørnholt, J. V., Midtvedt, T., et al. (2016). Fat and vitamin intakes during pregnancy have stronger relations with a pro-inflammatory maternal microbiota than does carbohydrate intake. *Microbiome* 4:55.

Maruyama, K., Hida, M., Kohgo, T., and Fukunaga, Y. (2009). Changes in salivary and fecal secretory IgA in infants under different feeding regimens. *Pediatr. Int.* 51, 342–345. doi: 10.1111/j.1442-200x.2008.02748.x

Meedya, S., Fahy, K., and Kable, A. (2010). Factors that positively influence breastfeeding duration to 6 months: a literature review. *Women Birth* 23, 135–145. doi: 10.1016/j.wombi.2010.02.002

Milani, C., Duranti, S., Bottacini, F., Casey, E., Turroni, F., Mahony, J., et al. (2017). The first microbial colonizers of the human gut: composition, activities, and health implications of the infant gut microbiota. *Microbiol. Mol. Biol. Rev. MMBR* 81:e00036-17.

Moossavi, S., Sepehri, S., Robertson, B., Bode, L., Goruk, S., Field, C. J., et al. (2019). Composition and variation of the human milk microbiota are influenced by maternal and early-life factors. *Cell Host Microbe* 25, 324–335.e4. doi: 10.1016/j.chom.2019.01.011

Rengarajan, S., Knoop, K. A., Rengarajan, A., Chai, J. N., Grajales-Reyes, J. G., Samineni, V. K., et al. (2020). A potential role for stress-induced microbial alterations in IgA-Associated irritable bowel syndrome with diarrhea. *Cell Rep. Med.* 1:100124. doi: 10.1016/j.xcrm.2020.100124

Shin, N., Whon, T. W., and Bae, J. (2015). *Proteobacteria* : microbial signature of dysbiosis in gut microbiota. *Trends Biotechnol.* 33, 496–503. doi: 10.1016/j.tibtech.2015.06.011

Smejda, K., Brzozowska, A., Podlecka, D., Polanska, K., and Jerzynska, J. (2019). Maternal stress and allergic diseases in children: a systematic review. *J. Dermatol. Skin Sci.* 1, 1–7.

Tun, H. M., Bridgman, S. L., Chari, R., Field, C. J., Guttman, D. S., Becker, A. B., et al. (2018). Roles of birth mode and infant gut microbiota in intergenerational transmission of overweight and obesity from mother to offspring. *JAMA Pediatr.* 172, 368–377. doi: 10.1001/jamapediatrics.2017.5535

van den Elsen, L. W. J., Garssen, J., Burcelin, R., and Verhasselt, V. (2019). Shaping the gut microbiota by breastfeeding: the gateway to allergy prevention? *Front. Pediatr.* 7:47. doi: 10.3389/fped.2019.00047

Williams, J. E., Carrothers, J. M., Lackey, K. A., Beatty, N. F., Brooker, S. L., Peterson, H. K., et al. (2019). Strong multivariate relations exist among milk, oral, and fecal microbiomes in mother-infant dyads during the first six months postpartum. *J. Nutr.* 149, 902–914. doi: 10.1093/jn/nxy299

Yang, R., Gao, R., Cui, S., Zhong, H., Zhang, X., Chen, Y., et al. (2019). Dynamic signatures of gut microbiota and influences of delivery and feeding modes during the first 6 months of life. *Physiol. Genom.* 51, 368–378. doi: 10.1152/physiolgenomics.00026.2019

Zijlmans, M. A. C., Korpela, K., Riksen-Walraven, J. M., de Vos, W. M., and de Weerth, C. (2015). Maternal prenatal stress is associated with the infant intestinal microbiota. *Psychoneuroendocrinology* 53, 233–245. doi: 10.1016/j.psyneuen.2015.01.006

Conflict of Interest: The authors declare that the research was conducted in the absence of any commercial or financial relationships that could be construed as a potential conflict of interest.

Publisher's Note: All claims expressed in this article are solely those of the authors and do not necessarily represent those of their affiliated organizations, or those of the publisher, the editors and the reviewers. Any product that may be evaluated in this article, or claim that may be made by its manufacturer, is not guaranteed or endorsed by the publisher.

Frontiers in Microbiology

Explores the habitable world and the potential of microbial life

The largest and most cited microbiology journal which advances our understanding of the role microbes play in addressing global challenges such as healthcare, food security, and climate change.

Discover the latest Research Topics

See more →

Frontiers

Avenue du Tribunal-Fédéral 34
1005 Lausanne, Switzerland
frontiersin.org

Contact us

+41 (0)21 510 17 00
frontiersin.org/about/contact